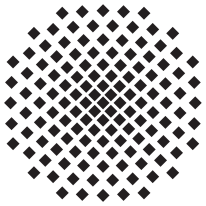

Universität Stuttgart

Spin density waves in bilayer cold polar molecules

Master Thesis

of

Amin Naseri Jorshari

First Supervisor: Prof. Dr. H. P. Büchler
Second Supervisor: Prof. Dr. G. Wunner

Institut für Theoretische Physik III
Universität Stuttgart

January 18, 2012

Contents

List of Figures

Chapter 1

Introduction

Following the breakthrough of the laser cooling over the atomic gas, by Steven Chu, Claude Cohen Tannoudji and William D. Phillips in 1985 [12], who honored with the Nobel Prize in 1997, the investigation upon the cold gases is snowballing rapidly. The observation of the Bose-Einstein condensation (BEC) (see Fig.1.1) in 1995 [4, 15], by Eric A. Cornell, Wolfgang Ketterle, Carl E. Wieman, have brought the second Nobel Prize in 2001 for the frontier settler of the field [8]. Cooling atoms through the quantum mechanical realm, accompanied by the tunable interaction of particles by means of external fields [5], has provided a new opportunity to observe the long-aged predictions besides many prospective of applications.

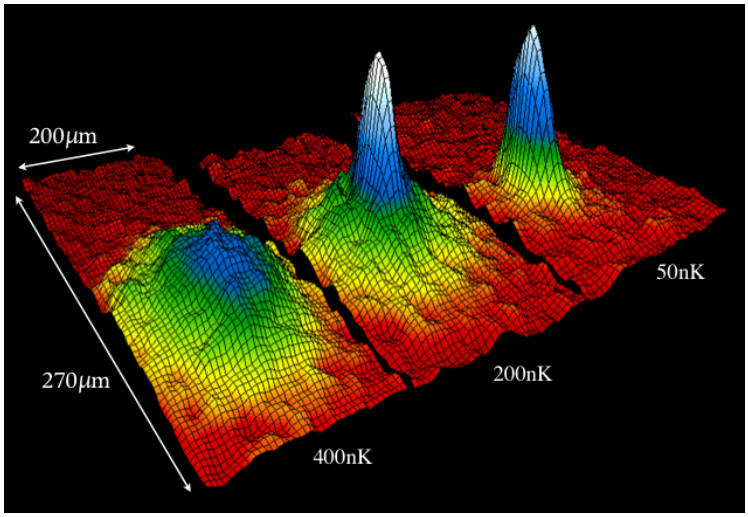

Figure 1.1: The velocity distribution of rubidium atoms taken by JILA-NIST [4]. The atoms are confined by magnetic field and cooled evaporatively. The condensate appears by cooling down the gas near 170nK, where a macroscopic fraction of atoms occupied common low-energy state. The velocity distribution has peaked abruptly as the temperature of the sample was lowered. The leftmost image shows the distribution just before the appearance of the condensation at 400nK. The middle one shows the moment of the condensation at 200nK, and the rightmost depicts after further cooling, where the sample is nearly pure condensate at 50nK. The field of the horizontal observation is $200\mu m$ by $270\mu m$. (The image is adopted from image gallery of NIST: `http://bec.nist.gov/gallery.html`)

Inspired by the experience done over the atoms, the territory of the cold and ultracold gases have been extended toward the molecules soil during the past decade. Currently, about fifty research groups are involved in the field of the cold molecules research and more than hundred paper is the annual outcome of the investigation over such crucially growing field [27]. The additional internal degree of freedom in molecules (see Fig. 1.2) as like vibrational and rotational levels, fine and hyperfine structure and symmetry-breaking doublet, offer a rich and challenging playground for a vast area of new experimental measurements and diverse applications. Molecules provides a significant advantage in compare with neutral atoms, as they possess tunable electric dipole moment which can be induced by a static dc electric field, in addition to their own intrinsic dipole moment. Molecules also have the capability to attain the transition dipole moment induced by a resonant microwave field, coupled with the internal rotational states. Therefore they have brought into the stage an inexperienced type of the systems allowing tunable interparticle interaction handled by means of external fields.

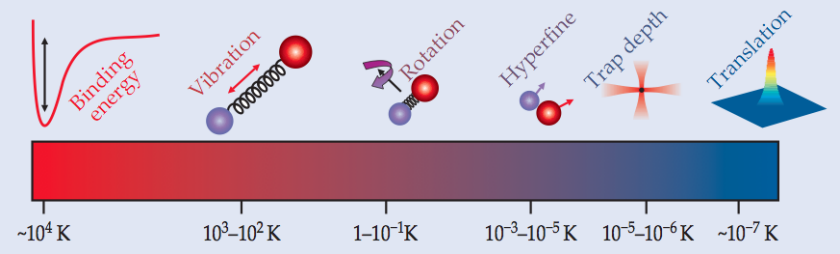

Figure 1.2: Molecules internal degree of freedoms and their corresponding energy scales, which offer a wide range of opportunities for quantum science in compare with the atoms. (The image is taken from Ref. [25])

Ultracold polar molecules open the prospective to explore quantum gases with the interparticle interactions, which are strong, long-range and spatially anisotropic. The interaction of molecules are in pronounced contrast to the gases of ultracold atoms, which are isotropic and extremely short-range and is labeled as the so-called contact interaction. Indeed, ultracold molecules offer a diverse scientific direction and promised application such as study of novel dynamics in the low-energy collisions, long-range collective quantum effects and quantum phase transitions, precise control of chemical reactions, tests of fundamental symmetries like parity and time reversal, and time variation of the fundamental constants; where has pushed further the traditional molecular science and actually has introduced a broadened multidisciplinary field that tied together the experimental and theoretical research on atomic, molecular, and optical physics and quantum information science [27, 11].

The main effort in the cold molecules experiment filed was focused over the creation of stable and dense ensembles of ultracold molecules during the past five years. Recently this goal has been accomplished by preparation of the degenerate gases of molecules in electronic vibrational ground states [33, 17, 14, 34, 35, 16] and the ultracold chemistry, molecular BEC, and coherent control of the ultracold molecular process would be feasible in close future.

On the theoretical point of view, a considerable number of research, looking for the exotic quantum phases in the cold polar molecule gases in various geometrical configurations have been attempted (for example see [9, 10, 36, 44, 7, 13, 28, 29]). As it is shown that a quasi-2D

gas of polar molecules would suppress inelastic collisions (see Ref. [22]), and so increases the lifetime of the trapped gas, most of the theoretical researches have been done over the low dimensional systems (see the caption of Fig. 1.3).

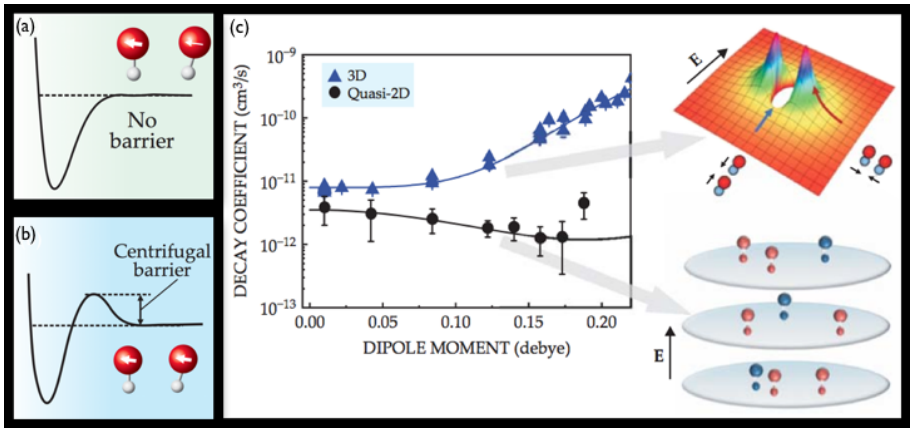

Figure 1.3: In a gas of cold polar molecules, when fermionic molecules are prepared in the same internal state, the relative wavefunction has to be antisymmetric. Hence, the molecules interact in a p-wave channel, and The centrifugal barrier suppress the chemical reaction. **(a)** The interaction of two molecules in mixture of internal state. **(b)** The centrifugal barrier due to p-wave relative wavefunction. **(c)** Attractive head-to-tail interaction of aligned dipolar molecules, due to applied electric field, decreases the centrifugal barrier, hence increases the decay of the system. But, confined molecules perpendicular to the quasi-2D layers shows repulsive side-by-side collision within a layer and suppresses the rate of decay. (The images are taken from Ref. [25])

Throughout this thesis, we have studied a number of the quantum phases of a two dimensional system of bilayer cold polar molecules. The bilayer system would be introduced in the following chapter. We have shown the instability of the system versus spin density wave (SDW) phase as a function of the interlayer separation or strength of the interparticle interaction. The order parameter and the condensation energy associated with the SDW phase have been presented. The instability of the bilayer cold polar molecules system to the interlayer superfluidity, in s-wave and p-wave channel also have been examined. Finally, the phase diagram of the system is presented as a function of the external governing parameters.

Chapter 2

Preliminaries

In the following chapter, we introduce a system of bilayer cold polar molecules which would be under investigation throughout this thesis. Besides, spin density wave phase and superfluidity phase are briefly reviewed.

2.1 Bilayer system of cold polar molecules

We consider two clouds of polar molecules [32, 29, 13] which are confined tightly in z direction by confinement length l_0. Two layers are separated by a distance l that is much larger than the confinement length $l_0 \ll l$, as it is depicted in Fig. 2.1. The translational motion of the molecules is given in 2 dimensions, but molecules possess a 3D rotational motion. The rotational states would be described by eigenstate $|J, M_J\rangle$ with J being total internal angular momentum of a molecule and M_J is its projection along the quantization axis. Polar molecules have permanent electric dipole moment d, coupled with the internal rotational degree of freedom. The operator of the dipole moment $\mathbf{d}$ have non-zero matrix element just only between states with different rotational quantum number. The transition dipole moment for $J = 0 \rightarrow J = 1$ reads as $d_t = |\langle 0, 0|\mathbf{d}|1, M_J\rangle| = d/\sqrt{3}$, with $M_J = 0, \pm 1$. The dipole moments establish a long-range and anisotropic interaction among molecules. The Hamiltonian for polar molecules H has the form

$$H = \sum_i \left(\frac{p_i^2}{2m} + B\mathbf{J}_i^2 \right) + \sum_{i,j} \frac{\mathbf{d}_i.\mathbf{d}_j - 3(\mathbf{d}_i.\hat{\boldsymbol{r}}_{ij})(\mathbf{d}_j.\hat{\boldsymbol{r}}_{ij})}{2r_{ij}^3}, \tag{2.1}$$

where $\mathbf{p} = (p_x, p_y)$ is the center-of-mass momentum of a molecule with mass m, r_{ij} being the distance between two molecules, $\hat{r}_{ij}$ is the unit vector operator, B is the effective rotational energy in the rigid rotor term, and $\mathbf{J} = (J_x, J_y, J_z)$ is the angular momentum operator.

The system is subject to a circularly polarized microwave electric field $\mathbf{E}_{ac}(t)$, propagating along z direction. The MW field couples the rotational ground state $|0, 0\rangle$ with the first excited state $|1, 1\rangle$ by the Rabi frequency $\Omega_R = d_t E_{ac}/\hbar$. The frequency of the field ω can be tuned close to the transition frequency $\omega_0 = 2B$ of the states $|0, 0\rangle$ and $|1, 1\rangle$ with detuning $\delta = \omega - \omega_0 \ll \omega_0$. Within rotating wave approximation (see Ref. [24]), the dressed-molecule states can be written

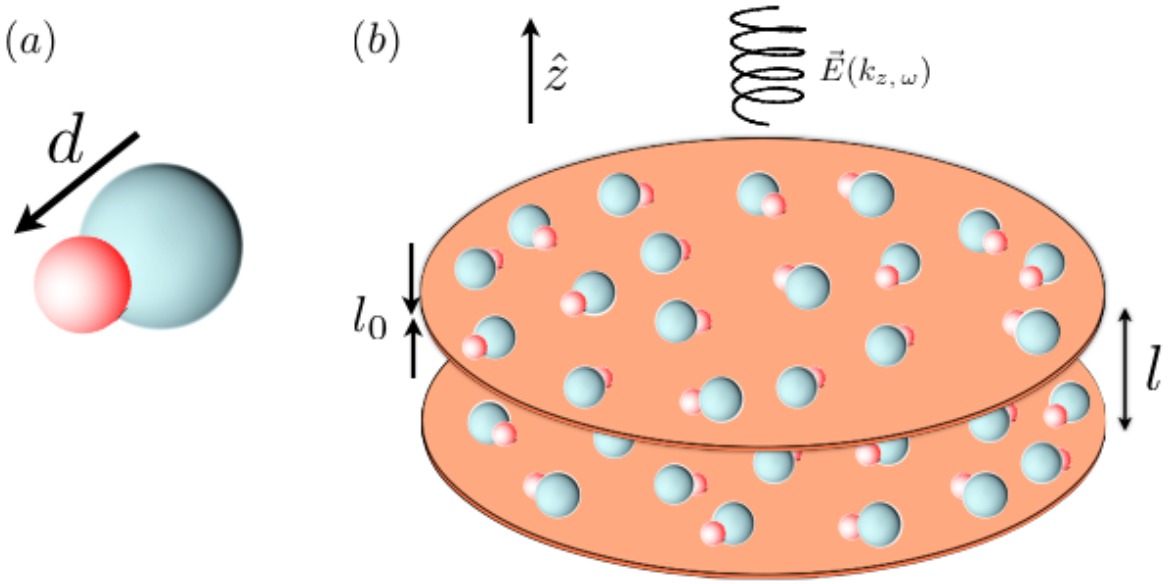

Figure 2.1: Bilayer system of cold polar molecules that composed of heteronuclear molecules which are confined tightly along z direction. **(a)** Molecules have a permanent electric dipole moment d. **(b)** The confinement length of the molecules is much smaller than the interlayer separation $l_0 \ll l$. Also, a MW field propagating along z direction would dress the molecules. The MW field is shown schematically.

$$|+\rangle = \alpha_+|0,0\rangle + \alpha_- e^{-i\omega t}|1,1\rangle,$$

$$|-\rangle = \alpha_-|0,0\rangle - \alpha_+ e^{-i\omega t}|1,1\rangle,$$

where $\alpha_+ = -\Gamma/\sqrt{\Gamma^2+\Omega_R^2}$, $\alpha_- = \Omega_R/\sqrt{\Gamma^2+\Omega_R^2}$, and $2\Gamma = \delta + \sqrt{\delta^2+4\Omega_R^2}$. It is possible to prepare the polar molecules in the internal state $|+\rangle_i$ by an adiabatic switching of the MW field. The effective interaction between polar molecules is given in the framework of Born-Oppenheimer approximation, in which the molecules are assumed to be at fixed positions and afterwards their states could be adiabatically connected to the states $|+\rangle_i \otimes |+\rangle_j$. At large distances, the dipolar interaction can be obtained perturbatively associated with dipole moment $\langle +|\mathbf{d}|+\rangle = d_{eff}(\cos\omega t, \sin\omega t, 0)$, where $d_{eff} = -\sqrt{2}d_t\alpha_+\alpha_-$. The time-averaged interaction between dipoles moments reads

$$V_{eff}^{\lambda\lambda'}(\boldsymbol{r}) = d_{eff}^2 \frac{l^2 - r^2/2}{(l^2+r^2)^{5/2}}, \tag{2.2}$$

where $\mathbf{r} = (r_x, r_y)$. The potential is defined for the interlayer interaction by $\lambda \neq \lambda'$, and for intralayer interaction $\lambda = \lambda'$, the relation reads with $l = 0$. In the short distances, the dipolar interaction between particles causes molecules depart from the state $|+\rangle$ and the perturbation breaks down. Therefore, in the short distances $r \leqslant r_\delta \equiv (d_t/\delta)^{1/3}$, one has to take into account the coupling of whole rotational states $|J, M_J\rangle$. The exact Born-Oppenheimer potential for

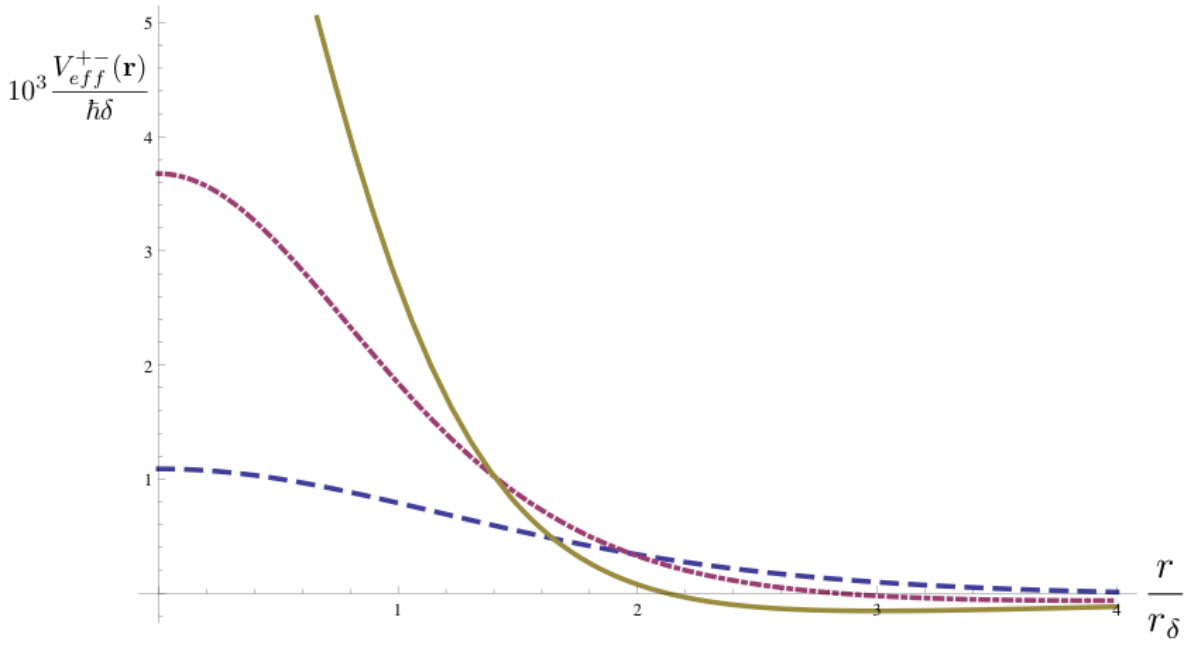

Figure 2.2: Interlayer Born-Oppenheimer potential for $\Omega_R/\delta = 1/8$. The solid (green), dash-dotted (red), and dashed (blue) lines correspond to $(l/r_\delta) = 1.5$, $(l/r_\delta) = 2$, and $(l/r_\delta) = 3$, respectively.

interlayer interactions and intralayer interaction at large distances are depicted in Fig. 2.2 and Fig. 2.3, respectively.

Fourier transform of the interaction potential

We Fourier transform the interaction potential in Eq. (2.2) by dividing the potential function into two parts as $V(\boldsymbol{r}) \equiv d_{eff}^2[\varphi_1(\boldsymbol{r}) + \varphi_2(\boldsymbol{r})]$, where $\varphi_1(\boldsymbol{r}) \equiv 1/(l^2 + r^2)^{3/2}$ and $\varphi_2(\boldsymbol{r}) \equiv -3r^2/2(l^2 + r^2)^{5/2}$. We have dropped the superscript $\lambda\lambda'$ and subscript eff. We will present the intralayer interaction by $V_{++}(\boldsymbol{r})$, $\tilde{V}_{++}(\boldsymbol{q})$, and the interlayer interaction as $V(\boldsymbol{r})$, $\tilde{V}(\boldsymbol{q})$. By keeping the interlayer separation at fixed value $z = l$, the Fourier transform of the first term reads

$$\begin{aligned} \tilde{\varphi}_1(\mathbf{q}) &= \int \frac{r dr d\theta}{(l^2 + r^2)^{3/2}} e^{-irq\cos\theta} \\ &= \frac{2\pi}{l} \exp(-lq). \end{aligned} \tag{2.3}$$

Fourier transform of the second term can be derived from the first term by constructing a relation as

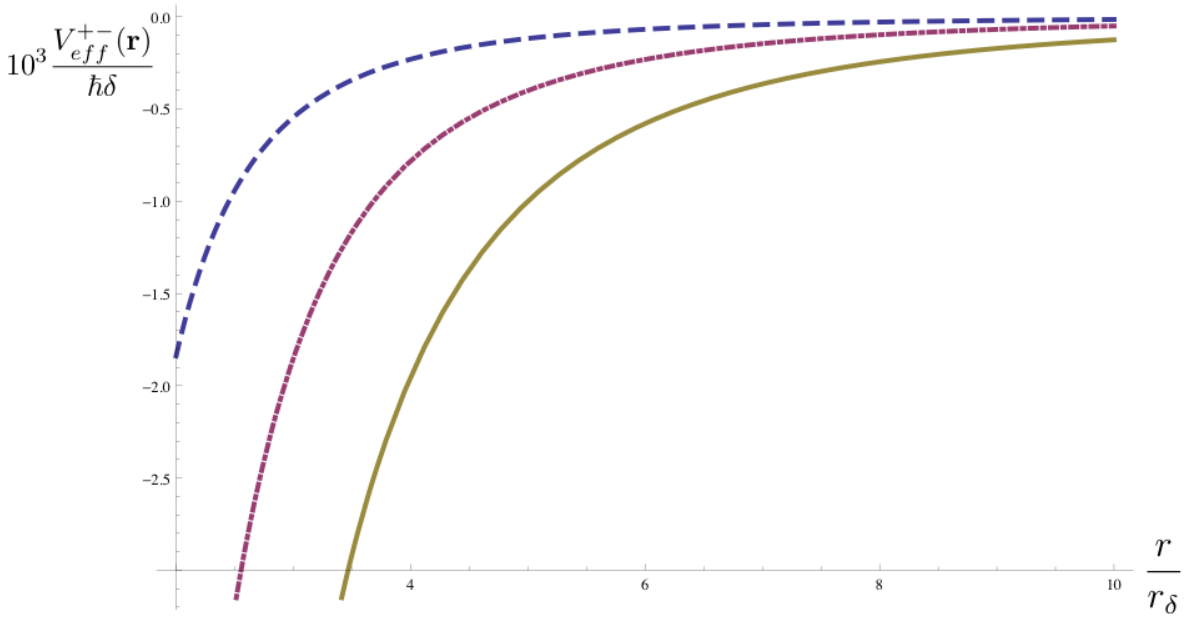

Figure 2.3: Intralayer interaction potential at the large distances $l \ll r$. The solid (green), dash-dotted (red), and dashed (blue) lines correspond to the $\Omega_R/\delta = 1/2$, $\Omega_R/\delta = 1/4$, and $\Omega_R/\delta = 1/8$, respectively.

$$\begin{aligned}\varphi_2(\boldsymbol{r}) = -\frac{3}{2}\frac{r^2}{(l^2+r^2)^{5/2}} &= \lim_{\lambda\to 1}\frac{1}{2}\frac{\partial}{\partial\lambda}\varphi_1(\lambda,\boldsymbol{r}) \\ &= \lim_{\lambda\to 1}\frac{1}{2}\frac{\partial}{\partial\lambda}\frac{1}{(l^2+\lambda^2 r^2)^{3/2}},\end{aligned}$$

and readily the Fourier transform obtains

$$\begin{aligned}\tilde{\varphi}_2(\boldsymbol{q}) &= \lim_{\lambda\to 1}\frac{1}{2}\frac{\partial}{\partial\lambda}\left[\frac{1}{\lambda^2}\frac{2\pi}{l}\exp\left(-\frac{lq}{\lambda}\right)\right] \\ &= \lim_{\lambda\to 1}\frac{1}{2}\frac{2\pi}{l\lambda^3}e^{-lq/\lambda}\left[-2+\frac{lq}{\lambda}\right] \\ &= \frac{2\pi}{l}e^{-lq}+\pi q e^{-lq}.\end{aligned}$$

The Fourier transform of the interaction potential can be achieved by sum of the both terms, which is

$$\tilde{V}(\mathbf{q}) = \pi d_{eff}^2 q e^{-ql}. \tag{2.4}$$

The interaction potential in momentum space $\tilde{V}(\mathbf{q})$ is shown in Fig. (2.4), and is positive for all value of $\mathbf{q}$ with a maximum at $lq = 1$. The Fourier transform of the intralayer interaction can be readily achieved by putting $l = 0$ in Eq. (2.4) which gives $\tilde{V}_{++}(\boldsymbol{q}) = \pi d_{eff}^2 q$.

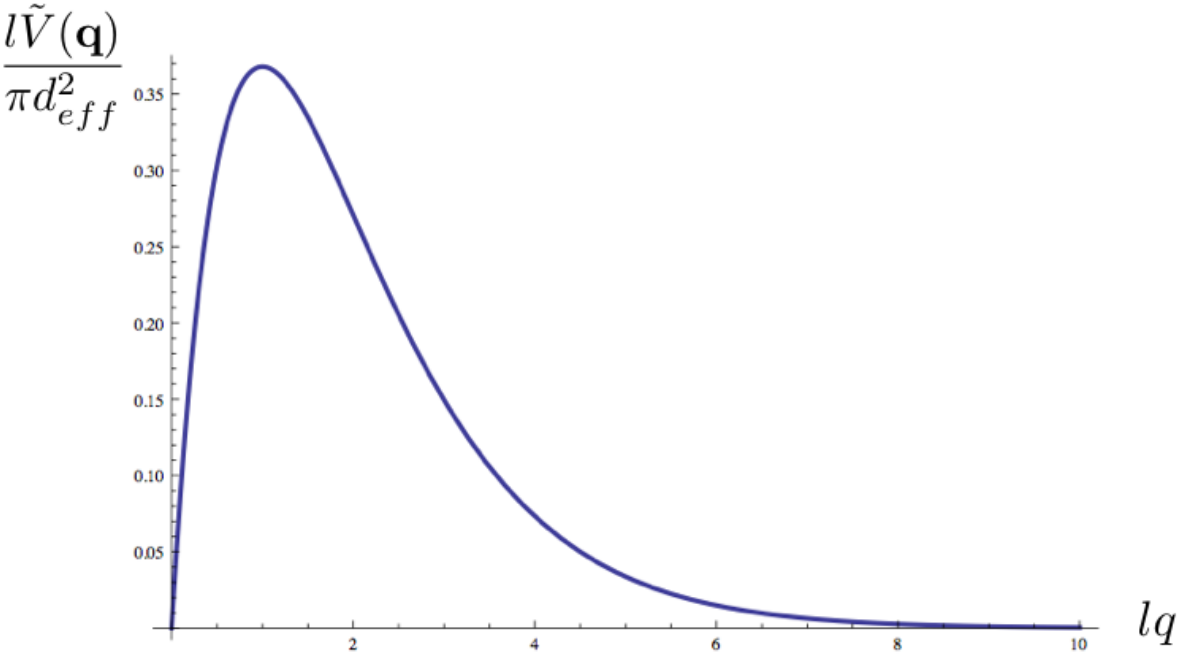

Figure 2.4: Fourier transform of the interlayer interaction which has a maximum at $lq = 1$.

Second-quantized representation

The Hamiltonian in the second quantization is written formally as

$$H = \sum_{\lambda} \int d\mathbf{x}\, \hat{\psi}^{\dagger}_{\lambda}(\mathbf{x}) \left(-\frac{\hbar^2}{2m} \nabla^2 \right) \hat{\psi}_{\lambda}(\mathbf{x}) + \frac{1}{2} \sum_{\lambda,\, \lambda'} \int d\mathbf{x} d\mathbf{y} \hat{\psi}^{\dagger}_{\lambda}(\mathbf{x}) \hat{\psi}^{\dagger}_{\lambda'}(\mathbf{y}) V(\mathbf{x}-\mathbf{y}) \hat{\psi}_{\lambda'}(\mathbf{y}) \hat{\psi}_{\lambda}(\mathbf{x}).$$

The field operators $\hat{\psi}^{\dagger}_{\lambda}(\mathbf{x})$ and $\hat{\psi}_{\lambda}(\mathbf{x})$ are creation and annihilation operators for a particle at the state with quantum numbers $\mathbf{x}$ and λ. We write the field operators in the basis of the plane-wave as

$$\begin{aligned} \hat{\psi}_{\lambda}(\mathbf{x}) &= \sum_{\mathbf{k},\, \lambda} \langle \mathbf{x}|\mathbf{k}\rangle \hat{a}_{\mathbf{k},\, \lambda}, \\ \hat{\psi}^{\dagger}_{\lambda}(\mathbf{x}) &= \sum_{\mathbf{k},\, \lambda} \langle \mathbf{k}|\mathbf{x}\rangle \hat{a}^{\dagger}_{\mathbf{k},\, \lambda}, \\ \langle \mathbf{x}|\mathbf{k}\rangle &= \frac{1}{\sqrt{L^2}} \exp\left(i\mathbf{k}.\mathbf{x}\right). \end{aligned}$$

where L^2 is the volume of the system, $\hat{a}^{\dagger}_{\mathbf{k},\, \lambda}$ and $\hat{a}_{\mathbf{k},\, \lambda}$ are creation and annihilation operators. By use of the following relation

$$\int d\mathbf{x} e^{i(\mathbf{k}-\mathbf{k}').\mathbf{x}} = L^2 \delta(\mathbf{k}-\mathbf{k}'),$$

the kinetic term takes the form

$$H_{Kin} = \sum_{\mathbf{k},\,\lambda} \frac{\hbar^2 k^2}{2m} \hat{a}^{\dagger}_{\mathbf{k},\,\lambda} \hat{a}_{\mathbf{k},\,\lambda}.$$

The interaction term can be written in the momentum space by replacing the operators and the interaction potential with their Fourier transforms as

$$\begin{aligned}
H_{int} &= \frac{1}{2} \sum_{\substack{\mathbf{k}_1,\,\mathbf{k}_2 \\ \mathbf{k}_3,\,\mathbf{k}_4}} \int d\mathbf{x} d\mathbf{y} \langle \mathbf{k}_1 | \mathbf{x} \rangle \hat{a}^{\dagger}_{\mathbf{k}_1,\,\lambda} \langle \mathbf{k}_2 | \mathbf{y} \rangle \hat{a}^{\dagger}_{\mathbf{k}_2,\,\lambda} \frac{1}{L^2} \int d\mathbf{q} \tilde{V}(\mathbf{q}) e^{i\mathbf{q}.(\mathbf{x}-\mathbf{y})} \langle \mathbf{y} | \mathbf{k}_3 \rangle \hat{a}_{\mathbf{k}_3,\,\lambda} \langle \mathbf{x} | \mathbf{k}_4 \rangle \hat{a}_{\mathbf{k}_4,\,\lambda} \\
&= \frac{1}{2L^6} \sum_{\substack{\mathbf{k}_1,\,\mathbf{k}_2 \\ \mathbf{k}_3,\,\mathbf{k}_4}} \int d\mathbf{x} d\mathbf{y} d\mathbf{q} e^{-i\mathbf{k}_1.\mathbf{x}} e^{-i\mathbf{k}_2.\mathbf{y}} \tilde{V}(\mathbf{q}) e^{i\mathbf{q}.(\mathbf{x}-\mathbf{y})} e^{i\mathbf{k}_3.\mathbf{y}} e^{i\mathbf{k}_4.\mathbf{x}} \hat{a}^{\dagger}_{\mathbf{k}_1,\,\lambda} \hat{a}^{\dagger}_{\mathbf{k}_2,\,\lambda} \hat{a}_{\mathbf{k}_3,\,\lambda} \hat{a}_{\mathbf{k}_4,\,\lambda} \\
&= \frac{1}{2L^6} \sum_{\substack{\mathbf{k}_1,\,\mathbf{k}_2 \\ \mathbf{k}_3,\,\mathbf{k}_4}} \int d\mathbf{q} \tilde{V}(\mathbf{q}) \hat{a}^{\dagger}_{\mathbf{k}_1,\,\lambda} \hat{a}^{\dagger}_{\mathbf{k}_2,\,\lambda} \hat{a}_{\mathbf{k}_3,\,\lambda} \hat{a}_{\mathbf{k}_4,\,\lambda} \underbrace{\int d\mathbf{x} e^{i(\mathbf{q}-\mathbf{k}_1+\mathbf{k}_4).\mathbf{x}}}_{L^2\delta(\mathbf{q}-\mathbf{k}_1+\mathbf{k}_4)} \underbrace{\int d\mathbf{y} e^{i(\mathbf{k}_3-\mathbf{k}_2-\mathbf{q}).\mathbf{y}}}_{L^2\delta(\mathbf{k}_3-\mathbf{k}_2-\mathbf{q})} \\
&= \frac{1}{2L^2} \sum_{\mathbf{q},\,\mathbf{k},\,\mathbf{k}'} \tilde{V}(\mathbf{q}) \hat{a}^{\dagger}_{\mathbf{k},\,\lambda} \hat{a}^{\dagger}_{\mathbf{k}',\,\lambda} \hat{a}_{\mathbf{k}'+q,\,\lambda} \hat{a}_{\mathbf{k}-q,\,\lambda},
\end{aligned}$$

where we have chose $\mathbf{k}_4 = \mathbf{k}_1 - \mathbf{q} \equiv \mathbf{k} - \mathbf{q}$ and $\mathbf{k}_3 = \mathbf{k}_2 + \mathbf{q} \equiv \mathbf{k}' + \mathbf{q}$, and the Fourier transform of the interaction potential $\tilde{V}(\mathbf{q})$ is given in Eq. (2.4). Therefore, the effective Hamiltonian for the bilayer system, by adding the chemical potential reads

$$H = \sum_{\mathbf{k},\,\lambda} \left[\epsilon(\mathbf{k}) - \mu_\lambda\right] \hat{c}^{\dagger}_{\mathbf{k}\lambda} \hat{c}_{\mathbf{k}\lambda} + \frac{1}{2L^2} \sum_{\substack{\mathbf{q},\,\mathbf{k},\mathbf{k}' \\ \lambda,\,\lambda'}} \tilde{V}(\mathbf{q}) \hat{c}^{\dagger}_{\mathbf{k}+\mathbf{q}\lambda} \hat{c}^{\dagger}_{\mathbf{k}'-\mathbf{q}\lambda'} \hat{c}_{\mathbf{k}'\lambda'} \hat{c}_{\mathbf{k}\lambda}, \tag{2.5}$$

where $\hat{c}^{\dagger}_{\mathbf{k}\lambda}$ and $\hat{c}_{\mathbf{k}\lambda}$ are creation and annihilation operators, respectively, for a molecule with momentum $\mathbf{k}$ in layer λ.

2.2 Spin density wave

We review the spin density wave phase in 1D following Gröner in Ref. [23]. The broken symmetry has been treated in the framework of the mean-field theory. However, the mean-field theory is not appropriate in 1D. Due to of the reduction of the phase space in 1D, the systems are unstable even in the absent of the interaction (see divergent behavior of 1D response function in Fig. A.1), and actually it would not be considered as a Fermi-liquid. By the way, mean-field theory can reveal the main features of the 1D model. The treatments beyond the mean-field theory can be found in Ref. [41].

We start by examining the divergent behavior of the response function in 1D. As discussed in App. A, the explicit integral form of the response function in one-dimension reads

$$\chi(q) = \int \frac{dk}{(2\pi)} \frac{f_k - f_{k+q}}{\epsilon_k - \epsilon_{k+q}}, \tag{2.6}$$

where f_k is the Fermi distribution function. The integral can be performed readily for 1D at zero-temperature by $f_k = \theta(k_F - k)$, which gives the result

$$\chi(q) = -\frac{m}{\pi\hbar^2 k_F} \ln\left|\frac{q+2k_F}{q-2k_F}\right|, \tag{2.7}$$

where m is the mass of the particle. This result can be compare with the response function in 2D and 3D which are given in Eq. (A.20). The situation in 1D is particular, where the response function diverges at $q = 2k_F$, as can be seen in Fig. A.1. The divergent behavior of the response function at $q = 2k_F$ comes from the particular topology of the Fermi surface in 1D, which is two points as is shown in Fig. 2.5. The response function in Eq. (2.6) shows that the most contribution of the integral comes from the pair of states, one empty and one full, which differ by $q = 2k_F$ and have the same energy. The whole states close to the Fermi-surface in 1D contribute to the such diverging behavior. However, in higher dimensions the number of such states reduced significantly in comparison with the states coupled by the same vector, but with the different energy (see Fig. 2.6).

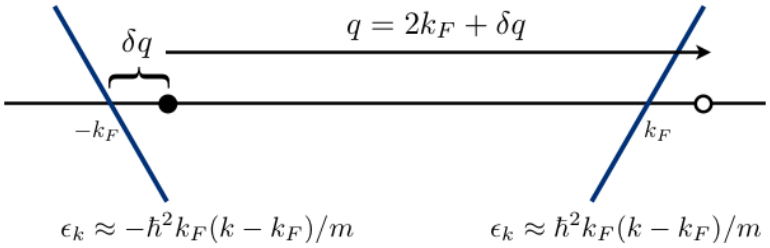

Figure 2.5: The linearized dispersion relation for a free fermionic gas, in the vicinity of the Fermi surface is shown. The Fermi surface is just two points. The states of the particle and hole close to the Fermi surface but in the opposite side, can be coupled by a single vector $q = 2k_F$ in 1D. (The image is reproduced from Ref. [23])

We consider a so-called one dimensional Hubbard Hamiltonian, as a system with the simplest possible interaction, to study the SDW in 1D. The Hamiltonian reads

$$H = \sum_{k,\sigma} \epsilon_k \hat{a}^\dagger_{k,\sigma} \hat{a}_{k,\sigma} + \frac{U}{N} \sum_{k,k',q} \hat{a}^\dagger_{k,\sigma} \hat{a}_{k+q,\sigma} \hat{a}^\dagger_{k',-\sigma} \hat{a}_{k'-q,-\sigma}, \tag{2.8}$$

where $\hat{a}^\dagger_{k,\sigma}$ and $\hat{a}_{k,\sigma}$ being the creation and annihilation operator, respectively, and U is the on-site Coulomb interaction. We split the density operators to its mean-value and the fluctuation around it to obtain

$$\begin{aligned} \hat{\rho}_{q\sigma} &= \sum_k \hat{a}^\dagger_{k\sigma}\, \hat{a}_{k+q\sigma} \\ &= \langle\hat{\rho}_{q\sigma}\rangle + (\hat{\rho}_{q\sigma} - \langle\hat{\rho}_{q\sigma}\rangle) \\ &= \langle\hat{\rho}_{q\sigma}\rangle + \delta\hat{\rho}_{q\sigma}. \end{aligned} \tag{2.9}$$

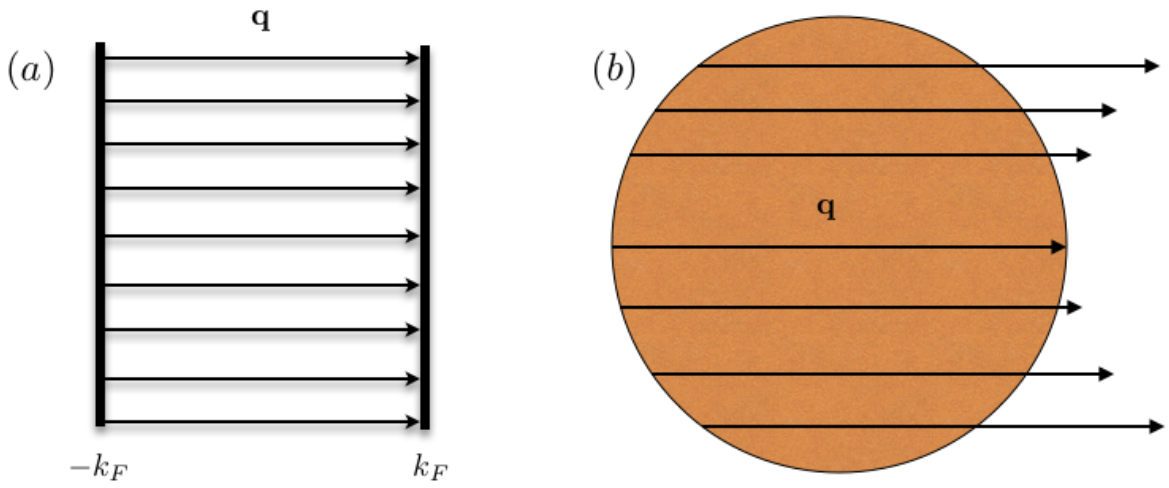

Figure 2.6: Topology of the Fermi surface in 1D and 2D of a free fermionic gas. The coupling vector of the particle-hole pairs are shown with arrows. (**a**) In 1D system, a single vector couples the whole particle and hole states in the vicinity of Fermi surface. (**b**) The number of the particle-hole pairs, with the same energy, coupled with a single vector $|\mathbf{q}| = 2k_F$, is significantly reduced in 2D. (The image is reproduced from Ref. [23])

By inserting this decomposition into the Hamiltonian in Eq. (2.8), after neglecting the quadratic term in the density operator fluctuation $\delta\hat{\rho}_{q\sigma}\delta\hat{\rho}_{-q-\sigma}$. We keep the expectation values at $q = 2k_F$, as it is the most interesting point due to divergent behavior of the response function. The mean-field Hamiltonian reads

$$H_{MF} = \sum_{k,\,\sigma} \epsilon_k \hat{a}^{\dagger}_{k,\,\sigma}\hat{a}_{k,\,\sigma} + \sum_{k} \left\{ \Delta e^{i\varphi} \left(\hat{a}^{\dagger}_{k+2k_F,\,\uparrow}\hat{a}_{k,\uparrow} + \hat{a}^{\dagger}_{k+2k_F,\,\downarrow}\hat{a}_{k,\downarrow} \right) + h.c. \right\} + \frac{2N|\Delta|^2}{U}, \tag{2.10}$$

where we have introduced

$$\begin{aligned} \mathbf{\Delta} &= |\Delta| \exp(i\varphi) \\ &= \frac{U}{N} \sum_{k} \langle \hat{\rho}_{2k_F\uparrow} \rangle \\ &= -\frac{U}{N} \sum_{k} \langle \hat{\rho}_{2k_F\downarrow} \rangle, \end{aligned} \tag{2.11}$$

which later would be clear that it is actually the order parameter of the SDW phase. The mean-field Hamiltonian can be diagonalized by means of the Bogolyubov transformation, by introducing the operators as

$$\begin{aligned} \hat{\gamma}_{1k} &= \tilde{M}_k\, \hat{a}_{1k} - \tilde{N}^{*}_{k}\, \hat{a}_{2k} = M_k e^{-i\varphi}\, \hat{a}_{1k} - N_k e^{i\varphi}\, \hat{a}_{2k}, \\ \hat{\gamma}_{2k} &= \tilde{N}_k\, \hat{a}_{1k} + \tilde{M}^{*}_{k}\, \hat{a}_{2k} = N_k e^{-i\varphi}\, \hat{a}_{1k} + M_k e^{i\varphi}\, \hat{a}_{2k}, \end{aligned} \tag{2.12}$$

where coefficients satisfy the relation $M_k^2+N_k^2=1$ to guaranty the canonical transformation of the operators. The subscript 1 and 2 refer to the states close to the k_F and $-k_F$, respectively. Diagonalized Hamiltonian reads

$$H_{MF}=\sum_{k,\sigma}E_k\hat{\gamma}^{\dagger}_{1k,\sigma}\hat{\gamma}_{1k,\sigma}+\sum_{k,\sigma}E_k\hat{\gamma}^{\dagger}_{2k,\sigma}\hat{\gamma}_{2k,\sigma}+\frac{2N|\Delta|^2}{U}, \tag{2.13}$$

with the dispersion relation for the quasi-particles as

$$E_k=\epsilon_k+sign(k-k_F)\sqrt{(\hbar^2k_F^2/m)^2(k-k_F)^2+\Delta^2}. \tag{2.14}$$

The dispersion relation shows a band gap in the single particle excitation. It has to be noted that the dispersion relation of the free system is approximated around the Fermi wavevector in Eq. (2.14) as $\epsilon_k\approx\hbar^2k_F(k-k_F)/m$. We analyze the order parameter $\mathbf{\Delta}$ to understand the nature of broken symmetry and its relation with the observable of the system.

At the first hand, we present the spin density, which in the second quantization takes the form

$$\begin{aligned} S(x) &= \frac{1}{2}\left[\hat{\Psi}^{\dagger}_{\uparrow}(x)\hat{\Psi}_{\uparrow}(x)-\hat{\Psi}^{\dagger}_{\downarrow}(x)\hat{\Psi}_{\downarrow}(x)\right] \\ &= \frac{1}{2}\sum_{k,k'}\left\{\hat{a}^{\dagger}_{k,\uparrow}\hat{a}_{k',\uparrow}-\hat{a}^{\dagger}_{k,\downarrow}\hat{a}_{k',\downarrow}\right\}e^{i(k'-k)x}, \end{aligned} \tag{2.15}$$

where we have used the expansion of the field operator in the plane-wave space as $\hat{\Psi}_{\sigma}(x)=\sum_k\hat{a}_{k,\sigma}exp(ikx)$. As we are interested in the paired states by $q=2k_F$, we single out the couplings with $k'=k\pm2k_F$. The expectation value of Eq. (2.15) reads

$$\begin{aligned} \langle S(x)\rangle &= \frac{1}{2}\sum_k\left\{\langle\hat{a}^{\dagger}_{k,\uparrow}\hat{a}_{k+2k_F,\uparrow}\rangle-\langle\hat{a}^{\dagger}_{k,\downarrow}\hat{a}_{k+2k_F,\downarrow}\rangle\right\}e^{i2k_Fx}+c.c. \\ &= \frac{1}{2}\left\{2|S|e^{i(2k_Fx+\varphi)}+2|S|e^{-i(2k_Fx+\varphi)}\right\} \\ &= 2|S|\cos(2k_Fx+\varphi), \end{aligned} \tag{2.16}$$

that we have introduced the complex parameter as

$$\begin{aligned} \mathbf{S}=|S|e^{i\varphi} &= \sum_k\langle\hat{a}^{\dagger}_{k,\uparrow}\hat{a}_{k+2k_F,\uparrow}\rangle=\langle\hat{\rho}_{2k_F\uparrow}\rangle \\ &= -\sum_k\langle\hat{a}^{\dagger}_{k,\downarrow}\hat{a}_{k+2k_F,\downarrow}\rangle=-\langle\hat{\rho}_{2k_F\downarrow}\rangle. \end{aligned} \tag{2.17}$$

We construct a relation between the order parameter and the spin density as

$$\mathbf{\Delta}=|\Delta|e^{i\varphi}=\frac{U}{N}\mathbf{S}. \tag{2.18}$$

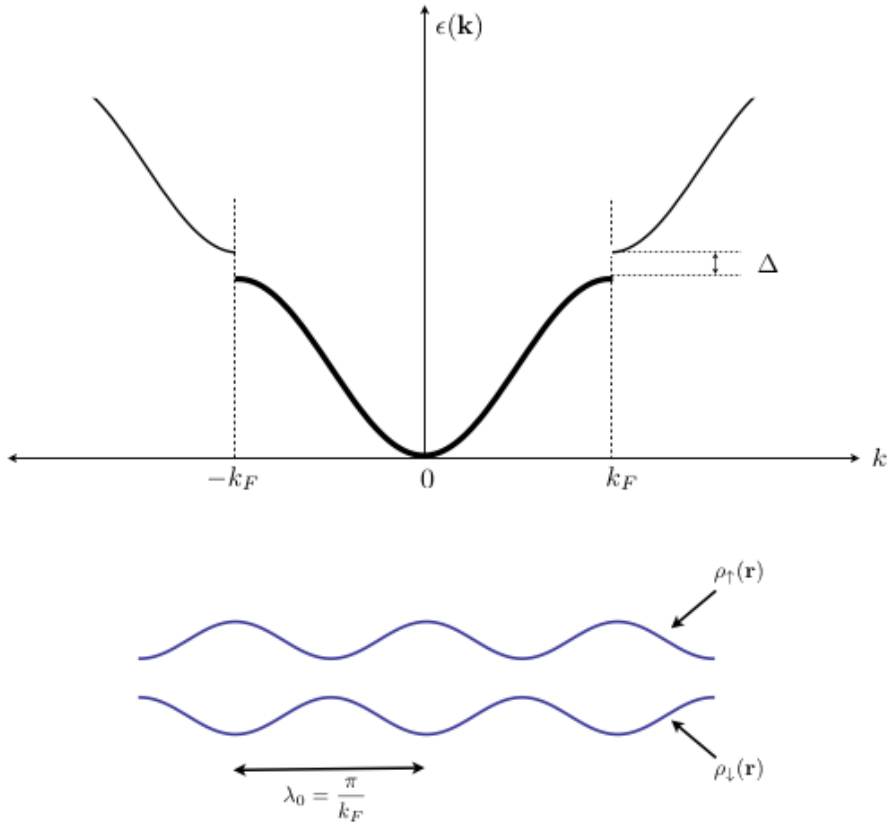

Figure 2.7: The dispersion relation of the spin density wave phase in 1D. The discrete translational symmetry of the SDW phase with a period $\lambda_0 = \pi/k_F$ determined by the Fermi wavevector. The modulation of the spin density wave is shown for two subbands: spin up and spin down density. (The image is reproduced from Ref. [23])

Hence, there is a direct relation between the spin density and order parameter whenever the expectation values $\langle \hat{a}^\dagger_{k,\sigma} \hat{a}_{k+2k_F,\sigma} \rangle$ takes on non-zero value. As the spin density shows a modulation, it is said that the system undergoes a phase transition into spin density wave phase. In the ground state of the SDW phase, both the spin rotational and the translational symmetry of the system are broken and the periodicity of the system being $\lambda_0 = \pi/k_F$. The Fermi surface is entirely removed (in 1D) as is depicted in Fig. 2.7. The SDW ground state can be taken as two charge density wave states, one for spin up and one for spin down that can be written as

$$\begin{aligned} \rho_\uparrow &= \rho_0 \left(1 + \cos\left(2k_F x + \varphi\right)\right), \\ \rho_\downarrow &= \rho_0 \left(1 + \cos\left(2k_F x + \varphi + \pi\right)\right), \end{aligned} \tag{2.19}$$

which is shown in Fig. 2.7. Finally, the ground state can be written as

$$|\Psi_0\rangle = \left(\prod_{|k|<k_F} \hat{\gamma}^\dagger_{1k,\uparrow} \hat{\gamma}^\dagger_{2k,\uparrow} \prod_{|k|<k_F} \hat{\gamma}^\dagger_{1k,\downarrow} \hat{\gamma}^\dagger_{2k,\downarrow} \right) |0\rangle. \tag{2.20}$$

2.3 Superfluidity

We present a brief review of the superfluidity. Actually, we take the terms "superconductivity" and "superconductivity" interchangeable as the microscopic mechanism describing both of these phenomenas is the same: conventional Bardeen-Cooper-Schrieffer (BCS) theory. The following description is adopted from Ref. [3], and it can also be found in more detail in references. [43, 19, 1].

The superfluidity stems from an attractive pairwise interaction which can form a bosonic-like state by coupling states with $\mathbf{k}\uparrow$ and $-\mathbf{k}\downarrow$, known as the Cooper pair. The origin of the attractive interaction between charged particles, in the framework of conventional BCS theory, are due to the exchange of the lattice vibration, so-called phonons. Indeed, the interaction among charged particles, say electrons, can be mediated by means of phonons through electron-phonon coupling. Such effective attractive interaction can be given for states in the vicinity of the Fermi surface as $|\epsilon_{\mathbf{k}} - \epsilon_{\mathbf{k}+\mathbf{q}}| < \delta \sim \omega_D$, where ω_D is the Debye frequency, the phonon characteristic frequency.

Given the existence of such attractive pairwise interaction, we continue by working over a simplified Hamiltonian as

$$H = \sum_{\mathbf{k},\sigma} \epsilon_{\mathbf{k}} \hat{c}^{\dagger}_{\mathbf{k},\sigma} \hat{c}_{\mathbf{k},\sigma} - \frac{g}{L^d} \sum_{\mathbf{k},\mathbf{k}',\mathbf{q}} \hat{c}^{\dagger}_{\mathbf{k}+\mathbf{q}\uparrow} \hat{c}^{\dagger}_{-\mathbf{k}\downarrow} \hat{c}_{-\mathbf{k}'+\mathbf{q}\downarrow} \hat{c}_{\mathbf{k}'\uparrow}, \tag{2.21}$$

where g being a positive constant. This model, which is globally referred as the BCS Hamiltonian, has to be taken as an effective Hamiltonian, which is valid over the thin shell around the Fermi surface as $|\epsilon_{\mathbf{k}} - \epsilon_{k_F}| < \delta/2$ and $|\epsilon_{\mathbf{k}'} - \epsilon_{k_F}| < \delta/2$. To examine the instability of the system described by the Hamiltonian in Eq. (2.21), we observe the fate of the Cooper pairs by means of the four-point correlation function (two-body Green function) as

$$C(\mathbf{q},\tau) = \frac{1}{L^{2d}} \sum_{\mathbf{k},\mathbf{k}'} \langle \hat{\psi}^{\dagger}_{\mathbf{k}+\mathbf{q}\uparrow}(\tau) \hat{\psi}^{\dagger}_{-\mathbf{k}\downarrow}(\tau) \hat{\psi}_{\mathbf{k}'+\mathbf{q}\downarrow}(0) \hat{\psi}_{-\mathbf{k}'\uparrow}(0) \rangle. \tag{2.22}$$

This two-body Green function describes the propagation of a Cooper pair under multiple scattering in an imaginary time τ. The pair states is scattered under the interaction with invariant center-of-mass-momentum like $|\mathbf{k}+\mathbf{q}\uparrow, -\mathbf{k}\downarrow\rangle \rightarrow |\mathbf{k}'+\mathbf{q}\uparrow, -\mathbf{k}'\downarrow\rangle$. Switching to the frequency representation, the correlation function takes the form

$$C(\mathbf{q}) \equiv C(\mathbf{q},\omega_m) = \frac{1}{\beta} \int_0^{\beta} d\tau e^{-i\omega_m \tau} C(\mathbf{q},\tau) = \frac{T^2}{L^{2d}} \sum_{\mathbf{k},\mathbf{k}'} \langle \hat{\psi}^{\dagger}_{\mathbf{k}+\mathbf{q}\uparrow} \hat{\psi}^{\dagger}_{-\mathbf{k}\downarrow} \hat{\psi}_{\mathbf{k}'+\mathbf{q}\downarrow} \hat{\psi}_{-\mathbf{k}'\uparrow} \rangle, \tag{2.23}$$

where $\beta = 1/T$ is the inverse temperature and $\omega_m = 2\pi n/\beta\hbar$ is the bosonic Matsubara frequency (see finite-temperature Green function chapters in for example references [19, 1, 3]). We treat perturbatively to solve the correlation function in Eq. (2.23). Ladder approximation which accounts the Cooper pair propagator in the lowest order, is shown in Fig. 2.8. The vertex part $\Gamma_{\mathbf{q}}$ (the effective interaction), is shown also in a so-called Dyson equation form. By translating the diagrams into an algebraic form we have

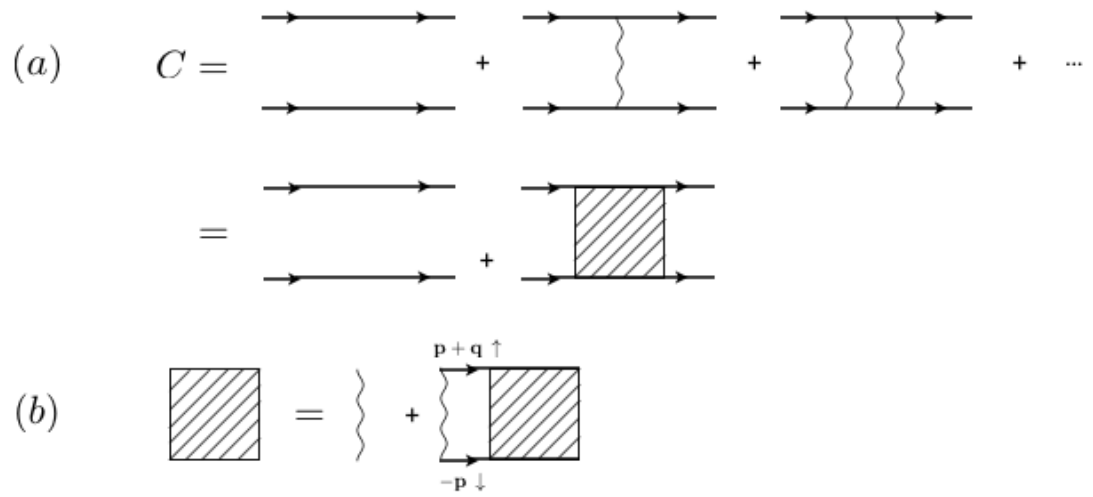

Figure 2.8: The propagation of a Cooper pair in an interacting system. (**a**) Two free Green functions, carry momenta $\mathbf{p}+\mathbf{q}$ and $-\mathbf{p}$, interact by transferring fixed value of momentum $\mathbf{q}$. (**b**) The vertex part of the propagator acts as a effective interaction, and obeys Dyson's equation. (The image is reproduced from Ref. [3])

$$\Gamma_{\mathbf{q}} = g + \frac{gT}{L^d}\sum_{\mathbf{p}} G_{\mathbf{p}+\mathbf{q}} G_{-\mathbf{p}} \Gamma_{\mathbf{q}}. \tag{2.24}$$

We solve Eq. (2.24) for $\Gamma_{\mathbf{q}}$ to obtain

$$\Gamma_{\mathbf{q}} = \frac{g}{1 - \frac{gT}{L^d}\sum_{\mathbf{p}} G_{\mathbf{p}+\mathbf{q}} G_{-\mathbf{p}}}. \tag{2.25}$$

We engage contour integral to calculate the denominator of the Eq. (2.25), by taking into account that the single-body Green function at non-zero temperature is $G_0(\mathbf{p},\, i\omega_m) = 1/(i\omega_m - \zeta_{\mathbf{p}})$ where $\zeta_{\mathbf{p}} = \hbar^2 p^2/2m - \mu$ being the dispersion relation of a free particle subtracted by chemical potential. The sum of momentum and frequency over multiplication of the propagators is written explicitly as

$$\begin{aligned} \frac{T}{L^d}\sum_{\mathbf{p}} G_{\mathbf{p}+\mathbf{q}} G_{-\mathbf{p}} &\equiv \frac{T}{L^d}\sum_{\mathbf{p},n} G_0(\mathbf{p}+\mathbf{q},\, -i\omega_n + i\omega_m) G_0(-\mathbf{p},\, i\omega_n) \\ &= \frac{T}{L^d}\sum_{\mathbf{p},n} \frac{1}{i\omega_n - \zeta_{-\mathbf{p}}} \frac{1}{-i\omega_n + i\omega_m - \zeta_{\mathbf{p}+\mathbf{q}}}. \end{aligned} \tag{2.26}$$

For evaluating the sum over frequency indices, we introduce the following function

$$F(\omega) = \frac{1}{\omega - \zeta_{-\mathbf{p}}} \frac{1}{-\omega + i\omega_m - \zeta_{\mathbf{p}+\mathbf{q}}}.$$

By employing Poisson's formula, we convert the sum to a contour integral

$$\sum_n F(i\omega_n) = \frac{-\beta}{2\pi i}\oint_R d\omega F(\omega) f(\omega), \tag{2.27}$$

where $f(\omega) = (\exp(\beta\omega)+1)^{-1}$ is the Fermi function. The contour is shown in Fig. 2.9 included two simple poles of $F(\omega)$ at $z = i\omega_m - \zeta_{\mathbf{p}+\mathbf{q}}$ and $z = \zeta_{-\mathbf{p}}$, and poles of $f(\omega)$ which are all along the imaginary axis at $i\omega_n$, where for fermionic propagator we have $i\omega = (i\pi/\beta)(2n+1)$ with $n = 0, \pm1, \pm2, \pm3\cdots$. There are two contour which we denote them by R and R'. The integral around contour R' is equal to the sum of the residues containing poles on the imaginary axis plus two residues of $F(\omega)$. Since the contour integral around R' vanishes when $R' \to \infty$, we have

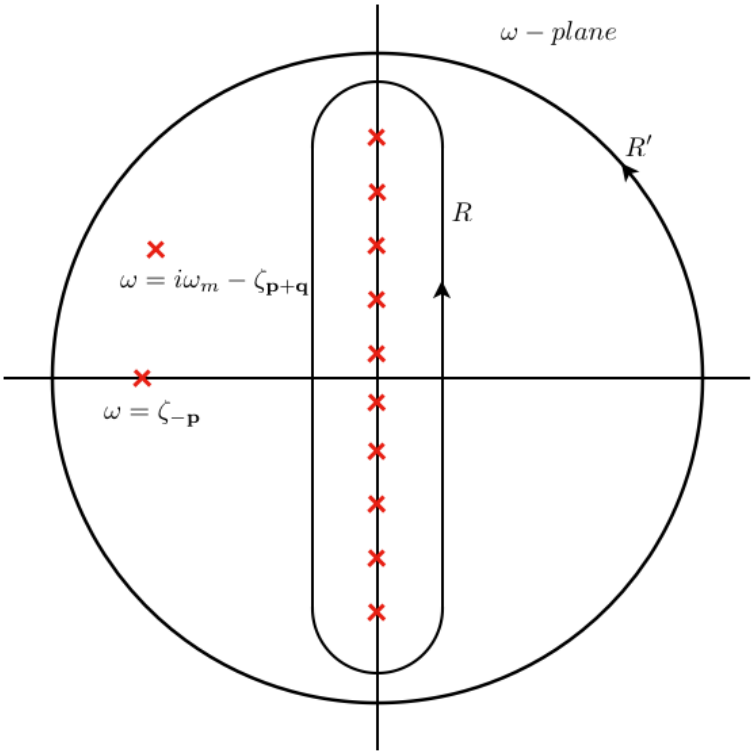

Figure 2.9: The contours which is used in the finite temperature calculations of two-body propagator. Two simple poles of $F(\omega)$ at $\omega = i\omega_m - \zeta_{\mathbf{p}+\mathbf{q}}$ and $\omega = \zeta_{-\mathbf{p}}$ are shown. The poles of $f(\omega)$ are along the imaginary axis.

$$\oint_{R'} = 0 = \oint_R d\omega F(\omega) f(\omega) + 2\pi i \sum \mathbf{Res}\, F(\omega) f(\omega)|_{\omega=\zeta_{-\mathbf{p}}, \omega=i\omega_m-\zeta_{\mathbf{p}+\mathbf{q}}},$$

We have the result of the sum by using the relation in Eq. (2.27), which reads

$$\frac{1}{\beta}\sum_n F(i\omega_n) = \sum \mathbf{Res}\, F(\omega) f(\omega)|_{\omega=\zeta_{-\mathbf{p}}, \omega=i\omega_m-\zeta_{\mathbf{p}+\mathbf{q}}}.$$

The residues can be readily evaluated as

$$\begin{aligned} \mathbf{Res}\, F(\omega)f(\omega)|_{\omega=\zeta_{-\mathbf{p}}} &= \frac{f(\zeta_{\mathbf{p}})}{i\omega_m - \zeta_{\mathbf{p}} - \zeta_{\mathbf{p+q}}}, \\ \mathbf{Res}\, F(\omega)f(\omega)|_{\omega=i\omega_m-\zeta_{\mathbf{p+q}}} &= \frac{f(i\omega_m - \zeta_{\mathbf{p+q}})}{i\omega_m - \zeta_{\mathbf{p}} - \zeta_{\mathbf{p+q}}}. \end{aligned} \tag{2.28}$$

We write down the sum in Eq. (2.31) by engaging Eq. (2.28) and the relation of the Fermi function as $f(i\omega_m - \zeta_{\mathbf{p+q}}) = f(\zeta_{\mathbf{p+q}}) - 1$ as

$$\frac{T}{L^d}\sum_{\mathbf{p},n} G_0(\mathbf{p}+\mathbf{q},\, -i\omega_n + i\omega_m)G_0(-\mathbf{p},\, i\omega_n) = \frac{1}{L^d}\sum_{p}\frac{1 - f(\zeta_{\mathbf{p+q}}) - f(\zeta_{\mathbf{p}})}{i\omega_m + \zeta_{\mathbf{p}} + \zeta_{\mathbf{p+q}}}. \tag{2.29}$$

We calculate the sum for the special case of $\mathbf{q} = (0,0)$ by taking the system as a spatially homogeneous and also the static configuration of the pairs $\omega_m = 0$. Replacing the sum over momentum by energy integral, and remembering the interval of validity of the attractive interaction, we obtain

$$\frac{T}{L^d}\sum G_{\mathbf{p}}G_{-\mathbf{p}} = \int_{-\omega_D}^{\omega_D} d\epsilon \nu^d(\epsilon)\frac{1-2f(\epsilon)}{2\epsilon} \approx \nu^d(\epsilon_F)\int_T^{\omega_D}\frac{d\epsilon}{\epsilon} = \nu^d(\epsilon_F)\ln\Big(\frac{\omega_D}{T}\Big), \tag{2.30}$$

where for a narrow vicinity of the Fermi surface, we have replaced the density of state by its value on the Fermi energy $\nu^d(\epsilon_F)$. Replacing the result into the vertex function, we obtain the result

$$\Gamma_{\mathbf{q}} = \frac{g}{1 - g\nu^d(\epsilon_F)\ln\left(\frac{\omega_D}{T}\right)}. \tag{2.31}$$

We see that even a weak attractive interaction $g \ll 1$ can contribute to the divergent of the pair formation. Hence, the system is unstable versus to the superconductivity. The critical temperature could be obtained by examining the condition where vertex function develops a singularity that leads to

$$T_c = \omega_D \exp\left[-\frac{1}{g\nu}\right], \tag{2.32}$$

which marks the transition temperature to the superconducting state.

We saw that below the critical temperature T_c, a macroscopic number of Cooper pairs would exist within the system. Thus, we decompose the pair of operators into the average value of Cooper pairs and the fluctuations around it. we write

$$\begin{aligned} \hat{c}^\dagger_{\mathbf{k}\uparrow}\hat{c}^\dagger_{-\mathbf{k}\downarrow} &= \langle \hat{c}^\dagger_{\mathbf{k}\uparrow}\hat{c}^\dagger_{-\mathbf{k}\downarrow}\rangle + \left(\hat{c}^\dagger_{\mathbf{k}\uparrow}\hat{c}^\dagger_{-\mathbf{k}\downarrow} - \langle \hat{c}^\dagger_{\mathbf{k}\uparrow}\hat{c}^\dagger_{-\mathbf{k}\downarrow}\rangle\right), \\ \hat{c}_{-\mathbf{k}\downarrow}\hat{c}_{\mathbf{k}\uparrow} &= \langle \hat{c}_{-\mathbf{k}\downarrow}\hat{c}_{\mathbf{k}\uparrow}\rangle + \left(\hat{c}_{-\mathbf{k}\downarrow}\hat{c}_{\mathbf{k}\uparrow} - \langle \hat{c}_{-\mathbf{k}\downarrow}\hat{c}_{\mathbf{k}\uparrow}\rangle\right). \end{aligned}$$

Such decomposition of the operators reveals the order nature of the superconductivity. In the normal phase $\langle \hat{c}^\dagger_{\mathbf{k}\uparrow}\hat{c}^\dagger_{-\mathbf{k}\downarrow}\rangle = \langle \hat{c}_{-\mathbf{k}\downarrow}\hat{c}_{\mathbf{k}\uparrow}\rangle = 0$. On the other hand, when this expectation value takes on non-zero value, it implies the existence of the macroscopic number of Cooper pairs within the system: superconducing state. Inserting those mean-field decompositions in the interaction term of Hamiltonian and neglecting terms quadratic in the fluctuations, we write

$$\begin{aligned}
\hat{c}^\dagger_{\mathbf{k}\uparrow}\hat{c}^\dagger_{-\mathbf{k}\downarrow}\hat{c}_{-\mathbf{k}'\downarrow}\hat{c}_{\mathbf{k}'\uparrow} &\approx \langle \hat{c}^\dagger_{\mathbf{k}\uparrow}\hat{c}^\dagger_{-\mathbf{k}\downarrow}\rangle\langle \hat{c}_{-\mathbf{k}'\downarrow}\hat{c}_{\mathbf{k}'\uparrow}\rangle \\
&+ \langle \hat{c}^\dagger_{\mathbf{k}\uparrow}\hat{c}^\dagger_{-\mathbf{k}\downarrow}\rangle \left(\hat{c}_{-\mathbf{k}'\downarrow}\hat{c}_{\mathbf{k}'\uparrow} - \langle \hat{c}_{-\mathbf{k}'\downarrow}\hat{c}_{\mathbf{k}'\uparrow}\rangle\right) \\
&+ \left(\hat{c}^\dagger_{\mathbf{k}\uparrow}\hat{c}^\dagger_{-\mathbf{k}\downarrow} - \langle \hat{c}^\dagger_{\mathbf{k}\uparrow}\hat{c}^\dagger_{-\mathbf{k}\downarrow}\rangle\right)\langle \hat{c}_{-\mathbf{k}'\downarrow}\hat{c}_{\mathbf{k}'\uparrow}\rangle \\
&= \hat{c}^\dagger_{\mathbf{k}\uparrow}\hat{c}^\dagger_{-\mathbf{k}\downarrow}\langle \hat{c}_{-\mathbf{k}'\downarrow}\hat{c}_{\mathbf{k}'\uparrow}\rangle + \hat{c}_{-\mathbf{k}'\downarrow}\hat{c}_{\mathbf{k}'\uparrow}\langle \hat{c}^\dagger_{\mathbf{k}\uparrow}\hat{c}^\dagger_{-\mathbf{k}\downarrow}\rangle - \langle \hat{c}_{-\mathbf{k}'\downarrow}\hat{c}_{\mathbf{k}'\uparrow}\rangle\langle \hat{c}^\dagger_{\mathbf{k}\uparrow}\hat{c}^\dagger_{-\mathbf{k}\downarrow}\rangle.
\end{aligned}$$

Therefore the BCS Hamiltonian after adding the chemical potential becomes

$$H - \mu\hat{N} \approx \sum_{\mathbf{k},\,\sigma}\left[\zeta_{\mathbf{k}}\hat{c}^\dagger_{\mathbf{k},\,\sigma}\hat{c}_{\mathbf{k},\,\sigma} - \left(\Delta^*\hat{c}_{-\mathbf{k}\downarrow}\hat{c}_{\mathbf{k}\uparrow} + \Delta\hat{c}^\dagger_{\mathbf{k}\uparrow}\hat{c}^\dagger_{-\mathbf{k}\downarrow}\right)\right] + \frac{L^d|\Delta|^2}{g}.$$

We have defined the order parameter as

$$\Delta = \frac{g}{L^d}\sum_{\mathbf{k}}\langle\Omega_s|\hat{c}_{-\mathbf{k}\downarrow}\hat{c}_{\mathbf{k}\uparrow}|\Omega_s\rangle = \frac{g}{L^d}\left(\sum_{\mathbf{k}}\langle\Omega_s|\hat{c}^\dagger_{\mathbf{k}\uparrow}\hat{c}^\dagger_{-\mathbf{k}\downarrow}|\Omega_s\rangle\right)^*, \tag{2.33}$$

where the expectation values are taken at the ground state of superconducting phase. By writing the operators in the Nambu spinor representation, we attempt to diagonalize the mean-field Hamiltonian as

$$\hat{\Psi}^\dagger_{\mathbf{k}} = \left(\hat{c}^\dagger_{\mathbf{k}\uparrow},\, \hat{c}_{-\mathbf{k}\downarrow}\right),\ \hat{\Psi}_{\mathbf{k}} = \begin{pmatrix} \hat{c}_{\mathbf{k}\uparrow} \\ \hat{c}^\dagger_{-\mathbf{k}\downarrow} \end{pmatrix},$$

and the Hamiltonian reads as

$$H - \mu\hat{N} = \sum_{\mathbf{k}}\hat{\Psi}^\dagger_{\mathbf{k}}\begin{pmatrix} \zeta_{\mathbf{k}} & -\Delta \\ -\Delta & -\zeta_{\mathbf{k}} \end{pmatrix}\hat{\Psi}_{\mathbf{k}} + \sum_{\mathbf{k}}\zeta_{\mathbf{k}} + \frac{L^d|\Delta|^2}{g}. \tag{2.34}$$

Now by canonical transformation of the Nambu operators, under which the anti-commutation relation of the fermionic operators are left invariant, the mean-field Hamiltonian can be brought to a diagonal form. We write the unitary transformation of the operators as

$$\hat{\chi}_{\mathbf{k}} \equiv \begin{pmatrix} \hat{\alpha}_{\mathbf{k}\uparrow} \\ \hat{\alpha}^\dagger_{-\mathbf{k}\downarrow} \end{pmatrix} = \begin{pmatrix} \cos\theta_{\mathbf{k}} & \sin\theta_{\mathbf{k}} \\ \sin\theta_{\mathbf{k}} & -\cos\theta_{\mathbf{k}} \end{pmatrix}\begin{pmatrix} \hat{c}_{\mathbf{k}\uparrow} \\ \hat{c}^\dagger_{-\mathbf{k}\downarrow} \end{pmatrix} \equiv U_{\mathbf{k}}\hat{\Psi}_{\mathbf{k}}.$$

We set $\tan(2\theta_{\mathbf{k}}) = -\Delta/\zeta_{\mathbf{k}}$ by putting $\cos(2\theta_{\mathbf{k}}) = \zeta_{\mathbf{k}}/\lambda_{\mathbf{k}}$ and $\sin(2\theta_{\mathbf{k}}) = -\Delta_{\mathbf{k}}/\lambda_{\mathbf{k}}$, where the dispersion relation of the quasi-particles can be obtained as

$$\lambda_{\mathbf{k}} = (\Delta_{\mathbf{k}}^2 + \zeta_{\mathbf{k}}^2)^{1/2}. \tag{2.35}$$

The diagonalized Hamiltonian reads

$$H - \mu\hat{N} = \sum_{\mathbf{k},\,\sigma} \lambda_{\mathbf{k}} \hat{\alpha}_{\mathbf{k}\sigma}^{\dagger} \hat{\alpha}_{\mathbf{k}\sigma} + \sum_{\mathbf{k}} (\zeta_{\mathbf{k}} - \lambda_{\mathbf{k}}) + \frac{\Delta^2 L^d}{g}. \tag{2.36}$$

The dispersion relation for quasi-particles excitation shows a energy gap which removed the Fermi surface entirely. The ground state of the superconducting state reads

$$|\Omega_s\rangle \equiv \prod_{\mathbf{k}} \hat{\alpha}_{\mathbf{k}\uparrow}^{\dagger} \hat{\alpha}_{-\mathbf{k}\downarrow}^{\dagger} |0\rangle \sim \prod_{\mathbf{k}} \left(\cos\theta_{\mathbf{k}} - \sin\theta_{\mathbf{k}} \hat{c}_{\mathbf{k}\uparrow}^{\dagger} \hat{c}_{-\mathbf{k}\downarrow}^{\dagger} \right) |0\rangle. \tag{2.37}$$

Finally, by solving Eq. (2.33) self-consistently we obtain the order parameter as

$$\begin{aligned} \Delta &= \frac{g}{L^d} \sum_{\mathbf{k}} \langle \Omega_s | \hat{c}_{-\mathbf{k}\downarrow} \hat{c}_{\mathbf{k}\uparrow} | \Omega_s \rangle = -\frac{g}{L^d} \sum_{\mathbf{k}} \sin\theta_{\mathbf{k}} \cos\theta_{\mathbf{k}} = \frac{g}{2L^d} \sum_{\mathbf{k}} \frac{\Delta}{(\Delta^2 + \zeta_{\mathbf{k}}^2)^{1/2}} \\ &\approx \frac{g\Delta}{2} \int_{-\omega_D}^{\omega_D} \frac{\nu(\zeta) d\zeta}{(\Delta^2 + \zeta^2)^{1/2}} = g\Delta \sinh^{-1}(\omega_D/\Delta), \end{aligned} \tag{2.38}$$

We have assumed that in the low-energy pairing and also in the vicinity of critical point, the order parameter can be taken momentum-independent. Solving the relation for Δ in the extreme limit $g\nu \ll 1$ we obtain

$$\Delta = \frac{\omega_D}{\sinh(1/g\nu)} \approx 2\omega_D \exp\left(-\frac{1}{g\nu}\right). \tag{2.39}$$

Comparing the explicit form of the order parameter with one we have achieved for the critical temperature in Eq. (2.32), we observe a relation between the order parameter at $T = 0$ and the critical temperature

$$\Delta \approx 2T_C. \tag{2.40}$$

Chapter 3

Spin density wave

In the preceding chapter, the dressed Born-Oppenheimer potential for the bilayer system has been presented. Our starting point would be the investigation of the instability of the system versus spin density wave (SDW) phase. In the following chapter, two methods for analyzing the instability would be presented. In the first approach, we add an external field coupled with the spin density and examine the response of the system in the mean-field theory regime. In the second, we use random phase approximation (RPA) in the many body field theory framework. Indeed, the both approaches stay in the limit of the weakly interacting system.

3.1 Hamiltonian for interlayer interaction

The Hamiltonian in the second quantization, including the intralayer and the interlayer interaction, is presented in Eq. (2.5). In this chapter, we are interested in the instabilities that is induced by the interlayer interaction. The effect of the intralayer interaction can be found in [29, 13]. It is shown in Ref. [29] that by tuning the external parameters of the system, it is possible to substantially suppress the intralayer instability. In the next chapter, we take the intralayer interaction to renormalize the parameters of the system. By the way, the Hamiltonian for the interlayer interaction *i.e.* the interaction of the particles in different layers reads

$$H = \sum_{\substack{\mathbf{k} \\ \lambda=1,2}} \left[\varepsilon(\mathbf{k}) - \mu_\lambda\right] c^\dagger_{\mathbf{k}\lambda}\, c_{\mathbf{k}\lambda} + \frac{1}{L^2} \sum_{\mathbf{q},\mathbf{k},\mathbf{k}'} \tilde{V}(\mathbf{q})\, c^\dagger_{\mathbf{k}+\mathbf{k}\lambda}\, c^\dagger_{\mathbf{k}'-\mathbf{q}\lambda'}\, c_{\mathbf{k}'\lambda'}\, c_{\mathbf{k}\lambda}, \tag{3.1}$$

where $c^\dagger_{\boldsymbol{k}\lambda}$ and $c_{\boldsymbol{k}\lambda}$ are fermionic creation and annihilation operators for a molecule with momentum $\boldsymbol{k}$ in layer λ. The first term sums the kinetic energy of the molecules $\varepsilon(\boldsymbol{k}) = \frac{\hbar^2 \boldsymbol{k}^2}{2m}$ with mass m, in both layers including the chemical potential for each layer. We restrict the calculations into zero-temperature $T = 0$. Therefore, the chemical potential is equal to the Fermi energy $\varepsilon^\lambda_F = \mu_\lambda$. The second sum counts the interaction of the particles in different layer $\lambda \neq \lambda'$. The particles interact by means of the potential $\tilde{V}(q)$ which is given as

$$\begin{aligned} \tilde{V}(q) &= \int d^2_{eff}\, \frac{(l^2 - r^2/2)}{(l^2 + r^2)^{5/2}}\, e^{-i\mathbf{q}.\mathbf{r}}\, d\mathbf{r} \\ &= \pi\, d^2_{eff}\; q\; \exp\left(-lq\right), \end{aligned} \tag{3.2}$$

where d_{eff} being the effective dipole moments of the molecules introduced in previous chapter, and l stands for layers separation.

The particles are confined in two layers. For such two states system, it is convenient to introduce the pseudospin-1/2 operator $2\,\hat{\mathbf{m}}_i = \hbar\, c^\dagger_{i\lambda}\, \boldsymbol{\sigma}_{\lambda\lambda'}\, c_{i\lambda'}$, where $\boldsymbol{\sigma}$ denotes the Pauli spin matrices belongs to particle i. The molecules in layer 1 and 2 will be represented by spinors $|\uparrow\rangle$ and $|\downarrow\rangle$, respectively. Therefore the Hamiltonian in Eq. (3.1) takes the form

$$H = \sum_{\substack{\boldsymbol{k}\\ \lambda=\uparrow\downarrow}} \left[\varepsilon(\boldsymbol{k}) - \mu_\lambda\right] c^\dagger_{\boldsymbol{k}\lambda}\, c_{\boldsymbol{k}\lambda} + \frac{1}{L^2} \sum_{\boldsymbol{q},\boldsymbol{k},\boldsymbol{k}'} \tilde{V}(\boldsymbol{q})\, c^\dagger_{\boldsymbol{k}+\boldsymbol{q}\uparrow}\, c^\dagger_{\boldsymbol{k}'-\boldsymbol{q}\downarrow}\, c_{\boldsymbol{k}'\downarrow}\, c_{\boldsymbol{k}\uparrow}\,. \tag{3.3}$$

In the normal state, given the unitary density of particle in both layers $n_1 = n_2 = n_0$, there would be no magnetization *i.e.* $\mathbf{M} = \langle\psi_N| \sum_i \hat{\mathbf{m}}_i |\psi_N\rangle = 0$. It implies the paramagnetic state *i.e.* absent of the interlayer correlations. The ground state of the normal phase is given by filling the lowest energy state up to the Fermi energy for either spin

$$|\psi_N\rangle = \prod_{|\boldsymbol{k}|<k_F} c^\dagger_{\boldsymbol{k}\uparrow} \prod_{|\boldsymbol{k}'|<k_F} c^\dagger_{\boldsymbol{k}'\downarrow}|0\rangle. \tag{3.4}$$

Before proceeding further, it is worthwhile to rearrange the Hamiltonian in Eq. (3.3) to obtain a concise form. Noticing that there are two pair of operators which act over the different space, spin-up and spin-down states, it is possible to exchange the operators in the interaction term without producing any extra terms due to anticommutation relation of fermionic operators

$$H = \underbrace{\sum_{\substack{\mathbf{k}\\ \lambda=\uparrow\downarrow}} \left[\varepsilon(\mathbf{k}) - \mu_\lambda\right] c^\dagger_{\mathbf{k}\lambda}\, c_{\mathbf{k}\lambda}}_{H_0} + \frac{1}{L^2} \sum_{\mathbf{q},\mathbf{k},\mathbf{k}'} \tilde{V}(\mathbf{q})\, c^\dagger_{\mathbf{k}+\mathbf{q}\uparrow}\, c_{\mathbf{k}\uparrow}\, c^\dagger_{\mathbf{k}'-\mathbf{q}\downarrow}\, c_{\mathbf{k}'\downarrow}. \tag{3.5}$$

By calling the kinetic part H_0 and introducing the density operator as

$$\rho_{\mathbf{q}\lambda} \;=\; \sum_k c^\dagger_{\mathbf{k}+\mathbf{q}\lambda}\, c_{\mathbf{k}\lambda}. \tag{3.6}$$

the Hamiltonians reads

$$H = H_0 + \frac{1}{L^2} \sum_{\mathbf{q}} \tilde{V}_{\mathbf{q}}\, \rho_{\mathbf{q}\uparrow}\, \rho_{-\mathbf{q}\downarrow}. \tag{3.7}$$

3.2 Instability versus spin density wave phase

In the following section, we examine the instability of the system to the SDW phase by means of two different method: Linear response theory and RPA method. Both approach are restricted within the weakly interacting system.

3.2.1 Mean-field instability

In the preceding section, the Hamiltonian in the pseudospin representation have been derived. We are ready to examine the stability of the system against the SDW phase. We are interested in the response of the system to an external field which is coupled to the spin density of the system

$$H = H_0 + \frac{1}{L^2}\sum_{\mathbf{q}} \tilde{V}_{\mathbf{q}}\, \rho_{\mathbf{q}\uparrow}\, \rho_{-\mathbf{q}\downarrow} + \sum_{\mathbf{q}} h_{\mathbf{q}}\, (\rho_{\mathbf{q}\uparrow} - \rho_{\mathbf{q}\downarrow}). \tag{3.8}$$

First of all, we decompose the density operator into its mean value (mean-field) and the fluctuations around the mean-value

$$\begin{aligned} \rho_{\boldsymbol{q}\lambda} &= \langle \rho_{\boldsymbol{q}\lambda} \rangle + (\rho_{\boldsymbol{q}\lambda} - \langle \rho_{\boldsymbol{q}\lambda} \rangle) \\ &= \langle \rho_{\boldsymbol{q}\lambda} \rangle + \delta\rho_{\boldsymbol{q}\lambda}, \end{aligned} \tag{3.9}$$

where the mean-value of the operator are taken at the ground state of the normal phase. We continue by neglecting the terms in the second order in the fluctuation terms $\delta\rho_{\boldsymbol{q}\lambda}\delta\rho_{-\boldsymbol{q}-\lambda}$ as

$$\begin{aligned} H &= H_0 + \frac{1}{L^2}\sum_{\boldsymbol{q}} \tilde{V}_{\boldsymbol{q}}\, (\langle \rho_{\boldsymbol{q}\uparrow} \rangle + \delta\rho_{\boldsymbol{q}\uparrow})\, (\langle \rho_{-\boldsymbol{q}\downarrow} \rangle + \delta\rho_{-\boldsymbol{q}\downarrow}) + \sum_{\boldsymbol{q}} h_{\boldsymbol{q}}\, (\rho_{\boldsymbol{q}\uparrow} - \rho_{\boldsymbol{q}\downarrow}) \\ &\simeq \underbrace{H_0 - \frac{1}{L^2}\sum_{\boldsymbol{q}} \tilde{V}_{\boldsymbol{q}}\, \langle \rho_{\boldsymbol{q}\uparrow} \rangle\, \langle \rho_{-\boldsymbol{q}\downarrow} \rangle}_{H_0'} + \frac{1}{L^2}\sum_{\boldsymbol{q}} \tilde{V}_{\boldsymbol{q}}\, (\rho_{\boldsymbol{q}\uparrow}\, \langle \rho_{-\boldsymbol{q}\downarrow} \rangle + \rho_{-\boldsymbol{q}\downarrow}\, \langle \rho_{\boldsymbol{q}\downarrow} \rangle) + \sum_{\boldsymbol{q}} h_{\boldsymbol{q}}\, (\rho_{\boldsymbol{q}\uparrow} - \rho_{\boldsymbol{q}\downarrow}) \\ &= H_0' + \sum_{\boldsymbol{q}} \{\rho_{\boldsymbol{q}\uparrow}\, (\frac{\tilde{V}_{\boldsymbol{q}}}{L^2}\, \langle \rho_{-\boldsymbol{q}\downarrow} \rangle + h_{\boldsymbol{q}}) + \rho_{\boldsymbol{q}\downarrow}\, (\frac{\tilde{V}_{\boldsymbol{q}}}{L^2}\, \langle \rho_{-\boldsymbol{q}\uparrow} \rangle - h_{\boldsymbol{q}})\} \\ &= H_0' + \underbrace{\sum_{\boldsymbol{q}} (\rho_{\boldsymbol{q}\uparrow} + \rho_{\boldsymbol{q}\downarrow})\, \frac{\tilde{V}_{\boldsymbol{q}} \langle \rho_{-\boldsymbol{q}\uparrow} + \rho_{-\boldsymbol{q}\downarrow} \rangle}{2L^2}}_{\varphi_{ch}^{ext}} + \underbrace{\sum_{\boldsymbol{q}} (\rho_{\boldsymbol{q}\uparrow} - \rho_{\boldsymbol{q}\downarrow}) (h_{\boldsymbol{q}} - \frac{\tilde{V}_{\boldsymbol{q}} \langle \rho_{-\boldsymbol{q}\uparrow} - \rho_{-\boldsymbol{q}\downarrow} \rangle}{2L^2})}_{\varphi_{s}^{ext}}, \end{aligned} \tag{3.10}$$

where the symmetry of the interaction $\tilde{V}_{\boldsymbol{q}} = \tilde{V}_{-\boldsymbol{q}}$ has been used in the third line. It is now apparent that the effect of the weak interaction term is reduced to a external fields. One of these external fields is coupled with the charge density $(\rho_{\boldsymbol{q}\uparrow} + \rho_{\boldsymbol{q}\downarrow})$ and the other is coupled to the spin density $(\rho_{\boldsymbol{q}\uparrow} - \rho_{\boldsymbol{q}\downarrow})$. The H_0' term contains unperturbed Hamiltonian plus a constant term. Therefore, we look to the induced density in the free system as a consequence of the external fields.

Upon the linear response theory (see App. A), it is possible to figure out the charge and spin density induced by external field. First, we examine the induced charge density in the system. The induced density is proportional to the external field times the response function χ_0 as

$$\rho^{ind} = \langle \rho_{\boldsymbol{q}\uparrow} + \rho_{\boldsymbol{q}\downarrow} \rangle = \chi_0(\boldsymbol{q})\, \varphi_{ch}^{ext} = \chi_0(\boldsymbol{q})\, \frac{\tilde{V}_{\boldsymbol{q}} \langle \rho_{\boldsymbol{q}\uparrow} + \rho_{\boldsymbol{q}\downarrow} \rangle}{2L^2}, \tag{3.11}$$

where we have used the hermiticity of the charge density operator $\langle \rho_{\boldsymbol{q}\uparrow} + \rho_{\boldsymbol{q}\downarrow} \rangle = \langle \rho_{-\boldsymbol{q}\uparrow} + \rho_{-\boldsymbol{q}\downarrow} \rangle$. There is no instability in the charge density and even there is not any induced charge density in the system by means of the external field coupled with spin density of the system. It has to be noted that charge density has to be zero, if Eq. (3.11) has to be valid. It is plausible intuitively, as the filed coupled with spin density cannot induced charge density.

Now, we turn to the spin density induced in the system. The response function $\chi_0(\boldsymbol{q})$ of a system for an external field coupled either to the spin density or charge density has the same form if the polarized particles have in common dispersion relation $\epsilon_{\boldsymbol{k}\uparrow} = \epsilon_{\boldsymbol{k}\downarrow}$. So, the induced spin density reads

$$\begin{aligned} S^{ind} &= \langle \rho_{\boldsymbol{q}\uparrow} - \rho_{\boldsymbol{q}\downarrow} \rangle = \chi_0(\boldsymbol{q})\, \varphi_s^{ext} = \chi_0(\boldsymbol{q})\, (h_{\boldsymbol{q}} - \frac{\tilde{V}_{\boldsymbol{q}} \langle \rho_{\boldsymbol{q}\uparrow} - \rho_{\boldsymbol{q}\downarrow} \rangle}{2L^2}), \\ \Rightarrow \quad S^{ind} &= \frac{\chi_0(\boldsymbol{q})\, h_{\boldsymbol{q}}}{1 + \frac{\chi_0(\boldsymbol{q})\, \tilde{V}_{\boldsymbol{q}}}{2\, L^2}}. \end{aligned} \tag{3.12}$$

If the denominator of the expression in Eq. (3.12) vanishes, then even for extremely weak external field $h_q \to 0$ there is a finite induced spin density within the system. Actually, it means that just an small fluctuations caused by interaction of the particle is enough to diverge the redistribution of the spin density of the system. The divergent of S^{ind} defines the instability condition as

$$\frac{\chi_0(\boldsymbol{q})\, \tilde{V}_{\boldsymbol{q}}}{L^2} = -2. \tag{3.13}$$

We examine the circumstances which satisfy Eq. (3.13). The response function introduced in App. A. The response function of a 2D system reads

$$\chi_0(\boldsymbol{q}) = -2\, \omega(E) \begin{cases} 1 & |q| \leq 2k_F, \\ \\ 1 - \sqrt{1 - (\frac{2\, k_F}{|\boldsymbol{q}|})^2} & |\boldsymbol{q}| > 2k_F, \end{cases} \tag{3.14}$$

in which $\omega(E)$ is the density of state per spin which is independent of the energy in two dimension. The density of state in 2D is $\omega(E) = \frac{m\, L^2}{2\, \pi\, \hbar^2}$, where L^2 is the surface of system and k_F is the Fermi wavevector. By negative sign of the response function (3.14) and permanent positive sign of the potential in k-space (see Eq. (3.2)), the equality in Eq. (3.13) can be satisfied. This instability of the spin-density-redistribution could be a sign of the phase transition of the system to spin density wave phase. Later, we compare the ground state energy of the system in both phase to check the phase transition possibility.

We obtain the instability equation explicitly as

$$\begin{aligned} & -2\, \omega(E)\, f(x)\, \frac{\tilde{V}_{\boldsymbol{q}}}{L^2} = -2 \\ \Rightarrow \quad & -2\, \frac{m\, L^2}{2\, \pi\, \hbar^2}\, f(x)\, \pi\, d_{eff}^2\, 2\, k_F\, x\, \exp\left(-2\, k_F\, lx\right) = -2, \end{aligned} \tag{3.15}$$

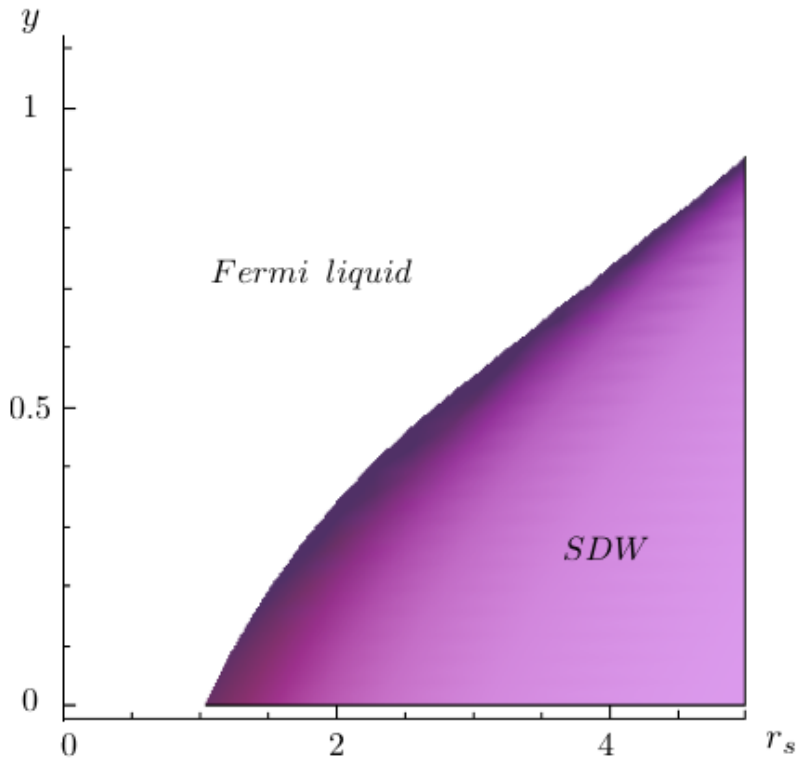

Figure 3.1: Instability of the Fermi liquid versus SDW as function of $y = lk_F$ and $r_s = md_{eff}^2 k_F/\hbar^2$.

where we have defined the dimensionless function

$$f(x) \equiv \frac{\chi_0(\boldsymbol{q})}{-2\,\omega(E)} = \begin{cases} 1 & x = \frac{|q|}{2k_F} \leq 1, \\ \\ 1 - \sqrt{1 - x^{-2}} & x = \frac{|q|}{2k_F} > 1, \end{cases} \tag{3.16}$$

and the dimensionless parameters are

$$\begin{cases} r_s = \frac{d_{eff}^2\, m\, k_F}{\hbar^2}, \\ \\ y = k_F\, l, \end{cases} \tag{3.17}$$

which r_s characterizes the strength of the dipole-dipole interaction and y measures the interlayer separation in the scale of the interparticle distance $\propto k_F$. The instability condition in Eq. (3.15), by means of the dimensionless parameters, takes the form

$$r_s\, x\, \exp\left(-2\, x\, y\right) f(x) \,= 1. \tag{3.18}$$

The phase diagram corresponds to the instability condition in Eq. (3.18) is shown in Fig. 3.1 as a function of y and r_s. One step further, we can show the critical points as a function of x and y. We minimize the r_s as a function of x to see the threshold of the instability (critical

points) with respect to x versus y. The function $f(x)$ in Eq. (3.18) has two parts, which are defined in Eq. (3.16). It can be readily obtained that r_s has a extremum point at $x = 1$ for all value of y as it increases monotonically for for $x \geqslant 1$. But for $x < 1$, there is a permanent minimum at $x = \frac{1}{2y}$. Owing to the regime of this part for $2y \leq 1$, the minimum lays out of the range of the regime as $x_{min} \geq 1$. Thus, for $2y \leq 1$ the minimum of this part emerged also at $x = 1$; and for $2y > 1$ it is placed at $x = \frac{1}{2y}$. We can show the threshold of the instability as a function of y and x as

$$x = \frac{q}{2k_F} = \begin{cases} 1 & y \leq \frac{1}{2}, \\ 1/2y & y > \frac{1}{2}, \end{cases} \tag{3.19}$$

which is depicted in Fig. 3.2. It is worthwhile to note that instability as a function of x and y appears just for $x \leq 1$ as all value of y.

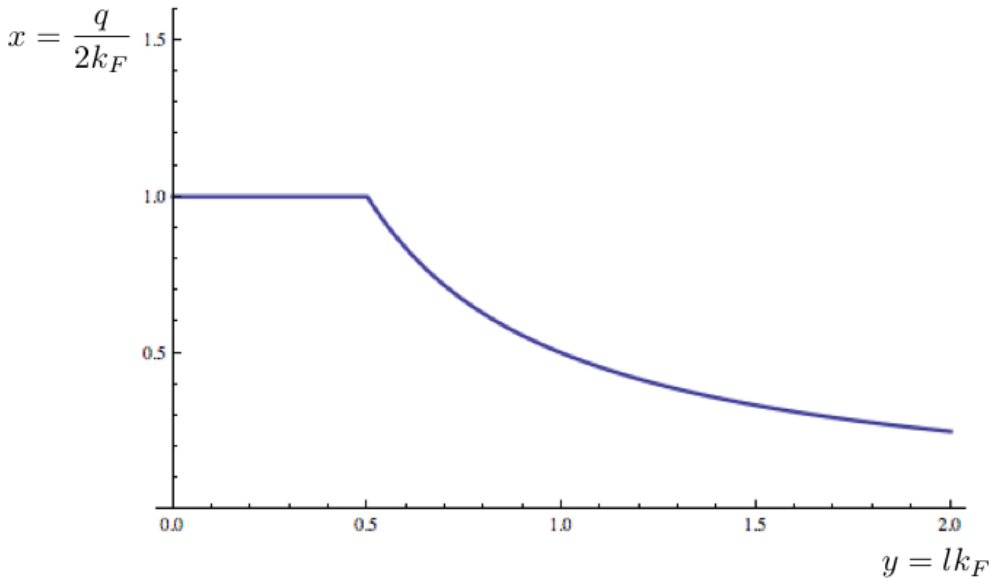

Figure 3.2: The critical points of the phase transition toward SDW. The threshold of the instability appears at the translational vector $|\mathbf{q}| = x2k_F$ associated with the unique external parameter as $y = lk_F$ and $r_s = md_{eff}^2 k_F/\hbar^2$.

In next section we examine the stability of the system through RPA method. Afterwards, we calculate the order parameter and the condensation energy of the SDW phase, self-consistently. But, before leaving this section it would not be time wasting to analyze the behavior of the bilayer system by a charge density perturbation. So similar to what is done up to now, we introduce an external field, coupled with the charge density, into the mean-field Hamiltonian

$$
\begin{aligned}
H &= H_0 + \frac{1}{L^2}\sum_q \tilde{V}_{\boldsymbol{q}}\,(\langle\rho\rangle + \Delta\rho)\,(\langle\rho\rangle + \Delta\rho) + \sum_{\boldsymbol{q}} h_{\boldsymbol{q}}\,(\rho_{\boldsymbol{q}\uparrow} + \rho_{\boldsymbol{q}\downarrow}) \\
&\simeq \underbrace{H_0 - \frac{1}{L^2}\sum_q \tilde{V}_{\boldsymbol{q}}\,\langle\rho_{\boldsymbol{q}\uparrow}\rangle\,\langle\rho_{-\boldsymbol{q}\downarrow}\rangle}_{H_0'} + \frac{1}{L^2}\sum_q \tilde{V}_{\boldsymbol{q}}\,(\rho_{\boldsymbol{q}\uparrow}\,\langle\rho_{-\boldsymbol{q}\downarrow}\rangle + \rho_{-\boldsymbol{q}\downarrow}\,\langle\rho_{\boldsymbol{q}\downarrow}\rangle) + \sum_{\boldsymbol{q}} h_{\boldsymbol{q}}\,(\rho_{\boldsymbol{q}\uparrow} + \rho_{\boldsymbol{q}\downarrow}) \\
&= H_0' + \sum_q \{\rho_{q\uparrow}\,(\frac{\tilde{V}_q}{L^2}\,\langle\rho_{-q\downarrow}\rangle + h_q) + \rho_{\boldsymbol{q}\downarrow}\,(\frac{\tilde{V}_{\boldsymbol{q}}}{L^2}\,\langle\rho_{-\boldsymbol{q}\uparrow}\rangle + h_{\boldsymbol{q}})\} \\
&= H_0' + \sum_{\boldsymbol{q}} (\rho_{\boldsymbol{q}\uparrow} + \rho_{\boldsymbol{q}\downarrow})\,(h_{\boldsymbol{q}} + \frac{\tilde{V}_{\boldsymbol{q}}\langle\rho_{-\boldsymbol{q}\uparrow} - \rho_{-\boldsymbol{q}\downarrow}\rangle}{2L^2}) + \sum_{\boldsymbol{q}} (\rho_{\boldsymbol{q}\uparrow} - \rho_{\boldsymbol{q}\downarrow})\,\frac{\tilde{V}_{\boldsymbol{q}}\langle\rho_{-\boldsymbol{q}\uparrow} + \rho_{-\boldsymbol{q}\downarrow}\rangle}{2L^2}. \qquad (3.20)
\end{aligned}
$$

Once again, there are two external fields which are coupled with the charge density and the spin density. We examine the effect of both of them. First, the induced charge density as a response to the external field

$$
\rho^{ind} = \langle\rho_{\boldsymbol{q}\uparrow} + \rho_{\boldsymbol{q}\downarrow}\rangle = \chi_0(\boldsymbol{q})\,\varphi_{ch}^{ext} = \chi_0(\boldsymbol{q})\,(h_{\boldsymbol{q}} + \frac{\tilde{V}_{\boldsymbol{q}}\,\rho^{ind}}{2L^2}),
$$

and readily solve for induced charge density we obtain

$$
\rho^{ind} = \frac{\chi_0(\boldsymbol{q})\,h_{\boldsymbol{q}}}{1 - \frac{\chi_0(\boldsymbol{q})\,\tilde{V}_{\boldsymbol{q}}}{2\,L^2}}. \qquad (3.21)
$$

As we saw in (3.16), the response function is negative versus positive sign of the potential V_q, which guarantee the stability of the system. In other words, by vanishing the external field, the induced field mutually disappears. For spin density, the system shows

$$
S^{ind} = \langle\rho_{\boldsymbol{q}\uparrow} + \rho_{\boldsymbol{q}\downarrow}\rangle = \chi_0(\boldsymbol{q})\,\varphi_{ch}^{ext} = \chi_0(\boldsymbol{q})\,\frac{\tilde{V}_{\boldsymbol{q}}\langle\rho_{\boldsymbol{q}\uparrow} + \rho_{\boldsymbol{q}\downarrow}\rangle}{2L^2}, \qquad (3.22)
$$

where obviously is unable to throw the system into trouble and, indeed, the induced density has to be zero in Eq. (3.22).

3.2.2 RPA approach to instability of the system

In the previous part, we have explored the instability of the system versus to the SDW phase, by analyzing the mean-field Hamiltonian in the presence of an external field. In the following part, we employ another approach to scrutinize the stability of the system. We have seen in the sprite of the mean-field approximation, spin density wave phase emerges by construction of the particle-hole pairs $\langle c_{k+q}^{\dagger} c_k\rangle$. Hence, by means of the two-body propagator, we analyze the fate of a particle-hole pair under multiple scattering in the Fermi liquid. The amplitude of the particle-hole propagator in the momentum $\boldsymbol{k}$ and energy ω space is written as

$$\begin{aligned}\Sigma(\boldsymbol{q},\omega) &= \Sigma_{\uparrow\uparrow}(\boldsymbol{q},\omega)+\Sigma_{\downarrow\downarrow}(\boldsymbol{q},\omega)\\ &= \sum_{\substack{\boldsymbol{k},\,\boldsymbol{k}'\\ \lambda=\uparrow\downarrow}}\langle\psi_N|\,T\left[c^{\dagger}_{\boldsymbol{k}-\boldsymbol{q}\lambda}c_{\boldsymbol{k}\lambda}c^{\dagger}_{\boldsymbol{k}'+\boldsymbol{q}\lambda}c_{\boldsymbol{k}'\lambda}\right]|\psi_N\rangle,\end{aligned} \tag{3.23}$$

where the operators are time ordered and the expectation value is taken in the ground state of the normal state. We have split the propagator into spin-up and spin-down pair propagators. This is actually the spin-polarized density fluctuation propagator, where we have put a fluctuation in the system and take another fluctuation at the end of propagation through the system. This is particle-hole channel and usually called Peierls channel, versus the particle-particle channel which called Cooper channel that is the case for exploring the instability to superconductivity. We engage the Feynman graphical perturbation theory for many body system to analyze this four-point correlation function (see for example Ref. [31], [19], [42] and [1]). The lowest order of the approximation for two-body (particle-hole) propagator is visualized in Fig. 3.3 as an infinite series of the diagrams, containing the interaction of consecutive polarized bubbles.

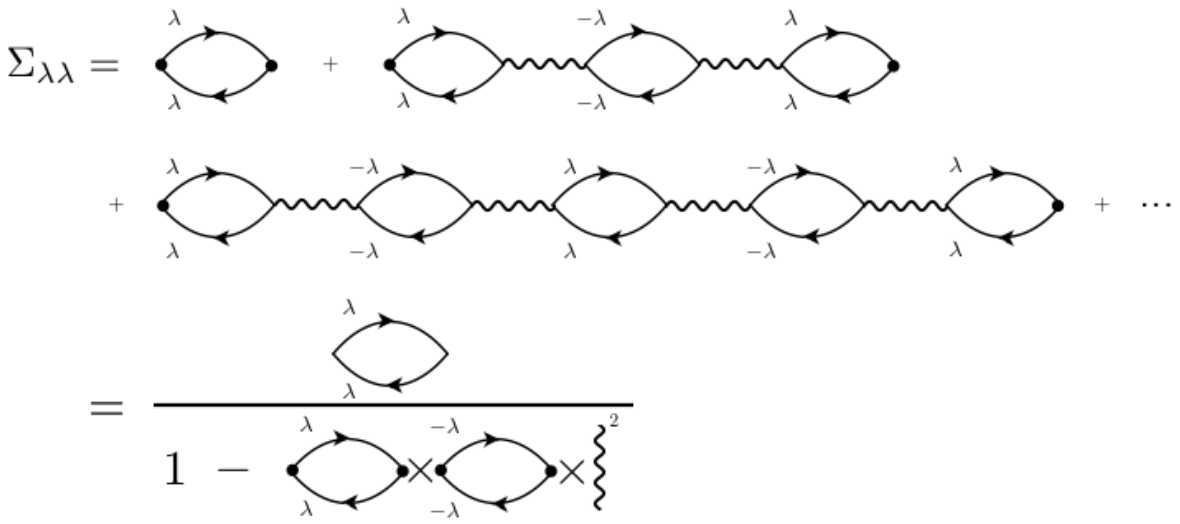

Figure 3.3: The approximation for propagation of a spin-polarized $\lambda =\uparrow, \downarrow$ particle-hole pair in interacting system. The pairs can interact with other pairs with opposite spin-polarization. Diagrams show a geometric series which the result of the sum is given diagrammatically.

The selective sum over bubbles diagrams in Fig. 3.3 is well-known as the *Random Phase Approximation*. Upon the bilayer Hamiltonian in Eq. (3.3), the interactions occur just between particles with opposite spin. Consequently, we have to consider the interactions between bubbles of opposite spin. In the graphical term, alternatively the spin of bubbles have to be changed. We sum up the series in Fig. 3.3, by representing a single bubble with $\Sigma_{0\,\lambda}$. As the sum is a geometrical series, we obtain

$$\Sigma(\boldsymbol{q},\omega)=\frac{\Sigma_{0\uparrow}(\boldsymbol{q},\omega)}{1-\tilde{V}_q^2\,\Sigma_{0\uparrow}(\boldsymbol{q},\omega)\,\Sigma_{0\downarrow}(\boldsymbol{q},\omega)}+\frac{\Sigma_{0\downarrow}(\boldsymbol{q},\omega)}{1-\tilde{V}_q^2\,\Sigma_{0\downarrow}(\boldsymbol{q},\omega)\,\Sigma_{0\uparrow}(\boldsymbol{q},\omega)}, \tag{3.24}$$

where $\tilde{V}_q$ is the interaction of the bubbles by exchanging momentum $\boldsymbol{q}$. Since the second term in the denominator is permanently positive, the amplitude of the pair propagator can diverge. This divergent implies that the system would be insatiable against formation of the particle-hole pairs. Hence, there could be a spontaneous broken symmetry: phase transition toward SDW phase where the ground state is composed of such particle-hole pairs. Owing to the equivalence between the particles with spin-up and spin-down polarization $\epsilon_\uparrow(k) = \epsilon_\downarrow(k)$, we define $\Sigma_{0\uparrow}(\boldsymbol{q},\omega) = \Sigma_{0\downarrow}(\boldsymbol{q},\omega) = \Sigma_0(\boldsymbol{q},\omega)$. The four-point correlation function takes the form

$$\Sigma(\boldsymbol{q},\omega) = \frac{2\Sigma_0(\boldsymbol{q},\omega)}{1 - \left[\tilde{V}_{\boldsymbol{q}}\,\Sigma_0(\boldsymbol{q},\omega)\right]^2},$$

and the instability condition reads

$$\tilde{V}_{\boldsymbol{q}}^2\,\Sigma_0^2(\boldsymbol{q},\omega) = 1. \tag{3.25}$$

The job is now to translate the single bubble into the algebraic form: finding the $\Sigma_0(\boldsymbol{q},\omega)$. A single bubble is composed of two free one-body propagator or free Green function G_0. We translate it to the analytical form by integrating over free indices of the momentum $\boldsymbol{k}$ and the frequency η. It turns out to be

$$i\Sigma_0(\boldsymbol{q},\omega) = (-1) \times \left(\frac{L}{2\pi}\right)^2 \int d\boldsymbol{k} \int \frac{d\eta}{2\pi}\, G_0(\boldsymbol{k},\,\eta) \times G_0(\boldsymbol{k}+\boldsymbol{q},\,\eta+\omega). \tag{3.26}$$

The minus is due to the fermion loop in the bubble. The free single-body Green function is

$$G_0(\boldsymbol{k},\omega) = \frac{\theta(k-k_F)}{\hbar\omega - \epsilon_{\boldsymbol{k}} + i\delta} + \frac{\theta(k_F-k)}{\hbar\omega - \epsilon_{\boldsymbol{k}} - i\delta}. \tag{3.27}$$

So the integral in Eq. (3.26) has four terms. First we do the integral over frequency. Two terms out of four terms have pole in the same imaginary half-plane of η. We close the contour in the opposite half-plane, thus their integral give no contribution. The other two terms have pole on the opposite sides of the half-plane and by use of contour integral we obtain the residues

$$\begin{aligned}
& \int \frac{d\eta}{2\pi}\, G_0(\boldsymbol{k},\,\eta) G_0(\boldsymbol{k}+\boldsymbol{q},\,\eta+\omega) \\
= & \int \frac{d\eta}{2\pi}\, \frac{\theta(k-k_F)}{\hbar\eta - \epsilon_{\boldsymbol{k}} + i\delta} \times \frac{\theta(k_F - |\boldsymbol{k}+\boldsymbol{q}|)}{\hbar\omega + \hbar\eta - \epsilon_{\boldsymbol{k}+\boldsymbol{q}} - i\delta} \\
+ & \int \frac{d\eta}{2\pi}\, \frac{\theta(k_F-k)}{\hbar\eta - \epsilon_{\boldsymbol{k}} - i\delta} \times \frac{\theta(|\boldsymbol{k}+\boldsymbol{q}| - k_F)}{\hbar\omega + \hbar\eta - \epsilon_{\boldsymbol{k}+\boldsymbol{q}} + i\delta} \\
= & \frac{2\pi i}{2\pi} \left\{ \frac{\theta(k-k_F)\theta(k_F - |\boldsymbol{k}+\boldsymbol{q}|)}{\hbar\omega - \epsilon_{\boldsymbol{k}+\boldsymbol{q}} + \epsilon_k - i\delta} - \frac{\theta(k_F-k)\theta(|\boldsymbol{k}+\boldsymbol{q}| - k_F)}{\hbar\omega - \epsilon_{\boldsymbol{k}+\boldsymbol{q}} + \epsilon_k + i\delta} \right\},
\end{aligned} \tag{3.28}$$

where in the last line the negative sign behind the second term in the bracket, is due to the counter-clockwise direction of the contour integral. By replacing this result in Eq. (3.26), the pair-bubble looks as

$$\Sigma_0(\boldsymbol{q},\omega) = \left(\frac{L}{2\pi}\right)^2 \int d\boldsymbol{k} \left\{ \frac{\theta(k_F-k)\theta(|\boldsymbol{k}+\boldsymbol{q}|-k_F)}{\hbar\omega - \epsilon_{\boldsymbol{k}+\boldsymbol{q}} + \epsilon_k + i\delta} - \frac{\theta(k-k_F)\theta(k_F-|\boldsymbol{k}+\boldsymbol{q}|)}{\hbar\omega - \epsilon_{\boldsymbol{k}+\boldsymbol{q}} + \epsilon_k - i\delta} \right\}, \quad (3.29)$$

which regardless of a factor of two for spin degeneracy, it has exactly the same form as the response function in Eq .(A.18). Put $\omega = 0$ corresponds to the time-independent case and neglecting the η, and using the relation that $\theta(x) = 1 - \theta(-x)$, it takes the form

$$\Sigma_0(\boldsymbol{q}) = \left(\frac{L}{2\pi}\right)^2 \int \frac{\theta(k_F-k) - \theta(k_F-|\boldsymbol{k}+\boldsymbol{q}|)}{\epsilon_k - \epsilon_{\boldsymbol{k}+\boldsymbol{q}}}\, d\boldsymbol{k}. \quad (3.30)$$

So we have

$$2\,\Sigma_0(\boldsymbol{q}) = \chi_0(\boldsymbol{q}). \quad (3.31)$$

and by replacing the final result in Eq. (3.25), we have exactly the same instability condition for the system as in Eq. (3.13). It can be written

$$\frac{|\chi_0(\boldsymbol{q})|\,\tilde{V}_{\boldsymbol{q}}}{L^2} = 2. \quad (3.32)$$

Hence as it was expected, both method released the same phase diagram for the bilayer system, which is depicted in Fig. 3.1.

3.3 Diagonalizing mean-field Hamiltonian

In the previous sections, the instability of the system versus SDW phase has been derived and the phase diagram is shown in Fig. 3.1. The calculations have been done in the frame work of linear response theory corresponds to the weakly interacting system. Hence, we continue with the mean-field Hamiltonian

$$\begin{aligned} H_{MF} &= \sum_{\boldsymbol{k}} [\varepsilon(\boldsymbol{k}) - \mu]\, c^\dagger_{\boldsymbol{k}\uparrow}\, c_{\boldsymbol{k}\uparrow} + \frac{1}{L^2} \sum_{\boldsymbol{q},\boldsymbol{k}} \tilde{V}_{\boldsymbol{q}}\, c^\dagger_{\boldsymbol{k}+\boldsymbol{q}\uparrow}\, c_{\boldsymbol{k}\uparrow}\, \tilde{\alpha}_{\boldsymbol{q}} \\ &+ \sum_{\boldsymbol{k}} [\varepsilon(\boldsymbol{k}) - \mu]\, c^\dagger_{\boldsymbol{k}\downarrow}\, c_{\boldsymbol{k}\downarrow} + \frac{1}{L^2} \sum_{\boldsymbol{q},\boldsymbol{k}} \tilde{V}_{\boldsymbol{q}}\, c^\dagger_{\boldsymbol{k}+\boldsymbol{q}\downarrow}\, c_{\boldsymbol{k}\downarrow}\, \tilde{\beta}_{\boldsymbol{q}} \\ &- \frac{1}{L^2} \sum_{\boldsymbol{q}} \tilde{V}_{\boldsymbol{q}}\, \tilde{\alpha}_{\boldsymbol{q}}\, \tilde{\beta}_{\boldsymbol{q}}, \end{aligned} \quad (3.33)$$

where we followed the same procedure as section 3.2.1, to neglect the quadratic terms for small fluctuations of number operators. We have introduced the complex parameters as

$$\begin{aligned}\tilde{\alpha}_{\boldsymbol{q}} &= \sum_{\boldsymbol{k}} \langle c^{\dagger}_{\boldsymbol{k}-\boldsymbol{q}\downarrow}\, c_{\boldsymbol{k}\downarrow}\rangle,\\ \tilde{\beta}_{\boldsymbol{q}} &= \sum_{\boldsymbol{k}} \langle c^{\dagger}_{\boldsymbol{k}+\boldsymbol{q}\uparrow}\, c_{\boldsymbol{k}\uparrow}\rangle. \end{aligned} \tag{3.34}$$

As can be seen in Eq. (3.33) the terms for either spins are uncoupled and well-separated. Therefore, we present the procedure of diagonalization just for one of the spin-polarization and then the same would be true for the other. In the following section, we analyze the degree of freedom of the Hamiltonian (3.33) to see how we can handle them and how many degree of freedom in coupling vector is permissible through the mean-field method.

3.3.1 Diagonalizing Hamiltonian for a one-dimensional lattice in a 2D space

Before start to diagonalize the Hamiltonian, we reduce the degree of freedom of the Hamiltonian (3.33) to the simplest case and just take a single coupling vector and its opposite direction $\pm\boldsymbol{q}$. The permissible value for $\boldsymbol{q}$ is shown in Fig. 3.2 for critical point where we are interested. Later, we try to increase the number of coupling vectors as much as possible. However, Hamiltonian for spin-up part is written in the form

$$\begin{aligned} H_{\uparrow} &= \sum_{\boldsymbol{k}} \left[\varepsilon(\boldsymbol{k}) - \mu\right]\, c^{\dagger}_{\boldsymbol{k}\uparrow}\, c_{\boldsymbol{k}\uparrow} + \frac{1}{L^2} \sum_{\substack{\boldsymbol{k}\\ \pm\boldsymbol{q}}} \tilde{V}_{\boldsymbol{q}}\, c^{\dagger}_{\boldsymbol{k}+\boldsymbol{q}\uparrow}\, c_{\boldsymbol{k}\uparrow}\, \tilde{\alpha}_{\boldsymbol{q}}\\ &= \sum_{\boldsymbol{k}} \left\{ \left[\varepsilon(\boldsymbol{k}) - \mu\right]\, c^{\dagger}_{\boldsymbol{k}\uparrow}\, c_{\boldsymbol{k}\uparrow} + \frac{1}{L^2}\, \tilde{V}_{\boldsymbol{q}} \left[c^{\dagger}_{\boldsymbol{k}+\boldsymbol{q}\uparrow}\, c_{\boldsymbol{k}\uparrow}\, \tilde{\alpha}_{\boldsymbol{q}} + c^{\dagger}_{\boldsymbol{k}\uparrow}\, c_{\boldsymbol{k}+\boldsymbol{q}\uparrow}\, \tilde{\alpha}^{*}_{\boldsymbol{q}} \right] \right\}, \end{aligned} \tag{3.35}$$

where the hermiticity of potential $\tilde{V}_{\boldsymbol{q}} = \tilde{V}_{-\boldsymbol{q}}$ is used besides the complex conjugation relation for $\tilde{\alpha}_{\boldsymbol{q}}$ as

$$\tilde{\alpha}_{\boldsymbol{q}} = \sum_{\boldsymbol{k}} \langle c^{\dagger}_{\boldsymbol{k}-\boldsymbol{q}\downarrow}\, c_{\boldsymbol{k}\downarrow}\rangle = \left(\sum_{\boldsymbol{k}} \langle c^{\dagger}_{\boldsymbol{k}+\boldsymbol{q}\downarrow}\, c_{\boldsymbol{k}\downarrow}\rangle \right)^{*} = \sum_{\boldsymbol{k}} \langle c^{\dagger}_{\boldsymbol{k}\downarrow}\, c_{\boldsymbol{k}+\boldsymbol{q}\downarrow}\rangle. \tag{3.36}$$

By singling out the coupling vector as $\pm\boldsymbol{q}$, we have encountered with the same situation as nearly free electron approximation [6] has accompanied with a periodic perturbation. The consequence of such approximation would be the appearance of band gap at the boundary of the Brillouin zones. So we have a one dimensional lattice with periodicity $\boldsymbol{q}$ within a two dimensional space.

As the first step, we take coupling vector $q \approx 2k_F$ corresponds to the critical points in Fig. 3.2. In this region, it would be shown in next section that the coupling of states is single *i.e.* each state at most is coupled with one state. Thereby, it is permissible to pick up a single coupling vector.

We restrict the Hamiltonian (3.35) by keeping sum over $\boldsymbol{k}$ just around the boundary of the first Brillouin zone (BZ), as is shown in Fig. 3.4. We rewrite the Eq. (3.35) by labeling the

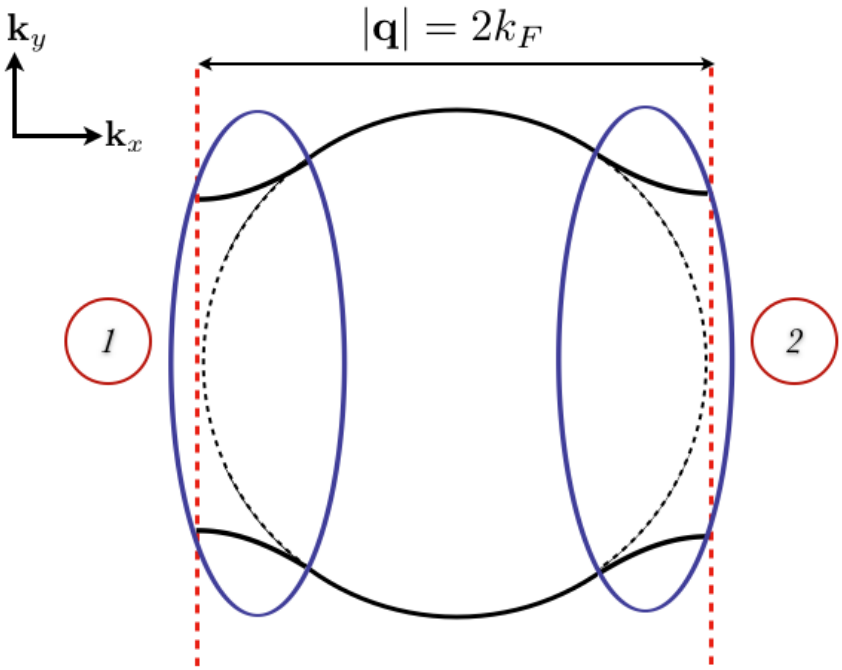

Figure 3.4: The appearance of the band gap at the boundary of the BZ for 1D lattice in a 2D space. The Fermi surface of the normal state is shown in dotted line.

operators acting over the states near boundary of lefthand side of the BZ by subscript one, and two for states near in righthand side of the BZ, to obtain

$$H_\uparrow = \sum_{\boldsymbol{k}} \left\{ \varepsilon_{1\boldsymbol{k}}\, c^\dagger_{1\boldsymbol{k}\uparrow}\, c_{1\boldsymbol{k}\uparrow} + \varepsilon_{2\boldsymbol{k}}\, c^\dagger_{2\boldsymbol{k}\uparrow}\, c_{2\boldsymbol{k}\uparrow} + \frac{1}{L^2}\, \tilde{V}_{\boldsymbol{q}} \left[c^\dagger_{1\boldsymbol{k}\uparrow}\, c_{2\boldsymbol{k}\uparrow}\, \tilde{\alpha}_{\boldsymbol{q}} + c^\dagger_{2\boldsymbol{k}\uparrow}\, c_{1\boldsymbol{k}\uparrow}\, \tilde{\alpha}^*_{\boldsymbol{q}} \right] \right\}, \quad (3.37)$$

that we absorbed the chemical potential into the dispersion relation terms to avoid lengthy equations.

Following the Bogolyubov diagonalization method [43], by means of the canonical transformation of the operators, which leaves invariant the commutation relation of the Fermionic operators, the transformed operators look

$$\begin{aligned} \gamma_{1\boldsymbol{k}} &= \tilde{M}_{\boldsymbol{k}}\, c_{1\boldsymbol{k}} - \tilde{N}^*_{\boldsymbol{k}}\, c_{2\boldsymbol{k}}, \\ \gamma_{2\boldsymbol{k}} &= \tilde{N}_{\boldsymbol{k}}\, c_{1\boldsymbol{k}} + \tilde{M}^*_{\boldsymbol{k}}\, c_{2\boldsymbol{k}}, \end{aligned} \quad (3.38)$$

where we have dropped the spin polarization symbol. The coefficients $\tilde{M}_{\boldsymbol{k}}$ and $\tilde{N}_{\boldsymbol{k}}$ construct the complex elements of the unitary matrix with the constrains

$$|\tilde{M}_{\boldsymbol{k}}|^2 + |\tilde{N}_{\boldsymbol{k}}|^2 = 1, \quad (3.39)$$

in order to guarantee the canonical anticommutation relation for new fermionic operators. Replacing the old operator by their transformed one, by using the matrix representation of

the inverse form of Eq. (3.39), we have

$$\begin{pmatrix} c_{1\boldsymbol{k}} \\ \\ c_{2\boldsymbol{k}} \end{pmatrix} = \begin{pmatrix} \tilde{M}^*_{\boldsymbol{k}} & \tilde{N}^*_{\boldsymbol{k}} \\ \\ -\tilde{N}_{\boldsymbol{k}} & \tilde{M}_{\boldsymbol{k}} \end{pmatrix} \begin{pmatrix} \gamma_{1\boldsymbol{k}} \\ \\ \gamma_{2\boldsymbol{k}} \end{pmatrix}. \tag{3.40}$$

The Hamiltonian reads

$$H_\uparrow = \sum_{\boldsymbol{k}} \begin{pmatrix} \gamma^\dagger_{1k} & \gamma^\dagger_{2k} \end{pmatrix} \begin{pmatrix} \tilde{M}_k & -\tilde{N}^*_k \\ \\ \tilde{N}_k & \tilde{M}^*_k \end{pmatrix} \begin{pmatrix} \epsilon_{1k} & \frac{\tilde{V}_q \tilde{\alpha}_q}{L^2} \\ \\ \frac{\tilde{V}_q \tilde{\alpha}^*_q}{L^2} & \epsilon_{1k} \end{pmatrix} \begin{pmatrix} \tilde{M}^*_k & \tilde{N}^*_k \\ \\ -\tilde{N}_k & \tilde{M}_k \end{pmatrix} \begin{pmatrix} \gamma_{1k} \\ \\ \gamma_{2k} \end{pmatrix}. \tag{3.41}$$

The complex parameters in Eq. (3.41) can be written explicitly as

$$\begin{cases} \tilde{\alpha}_k = \alpha_k \, e^{-i\varphi}, \\ \tilde{M}_k = M_k \, e^{\frac{i\varphi}{2}}, \\ \tilde{N}_k = N_k \, e^{\frac{i\varphi}{2}}, \end{cases} \tag{3.42}$$

After multiplying the middle matrices in $H_\uparrow$, it takes the form

$$H_\uparrow = \sum_{\boldsymbol{k}} \begin{pmatrix} \gamma^\dagger_{1k} & \gamma^\dagger_{2k} \end{pmatrix} \begin{pmatrix} M^2\,\epsilon_{1k} - 2\,M\,N\,\alpha\,\frac{V_q}{L^2} + N^2\,\epsilon_{2k} & -N\,M\,\epsilon_{1k} + \alpha\,(M^2 - N^2)\,\frac{V_q}{L^2} + M\,N\,\epsilon_{2k} \\ \\ -N\,M\,\epsilon_{1k} + \alpha\,(M^2 - N^2)\,\frac{V_q}{L^2} + M\,N\,\epsilon_{2k} & M^2\,\epsilon_{1k} + 2\,M\,N\,\alpha\,\frac{V_q}{L^2} + N^2\,\epsilon_{2k} \end{pmatrix} \begin{pmatrix} \gamma_{1k} \\ \\ \gamma_{2k} \end{pmatrix}, \tag{3.43}$$

where we dropped the momentum subscript of α, M and N. By vanishing the off-diagonal terms of the Hamiltonian in Eq. (3.43), actually the elements of the unitary matrix would be found. So we obtain

$$-N\,M\,\epsilon_{1\boldsymbol{k}} + \alpha\,(M^2 - N^2)\,\frac{\tilde{V}_{\boldsymbol{q}}}{L^2} + M\,N\,\epsilon_{2\boldsymbol{k}} = 0, \tag{3.44}$$

and employing Eq. (3.39), the solution for the elements of the transformation matrix are found by setting

$$\begin{aligned} M &= \cos\theta, \\ N &= \sin\theta, \end{aligned} \tag{3.45}$$

and using the relations

$$\begin{aligned} 2MN &= \sin 2\theta, \\ M^2 - N^2 &= \cos 2\theta, \\ \tan 2\theta &= \frac{2\,\alpha\,\tilde{V}_q/L^2}{\epsilon_{1k} - \epsilon_{2k}}. \end{aligned} \tag{3.46}$$

We achieved readily

$$M^2 = \cos^2\theta = \frac{1+\cos 2\theta}{2},$$
$$N^2 = \sin^2\theta = \frac{1-\cos 2\theta}{2}, \tag{3.47}$$

and finally, it is solved for trigonometric functions

$$\cos 2\theta = \frac{1}{\sqrt{1+\tan^2 2\theta}} = \frac{(\epsilon_{1k}-\epsilon_{2k})/2}{\sqrt{[(\epsilon_{1k}-\epsilon_{2k})/2]^2 + (\alpha\,\tilde{V}_q/L^2)^2}},$$
$$\sin 2\theta = \frac{\tan 2\theta}{\sqrt{1+\tan^2 2\theta}} = \frac{\alpha\,\tilde{V}_q/L^2}{\sqrt{[(\epsilon_{1k}-\epsilon_{2k})/2]^2 + (\alpha\,\tilde{V}_q/L^2)^2}}. \tag{3.48}$$

We use the results of Eq. (3.48) and the diagonal terms would be obtained

$$\begin{aligned} M^2\,\epsilon_{1k} + N^2\,\epsilon_{2k} \pm 2\,M\,N\,\alpha\,\tilde{V}_q &= \frac{1+\cos 2\theta}{2}\,\epsilon_{1k} + \frac{1-\cos 2\theta}{2}\,\epsilon_{2k} \pm \alpha\,V_q \sin 2\theta \\ &= \frac{\epsilon_{1k}+\epsilon_{2k}}{2} \pm \sqrt{\left(\frac{\epsilon_{1k}-\epsilon_{2k}}{2}\right)^2 + \left(\frac{\alpha\,\tilde{V}_q}{L^2}\right)^2}, \end{aligned} \tag{3.49}$$

where the subscript i referring to the side of the Brillouin zone boundary. The diagonalized spin-up Hamiltonian takes the form

$$H_\uparrow = \sum_{k,\,i} E^{\pm}_{\boldsymbol{k}}\gamma^\dagger_{i\boldsymbol{k}}\gamma_{i\boldsymbol{k}}, \tag{3.50}$$

where it has two part respect two side of boundary zone with eigenvalue

$$E^{\pm}_{\boldsymbol{k}} = \frac{\epsilon_{1\boldsymbol{k}}+\epsilon_{2\boldsymbol{k}}}{2} \pm \sqrt{\left(\frac{\epsilon_{1\boldsymbol{k}}-\epsilon_{2\boldsymbol{k}}}{2}\right)^2 + \left(\frac{\alpha\,\tilde{V}_{\boldsymbol{q}}}{L^2}\right)^2}. \tag{3.51}$$

The eigenenergy E^- refers to the states in the first BZ and the other E^+ belongs to the second BZ. The Hamiltonian for spin-down $H_\downarrow$ can be written down in the analogy with $H_\uparrow$. Therefore, the full Hamiltonian in Eq. (3.33) reads

$$\begin{aligned} H_{MF} &= H_\uparrow + H_\downarrow - \frac{1}{L^2}\sum_{\pm\boldsymbol{q}} \tilde{V}_{\boldsymbol{q}}\,\tilde{\alpha}_{\boldsymbol{q}}\,\tilde{\beta}_{\boldsymbol{q}} \\ &= \sum_{\substack{\boldsymbol{k},\,i \\ \lambda=\uparrow\downarrow}} E^{\pm}_{i\boldsymbol{k}}\gamma^\dagger_{i\boldsymbol{k}\lambda}\gamma_{i\boldsymbol{k}\lambda} - \frac{\tilde{V}_{\boldsymbol{q}}}{L^2}\left(\tilde{\alpha}\tilde{\beta} + \tilde{\alpha}^*\tilde{\beta}^*\right). \end{aligned} \tag{3.52}$$

We define the complex order parameter as

$$\tilde{\Delta} = \frac{\tilde{V}_{\boldsymbol{q}}}{L^2}\tilde{\beta}^* = -\frac{\tilde{V}_{\boldsymbol{q}}}{L^2}\tilde{\alpha}. \tag{3.53}$$

We have supposed that the order parameter is momentum independent. This hypothesis is valid in the weak coupling limit and in the vicinity of the critical point, where we are concerned. The mean-field Hamiltonian takes the diagonal form

$$H_{MF} \quad = \quad \sum_{\substack{\boldsymbol{k},\, i \\ \lambda=\uparrow\downarrow}} E^{\pm}_{i\boldsymbol{k}} \gamma^{\dagger}_{i\boldsymbol{k}\lambda}\gamma_{ik\lambda} + \frac{2\Delta^2 L^2}{\tilde{V}_{\boldsymbol{q}}}. \tag{3.54}$$

Resolving the dispersion relations by $\epsilon_{ik} \to (\epsilon_{ik} - \mu)$ as it had been said before, the eigenvalue of the diagonalized Hamiltonian looks

$$E^{\pm}_{\boldsymbol{k}} = \frac{\epsilon_{1\boldsymbol{k}} + \epsilon_{2\boldsymbol{k}}}{2} \pm \sqrt{\left(\frac{\epsilon_{1\boldsymbol{k}} - \epsilon_{2\boldsymbol{k}}}{2}\right)^2 + \Delta^2} \quad - \quad \mu. \tag{3.55}$$

The diagonalization of the mean-field Hamiltonian, containing just single coupling vector $\boldsymbol{q}$, is done and as it is expected there is a band gap in the single particle excitation spectrum at the boundary of the BZ. In the next par,t we look to the circumstances that increases the number of the coupling as much as it remains finite, which is needed throughout the presented procedure of the diagonalization.

We compare the energy of the ground state in SDW phase (3.54) and normal state *i.e.* Fermi liquid in the coming sections. It is apparent that order parameter is zero in normal state as $\tilde{\alpha}$ and $\tilde{\beta}$ which construct the order parameter (3.53) vanish in normal state as the expectation value of those pairs are mutually zero *i.e.* $\langle\psi_N|a^{\dagger}_{\boldsymbol{k}-\boldsymbol{q}}a_{\boldsymbol{k}}|\psi_N\rangle = 0$. Hence the Hamiltonian (3.54) coincide with the normal state Hamiltonian within the framework of mean-field.

The ground state in the SDW phase, considering the quasiparticle operators in Eq. (3.39), would be achieved by filling the lowest energy state up to Fermi energy. We fix the chemical potential, which is equal to the Fermi energy of normal state at zero temperature. Within our weakly interacting system, we believe that SDW phase modifies states close to the boundary zones and elsewhere it would be the same as the normal Fermi liquid. We write the ground state in the SDW phase as

$$|\psi_{SDW}\rangle = \prod_{E_{\boldsymbol{k}}<0} \gamma^{\dagger}_{1\boldsymbol{k}\uparrow}\gamma^{\dagger}_{2\boldsymbol{k}\uparrow} \prod_{E_{\boldsymbol{k}}<0} \gamma^{\dagger}_{1\boldsymbol{k}\downarrow}\gamma^{\dagger}_{2\boldsymbol{k}\downarrow}|0\rangle, \tag{3.56}$$

where obviously the Fermi energy in SDW phase is different from the one in Normal state and $E_{\boldsymbol{k}}$ is given in Eq. (3.55).

3.3.2 Diagonalizing Hamiltonian for a triangular lattice in a 2D space

In the preceding section, we have diagonalized the mean-field Hamiltonian concerning a single coupling vector (see Eq. (3.54)). In the following part, we look to the Hamiltonian with more allowed coupling vector and analyze the effect of the increasing the number of the coupling within the framework of the mean-field approximation.

In the two dimensional reciprocal space, two linearly independent vectors are sufficient and necessary to span the whole space. Hence, there would be two independent translational vectors. Introducing another translational vector could have two distinct consequences. On the one hand, it can scale the translational vectors of the lattice by rational factor if it could be written as a linear sum of the basis vectors, with the coefficient being rational numbers. On the other hand, it can totally destroy the lattice if the new introduced vector cannot be expressed as the linear combination of the basis vectors. In the latter case, actually each state couples to the infinite number of the states and upon the current mean-field method, it is impossible to diagonalize the Hamiltonian. Hereby, the two dimensional lattice would be the favorable model which can be dealt within the restriction of the mean-field theory. So we choose two vectors as the basis vectors with the amplitude $\mathbf{q}_1 = \boldsymbol{q}_2$. The amplitude of the translational vectors are restricted over the permissible values at the critical points which are depicted in Fig. 3.2.

The orientation of the basis vectors can be determined by taking into account that the ground state energy of SDW phase has to have the lowest energy. Considering that construction of particle-hole pairs lead to the reduction of the ground state energy, equilateral triangular lattice (hexagonal lattice) provides the higher number of coupling, upon the isotropic symmetry of the space. Besides, the triangular lattice provides highest number of discrete rotational symmetry.

Concerning the triangular lattice in Fig. 3.5 for the states far from the vertexes of the lattice, we have three independent terms in the Hamiltonian. The diagonalized form, inspired by Eq. (3.54), reads

$$\begin{aligned} H_{MF} &= \sum_{\substack{k\in\boldsymbol{q}_1 \\ i,\,\lambda=\uparrow\downarrow}} E^{\pm}_{i\boldsymbol{k}}\gamma^{\dagger}_{i\boldsymbol{k}\lambda}\gamma_{i\boldsymbol{k}\lambda} + \frac{2\Delta^2 L^2}{\tilde{V}_{\boldsymbol{q}_1}} \\ &+ \sum_{\substack{\boldsymbol{k}\in\boldsymbol{q}_2 \\ i,\,\lambda=\uparrow\downarrow}} E^{\pm}_{i\boldsymbol{k}}\gamma^{\dagger}_{i\boldsymbol{k}\lambda}\gamma_{i\boldsymbol{k}\lambda} + \frac{2\Delta^2 L^2}{\tilde{V}_{\boldsymbol{q}_2}} \\ &+ \sum_{\substack{\boldsymbol{k}\in\boldsymbol{q}_3 \\ i,\,\lambda=\uparrow\downarrow}} E^{\pm}_{i\boldsymbol{k}}\gamma^{\dagger}_{i\boldsymbol{k}\lambda}\gamma_{i\boldsymbol{k}\lambda} + \frac{2\Delta^2 L^2}{\tilde{V}_{\boldsymbol{q}_3}}, \end{aligned} \tag{3.57}$$

where each line corresponds to the one sides of the triangle in reciprocal lattice. The sum over i is restricted over the two side of each coupling vector (area in the vicinity of the boundaries of the BZs). The eigenvalues are the same as one in Eq. (3.55) whenever the Fermi surface does not include the vertex of the lattice (except the origin). As there are three equivalent independent term in Hamiltonian so the total ground state energy would be

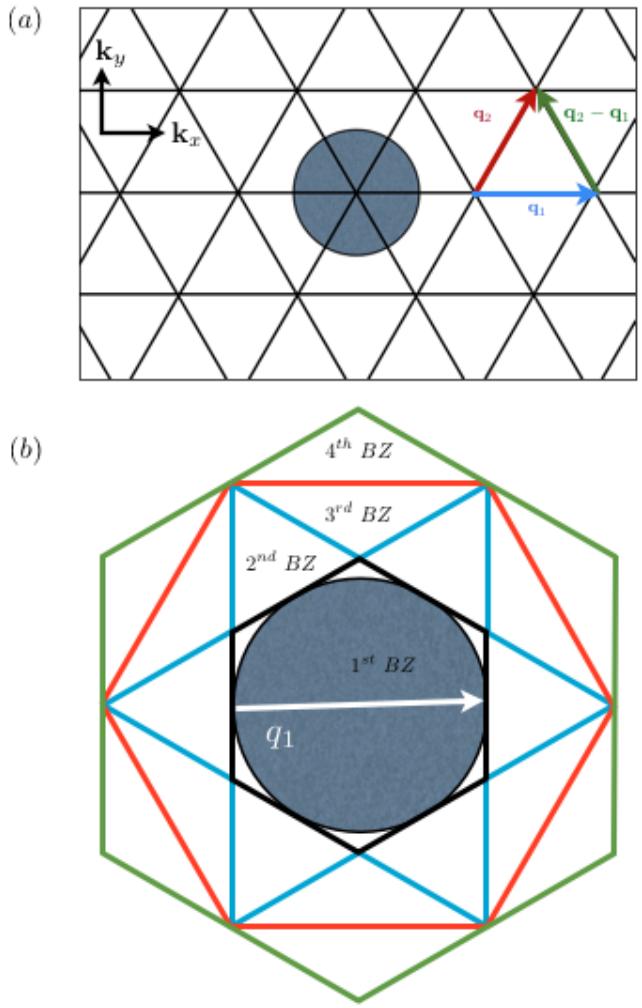

Figure 3.5: (**a**) The schematic representation of the triangular lattice and the relative configuration of the Fermi surface. Two independent translational vectors are also shown with the blue and red arrows indicated by $\boldsymbol{q}_1$ and $\boldsymbol{q}_2$, respectively. The third side of the triangles are shown by the green arrow as the $\boldsymbol{q}_2 - \boldsymbol{q}_1$. (**b**) The Brillouin zones of the triangular lattice and the relative placement of the Fermi surface have been shown. The typical couplings of the state by vector $\boldsymbol{q}_1$ is depicted for illustrations of the pairing.

$$\begin{aligned} E^0_{SDW} = \langle \psi_{SDW} | H_{MF} | \psi_{SDW} \rangle &= 3 \times 2 \sum_{1^{st}BZ} \left(\frac{\epsilon_{1\boldsymbol{k}} + \epsilon_{2\boldsymbol{k}}}{2} - \sqrt{\left(\frac{\epsilon_{1\boldsymbol{k}} - \epsilon_{2\boldsymbol{k}}}{2} \right)^2 + \Delta^2} - \mu \right) \\ &+ 3 \times 2 \sum_{2^{nd}BZ} \left(\frac{\epsilon_{1\boldsymbol{k}} + \epsilon_{2\boldsymbol{k}}}{2} + \sqrt{\left(\frac{\epsilon_{1\boldsymbol{k}} - \epsilon_{2\boldsymbol{k}}}{2} \right)^2 + \Delta^2} - \mu \right) \\ &+ 3 \times \frac{2\Delta^2 L^2}{\tilde{V}_{\boldsymbol{q}}}. \end{aligned} \tag{3.58}$$

3.4 Condensation energy and order parameter

Following the diagonalized mean-field Hamiltonian in Eq. (3.54) corresponds to the one-dimensional lattice, we start to find out the ground state energy of the system in the SDW phase. We derive the condensation energy in order to admit the phase transition of the system as a consequence of the instability versus SDW phase. All calculation is restricted to the zero temperature $T = 0$. The ground state energy and order parameter has to be calculated self-consistently. So we present them alternatively together, as their consistency has to be check throughout the calculations.

We calculate the parameter of the system corresponds to the critical points, which is depicted in Fig. 3.2. It has to be said that the validity of the calculation is just in the vicinity of the critical point. Hereby, we try to calculate the condensation energy and the order parameter self-consistently for the phase diagram.

We look to the relation of the order parameter and the ground state energy before leaving this section. The ground state energy is written

$$\begin{aligned} E^0_{SDW} = \langle\psi_{SDW}|H_{MF}|\psi_{SDW}\rangle &= 2\sum_{k<k'_F}\left(\frac{\epsilon_{1\boldsymbol{k}}+\epsilon_{2\boldsymbol{k}}}{2}-\sqrt{\left(\frac{\epsilon_{1\boldsymbol{k}}-\epsilon_{2\boldsymbol{k}}}{2}\right)^2+\Delta^2}-\mu\right) \\ &+ 2\sum_{k>k'_F}\left(\frac{\epsilon_{1\boldsymbol{k}}+\epsilon_{2\boldsymbol{k}}}{2}+\sqrt{\left(\frac{\epsilon_{1\boldsymbol{k}}-\epsilon_{2\boldsymbol{k}}}{2}\right)^2+\Delta^2}-\mu\right) \\ &+ \frac{2\Delta^2L^2}{\tilde{V}_{\boldsymbol{q}}}, \end{aligned} \tag{3.59}$$

where the first sum is over the first Brillouin zone and the second sum for the second Brillouin zone. The Fermi wavevector in SDW phase is shown with prime sign. The prefactor 2 is for spin degeneracy. Now, upon the definition of the order parameter (3.53), it is written by use of (3.34)

$$\tilde{\Delta} = \Delta e^{i\varphi} = \frac{\tilde{V}_{\boldsymbol{q}}}{L^2}\tilde{\beta}^* = \frac{\tilde{V}_{\boldsymbol{q}}}{L^2}\sum_{\boldsymbol{k}}\langle a^\dagger_{\boldsymbol{k}+\boldsymbol{q}\uparrow}\, a_{\boldsymbol{k}\uparrow}\rangle, \tag{3.60}$$

We employ the transformed operator to rewrite the pair expectations value as

$$\begin{aligned} \langle c^\dagger_{\boldsymbol{k}+\boldsymbol{q}\uparrow}\, c_{\boldsymbol{k}\uparrow}\rangle &= \langle c^\dagger_{1\boldsymbol{k}\uparrow}\, c_{2\boldsymbol{k}\uparrow}\rangle \\ &= \tilde{N}\tilde{M}e^{i\varphi} \\ &= \frac{\sin 2\theta}{2}e^{i\varphi} \\ &= \frac{\tilde{\beta}\,\tilde{V}_{\boldsymbol{q}}/2L^2}{\sqrt{((\epsilon_{1\boldsymbol{k}}-\epsilon_{2\boldsymbol{k}})/2)^2+(\beta\,\tilde{V}_{\boldsymbol{q}}/L^2)^2}}. \end{aligned} \tag{3.61}$$

The order parameter so can be written as

$$\Delta\frac{\tilde{V}_{\boldsymbol{q}}}{2L^2}=\sum_{\boldsymbol{k}}\frac{\Delta}{\sqrt{((\epsilon_{1\boldsymbol{k}}-\epsilon_{2\boldsymbol{k}})/2)^2+\Delta^2}}. \tag{3.62}$$

The order parameter generally is momentum-dependent. But as we mentioned, for weakly interacting system, we take the order parameter momentum-independent. Equation (3.62) is valid up to first Brillouin zone filled state. For the states of the higher bands, we have to diagonalize the mean-field Hamiltonian once again. The order parameter can also be derived by minimizing the ground state energy with respect to the order parameter consistent with the Landau theory approach. Hence we minimize E^0_{SDW} (3.59) as a function of the order parameter. So we have

$$\begin{aligned}\frac{\partial E^0_{SDW}}{\partial\Delta} &= -2\sum_{1^{st}BZ}\frac{\Delta}{\sqrt{\left(\frac{\epsilon_{1\boldsymbol{k}}-\epsilon_{2\boldsymbol{k}}}{2}\right)^2+\Delta^2}}+2\sum_{2^{nd}BZ}\frac{\Delta}{\sqrt{\left(\frac{\epsilon_{1\boldsymbol{k}}-\epsilon_{2\boldsymbol{k}}}{2}\right)^2+\Delta^2}}+\frac{4\Delta L^2}{\tilde{V}_{\boldsymbol{q}}}\\ &= 0,\end{aligned} \tag{3.63}$$

and can be readily solved for a self-consistent equation

$$\begin{aligned}\Delta &= \frac{\tilde{V}_{\boldsymbol{q}}}{2L^2}\sum_{1^{st}BZ}\frac{\Delta}{\sqrt{((\epsilon_{1\boldsymbol{k}}-\epsilon_{2\boldsymbol{k}})/2)^2+\Delta^2}}\\ &- \frac{\tilde{V}_{\boldsymbol{k}}}{2L^2}\sum_{2^{nd}BZ}\frac{\Delta}{\sqrt{((\epsilon_{1\boldsymbol{k}}-\epsilon_{2\boldsymbol{k}})/2)^2+\Delta^2}}.\end{aligned} \tag{3.64}$$

So we are ready to calculate explicitly the ground state energy and order parameter self-consistently in the coming sections.

3.4.1 In the case of $q = 2k_F$

Concerning the critical points of the system in Fig. 3.2, a large area of the diagram associated with $y \leq 1/2$, corresponds to the instability at $q = 2k_F$. Obviously, the interaction strength at the critical points r_s varies continuously upon this part of the critical points diagram (see Fig. 3.1). We start to calculate the order parameter, since we would need the order parameters through the calculation of the condensation energy.

Order parameter for $q = 2k_F$

In this regime, we suppose particle-hole coupling take place within a narrow area close to the Fermi surface. Hence, we introduce a cutoff λ, as shown in Fig. 3.6, in which the states are coupled by means of the vector $|\boldsymbol{q}| = 2k_F$ to the states at other side of the Fermi surface. Such coupling $|\boldsymbol{q}| = 2k_F$ implies that the band gap appears on the Fermi surface. Hence, we are dealing with the first Brillouin zone and the second band is empty. In the weak coupling regime, we treat the states out of the cutoff, states far from the Fermi surface, as the states in the normal phase *i.e.* $\Delta = 0$. As we discuss later, the final results of the calculation have

to be independent of the cutoff λ, which could be done in the regime of the extremely weak coupling $\Delta \ll \epsilon_F$.

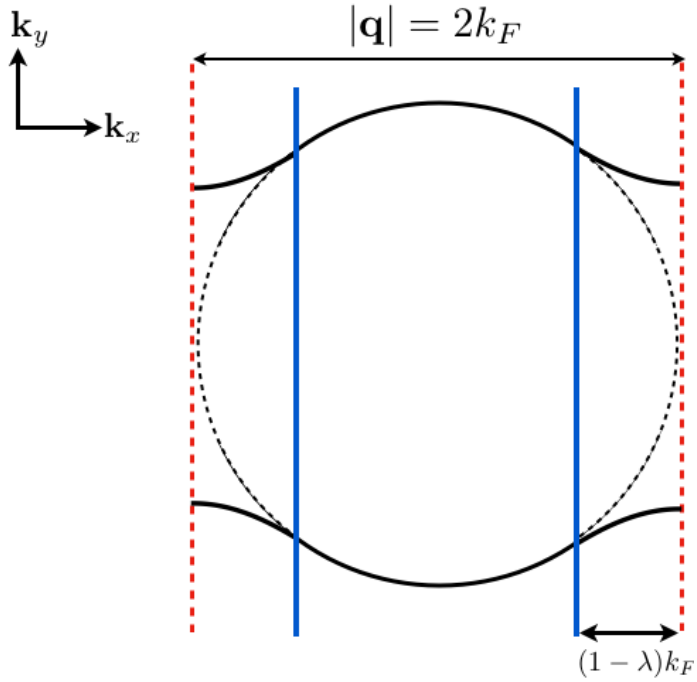

Figure 3.6: The Fermi surface of the SDW phase. The cutoff splits the states to the two distinct areas: the states in the vicinity of the Fermi surface and the states far from it.

The particular form of the self-consistent order parameter equation has a significant practical importance in the following calculation. Actually, by vanishing the order parameter in Eq. (3.62), it reduces to the instability equation (3.13). In the present regime it is written

$$\begin{aligned} -2 &= \frac{\chi_0(\boldsymbol{q})\,\tilde{V}_{\boldsymbol{q}}}{L^2}, \\ \Rightarrow 1 &= \frac{\tilde{V}_{\boldsymbol{q}}}{L^2}\,\omega(E), \end{aligned} \tag{3.65}$$

where the form of the response function $\chi_0(q)$ in $q \leq 2k_F$ is used. We perform the vanishing limit of the order parameter in Eq. (3.62) to see this correspondence as

$$\begin{aligned}
\lim_{\Delta\to 0}\left\{\Delta \;&=\; \frac{\tilde{V}_{\boldsymbol{q}}}{2L^2}\sum_{k}\frac{\Delta}{\sqrt{((\epsilon_{1\boldsymbol{k}}-\epsilon_{2\boldsymbol{k}})/2)^2+\Delta^2}}\right\},\\
\Rightarrow 1 \;&=\; \frac{\tilde{V}_{\boldsymbol{q}}}{2L^2}\sum_{\boldsymbol{k}}\frac{1}{\sqrt{((\epsilon_{1\boldsymbol{k}}-\epsilon_{2\boldsymbol{k}})/2)^2}},\\
\Rightarrow 1 \;&=\; \frac{\tilde{V}_{\boldsymbol{q}}}{L^2}\sum_{\boldsymbol{k}}\frac{1}{\epsilon_{1\boldsymbol{k}}-\epsilon_{2\boldsymbol{k}}},\\
\Rightarrow 1 \;&=\; \frac{\tilde{V}_{\boldsymbol{q}}}{L^2}\,\omega(E). \qquad (3.66)
\end{aligned}$$

In the fourth line we have just written the result of the sum in the third line. Later, we show it clearly.

As it is suggested that the order parameter in the form which is presented in Eq. (3.62) is valid just within the cutoff, which is introduced in Fig. 3.6, and elsewhere we deal with the vanishing limit of the order parameter $\Delta \to 0$ which is equal the instability equation. Hence, first we have achieved the representation of the response function in the current regime $q = 2k_F$, in order to employ it in the self-consistent order parameter equation. As the direction of $\boldsymbol{q}$ is arbitrary, we fixed it along $\hat{\boldsymbol{x}}$-direction. So the response function reads

$$\begin{aligned}
\chi^0(|\boldsymbol{q}|=2k_F) \;&=\; 2\sum_{\boldsymbol{k}}\frac{\theta(k_F-k)-\theta(k_F-|\overbrace{\boldsymbol{k}+\boldsymbol{q}}^{k'}|)}{\epsilon_{|\boldsymbol{k}|}-\epsilon_{|\boldsymbol{k}+\boldsymbol{q}|}}\\
&=\; 2\left(\frac{L}{2\pi}\right)^2\frac{2m}{\hbar^2}\int\left\{\frac{\theta(k_F-k)}{k^2-(\boldsymbol{k}+\boldsymbol{q})^2}d\boldsymbol{k}-\frac{\theta(k_F-k')}{(\boldsymbol{k}'-\boldsymbol{q})^2-k'^2}d\boldsymbol{k}'\right\}\\
&=\; 2\left(\frac{L}{2\pi}\right)^2\frac{2m}{\hbar^2}4\int_0^{k_F}\int_0^{\sqrt{k_F^2-k_x^2}}\left\{\frac{1}{-q^2+2k_xq}-\frac{1}{q^2+2k_xq}\right\}dk_xdk_y\\
&=\; 2\left(\frac{L}{2\pi}\right)^2\frac{2m}{\hbar^2}\int_0^1\int_0^{\sqrt{1-x^2}}\left\{\frac{1}{1+x}-\frac{1}{x-1}\right\}dxdy\\
&=\; -\frac{2}{\pi}\omega(E)\int_0^1\left\{\sqrt{\frac{1+x}{1-x}}+\sqrt{\frac{1-x}{1+x}}\right\}dx\\
&=\; -2\omega(E), \qquad (3.67)
\end{aligned}$$

where we have used the definition of the response function is given in Eq. (A.18). In the third line, the prefactor 4 corresponds to the four quadrants of the integral domain in the k-space. The coupling vector is supposed to be lying along x-direction with the length twice the Fermi wavenumber $q = 2k_F$. It has to be noted that for state near the boundary zone in the righthand side of the BZ, coupling vector $\boldsymbol{q}$ directed in along the negative direction and in other side is taken vice versa. Therefore, their inner product is $\boldsymbol{k}.\boldsymbol{q} = -k_xq$, which is employed in the third line. In the last lines the integral's variable is normalized by Fermi wavelength $x = k_x/k_F$ and $y = k_y/k_F$ that $\boldsymbol{k}$ is considered as $k^2 = k_x^2 + k_y^2$. The density of state in 2D is

engaged as $\omega(E) = mL^2/2\pi\hbar^2$, which is independent of the energy. In the normal state, the Fermi surface is a circle with the radius of k_F and the integral is performed with respect to this circle of the Fermi surface.

Now upon the idea of the cutoff in Fig. 3.6, we rewrite the self-consistent equation of the order parameter. We had mentioned that in the weak coupling regime, the order parameter is taken momentum independent. Beginning from (3.62) and taking into account that the sum is over the first BZ we have

$$\begin{aligned}
\Delta &= \Delta \frac{\tilde{V}_{\boldsymbol{q}}}{2L^2} \sum_{\boldsymbol{k}} \frac{1}{\sqrt{\left(\frac{\epsilon_{1\boldsymbol{k}}-\epsilon_{2\boldsymbol{k}}}{2}\right)^2 + \Delta^2}} \\
&= \Delta \frac{\tilde{V}_{\boldsymbol{q}}}{2L^2} \frac{m}{\hbar^2} \sum_{\boldsymbol{k}} \frac{1}{\sqrt{\left[\frac{1}{4}\left(q^2 + 2\boldsymbol{k}.\boldsymbol{q}\right)\right]^2 + \Delta^2}} \\
&= \Delta\, \omega(E)\, \frac{\tilde{V}_{\boldsymbol{q}}}{L^2}\, \frac{1}{4\pi} \int^{1^{st}BZ} \frac{dxdy}{\sqrt{(1-|x|)^2 + \Delta'^2}},
\end{aligned} \tag{3.68}$$

where the same reasoning as in the calculation of the response function in Eq. (3.67) is employed in the mid-steps. The order parameter is renormalized by twice Fermi energy $\Delta' = \Delta/2\epsilon_F$. The last integral in Eq. (3.68) is over the whole first BZ, and now the area in and out of the cutoff have to be separated. We perform the integral within the cutoff by finding the limits of the integral. We attempt to derive the Fermi surface by solving the dispersion relation for y-component. By use of the dispersion relation for the first BZ (3.55), we write

$$\begin{aligned}
\mu &= \frac{\epsilon_{1\boldsymbol{k}} + \epsilon_{2\boldsymbol{k}}}{2} - \sqrt{\left(\frac{\epsilon_{1\boldsymbol{k}} - \epsilon_{2\boldsymbol{k}}}{2}\right)^2 + \Delta^2} \\
&= \frac{\hbar^2}{2m}\frac{1}{2}\left[\boldsymbol{k}^2 + (\boldsymbol{k}+\boldsymbol{q})^2\right] - \sqrt{\left\{\frac{\hbar^2}{2m}\frac{1}{2}\left[k^2 - (\boldsymbol{k}+\boldsymbol{q})^2\right]\right\}^2 + \Delta^2} \\
&= \epsilon_F \left[x^2 + y^2 + 2(1-|x|) - 2\sqrt{(1-|x|)^2 + \Delta'^2}\right],
\end{aligned}$$

and concerning the relation $\mu = \epsilon_F$ at zero-temperature, we solve this equation for y to obtain

$$y = \sqrt{2\sqrt{(1-|x|)^2 + \Delta'^2} - (1-|x|)^2}. \tag{3.69}$$

It is possible to do the integral over the Fermi surface of the SDW phase. So by separating Eq. (3.68) with respect to the cutoff, we continue with its integral part as

$$\int^{1^{st}BZ} \frac{dxdy}{\sqrt{(1-|x|)^2+\Delta'^2}} = 4\int_0^{\lambda}\int_0^{\sqrt{1-x^2}} \left\{\frac{1}{1+x}-\frac{1}{x-1}\right\} dxdy + 4\int_{\lambda}^{1}\int_0^{\sqrt{2\sqrt{(1-x)^2+\Delta'^2}-(1-x)^2}} \frac{dxdy}{\sqrt{(1-x)^2+\Delta'^2}}, \tag{3.70}$$

where sign of absolute value function is dropped as the integral is just over the positive value, and the prefactor 4 counts the other regions. By adding and subtracting a term in order to make the first integral same as the response function integral in Eq. (3.67). Before go further, we do some approximation to simplify the upper limit of the second integral in (3.70).

In the weak coupling regime $\Delta' \ll 1$, for area near to the boundary zone $(1-|x|) \ll 1$, the second term in the square root of upper limit of second integral y, can be neglected in comparison with the first term

$$(1-|x|)^2 \ll \sqrt{(1-|x|)^2+\Delta'^2}. \tag{3.71}$$

then the upper limit is written like

$$y = \sqrt{2\sqrt{(1-|x|)^2+\Delta'^2}}. \tag{3.72}$$

Hereby, the integrals appears as

$$\begin{aligned}(3.70) &= 4\int_0^{1}\int_0^{\sqrt{1-x^2}} \left\{\frac{1}{1+x}-\frac{1}{x-1}\right\} dxdy \\ &+ 4\int_{\lambda}^{1}\int_0^{\sqrt{2\sqrt{(1-x)^2+\Delta'^2}}} \frac{dxdy}{\sqrt{(1-x)^2+\Delta'^2}} - 4\int_{\lambda}^{1}\int_0^{\sqrt{1-x^2}} \left\{\frac{1}{1+x}-\frac{1}{x-1}\right\} dxdy \\ &= 4\pi + 4\int_{\lambda}^{1}\left\{\frac{\sqrt{2}}{\left[(1-x)^2+\Delta'^2\right]^{\frac{1}{4}}} - \frac{2}{\sqrt{1-x^2}}\right\} dx, \end{aligned} \tag{3.73}$$

that the first integral is exactly the same as one in the response function integral in Eq. (3.67). For states close to the boundary $(1-|x|) \ll 1$, we approximate further $1-x^2 = (1-x)(1+x) \approx 2(1-x)$. So we have

$$(3.73) \approx 4\pi + 4\sqrt{2}\int_{\lambda}^{1}\left\{\frac{1}{\left[(1-x)^2+\Delta'^2\right]^{\frac{1}{4}}} - \frac{1}{\sqrt{1-x}}\right\} dx, \tag{3.74}$$

and by renaming the integral variable as $\frac{1-|x|}{\Delta'} = z$, we continue

$$(3.74) \quad = \quad 4\pi + 4\sqrt{2\Delta'} \int_0^{\frac{1-\lambda}{\Delta'}} \left[\frac{1}{(1+z^2)^{\frac{1}{4}}} - \frac{1}{\sqrt{z}} \right] dz. \tag{3.75}$$

By taking the vanishing limit of the order parameter $\Delta' \to 0$, as the weak coupling regime, there would be a well-define integral. We see that by taking such limit the upper limit goes to the infinity and we have got ride of the cutoff

$$\lim_{\Delta' \to 0} \frac{1-\lambda}{\Delta'} \to \infty.$$

We perform the integral

$$\begin{aligned} (3.70) = (3.75) \quad &= \quad 4\pi + 4\sqrt{2\Delta'} \lim_{\Delta' \to 0} \int_0^{\frac{1-\lambda}{\Delta'}} \left[\frac{1}{(1+z^2)^{\frac{1}{4}}} - \frac{1}{\sqrt{z}} \right] dz \\ &= \quad 4\pi + 4\sqrt{2\Delta'} \int_0^{\infty} \left[\frac{1}{(1+z^2)^{\frac{1}{4}}} - \frac{1}{\sqrt{z}} \right] dz \\ &= \quad 4\pi - 8\sqrt{2\pi\Delta'} \, \frac{\Gamma(\frac{3}{4})}{\Gamma(\frac{1}{4})}, \end{aligned} \tag{3.76}$$

where $\Gamma(z)$ is the gamma function. By replacing the integral (3.70) in the order parameter equation (3.68) we obtain

$$\begin{aligned} \Delta' \quad &= \quad \Delta' \, \omega(E) \, \frac{\tilde{V}_{\boldsymbol{q}}}{L^2} \left(1 - 2\sqrt{\frac{2}{\pi}} \, \frac{\Gamma(\frac{3}{4})}{\Gamma(\frac{1}{4})} \, \sqrt{\Delta'} \right) \\ &= \quad \Delta' \, \omega(E) \, \frac{\tilde{V}_{\boldsymbol{q}}}{L^2} \left(1 - 0.54\sqrt{\Delta'} \right). \end{aligned} \tag{3.77}$$

Now we solved Eq. (3.77) for Δ' to get

$$\begin{aligned} \Delta' \quad &= \quad \left[\sqrt{\frac{\pi}{8}} \, \frac{\Gamma(\frac{1}{4})}{\Gamma(\frac{3}{4})} \right]^2 \left(1 - \frac{L^2}{\omega(E) \, \tilde{V}_{\boldsymbol{q}}} \right)^2 \\ &= \quad \frac{1}{(0.54)^2} \left(1 - \frac{L^2}{\omega(E) \, \tilde{V}_{\boldsymbol{q}}} \right)^2. \end{aligned} \tag{3.78}$$

It is convenient to introduce the critical parameters, in which the order parameter vanishes and that is the very moment of phase transition. Obviously the order parameter vanishes at the critical points that we have derived before in Eq. (3.13) and is apparent in Eq. (3.78). By the way, we use Eq. (3.78) to find critical parameter by

$$1 \quad = \quad \frac{L^2}{\omega(E) \, \tilde{V}^c_{\boldsymbol{q}}}, \tag{3.79}$$

in which the order parameter vanishes. By use of $x = q/2k_F$, $y = lk_F$ and $r_s = d_{eff}^2\, m\, k_F/\hbar^2$, which are introduced in the Sec. 3.2.1, we rewrite the potential in Eq. (3.2) at the critical points as

$$\begin{aligned} \tilde{V}_{\boldsymbol{q}}^c &= r_s^c \frac{2\hbar^2}{m} x \, \exp\left(-2yx\right)|_{x=1} \\ &= r_s^c \frac{2\hbar^2}{m} \, \exp\left(-2y\right). \end{aligned} \tag{3.80}$$

Replace it in Eq. (3.79), the critical strength obtain

$$\begin{aligned} \tilde{V}_q^c &= \frac{L^2}{\omega(E)} \\ &= L^2 \frac{2\pi\hbar^2}{mL^2}, \\ &\Rightarrow \quad r_s^c = \pi e^{2y}. \end{aligned} \tag{3.81}$$

Finally, we write down explicitly the order parameter by engaging this critical strength in Eq. (3.78) as

$$\begin{aligned} \Delta' &= \frac{\pi}{8} \left(\frac{\Gamma(\frac{1}{4})}{\Gamma(\frac{3}{4})}\right)^2 \left(1 - \frac{r_s^c}{r_s}\right)^2 \\ &= 3.44 \left(1 - \frac{r_s^c}{r_s}\right)^2, \end{aligned} \tag{3.82}$$

which is valid throughout the critical points in the interval ($y \leq \frac{1}{2}$, $x = 1$) corresponds to the critical strength as defined in Eq. (3.81).

Condensation energy for $q = 2k_F$

The order parameter in the regime $q = 2k_F$ is found in preceding part. We turn to the condensation energy in the same regime. As it has been said, these two quantities have to be calculated self-consistently. Thereby, the order parameter has to minimize the ground state energy in each step of the calculation.

The starting point would be Eq. (3.59). In the current regime $q = 2k_F$, the first band is just filled. So we have

$$
\begin{aligned}
E^{SDW} &= 2\sum_{1^{st}BZ}\left[\frac{\epsilon_{1k}+\epsilon_{2\boldsymbol{k}}}{2}-\sqrt{\left(\frac{\epsilon_{1\boldsymbol{k}}-\epsilon_{2\boldsymbol{k}}}{2}\right)^2+\Delta^2}-\mu\right]+\frac{2\Delta^2L^2}{\tilde{V}_{\boldsymbol{q}}}\\
&= 2\sum_{1^{st}BZ}\left\{\frac{\hbar^2}{2m}\frac{1}{2}\left[k^2+(\boldsymbol{k}+\boldsymbol{q})^2\right]-\sqrt{\left\{\frac{\hbar^2}{2m}\frac{1}{2}\left[k^2-(\boldsymbol{k}+\boldsymbol{q})^2\right]\right\}^2+\Delta^2}-\epsilon_F\right\}+\frac{2\Delta^2L^2}{\tilde{V}_{\boldsymbol{q}}}\\
&= 2\frac{\hbar^2}{2m}\left(\frac{L^2}{2\pi}\right)k_F^4\int^{1^{st}BZ}\left\{x^2+y^2+2(1-|x|)-2\sqrt{(1-|x|)^2+\Delta'^2}-1\right\}dxdy+\frac{8\Delta'^2\epsilon_F^2L^2}{\tilde{V}_{\boldsymbol{q}}}\\
&= E^N\frac{2}{\pi}\int^{1^{st}BZ}\left\{y^2+(1-|x|)^2-2\sqrt{(1-|x|)^2+\Delta'^2}\right\}dxdy+\frac{8\Delta'^2\epsilon_F^2L^2}{\tilde{V}_{\boldsymbol{q}}},
\end{aligned}
\tag{3.83}
$$

where we have used $\boldsymbol{k}.\boldsymbol{q}=-k_xq$ and introduced $x=k_x/k_F$, $y=k_y/k_F$ by $k^2=k_x^2+k_y^2$, and also normalized the order parameter $\Delta'=\Delta/2\epsilon_F$. In the last line we used the total energy per spin in the normal state that is

$$
\begin{aligned}
E^N &= \left(\frac{L}{2\pi}\right)^2\int_0^{k_F}\frac{\hbar^2k^2}{2m}d^2k\\
&= \left(\frac{L}{2\pi}\right)^2\frac{\hbar^2k_F^4}{2m}\int_0^{\lambda}\int_0^{\sqrt{1-x^2}}(x^2+y^2)dxdy\\
&= \frac{\hbar^2L^2k_F^4}{8\pi m}.
\end{aligned}
\tag{3.84}
$$

Similar to the case of the order parameter, we introduce the idea of the cutoff which is shown in Fig. 3.6. It is mentioned that we use the dispersion relation of the SDW in the vicinity of the boundary zone, and elsewhere the dispersion relation of the normal state. Therefore, we split the integral in (3.83) to two parts: one for states close to the boundary zones, and other far from it as

$$
\begin{aligned}
&\int^{1^{st}BZ}\left\{y^2+(1-|x|)^2-2\sqrt{(1-|x|)^2+\Delta'^2}\right\}dxdy\\
=\;& 4\int_0^{\lambda}\int_0^{\sqrt{1-x^2}}\left(x^2+y^2-1\right)dxdy\\
+\;& 4\int_{\lambda}^{1}\int_0^{\sqrt{2\sqrt{(1-|x|)^2+\Delta'^2}-(1-|x|)^2}}\left\{y^2+(1-x)^2-2\sqrt{(1-x)^2+\Delta'^2}\right\}dxdy.
\end{aligned}
\tag{3.85}
$$

The prefactor 4 counts the number of quadrants as the integrals are over positive one. At each step of the calculation of the ground state energy, we check the consistency of the calculation with the order parameter, at the same level of calculations. So we take the derivative of Eq. (3.85) with respect to Δ', by use of the Leibniz integral rule, which is the derivative of a function with the definite integral form as

$$F(x) = \int_{\mathbf{b}(x)}^{\mathbf{a}(x)} f(x,y)dy.$$

The derivative takes the form

$$\frac{dF(x)}{dx} = f(x,\mathbf{b}(x))\,\frac{d\mathbf{b}(x)}{dx} - f(x,\mathbf{a}(x))\,\frac{d\mathbf{a}(x)}{dx} + \int_{\mathbf{b}(x)}^{\mathbf{a}(x)} \frac{\partial f(x,y)}{\partial x}dy.$$

By employing this relation for the ground state energy in Eq. (3.83), we obtain

$$\begin{aligned}
0 &= \partial_{\Delta'} E^{SDW} = \partial_{\Delta'}\Big\{E^N\,\frac{2}{\pi}\,(3.85) + \frac{8\Delta'^2\,\epsilon_F^2\,L^2}{\tilde{V}_{\boldsymbol{q}}}\Big\} \\
&= E^N\,\frac{2}{\pi}\Bigg\{\Bigg[\Big\{\sqrt{2\sqrt{(1-|x|)^2+\Delta'^2}-(1-|x|)^2}\;\Big\}^2 + (1-x)^2 - 2\sqrt{(1-x)^2+\Delta'^2}\;\Bigg]\,\frac{d(...)}{d\Delta'} \\
&- (...)\times 0 \\
&+ 4\int_\lambda^1 \int_0^{\sqrt{2\sqrt{(1-|x|)^2+\Delta'^2}-(1-|x|)^2}} \partial_{\Delta'}\left\{y^2+(1-x)^2-2\sqrt{(1-x)^2+\Delta'^2}\right\}dxdy\Bigg\} \\
&+ \frac{16\Delta'\,\epsilon_F^2\,L^2}{\tilde{V}_{\boldsymbol{q}}},
\end{aligned}$$

where the second line is merely zero. By using the relation

$$\omega(E) = \frac{E^N}{\epsilon_F^2} = \frac{\frac{\hbar^2L^2k_F^4}{8\pi m}}{\left(\frac{\hbar^2k_F^2}{2m}\right)^2} = \frac{mL^2}{2\pi\hbar^2}, \tag{3.86}$$

we obtain for the order parameter

$$\Delta' \;\propto\; \Delta'\,\omega(E)\,\frac{\tilde{V}_{\boldsymbol{q}}}{L^2}\,\frac{1}{\pi}\int_\lambda^1\int_0^{\sqrt{2\sqrt{(1-x)^2+\Delta'^2}-(1-x)^2}} \frac{dxdy}{\sqrt{(1-x)^2+\Delta'^2}}, \tag{3.87}$$

which the rhs is equal to the order parameter by use of Eq. (3.70), regardless of the Δ-independent term.

We continue from Eq. (3.85). By engaging the same trick as in the order parameter calculation, we introduce the complete form of the normal ground state energy as

$$\begin{aligned}
(3.85) &= 4\pi + 4\int_\lambda^1\int_0^{\sqrt{2\sqrt{(1-|x|)^2+\Delta'^2}-(1-|x|)^2}} \left\{y^2+(1-x)^2-2\sqrt{(1-x)^2+\Delta'^2}\right\}dxdy \\
&- 4\int_\lambda^1\int_0^{\sqrt{1-x^2}} \left(x^2+y^2-1\right)dxdy,
\end{aligned} \tag{3.88}$$

and by engaging Eq. (3.88) in Eq. (3.84), after a manipulation and neglecting the square term versus the square root term $(1-x)^2 \ll \sqrt{(1-x)^2+\Delta'^2}$ for the area close to the boundary $(1-|x|) \ll 1$, we continue for condensation energy as

$$\begin{aligned} E^{con} &= E^N - E^{SDW} \\ &= E^N \frac{8}{\pi}\Bigg\{ \int_\lambda^1 \int_0^{\sqrt{1-x^2}} \left(x^2+y^2-1\right) dxdy \\ &- \int_\lambda^1 \int_0^{\sqrt{2\sqrt{(1-x)^2+\Delta'^2}}} \left\{ y^2 - 2\sqrt{(1-x)^2+\Delta'^2} \right\} dxdy \Bigg\} \\ &- \frac{8\Delta'^2 \epsilon_F^2 L^2}{\tilde{V}_{\boldsymbol{q}}}. \end{aligned} \tag{3.89}$$

We perform the integrals to obtain

$$\begin{aligned} &\int_\lambda^1 \int_0^{\sqrt{1-x^2}} \left(x^2+y^2-1\right) dxdy - \int_\lambda^1 \int_0^{\sqrt{2\sqrt{(1-x)^2+\Delta'^2}}} \left\{ y^2 - 2\sqrt{(1-x)^2+\Delta'^2} \right\} dxdy \\ = &\int_\lambda^1 \frac{2}{3}\Bigg\{ -(1-x^2)^{\frac{3}{2}} + 2^{\frac{3}{2}} \left[(1-x)^2+\Delta'^2\right]^{\frac{3}{4}} \Bigg\} dx. \end{aligned} \tag{3.90}$$

We approximate the first integrand by $(1-x^2)^{\frac{3}{2}} = (1+x)^{\frac{3}{2}}(1-x)^{\frac{3}{2}} \approx 2^{\frac{3}{2}}(1-x)^{\frac{3}{2}}$, which is valid for the area close to the boundary of BZ. We continue to obtain

$$(3.90) = \frac{2^{\frac{5}{2}}}{3} \int_\lambda^1 \Bigg\{ \left[(1-x)^2+\Delta'^2\right]^{\frac{3}{4}} - (1-x)^{\frac{3}{2}} \Bigg\} dx. \tag{3.91}$$

Before going further, we check the consistency of Eq. (3.91), to be minimized by the order parameter over the same level of approximation in Eq. (3.74). As the prefactors are out of the interest, we just check the delta-dependent integrals. By taking the derivative of Eq. (3.91)

$$\partial_{\Delta'}(3.91) \propto \sqrt{2} \int_\lambda^1 \frac{1}{\left[(1-x)^2+\Delta'^2\right]^{\frac{1}{4}}} dx,$$

which corresponds to the Δ'-dependent part of Eq. (3.74).

Renaming the variable of the integral in Eq. (3.91), with $z = (1-x)/\Delta'$, and taking the vanishing limit of the integral in the framework of the weak coupling $\Delta' \ll \epsilon_F$, the integral emerges like

$$
\begin{aligned}
(3.91) \quad &= \frac{2^{\frac{5}{2}}}{3}\Delta'^{\frac{5}{2}} \lim_{\Delta'\to 0}\int_0^{\frac{1-\lambda}{\Delta'}} \left\{ \left[1+z^2\right]^{\frac{3}{4}} - z^{\frac{3}{2}} \right\} dx \\
&= \frac{2^{\frac{5}{2}}}{3}\Delta'^{\frac{5}{2}} \int_0^{\infty} \left\{ \left[1+z^2\right]^{\frac{3}{4}} - z^{\frac{3}{2}} \right\} dx. \qquad (3.92)
\end{aligned}
$$

This integral is divergent. Obviously, this tangle is not a physical consequence of the ground state energy, which is finite in its discrete form in Eq. (3.83). It is the result of the approach in the continuum limit which is chosen for calculation *i.e.* introducing cutoff in the vanishing coupling energy $\Delta' \ll \epsilon_F$. We can get rid of this disaster, by adding and subtracting a term correspond to the derivative of the integrand in Eq. (3.91), the integral in Eq. (3.92) would become convergent. Therefore, we show the following relation for the integrand

$$
\begin{aligned}
\Delta'^2 \times \lim_{\Delta'^2\to 0} \frac{\left[(1-x)^2+\Delta'^2\right]^{\frac{3}{4}} - (1-x)^{\frac{3}{2}}}{\Delta'^2} &= \frac{\partial}{\partial\zeta}\Big\{ \left[(1-x)^2+\zeta\right]^{\frac{3}{4}} \Big\}|_{\zeta=0} \\
&= \frac{3}{4}\frac{1}{\sqrt{1-x}}\Delta'^2, \qquad (3.93)
\end{aligned}
$$

We rewrite the integral in Eq. (3.91) once agin as

$$
\begin{aligned}
(3.91) \quad &= \frac{2^{\frac{5}{2}}}{3}\int_\lambda^1 \left\{ \left[(1-x)^2+\Delta'^2\right]^{\frac{3}{4}} - (1-x)^{\frac{3}{2}} - \frac{3}{4}\frac{1}{\sqrt{1-x}}\Delta'^2 \right\} dx + \frac{2^{\frac{5}{2}}}{3}\int_\lambda^1 \frac{3}{4}\frac{1}{\sqrt{1-x}}\Delta'^2\, dx \\
&= \frac{2^{\frac{5}{2}}}{3}\Delta'^{\frac{5}{2}}\int_0^{\infty} \left\{ \left[1+z^2\right]^{\frac{3}{4}} - z^{\frac{3}{2}} - \frac{3}{4\sqrt{z}} \right\} dx + \sqrt{2}\int_\lambda^1 \frac{1}{\sqrt{1-x}}\Delta'^2\, dx. \qquad (3.94)
\end{aligned}
$$

The first integral in Eq. (3.94) is convergent, contrary to integral in Eq. (3.92). If we scrutinize the SDW ground state energy in its discrete form in (3.83), we see that in the weak coupling regime $\Delta \ll \epsilon_F$ the sum in the ground state energy has a term proportional to the square of the order parameter times the response function as

$$
\begin{aligned}
& 2\sum_{1^{st}BZ}\left[\frac{\epsilon_{1k}+\epsilon_{2k}}{2} - \sqrt{\left(\frac{\epsilon_{1k}-\epsilon_{2k}}{2}\right)^2 + \Delta^2} - \mu \right] \\
= \; & 2\sum_{1^{st}BZ}\left[\frac{\epsilon_{1k}+\epsilon_{2k}}{2} - \left(\frac{\epsilon_{1k}-\epsilon_{2k}}{2}\right)\sqrt{1+\left(\frac{\epsilon_{1k}-\epsilon_{2k}}{2}\right)^{-2}\Delta^2} - \mu \right] \\
\approx \; & 2\sum_{1^{st}BZ}\left[\frac{\epsilon_{1k}+\epsilon_{2k}}{2} - \left(\frac{\epsilon_{1k}-\epsilon_{2k}}{2}\right)\left\{1+\frac{1}{2}\left(\frac{\epsilon_{1k}-\epsilon_{2k}}{2}\right)^{-2}\Delta^2\right\} - \mu \right] \\
\propto \; & 2\,\Delta^2 \sum_{1^{st}BZ}\frac{1}{\epsilon_{1k}-\epsilon_{2k}}. \qquad (3.95)
\end{aligned}
$$

The last term is in the close similarity with the response function in Eq. (3.67). Therefore, the extra term in Eq. (3.94) is just the response function, at the same level of approximation

in Eq. (3.74). So we return to the extra term in Eq. (3.94), and give up the cutoff idea to obtain the original form of the response function with the correct coefficient

$$\begin{aligned}\sqrt{2}\Delta'^2\int_\lambda^1 \frac{1}{\sqrt{1-x}}\,dx \quad &\rightarrow \quad \Delta'^2\int_0^1\left\{\sqrt{\frac{1+x}{1-x}}+\sqrt{\frac{1-x}{1+x}}\right\}dx \\ &= \quad \pi\Delta'^2. \end{aligned} \tag{3.96}$$

By performing the first integral in Eq. (3.94) and insert it in the condensation energy, we obtain

$$\begin{aligned} E^{con} &= E^N - E^{SDW} \\ &= E^N\frac{8}{\pi}\left\{\frac{2^{\frac{5}{2}}}{3}\Delta'^{\frac{5}{2}}\int_0^\infty\left\{\left[1+z^2\right]^{\frac{3}{4}}-z^{\frac{3}{2}}-\frac{3}{4\sqrt{z}}\right\}dx+\pi\Delta'^2\right\}-\frac{8\Delta'^2\,\epsilon_F^2\,L^2}{\tilde{V}_{\boldsymbol{q}}} \\ &= E^N\left\{\frac{16}{5}\sqrt{\frac{2}{\pi}}\,\frac{\Gamma(-\frac{1}{4})}{\Gamma(\frac{1}{4})}\,\Delta'^{\frac{5}{2}}+8\Delta'^2\right\}-\frac{8\Delta'^2\,\epsilon_F^2\,L^2}{\tilde{V}_{\boldsymbol{q}}}. \\ &. \end{aligned} \tag{3.97}$$

Once again, we check the consistency of the condensation energy and the order parameter. Minimizing Eq. (3.97) with respect to Δ' and using Eq. (3.86), we write

$$\begin{aligned} 0 &= \partial_{\Delta'}E^{con} = E^N\left\{\frac{16}{5}\sqrt{\frac{2}{\pi}}\,\frac{\Gamma(-\frac{1}{4})}{\Gamma(\frac{1}{4})}\,\frac{5}{2}\Delta'^{\frac{3}{2}}+16\Delta'\right\}-\frac{16\Delta'\,\epsilon_F^2\,L^2}{\tilde{V}_{\boldsymbol{q}}}, \\ \Rightarrow\quad \Delta' &= \Delta'\,\omega(E)\,\frac{\tilde{V}_{\boldsymbol{q}}}{L^2}\left(1+\frac{1}{\sqrt{2\pi}}\,\frac{\Gamma(\frac{-1}{4})}{\Gamma(\frac{1}{4})}\sqrt{\Delta'}\right) \\ &= \Delta'\,\omega(E)\,\frac{\tilde{V}_{\boldsymbol{q}}}{L^2}\left(1-0.54\sqrt{\Delta'}\right), \end{aligned} \tag{3.98}$$

which is exactly the same as the final equation for the order parameter in Eq. (3.77). We solve Eq. (3.98) to obtain

$$\omega(E)\frac{L^2}{V_q} \quad = \quad \frac{E^N}{\epsilon_F^2}\frac{L^2}{\tilde{V}_{\boldsymbol{q}}} = \left(1+\frac{1}{\sqrt{2\pi}}\,\frac{\Gamma(\frac{-1}{4})}{\Gamma(\frac{1}{4})}\sqrt{\Delta'}\right),$$

and place it in Eq. (3.97) we have

$$\begin{aligned} E^{con} &= E^N\left\{\frac{16}{5}\sqrt{\frac{2}{\pi}}\,\frac{\Gamma(-\frac{1}{4})}{\Gamma(\frac{1}{4})}\,\Delta'^{\frac{5}{2}}+8\Delta'^2\right\}-\frac{8\Delta'^2\,\epsilon_F^2\,L^2}{\tilde{V}_{\boldsymbol{q}}} \\ &= E^N\left\{\frac{16}{5}\sqrt{\frac{2}{\pi}}\,\frac{\Gamma(-\frac{1}{4})}{\Gamma(\frac{1}{4})}\,\Delta'^{\frac{5}{2}}+8\Delta'^2-8\Delta'^2-\frac{8}{\sqrt{2\pi}}\,\frac{\Gamma(\frac{-1}{4})}{\Gamma(\frac{1}{4})}\sqrt{\Delta'}\right\} \\ &= E^N\left(\frac{8}{\sqrt{2\pi}}-\frac{16}{5}\sqrt{\frac{2}{\pi}}\right)\,\frac{\Gamma(-\frac{1}{4})}{\Gamma(\frac{1}{4})}\,\Delta'^{\frac{5}{2}} \\ &= 0.87\,E^N\,\Delta'^{\frac{5}{2}}. \end{aligned} \tag{3.99}$$

We engage the final form of the order parameter in Eq. (3.82) to obtain the ultimate form of the condensation energy as

$$E^{con} = 19.06\, E^N \left(1 - \frac{r_s^c}{r_s}\right)^5 . \tag{3.100}$$

The positive sign of the condensation energy provides that the system in SDW phase has a lower energy rather than the normal state. As we showed in Sec. 3.3.2, the lowest energy in the SDW phase, in the framework of mean-field theory, achieved by a triangular lattice. Then the lowest condensation energy is three times of the Eq. (3.99).

3.4.2 In the case of partially-filled second Brillouin zone $q \leq 2k_F$

The critical points in Fig. 3.2, correspond to the area within interval ($y \leq \frac{1}{2}$, $x = 1$) is studied in the preceding section. In this section, we analyze the parts of the critical points correspond to the interval ($y > \frac{1}{2}$, $x < 1$).This regime $q < 2k_F$, shows a rich phases and increased number coupling in compare to the other regime $q = 2k_F$.

As it is represented in the section 3.3.2, the lowest energy in the SDW phase is provided by the triangular lattice (the Fermi surface in such reciprocal space is depicted in Fig. 3.5). We start to study the phase diagram in the current regime by decreasing the coupling vector $\boldsymbol{q}$ for fixed Fermi energy or equivalently, we increase the Fermi energy versus the fixed coupling vector. By changing the ratio of Fermi wavevector and the coupling vector, we are interested in the behavior of the system by changing the configuration of the system y throughout the critical points (see Fig. 3.2).

It is apparent that by increasing the Fermi surface over the fixed lattice basis, gradually more and more Brillouin zones would be included inside the Fermi surface. While blowing the Fermi surface, the system encounters with the moment where the Fermi surface placed precisely at the vertexes and so-called nesting happens. As the system enters to a new BZ, consequently a new term would appear in the ground state energy. Hence, the ground state of the system shows a sudden change whenever it passes such nesting points. Actually, the system undergoes a phase transition from SDW phase to SDW phase, due to non-analytical behavior of the ground state at the nesting moments. The behavior of the condensation energy is shown schematically in Fig. 3.7 versus an external parameter. This transition from SDW to SDW would be a first order phase transition as the first derivation of the energy shows a singularity.

In the following, the order parameter and condensation energy, corresponding to the case that the Fermi surface lied over the first and second BZ, would be presented presented. The procedure is the same as done in previous section. We first present the calculations for order parameter.

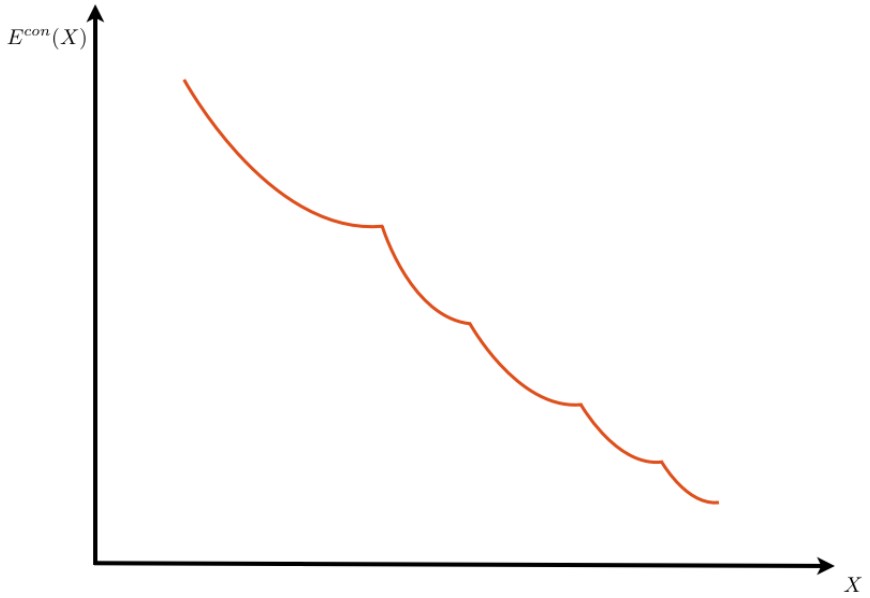

Figure 3.7: The schematic representation of the condensation energy versus an external parameter, say strength of the interaction r_s or interlayer separation y. The non-analytical points, where marked by sudden drop of the diagram, are associated with the nesting points where the translational vector $|\boldsymbol{q}|$ and Fermi energy k_F are commensurate: $q = (m/n)k_F$ by integral m and n.

Order parameter for $q < 2k_F$: case of $\beta^2 \gg 2\Delta'$

Since the Fermi surface is expanded into the second BZ, the corresponding term has to be included into condensation energy. Because the couplings of each particle is yet single, one particle coupled to at most one hole, then it suffices to consider a one dimensional lattice and at the end of calculations, we count the 3 independent coupling area of the triangular lattice by a factor of three.

We start to calculate the order parameter by use of Eq. (3.64) and also rename the coupling vector as $\boldsymbol{q} = 2\boldsymbol{p}$. So the interaction potential looks like

$$\tilde{V}(\boldsymbol{q} = 2\boldsymbol{p}) \quad = \quad \pi\, d_{eff}^2\; 2p\; \exp\left(-2lp\right), \tag{3.101}$$

The self-consistent equation order parameter in Eq. (3.64), can be written

$$\begin{aligned} \Delta \quad &= \quad \frac{\tilde{V}_{2\mathbf{p}}}{2L^2}\,\Delta \sum_{1^{st}BZ} \frac{1}{\sqrt{\left((\epsilon_{1k} - \epsilon_{2k})/2\right)^2 + \Delta^2}} \\ &- \quad \frac{\tilde{V}_{2\mathbf{p}}}{2L^2}\,\Delta \sum_{2^{nd}BZ} \frac{1}{\sqrt{\left((\epsilon_{1k} - \epsilon_{2k})/2\right)^2 + \Delta^2}}, \end{aligned} \tag{3.102}$$

where once again we took the order parameter as k-independent for the region in the vicinity of the critical point. We introduce the idea of cutoff, the same as we did in previous sections,

but this time two different cutoff: one for the first BZ λ_1 and the other for the second BZ λ_2, which is depicted in Fig. 3.8. Hereby, the continuum limit of the order parameter is written

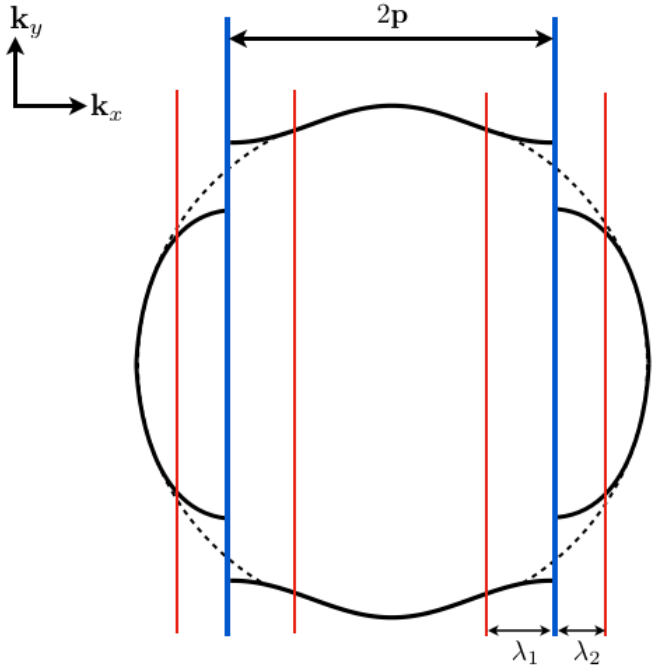

Figure 3.8: The Fermi surface in the SDW phase (solid line) and normal phase (dashed line) are shown. Two cutoffs are introduced: one in the first BZ and the second in the second BZ.

$$\Delta' = \frac{\Delta' \tilde{V}_{2\mathbf{p}}}{2L^2} \left(\frac{L}{2\pi}\right)^2 \frac{m}{\hbar^2} \left\{ \int^{1^{st}BZ} \frac{dxdy}{\sqrt{(1-|x|)^2 + \Delta'^2}} - \int^{2^{st}BZ} \frac{dxdy}{\sqrt{(1-|x|)^2 + \Delta'^2}} \right\}, \tag{3.103}$$

where the the order parameter is normalized as $\Delta' = \Delta/2\epsilon_{\boldsymbol{p}}$ and the variables as $x = k_x/p$ and $y = k_y/p$, where $k^2 = k_x^2 + k_y^2$, and also we used $\boldsymbol{k}.\boldsymbol{q} = 2\boldsymbol{k}.\boldsymbol{p} = 2k_x p$. Before proceeding further, we derive the Fermi surface (Fig. 3.8) as a function of x for y by use of Eq. (3.55), for both BZ as

$$\begin{aligned} \mu &= \frac{\epsilon_{1\boldsymbol{k}} + \epsilon_{2\boldsymbol{k}}}{2} \pm \sqrt{\left(\frac{\epsilon_{1\boldsymbol{k}} - \epsilon_{2\boldsymbol{k}}}{2}\right)^2 + \Delta^2} \\ &= \frac{\hbar^2}{2m}\frac{1}{2}\left[k^2 + (\boldsymbol{k}+\boldsymbol{q})^2\right] \pm \sqrt{\left\{\frac{\hbar^2}{2m}\frac{1}{2}\left[k^2 - (\boldsymbol{k}+\boldsymbol{q})^2\right]\right\}^2 + \Delta^2} \\ &= \frac{\hbar^2 p^2}{2m}\left[x^2 + y^2 + 2(1-|x|) \pm 2\sqrt{(1-|x|)^2 + \Delta'^2}\right], \end{aligned} \tag{3.104}$$

and by introducing the dimensionless parameters

$$\begin{cases} \alpha = \frac{k_F}{p}, \\ \\ \beta^2 = 1 + \alpha^2. \end{cases} \tag{3.105}$$

Then Eq. (3.104) can be written as

$$1 + \beta^2 = \alpha^2 = \frac{\epsilon_F}{\epsilon_p} = x^2 + y^2 + 2(1 - |x|) \pm 2\sqrt{(1 - |x|)^2 + \Delta'^2}.$$

Thus can be readily solved for y to obtain

$$y = \sqrt{\beta^2 \mp 2\sqrt{(1 - |x|)^2 + \Delta'^2} - (1 - |x|)^2}, \tag{3.106}$$

where positive result corresponds to the first BZ and negative one for the second BZ. We put the order parameter zero, for the area far from the boundary zone in Eq. (3.103), and the integral of the order parameter reduces to the response function, as is showed in Sec. 3.4.1. Hence, there would be

$$\begin{aligned} \Delta' = \frac{\Delta'\tilde{V}_{2\boldsymbol{p}}}{2L^2} \left(\frac{L}{2\pi}\right)^2 \frac{m}{\hbar^2} 4 \Bigg\{ \pi \quad &+ \quad \int_{1-\lambda_1}^{1} \int_{0}^{\sqrt{\beta^2 + 2\sqrt{(1-x)^2+\Delta'^2} - (1-x)^2}} \frac{dxdy}{\sqrt{(1-x)^2 + \Delta'^2}} \\ &- \quad \int_{1-\lambda_1}^{1} \int_{0}^{\sqrt{1+\beta^2-x^2}} \left(\frac{1}{1-x} + \frac{1}{1+x}\right) dxdy \\ &- \quad \int_{1}^{1+\lambda_2} \int_{0}^{\sqrt{\beta^2 - 2\sqrt{(1-x)^2+\Delta'^2} - (1-x)^2}} \frac{dxdy}{\sqrt{(1-x)^2 + \Delta'^2}} \\ &- \quad \int_{1}^{1+\lambda_2} \int_{0}^{\sqrt{1+\beta^2-x^2}} \left(\frac{1}{1-x} + \frac{1}{1+x}\right) dxdy \Bigg\}, \end{aligned} \tag{3.107}$$

where π is the integral of the response function in the regime $q = 2p \leq 2k_F$, and is shown in Eq. (3.67). The integrals in the second and fourth lines are subtracted from the complete integral of the response function to give the correct limit of the integral. In the upper limits of integrals, we neglect the square term in compare with square root one, for $(1-x)^2 \ll \sqrt{(1-x)^2 + \Delta'^2}$ which is valid for the area extremely close to the boundary zone $(1 - x) \ll 1$. Also, for the integrals of the response function, second and fourth integral after writing them in common denominator, we approximate within the same regime as $1 - x^2 \approx 2(1 - x)$. It has to be noted that the integral in the second BZ just has value for $\beta^2 \geq 2\sqrt{(1-x)^2 + \Delta'^2}$. We take the cutoff in the second BZ to has a definite value equal to its maximum value as

$$\begin{aligned} \beta^2 &= 2\sqrt{\lambda_2^2 + \Delta'^2}, \\ \Rightarrow \lambda_2 &= \sqrt{\frac{\beta^4}{4} - \Delta'^2}. \end{aligned} \tag{3.108}$$

By performing the y-component integral and renaming the variables by $z = (1-x)/\Delta'$ for the first band and $z = (x-1)/\Delta'$ for the second band, by make use of $\omega(E) = mL^2/2\pi\hbar^2$, there would be

$$\begin{aligned}\Delta' = \frac{\tilde{V}_{2\boldsymbol{p}}}{L^2}\,\omega(E)\,\frac{\Delta'}{\pi}\Bigg\{\pi \;&+\; \beta\int_0^{\frac{\lambda_1}{\Delta'}}\left[\frac{\sqrt{1+\sigma\sqrt{1+z^2}}}{\sqrt{1+z^2}} - \frac{\sqrt{1+\sigma z}}{z}\right]dz \\ &-\; \beta\int_0^{\frac{\lambda_2}{\Delta'}}\left[\frac{\sqrt{1-\sigma\sqrt{1+z^2}}}{\sqrt{1+z^2}} - \frac{\sqrt{1-\sigma z}}{z}\right]dz\Bigg\},\end{aligned} \tag{3.109}$$

that we have introduced a new parameter $\sigma = 2\Delta'/\beta^2$. These integrals cannot be done analytically. So we expand them for small σ in the regime $\beta^2 \gg 2\Delta'$, which implies the region far from the band gap but yet within the cutoff $\beta^2 < 2\lambda$. Keep the approximation up to the first order in σ leaves the integral convergent as

$$\begin{aligned}\Delta' &= \frac{\tilde{V}_{2\boldsymbol{p}}}{L^2}\,\omega(E)\,\frac{\Delta'}{\pi}\Bigg\{\pi \;+\; \beta\int_0^{\frac{\lambda_1}{\Delta'}}\left[\frac{1+\frac{1}{2}\sigma\sqrt{1+z^2}}{\sqrt{1+z^2}} - \frac{1+\frac{1}{2}\sigma z}{z}\right]dz \\ &\qquad -\; \beta\int_0^{\frac{\lambda_2}{\Delta'}}\left[\frac{1-\frac{1}{2}\sigma\sqrt{1+z^2}}{\sqrt{1+z^2}} - \frac{1-\frac{1}{2}\sigma z}{z}\right]dz\Bigg\} \\ &= \frac{\tilde{V}_{2\boldsymbol{p}}}{L^2}\,\omega(E)\,\frac{\Delta'}{\pi}\Bigg\{\pi \;+\; \beta\int_0^{\frac{\lambda_1}{\Delta'}}\left[\frac{1}{\sqrt{1+z^2}} - \frac{1}{z}\right]dz - \beta\int_0^{\frac{\lambda_2}{\Delta'}}\left[\frac{1}{\sqrt{1+z^2}} - \frac{1}{z}\right]dz\Bigg\} \\ &= \frac{\tilde{V}_{2\boldsymbol{p}}}{L^2}\,\omega(E)\,\frac{\Delta'}{\pi}\Bigg\{\pi \;+\; \beta\int_{\frac{\lambda_2}{\Delta'}}^{\frac{\lambda_1}{\Delta'}}\left[\frac{1}{\sqrt{1+z^2}} - \frac{1}{z}\right]dz\Bigg\}.\end{aligned} \tag{3.110}$$

Now by taking the infinite limit of the first band cutoff $\lambda_1 \to \infty$, simultaneously keeping the order parameter finite and small, and also using the definite value of the second band cutoff in Eq. (3.108), we perform the integral in Eq. (3.110) by renaming the lower limit of the second integral with $a = \lambda_2/\Delta' = \sqrt{\sigma^{-2}-1}$, we obtain

$$\begin{aligned}\Delta' &= \frac{\tilde{V}_{2\boldsymbol{p}}}{L^2}\,\omega(E)\,\frac{\Delta'}{\pi}\Bigg\{\pi \;+\; \beta\int_a^{\infty}\left[\frac{1}{\sqrt{1+z^2}} - \frac{1}{z}\right]dz\Bigg\} \\ &= \frac{\tilde{V}_{2\boldsymbol{p}}}{L^2}\,\omega(E)\,\frac{\Delta'}{\pi}\Big\{\pi \;+\; \beta\left[\ln(2a) - \sinh^{-1}(a)\right]\Big\}.\end{aligned} \tag{3.111}$$

We expand the $\sinh^{-1}(a)$ in the infinite limit $a = \sqrt{\sigma^{-2}-1} \gg 1$, which is valid for $\sigma = 2\Delta'\beta^2 \ll 1$, to obtain

$$\lim_{x\to\infty}\sinh^{-1}(x) \approx \ln(2x) + \frac{1}{4x^2} + \cdots, \tag{3.112}$$

and engaging this expansion in Eq. (3.111), leads to

$$\begin{aligned}
\Delta' &= \frac{V_{2p}}{L^2}\,\omega(E)\,\frac{\Delta'}{\pi}\Big\{\pi+\beta\left[\ln(2a)-\ln(2a)-\frac{a^{-2}}{4}\right]\Big\} \\
&= \frac{\tilde{V}_{2\boldsymbol{p}}}{L^2}\,\omega(E)\,\frac{\Delta'}{\pi}\Big\{\pi-\frac{\beta}{4}\frac{1}{\frac{1}{\sigma^{-2}}-1}\Big\} \\
&\approx \frac{\tilde{V}_{2\boldsymbol{p}}}{L^2}\,\omega(E)\,\frac{\Delta'}{\pi}\Big\{\pi-\frac{\beta}{4}\sigma^2\Big\} \\
&= \frac{\tilde{V}_{2\boldsymbol{p}}}{L^2}\,\omega(E)\,\Delta'\Big\{1-\frac{\Delta'^2}{\pi\beta^3}\Big\},
\end{aligned} \tag{3.113}$$

which reveals the explicit form of the order parameter. We solve it for Δ' to obtain

$$\Delta' = \sqrt{\pi\beta^3}\left(1-\frac{L^2}{\tilde{V}_{2\boldsymbol{p}}\omega(E)}\right)^{1/2}. \tag{3.114}$$

As we did in previous section, we rewrite the order parameter associated with the critical strength which vanishes the order parameter. Regarding the critical points in Fig. 3.2, we rewrite the dimensionless parameter α, introduced in Eq. (3.105) to obtain

$$\alpha = \begin{cases} 1 & y \le \frac{1}{2}, \\ \\ 2y & y > \frac{1}{2}, \end{cases} \tag{3.115}$$

and for Eq. (3.114) at the critical moment, we have

$$\begin{aligned}
\frac{L^2}{\omega(E)} &= \tilde{V}^c_{2\boldsymbol{p}} \\
&= r_s^c\,\frac{2\hbar^2}{m\alpha}\,\exp\left(-\frac{2y}{\alpha}\right)\Big|_{\alpha=2y} \\
&= r_s^c\,\frac{2\hbar^2}{2mey}.
\end{aligned} \tag{3.116}$$

At the end, the ultimate form of the order parameter looks

$$\Delta' = \sqrt{\pi\beta^3}\left(1-\frac{r_s^c}{r_s}\right)^{1/2}, \tag{3.117}$$

where $r_s^c = 2\pi ey$ by use of Eq. (3.116).

Condensation energy for $q < 2k_F$: case of $\beta^2 \gg 2\Delta'$

We start from Eq. (3.59), the exact ground state energy of SDW phase including sum over first and second BZ. Similar to the calculation for the order parameter we rename the coupling

vector $\boldsymbol{q} = 2\boldsymbol{p}$, and we introduce the cutoffs for both band as is shown in Fig. 3.8. We divide the integral of the energy for area within the cutoff and outside the cutoff. The same as the order parameter, we perform the calculation for one dimensional lattice and at the end compensate it by a factor of three. The ground state energy reads

$$\begin{aligned}
E^0_{SDW} &= 2\sum_{1^{st}BZ}\left(\frac{\epsilon_{1\boldsymbol{k}}+\epsilon_{2\boldsymbol{k}}}{2}-\sqrt{\left(\frac{\epsilon_{1\boldsymbol{k}}-\epsilon_{2\boldsymbol{k}}}{2}\right)^2+\Delta^2}-\mu\right)\\
&+ 2\sum_{2^{nd}BZ}\left(\frac{\epsilon_{1\boldsymbol{k}}+\epsilon_{2\boldsymbol{k}}}{2}+\sqrt{\left(\frac{\epsilon_{1\boldsymbol{k}}-\epsilon_{2\boldsymbol{k}}}{2}\right)^2+\Delta^2}-\mu\right)+\frac{2\Delta^2L^2}{\tilde{V}_{2\boldsymbol{p}}}\\
&= 2\sum_{1^{st}BZ}\left\{\frac{\hbar^2}{2m}\frac{1}{2}\left[k^2+(\boldsymbol{k}+\boldsymbol{q})^2\right]-\sqrt{\left\{\frac{\hbar^2}{2m}\frac{1}{2}\left[k^2-(\boldsymbol{k}+\boldsymbol{q})^2\right]\right\}^2+\Delta^2}-\epsilon_F\right\}\\
&+ 2\sum_{2^{nd}BZ}\left\{\frac{\hbar^2}{2m}\frac{1}{2}\left[k^2+(\boldsymbol{k}+\boldsymbol{q})^2\right]+\sqrt{\left\{\frac{\hbar^2}{2m}\frac{1}{2}\left[k^2-(\boldsymbol{k}+\boldsymbol{q})^2\right]\right\}^2+\Delta^2}-\epsilon_F\right\}\\
&+ \frac{2\Delta^2L^2}{\tilde{V}_{2\boldsymbol{p}}}\\
&= 2\frac{\hbar^2}{2m}\left(\frac{L^2}{2\pi}\right)p^4\int^{1^{st}BZ}\left\{x^2+y^2+2(1-|x|)-2\sqrt{(1-|x|)^2+\Delta'^2}-\alpha^2\right\}dxdy\\
&+ 2\frac{\hbar^2}{2m}\left(\frac{L^2}{2\pi}\right)p^4\int^{2^{nd}BZ}\left\{x^2+y^2+2(1-|x|)+2\sqrt{(1-|x|)^2+\Delta'^2}-\alpha^2\right\}dxdy\\
&+ \frac{8\Delta'^2\epsilon_{\boldsymbol{p}}^2L^2}{\tilde{V}_{2\boldsymbol{p}}},
\end{aligned}\tag{3.118}$$

where we normalized variables as $x = k_x/p$, $y = k_y/p$, $\Delta' = \Delta/2\epsilon_p$ and α is introduced in Eq. (3.105). The orientation of the coupling vector is such that $\boldsymbol{k}.\boldsymbol{q} = 2\boldsymbol{k}.\boldsymbol{p} = -2k_xp$. We solved y-component as the function of x-component in Eq. (3.106) for the upper limits of the integral. The ground state energy looks

$$\begin{aligned}
E^{SDW} &= \frac{16E^N}{3\pi\alpha^4}\Bigg\{\int_0^{1-\lambda_1}\int_0^{\sqrt{1+\beta^2-x^2}}\Big\{y^2+x^2-\beta^2-1\Big\}dxdy\\
&+ \int_{1-\lambda_1}^{1}\int_0^{\sqrt{\beta^2+2\sqrt{(1-x^2)+\Delta'^2}-(1-x)^2}}\Big\{y^2+(1-x)^2-2\sqrt{(1-x)^2+\Delta'^2}-\beta^2\Big\}dxdy\\
&+ \int_{1}^{1+\lambda_2}\int_0^{\sqrt{\beta^2+2\sqrt{(1-x^2)+\Delta'^2}-(1-x)^2}}\Big\{y^2+(1-x)^2+2\sqrt{(1-x)^2+\Delta'^2}-\beta^2\Big\}dxdy\\
&+ \int_{1+\lambda_2}^{\alpha^2}\int_0^{\sqrt{1+\beta^2-x^2}}\Big\{y^2+x^2-\beta^2-1\Big\}dxdy\Bigg\}+\frac{8\Delta'^2L^2\epsilon_{\boldsymbol{p}}^2}{\tilde{V}_{2\boldsymbol{p}}}.
\end{aligned}\tag{3.119}$$

Before proceeding further, it is good to mention that by doing the same as we did in previous section, we can check the consistency of Eq. (3.119) with the order parameter, at the same level of calculation in Eq. (3.107). Actually, it is the same as the Eq. (3.86) just an extra integral for the second BZ which has the same form.

We add and subtracts terms a term to Eq. (3.119), to make the integral outside the cutoff in the form of the ground state energy of the normal phase. By neglecting the square term in compare with the square root term, for $(1-x)^2 \ll \sqrt{1-x}$ for area close to the boundary $(1-x) \ll 1$. Also, we approximate further as $(1-x^2) \approx 2(1-x)$ in the integral outside the cutoff. The y-component of the integral takes the form

$$E^{con} = \frac{16E^N}{3\pi\alpha^4}\Bigg\{ \int_{1-\lambda_1}^{1} \Big\{ \Big[\beta^2 + 2\sqrt{(1-x)^2+\Delta'^2}\Big]^{3/2} \quad - \quad \big[\beta^2 + 2(1-x)\big]^{3/2} \Big\} dx + \int_{1}^{1+\lambda_2} \Big\{ \Big[\beta^2 - 2\sqrt{(1-x)^2+\Delta'^2}\Big]^{3/2} \quad - \quad \big[\beta^2 + 2(1-x)\big]^{3/2} \Big\} dx \Bigg\} + \frac{8\Delta'^2 L^2 \epsilon_{\boldsymbol{p}}^2}{\tilde{V}_{2\boldsymbol{p}}}, \tag{3.120}$$

which $E^{con} = E^N - E^{SDW}$. Now by renaming the integrals variables as $z = (1-x)/\Delta'$ for the first BZ integral and $z = (1-x)/\Delta'$ for the second one and introducing $\sigma = 2\Delta'/\beta^2$ we write the integral as

$$E^{con} = \frac{16E^N}{3\pi\alpha^4}\Delta'\beta^3\Bigg\{ \int_{0}^{\frac{\lambda_1}{\Delta'}} \big\{(1+\sigma\sqrt{1+z^2})^{3/2} \quad - \quad (1+\sigma z)^{3/2}\big\} dz + \int_{0}^{\frac{\lambda_2}{\Delta'}} \big\{(1-\sigma\sqrt{1+z^2})^{3/2} \quad - \quad (1-\sigma z)^{3/2}\big\} dz \Bigg\} + \frac{8\Delta'^2 L^2 \epsilon_{\boldsymbol{p}}^2}{\tilde{V}_{2\boldsymbol{p}}}. \tag{3.121}$$

In Eq. (3.121), the cutoff in the second BZ has a definite value which is presented in Eq. (3.108). By the way, the integral in this form cannot be done analytically and similar to the calculations for the order parameter we expand the integrands for small σ. So we have for the integrals in Eq. (3.121) up to first order

$$\begin{aligned} & \int_0^{\frac{\lambda_1}{\Delta'}} \Big\{(1+\sigma\sqrt{1+z^2})^{3/2} - (1+\sigma z)^{3/2}\Big\} dz + \int_0^{\frac{\lambda_2}{\Delta'}} \Big\{(1-\sigma\sqrt{1+z^2})^{3/2} - (1-\sigma z)^{3/2}\Big\} dz \\ = & \int_0^{\frac{\lambda_1}{\Delta'}} \Big\{(1+\frac{3}{2}\sigma\sqrt{1+z^2}) - (1+\frac{3}{2}\sigma z)\Big\} dz + \int_0^{\frac{\lambda_2}{\Delta'}} \Big\{(1-\frac{3}{2}\sigma\sqrt{1+z^2}) - (1-\frac{3}{2}\sigma z)\Big\} dz \\ = & \frac{3}{2}\sigma\Big\{\int_0^{\frac{\lambda_1}{\Delta'}} (\sqrt{1+z^2}-z)dz - \int_0^{\frac{\lambda_2}{\Delta'}} (\sqrt{1+z^2}-z)dz\Big\} \\ = & \frac{3}{2}\sigma\int_{\frac{\lambda_2}{\Delta'}}^{\frac{\lambda_1}{\Delta'}} (\sqrt{1+z^2}-z)dz. \end{aligned} \tag{3.122}$$

The lower limit of the last integral is $\lambda_2/\Delta' = \sqrt{\sigma^{-2}-1} = a$ and the upper limit has to go to infinity $\lambda_1/\Delta' \to \infty$. But in this regime this integral is divergent and has to be behaved through the same way that we did in previous section: as it was shown the leading term in the discrete form of the ground state energy is proportional to the response function times square of the order parameter. we add and subtract a term which is equal to the response function at the same level of approximation. So we have

$$(3.122) = \frac{3}{2}\sigma \left\{ \int_a^\infty (\sqrt{1+z^2} - z - \frac{1}{2z})dz + \int_a^\infty \frac{1}{2z}dz \right\}. \tag{3.123}$$

First we calculate the extra term. It is the same as the integral of the response function in Eq. (3.110). So this integral form of the response function in Eq. (3.110) has to give the value of the response function which is π (look Eq. (3.67)). Then, the following relation is valid

$$\beta \int_a^\infty \frac{1}{z}dz \equiv \pi.$$

The extra term in Eq. (3.123) achieves the value as

$$\int_a^\infty \frac{1}{2z}dz \equiv \frac{\pi}{2\beta}. \tag{3.124}$$

Now the first integral in Eq. (3.123) would be

$$\int_a^\infty (\sqrt{1+z^2} - z - \frac{1}{2z})dz = \frac{1}{4}\left[1 + 2a(a - \sqrt{1+a^2}) - 2\sinh^{-1}(a) + 2\ln(2a)\right]. \tag{3.125}$$

By expanding the result, term by term for large a, which is valid for small σ, and keep the terms up to the second order we have

$$\begin{aligned} 1 + 2a(a - \sqrt{1+a^2}) &= 1 + 2\sqrt{\sigma^{-2}-1}(\sqrt{\sigma^{-2}-1} - \sigma^{-1}) \\ &= 1 + 2(\sigma^{-2}-1) - 2\,\frac{\sqrt{\sigma^{-2}-1}}{\sigma} \\ &\approx 1 + 2(\frac{1}{\sigma^2} - 1) - \frac{2}{\sigma^2}(1 - \frac{\sigma^2}{2} - \frac{\sigma^4}{8}) \\ &= \frac{\sigma^2}{4}. \end{aligned} \tag{3.126}$$

We expand $\sinh^{-1} x$ around for large value by means of Eq. (3.112). Thus, the sum of the hyperbolic and logarithm terms in Eq. (3.125) leads to

$$2[-\sinh^{-1}(a) + \ln(2a)] \approx -\frac{2}{4}\frac{1}{a^2} = -\frac{2}{4}\frac{1}{\sigma^{-2}-1} \approx -\frac{2}{4}\sigma^2. \tag{3.127}$$

Finally, gathering all the terms and inserting back the integrals at the original place in Eq. (3.121), we write down the condensation energy as

$$\begin{aligned} E^{con} &= \frac{16E^N}{3\pi\alpha^4}\Delta'\beta^3\frac{3\sigma}{2}\left\{\frac{1}{4}(\frac{1}{4}\sigma^2-\frac{2}{4}\sigma^2)+\frac{\pi}{2\beta}\right\}-\frac{8\Delta'^2L^2\epsilon_{\boldsymbol{p}}^2}{\tilde{V}_{2\boldsymbol{p}}} \\ &= \frac{8E^N}{\alpha^4}\left\{\Delta'^2-\frac{\Delta'^4}{2\pi\beta^3}\right\}-\frac{8\Delta'^2L^2\epsilon_{\boldsymbol{p}}^2}{\tilde{V}_{2\boldsymbol{p}}}. \end{aligned} \tag{3.128}$$

That is the moment we can check, once agin, that the order parameter minimize the condensation energy

$$\begin{aligned} \partial_{\Delta'}E^{con} &= \frac{8E^N}{\alpha^4}\left\{2\Delta'-4\frac{\Delta'^3}{2\pi\beta^3}\right\}-\frac{16\Delta' L^2\epsilon_{\boldsymbol{p}}^2}{\tilde{V}_{2\boldsymbol{p}}}=0, \\ \Rightarrow\quad \Delta' &= \frac{\tilde{V}_{2\boldsymbol{p}}}{L^2}\,\omega(E)\,\Delta'\Big\{1-\frac{\Delta'^2}{\pi\beta^3}\Big\}, \end{aligned} \tag{3.129}$$

which is the same as the order parameter in Eq. (3.113), where we have used Eq. (3.86) and the relation

$$\frac{E^N}{\alpha^4\,\epsilon_{\boldsymbol{p}}^2}=\frac{E^N}{\epsilon_F^2}=\omega(E). \tag{3.130}$$

to derive Eq. (3.129). Now by engaging Eq. (3.129) in the form

$$\frac{L^2\epsilon_{\boldsymbol{p}}^2}{\tilde{V}_{2\boldsymbol{p}}}=\frac{8E^N}{\alpha^4}(1-\frac{\Delta'^2}{\pi\beta^3}). \tag{3.131}$$

We rewrite the condensation energy inEq. (3.128) as

$$\begin{aligned} E^{con} &= \frac{E^N}{\alpha^4}\left\{8\Delta'^2-\frac{4\Delta'^4}{\pi\beta^3}-8\Delta'^2+\frac{8\Delta'^4}{\pi\beta^3}\right\} \\ &= \frac{E^N}{\alpha^4}\frac{4\Delta'^4}{\pi\beta^3}. \end{aligned} \tag{3.132}$$

By replacing the final form of the order parameter in Eq. (3.117), the ultimate form of the condensation energy would be

$$E^{con}=E^N\,\frac{4\pi\beta^3}{(1+\beta^2)^2}\left(1-\frac{r_s^c}{r_s}\right)^2. \tag{3.133}$$

So the order parameter and the condensation energy are obtained self-consistency for the region of the phase diagram associated with $q<2k_F$ and $\beta^2\gg 2\Delta'$. The results of this regime do not merge into the results of the regime corresponds to $q=2k_F$ when $\beta\to 0$. Therefore, we once again solve the order parameter and the condensation energy with the same configuration of the Fermi surface but this time for $\beta^2\ll 2\Delta'$.

Order parameter for $q < 2k_F$: case of $\beta^2 \ll 2\Delta'$.

In this part, once again we repeat the procedure of the self-consistent calculations to obtain the order parameter and the condensation energy corresponded to the interval $(y > \frac{1}{2}, x < 1)$ of the critical points in Fig. 3.2. We perform the calculations in the asymptotic regime for $\beta^2 \ll 2\Delta'$ where $\sqrt{1+\beta^2}\, q = 2k_F$. Similar to the previous part, we obtain the parameters for a one-dimensional lattice and by a factor of three, we count the effect of the triangular lattice. We start by the integral form of the order parameter in Eq. (3.109). We write the equation into the favorable parameters associated with the current regime as

$$\begin{aligned}
\Delta' = \frac{\tilde{V}_{2\boldsymbol{p}}}{L^2}\,\omega(E)\,\frac{\Delta'}{\pi}\Bigg\{\pi \;&+\; \beta\int_0^{\frac{\lambda_1}{\Delta'}}\left[\frac{\sqrt{1+\sigma\sqrt{1+z^2}}}{\sqrt{1+z^2}} - \frac{\sqrt{1+\sigma z}}{z}\right]dz \\
&-\; \beta\int_0^{\frac{\lambda_2}{\Delta'}}\left[\frac{\sqrt{1-\sigma\sqrt{1+z^2}}}{\sqrt{1+z^2}} - \frac{\sqrt{1-\sigma z}}{z}\right]dz\Bigg\} \\
= \frac{\tilde{V}_{2\boldsymbol{p}}}{L^2}\,\omega(E)\,\frac{\Delta'}{\pi}\Bigg\{\pi \;&+\; \sqrt{2\Delta'}\int_0^{\frac{\lambda_1}{\Delta'}}\left[\frac{\sqrt{\frac{\beta^2}{2\Delta'}+\sqrt{1+z^2}}}{\sqrt{1+z^2}} - \frac{\sqrt{\frac{\beta^2}{2\Delta'}+z}}{z}\right]dz \\
&-\; \sqrt{2\Delta'}\int_0^{\frac{\lambda_2}{\Delta'}}\left[\frac{\sqrt{\frac{\beta^2}{2\Delta'}-\sqrt{1+z^2}}}{\sqrt{1+z^2}} - \frac{\sqrt{\frac{\beta^2}{2\Delta'}-z}}{z}\right]dz\Bigg\},
\end{aligned} \tag{3.134}$$

where $\sigma = 2\Delta'/\beta^2$. In the limit $\beta^2 \ll 2\Delta'$, the first term in the second integral dose not contribute as it is imaginary. The reason is actually absence of the states in the vicinity of the band gap. We attempt to explain the physical reason by employing the one dimensional system. The density of state vanishes close to the boundary of the BZ within the interval of $\epsilon_{\boldsymbol{p}} - \Delta < \epsilon_{\boldsymbol{k}} < \epsilon_{\boldsymbol{k}} + \Delta$, where $2\boldsymbol{p} = \boldsymbol{q}$ and $\boldsymbol{q}$ is the translational vector in 1D lattice. In the current regime $\beta^2 \ll 2\Delta'$, the second BZ states fall into the interval $\epsilon_{\boldsymbol{p}} < \epsilon_{\boldsymbol{p}} < \epsilon_F = \alpha^2\epsilon_{\boldsymbol{p}} = (1+\beta^2)\epsilon_{\boldsymbol{p}}$, and it can be shown that it is within the forbidden interval. The lhs limit is larger than the lhs of the forbidden area as obviously $\epsilon_{\boldsymbol{p}} - \Delta < \epsilon_{\boldsymbol{p}}$. The rhs can be shown that is smaller than the rhs of the forbidden one as $(1+\beta^2)\epsilon_{\boldsymbol{p}} < \epsilon_{\boldsymbol{p}} + \Delta \Rightarrow \beta^2\epsilon_{\boldsymbol{p}} < \Delta \Rightarrow \beta^2 < 2\Delta'$, which is indeed true as we are dealing with the regime $\beta^2 \ll 2\Delta'$. This reasoning is also true in 2D. We continue with Eq. (3.134), By neglecting the term in the second integral corresponds to the second BZ of the SDW phase, it reads

$$\begin{aligned}
\Delta' = \frac{\tilde{V}_{2\boldsymbol{p}}}{L^2}\,\omega(E)\,\frac{\Delta'}{\pi}\Bigg\{\pi + \sqrt{2\Delta'}\int_0^{\frac{\lambda_1}{\Delta'}}&\left[\frac{\sqrt{\frac{\beta^2}{2\Delta'}+\sqrt{1+z^2}}}{\sqrt{1+z^2}} - \frac{\sqrt{\frac{\beta^2}{2\Delta'}+z}}{z}\right]dz \\
&+\sqrt{2\Delta'}\int_0^{\frac{\lambda_2}{\Delta'}}\frac{\sqrt{\frac{\beta^2}{2\Delta'}-z}}{z}dz\Bigg\}.
\end{aligned} \tag{3.135}$$

Once again, considering the square root in the second integral, the upper limit has to be restricted with its maximum value as

$$\begin{aligned} \frac{\beta^2}{2\Delta'} &\geq \frac{\lambda_2}{\Delta'}, \\ \Rightarrow \quad \lambda_2 &= \frac{\beta^2}{2}. \end{aligned} \tag{3.136}$$

Rearranging Eq. (3.135), we have

$$\begin{aligned} \Delta' = \frac{\tilde{V}_{2\boldsymbol{p}}}{L^2}\,\omega(E)\,\frac{\Delta'}{\pi}\Bigg\{\pi \;&+\; \sqrt{2\Delta'}\int_{\frac{\lambda_2}{\Delta'}}^{\frac{\lambda_1}{\Delta'}}\left\{\frac{\sqrt{\frac{\beta^2}{2\Delta'}+\sqrt{1+z^2}}}{\sqrt{1+z^2}}-\frac{\sqrt{\frac{\beta^2}{2\Delta'}+z}}{z}\right\}dz \\ &+\; \sqrt{2\Delta'}\int_{0}^{\frac{\lambda_2}{\Delta'}}\frac{\sqrt{\frac{\beta^2}{2\Delta'}+\sqrt{1+z^2}}}{\sqrt{1+z^2}}dz \\ &+\; \sqrt{2\Delta'}\int_{0}^{\frac{\lambda_2}{\Delta'}}\left\{\frac{\sqrt{\frac{\beta^2}{2\Delta'}-z}}{z}-\frac{\sqrt{\frac{\beta^2}{2\Delta'}+z}}{z}\right\}dz\Bigg\}. \end{aligned} \tag{3.137}$$

We expand the integrands as a perturbation of $\beta^2/2\Delta'$, except the last integral that we keep it without expansion (in the last integral the term $\beta^2/2\Delta'$ is comparable with z). After rearranging, there would be

$$\begin{aligned} \Delta' \simeq \frac{\tilde{V}_{2\boldsymbol{p}}}{L^2}\,\omega(E)\,\frac{\Delta'}{\pi}\Bigg\{\pi \;&+\; \sqrt{2\Delta'}\int_{0}^{\frac{\lambda_1}{\Delta'}}\left\{\frac{1}{(1+z^2)^{\frac{1}{4}}}-\frac{1}{\sqrt{z}}\right\}dz \\ &+\; \sqrt{2\Delta'}\int_{0}^{\frac{\lambda_2}{\Delta'}}\frac{1}{\sqrt{z}}dz \\ &+\; \sqrt{2\Delta'}\int_{\frac{\lambda_2}{\Delta'}}^{\frac{\lambda_1}{\Delta'}}\frac{1}{2}\frac{\beta^2}{2\Delta'}\left\{\frac{1}{(1+z^2)^{\frac{3}{4}}}-\frac{1}{z^{\frac{3}{2}}}\right\}dz \\ &-\; \sqrt{2\Delta'}\int_{\frac{\lambda_2}{\Delta'}}^{\frac{\lambda_1}{\Delta'}}\frac{1}{8}\frac{\beta^4}{4\Delta'^2}\left\{\frac{1}{(1+z^2)^{\frac{5}{4}}}-\frac{1}{z^{\frac{5}{2}}}\right\}dz \\ &+\; \sqrt{2\Delta'}\int_{\frac{\lambda_2}{\Delta'}}^{\frac{\lambda_1}{\Delta'}}\frac{1}{2}\frac{\beta^2}{2\Delta'}\frac{1}{(1+z^2)^{\frac{3}{4}}}dz \\ &-\; \sqrt{2\Delta'}\int_{\frac{\lambda_2}{\Delta'}}^{\frac{\lambda_1}{\Delta'}}\frac{1}{8}\frac{\beta^4}{4\Delta'^2}\frac{1}{(1+z^2)^{\frac{5}{4}}}dz \\ &+\; \sqrt{2\Delta'}\int_{0}^{\frac{\lambda_2}{\Delta'}}\left\{\frac{\sqrt{\frac{\beta^2}{2\Delta'}-z}}{z}-\frac{\sqrt{\frac{\beta^2}{2\Delta'}+z}}{z}\right\}dz\Bigg\}, \end{aligned} \tag{3.138}$$

where we have separated the first integral, which is obtained by adding and subtracting a term is become equal to the order parameter in the regime $q = 2k_F$. The other terms are

corrections respect to the extension of the Fermi surface into the second BZ. Performing the integrals it looks

$$\begin{aligned}
\Delta' &= \Delta'\,\omega(E)\,\frac{\tilde{V}_{2\boldsymbol{p}}}{L^2}\left\{1-2\sqrt{\frac{2}{\pi}}\,\frac{\Gamma(\frac{3}{4})}{\Gamma(\frac{1}{4})}\,\sqrt{\Delta'}\right\} \\
&+ \omega(E)\,\frac{\tilde{V}_{2\boldsymbol{p}}}{L^2}\frac{1}{\sqrt{2\pi}}\frac{\Gamma(\frac{5}{4})}{\Gamma(\frac{3}{4})}\beta^2\sqrt{\Delta'} \\
&= \omega(E)\,\frac{\tilde{V}_{2\boldsymbol{p}}}{L^2}\Delta'\left\{1-0.54\,\sqrt{\Delta'}\right\} \\
&+ 0.29\,\omega(E)\,\frac{\tilde{V}_{2\boldsymbol{p}}}{L^2}\beta^2\sqrt{\Delta'}, \qquad (3.139)
\end{aligned}$$

where the first line of the result is exactly the same as the order parameter in the regime corresponds to $q = 2k_F$ in Eq. (3.77). The next term is the correction. We solve the quadratic equation to obtain the order parameter

$$\begin{aligned}
\sqrt{\Delta'} &= \frac{(\omega(E)\frac{\tilde{V}_{2\boldsymbol{p}}}{L^2}-1)+\sqrt{(\omega(E)\frac{\tilde{V}_{2\boldsymbol{p}}}{L^2}-1)^2+0.65\,(\omega(E)\frac{\tilde{V}_{2\boldsymbol{p}}}{L^2})^2\beta^2}}{1.08\,\omega(E)\frac{\tilde{V}_{2\boldsymbol{p}}}{L^2}}, \\
\Rightarrow\quad \Delta' &= \left\{\frac{(\omega(E)\frac{\tilde{V}_{2\boldsymbol{p}}}{L^2}-1)+\sqrt{(\omega(E)\frac{\tilde{V}_{2\boldsymbol{p}}}{L^2}-1)^2+0.65\,(\omega(E)\frac{\tilde{V}_{2\boldsymbol{p}}}{L^2})^2\beta^2}}{1.08\,\omega(E)\frac{\tilde{V}_{2\boldsymbol{p}}}{L^2}}\right\}^2. \qquad (3.140)
\end{aligned}$$

The disaster which is happened, is that the order parameter dose not vanish at the critical point $\omega(E)V_{2p}/L^2 = 1$. The reason is that we have neglected one of the term in Eq. (3.134).This non-vanishing order parameter is not a physical effect, because the order parameter in its discrete form in Eq. (3.102) merges to the instability equation at critical point. The problem has been created as the problematic approximations: in spite of vanishing limit of the order parameter $\Delta' \to 0$, we have introduced $\beta^2 \ll 2\Delta'$.

Any way, the aim was that to show that the order parameter for the regime $q < 2k_F$, coincides with its expression in regime $q = 2k_F$, which it does indeed:

$$\lim_{\beta\to 0}(3.139) = (3.77). \qquad (3.141)$$

Condensation energy for $q < 2k_F$: case of $\beta^2 \ll 2\Delta'$

After that we have checked the correct asymptotic behavior of the order parameter in different regime, we do the same for the condensation energy. We start with Eq. (3.121) and reform it as is proper for current regime

$$
\begin{aligned}
E^{con} &= \frac{16E^N}{3\pi\alpha^4}\,2^{\frac{3}{2}}\Delta'^{\frac{5}{2}}\Bigg\{\int_0^{\frac{\lambda_1}{\Delta'}}\Big\{(1+\sigma\sqrt{1+z^2})^{3/2} \;-\; (1+\sigma z)^{3/2}\Big\}dz \\
&\qquad + \int_0^{\frac{\lambda_2}{\Delta'}}\Big\{(1-\sigma\sqrt{1+z^2})^{3/2} \;-\; (1-\sigma z)^{3/2}\Big\}dz\Bigg\} + \frac{8\Delta'^2L^2\epsilon_{\boldsymbol{p}}^2}{\tilde{V}_{2\boldsymbol{p}}} \\
&= \frac{16E^N}{3\pi\alpha^4}\,2^{\frac{3}{2}}\Delta'^{\frac{5}{2}}\Bigg\{\int_0^{\frac{\lambda_1}{\Delta'}}\Big\{(\frac{\beta^2}{2\Delta'}+\sqrt{1+z^2})^{3/2} \;-\; (\frac{\beta^2}{2\Delta'}+z)^{3/2}\Big\}dz \\
&\qquad + \int_0^{\frac{\lambda_2}{\Delta'}}\Big\{(\frac{\beta^2}{2\Delta'}-\sqrt{1+z^2})^{3/2} \;-\; (\frac{\beta^2}{2\Delta'}-z)^{3/2}\Big\}dz\Bigg\} + \frac{8\Delta'^2L^2\epsilon_{\boldsymbol{p}}^2}{V_{2\boldsymbol{p}}}.
\end{aligned}
\tag{3.142}
$$

Once again, the integral of the second BZ has no contribution, as it lays over the forbidden region. The upper limit of the integral, owing to the square root of the integrand, has to have restricted value up to $\lambda_2 = \beta^2/2$. We expand the integrands and keep the terms up to the second order in $\beta^2/2\Delta' \ll 1$. We continue with integrals as

$$
\begin{aligned}
&\int_0^{\frac{\lambda_1}{\Delta'}}\Big\{(\frac{\beta^2}{2\Delta'}+\sqrt{1+z^2})^{3/2}-(\frac{\beta^2}{2\Delta'}+z)^{3/2}\Big\}dz - \int_0^{\frac{\lambda_2}{\Delta'}}(\frac{\beta^2}{2\Delta'}-z)^{3/2}dz \\
\approx\;& \int_0^{\frac{\lambda_1}{\Delta'}}\Big\{(1+z^2)^{\frac{3}{4}}+\frac{3}{2}\frac{\beta^2}{2\Delta'}(1+z^2)^{\frac{1}{4}}+\frac{3}{8}\frac{\beta^4}{4\Delta'^2}\frac{1}{(1+z^2)^{\frac{1}{4}}}\Big\}dz \\
-\;& \int_{\frac{\lambda_2}{\Delta'}}^{\frac{\lambda_1}{\Delta'}}\Big\{z^{\frac{3}{2}}+\frac{3}{2}\frac{\beta^2}{2\Delta'}\sqrt{z}+\frac{3}{8}\frac{\beta^4}{4\Delta'^2}\frac{1}{\sqrt{z}}\Big\}dz \\
-\;& \int_0^{\frac{\lambda_2}{\Delta'}}\Big\{(\frac{\beta^2}{2\Delta'}+z)^{\frac{3}{2}}+(\frac{\beta^2}{2\Delta'}-z)^{\frac{3}{2}}\Big\}dz.
\end{aligned}
\tag{3.143}
$$

After adding and subtracting some terms to obtain the integral of the condensation energy in $q = 2k_F$, we continue

$$
\begin{aligned}
(3.143) \;=\;& \int_0^{\frac{\lambda_1}{\Delta'}}\Big\{(1+z^2)^{\frac{3}{4}}-z^{\frac{3}{2}}\Big\}dz \\
+\;& \int_0^{\frac{\lambda_2}{\Delta'}} z^{\frac{3}{2}}dz \\
+\;& \int_{\frac{\lambda_2}{\Delta'}}^{\frac{\lambda_1}{\Delta'}}\Bigg\{\frac{3}{2}\frac{\beta^2}{2\Delta'}\Big[(1+z^2)^{\frac{1}{4}}-z^{\frac{1}{4}}\Big]+\frac{3}{8}\frac{\beta^4}{4\Delta'^2}\Big[\frac{1}{(1+z^2)^{\frac{1}{4}}}-\frac{1}{z^{\frac{1}{4}}}\Big]\Bigg\}dz \\
+\;& \int_0^{\frac{\lambda_2}{\Delta'}}\Big\{\frac{3}{2}\frac{\beta^2}{2\Delta'}(1+z^2)^{\frac{1}{4}}+\frac{3}{8}\frac{\beta^4}{4\Delta'^2}\frac{1}{(1+z^2)^{\frac{1}{4}}}\Big\}dz \\
-\;& \int_0^{\frac{\lambda_2}{\Delta'}}\Big\{(\frac{\beta^2}{2\Delta'}+z)^{\frac{3}{2}}+(\frac{\beta^2}{2\Delta'}-z)^{\frac{3}{2}}\Big\}dz.
\end{aligned}
\tag{3.144}
$$

The first line is exactly the integral of the condensation energy in $q = 2k_F$ regime (see Eq. (3.92)). The other lines constitute the correction correspond to the current regime. The integrals can be evaluated. The condensation energy would be

$$\begin{aligned} E^{con} &\approx \frac{E^N}{\alpha^4}\left\{\frac{16}{5}\sqrt{\frac{2}{\pi}}\,\frac{\Gamma(-\frac{1}{4})}{\Gamma(\frac{1}{4})}\,\Delta'^{\frac{5}{2}} + 8\Delta'^{2}\right\} - \frac{8\Delta'^{2}\,\epsilon_F^2\,L^2}{\alpha^4\tilde{V}_{2\boldsymbol{p}}} \\ &+ \frac{16\sqrt{2}}{3\sqrt{\pi}}\frac{\Gamma(-\frac{1}{4})}{\Gamma(\frac{1}{4})}\frac{E^N\beta^2}{\alpha^4}\Delta'^{\frac{3}{2}}. \end{aligned} \tag{3.145}$$

By use of the order parameter in Eq. (3.139), we obtain the relation

$$\frac{L^2}{\tilde{V}_{2\boldsymbol{p}}} = \frac{E^N}{\alpha^4\epsilon_p}\left\{1 - 2\sqrt{\frac{2}{\pi}}\,\frac{\Gamma(\frac{3}{4})}{\Gamma(\frac{1}{4})}\,\sqrt{\Delta'} + \omega(E)\,\frac{\tilde{V}_{2\boldsymbol{p}}}{L^2}\,\frac{1}{\sqrt{2\pi}}\,\frac{\Gamma(\frac{5}{4})}{\Gamma(\frac{3}{4})}\beta^2\sqrt{\Delta'}\right\}. \tag{3.146}$$

We insert this relation into Eq. (3.145), and by expanding $\alpha^4 = (1+\beta^2)^2$ for small β^2, the ultimate form of the condensation energy would be

$$\begin{aligned} E^{con} &= \frac{E^N}{\alpha^4}\left\{\left[\frac{16\sqrt{2}}{5\sqrt{\pi}}\frac{\Gamma(-\frac{1}{4})}{\Gamma(\frac{1}{4})} + \frac{16\sqrt{2}}{\sqrt{\pi}}\frac{\Gamma(\frac{3}{4})}{\Gamma(\frac{1}{4})}\right]\Delta'^{\frac{5}{2}}\right. \\ &+ \left.\left[\frac{32^2}{\pi^{\frac{3}{2}}}\frac{\Gamma(\frac{1}{4})}{\Gamma(-\frac{1}{4})} - \frac{8}{\sqrt{2\pi}}\frac{\Gamma(\frac{5}{4})}{\Gamma(\frac{3}{4})}\right]\beta^2\,\Delta'^{\frac{3}{2}}\right\} \\ &\approx E^N\left\{0.86\,\Delta'^{\frac{5}{2}} - \beta^2\left[6.9\,\Delta'^{\frac{5}{2}} - 1.1\times 10^3\,\Delta'^{\frac{3}{2}}\right]\right\}. \end{aligned} \tag{3.147}$$

The condensation energy in Eq. (3.145) has the correction term proportional to the β^2, in comparison with the equation in the regime $q = 2k_F$. So in the vanishing limit of β, the order parameters and the condensation energies in both regimes evolve continuously to each other.

3.4.3 In the case of partially-filled second BZ: nesting case

We have studied up to now the situations of the partially-filled first BZ, accompanied with nesting as $q = 2k_F$, and also the case of the partially-filled second BZ upon the lattice idea, which is introduced in Sec. 3.3.2. Fortunately in those cases, there was at most a single coupling for each particle, and it was possible to treat the case as a-one dimensional lattice and compensate the triangular lattice by a factor of three. But in the case that Fermi surface is settled at the vertex, as is shown in Fig. 3.9, there is a higher number of couplings for the states close to the vertex of the lattice. So once again we have to normalize the mean-field Hamiltonian concerning the present coupling at the vertex. The part of the Hamiltonian for the region close to the vertexes is involved with three different BZs. Obviously, the particle-hole pairs where are accommodated at the boundary of the first band and second band have to be included in the condensation energy and the order parameter calculations.

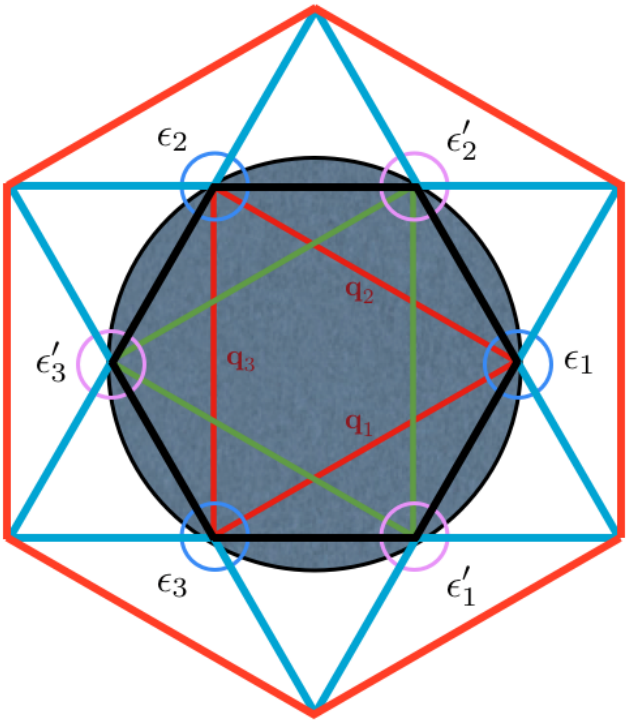

Figure 3.9: The Fermi surface is shown relaxed at the vertex of the translational vectors. The hexagon in the middle (black thick line), represents the first Brillouin zone which is totally filled. The Fermi surface is lied partially over second BZ and at the border of third BZ. Two triangles show the type of the coupling for states in the vicinity of the vertexes.

Another particular feature of the current regime is the nesting, that is the coupling vector fits the Fermi surface as $q = \sqrt{3}k_F$. As it was mentioned before, when nesting happens, the system undergoes a first-order phase transition from SDW phase to SDW phase. The reason is that by reaching to the such vertex, a new term would appear in the condensation energy associated with the energy of the states in the new BZ.

Below we start to diagonalize the mean-field Hamiltonian associated with the vertex area of the lattice. We go back to the mean-field Hamiltonian in Eq. (3.33) and we try to diagonalize it. Upon the type of the couplings, which are depicted in Fig. 3.9, there are two independent coupling region *i.e.* two equilateral triangles. Thus, the calculations would be presented for just one of those triangle and also just for one of the spin polarization. Labeling the angles of the triangle as is shown in Fig. 3.9, we write down the Hamiltonian as

$$H_{\downarrow}^{vertex} = \sum_k \left\{ \epsilon_1 c_1^\dagger c_1 + \epsilon_2 c_2^\dagger c_2 + \epsilon_2 c_2^\dagger c_2 + \left[\tilde{\Delta} c_1^\dagger c_2 + \tilde{\Delta}^* c_2^\dagger c_1 + \tilde{\Delta} c_1^\dagger c_3 + \tilde{\Delta}^* c_3^\dagger c_1 + \tilde{\Delta} c_2^\dagger c_3 + \tilde{\Delta}^* c_3^\dagger c_2 \right] \right\}, \tag{3.148}$$

where we have dropped the momentum subscript of the operators and the parameters. The terms in the square bracket represent the coupling between different area which are labeled by the subscript from one to three. To diagonalize the Hamiltonian, we write it in the matrix

form and diagonalize the matrix by means of unitary transformation to keep the fermionic commutation relation invariant. the Hamiltonian reads

$$H_{\downarrow}^{vertex} = \sum_{k} \begin{pmatrix} c_1^\dagger & c_2^\dagger & c_3^\dagger \end{pmatrix} \begin{pmatrix} \epsilon_1 & \tilde{\Delta} & \tilde{\Delta} \\ \tilde{\Delta}^* & \epsilon_2 & \tilde{\Delta} \\ \tilde{\Delta}^* & \tilde{\Delta}^* & \epsilon_3 \end{pmatrix} \begin{pmatrix} c_1 \\ c_2 \\ c_3 \end{pmatrix}. \tag{3.149}$$

We are interested in the eigenvalue of the following equation

$$det \begin{vmatrix} \epsilon_1 - \lambda & \tilde{\Delta} & \tilde{\Delta} \\ \tilde{\Delta}^* & \epsilon_2 - \lambda & \tilde{\Delta} \\ \tilde{\Delta}^* & \tilde{\Delta}^* & \epsilon_3 - \lambda \end{vmatrix} = 0. \tag{3.150}$$

The characteristic polynomial of the matrix is a linear equation of the third order, that can be written as

$$-\lambda^3 + \lambda^2 \underbrace{(\epsilon_1 + \epsilon_2 + \epsilon_3)}_{\alpha} + \lambda \underbrace{(3\Delta^2 - \epsilon_1\epsilon_2 - \epsilon_1\epsilon_3 - \epsilon_2\epsilon_3)}_{\beta} + \underbrace{\epsilon_1\epsilon_2\epsilon_3 + \Delta^2(Re\tilde{\Delta} - \epsilon_1 - \epsilon_2 - \epsilon_3)}_{\gamma} = 0. \tag{3.151}$$

We solve this cubic equation by means of trigonometric method (see Ref. [45]) after writing Eq. (3.151) as

$$t^3 - pt^3 + q = 0, \tag{3.152}$$

where we have renamed the variable as

$$\lambda = t + \frac{\alpha}{3},$$

and the coefficients are

$$\begin{aligned} p &= \tfrac{3\beta+\alpha^2}{3}, \\ q &= \tfrac{2\alpha^3+9\alpha\beta+27\gamma}{27}, \end{aligned} \tag{3.153}$$

that α, β and γ are introduced in Eq. (3.151), and the real roots are

$$t_j = 2\sqrt{\frac{p}{3}} \cos\left(\frac{1}{3}\arccos\left(\frac{3q}{2p}\sqrt{\frac{3}{p}}\right) - j\frac{2\pi}{3}\right), \qquad \text{for} \qquad j = 0, 1, 2. \tag{3.154}$$

The three different real roots correspond to the eigenvalue of three different zone. The eigenenergies are written as

$$E_{i,j} = t_{i,j} + \frac{\alpha}{3},$$

where index i associated with the one of the vertex of the triangle in Fig. 3.9, and index j counts the BZs in the vicinity of the vertexes. The diagonalized Hamiltonian in Eq. (3.148) takes the form

$$H_{\downarrow}^{vertex} = \sum_{\substack{1^{st}BZ \\ i}} E_i^{1^{st}}(k)\gamma_{i,k}^{\dagger}\gamma_{i,k} + \sum_{\substack{2^{nd}BZ \\ i}} E_i^{2^{nd}}(k)\gamma_{i,k}^{\dagger}\gamma_{i,k} + \sum_{\substack{3^{rd}BZ \\ i}} E_i^{3^{rd}}(k)\gamma_{i,k}^{\dagger}\gamma_{i,k}. \tag{3.155}$$

The explicit form of the eigenenergies are so lengthy. The calculation of the ground state energy and the order parameter cannot be accomplished. But the point is that contrary to the former calculation the gap equation is phase-dependent, as is apparent in Eq. (3.151), where in the γ coefficient there is a term of $Re\Delta$. As we said the system undergoes a phase transitions from SDW phase to SDW phase, whenever nesting happens.

3.5 Summary

The instability of the bilayer system versus the spin density wave phase, under interlayer interaction, has been studied. The phase diagram as a function of the external parameters of the system is depicted in Fig. 3.1. It is expected that the translational symmetry and the isotropy of the spin would be broken in the SDW phase. Upon the idea of the pseudospin, SDW means that density of molecules in each layer starts to modulate.

The system is brought onto the critical point by varying the strength of the interaction r_s or the interlayer separation y. The threshold of the instability is shown in Fig. 3.2, versus y and the module of the coupling vector $x = q/2k_F$. In the means-field framework, it is shown that the triangular lattice with equal sides of q (see Fig. 3.5), has the lowest energy in the SDW phase. We have studied the phase diagram, associated with the different relative configuration of the Fermi surface and the triangular lattice. It is shown that for $y \leq \frac{1}{2}$ the instability appears for $q = 2k_F$, as the Fermi surface is relaxed on the boundary of the first and the second Brillouin zone, but associated with different critical strength of the interaction. For $y \geq \frac{1}{2}$, the instability starts for $x = q/2k_F = 1/2y$. Thus for any fixed y configuration, there is a unique critical interaction strength in which the system undergoes a phase transition from Fermi liquid to spin density phase.

We have derived the condensation energy and the order parameter, self-consistently, for some parts of the phase diagram in Sec. 3.4, where was possible to obtain analytically. We have performed the calculations for the parts of the phase diagram associated with the parameters as ($q = 2k_F$ and $y \leq \frac{1}{2}$), in the Sec. 3.4.1. Case of the partially-filled-second BZ, with the constraint of ($x = \frac{q}{2k_F} = \frac{1}{2y}$ and $y > \frac{1}{2}$), is calculated in Sec. 3.4.2. Furthermore, we discussed the situation for the region $y \geq \frac{1}{2}$, where the Fermi surface is placed at the vertex of the lattice. In the latter case, nesting happens, where the ratio of the Fermi wavenumber and

coupling vector is a rational number. It is mentioned that upon such commensurate situation, it is not possible to obtain the order parameter and the condensation energy analytically. But, it is discussed that due to the involvement of the third BZ, there is an extra term in the condensation energy and the order parameter equation. As much further extending the Fermi surface into higher value of $y = lk_F$, more and more Brillouin zones would be involved into the calculations (see Fig. 3.2).

At each vertex of the lattice, Fermi surface would enter a new BZ and thus a new term comes into the condensation energy. Owing to this new term, the ground state energy shows a singularity. Therefore, the system undergoes a phase transition from SDW to SDW phase, whenever such commensurability happens. Intuitively the ground state energy as a function of an external parameter, say X, is depicted in Fig. 3.7, which shows sudden changes in the condensation energy at the commensurate points. Since the first derivative of the energy with respect to the external parameter X is singular, it is expected that there would be a first order phase transition. The phase diagram is shown in Fig. 3.10, which includes the new SDW phases at the commensurate points.

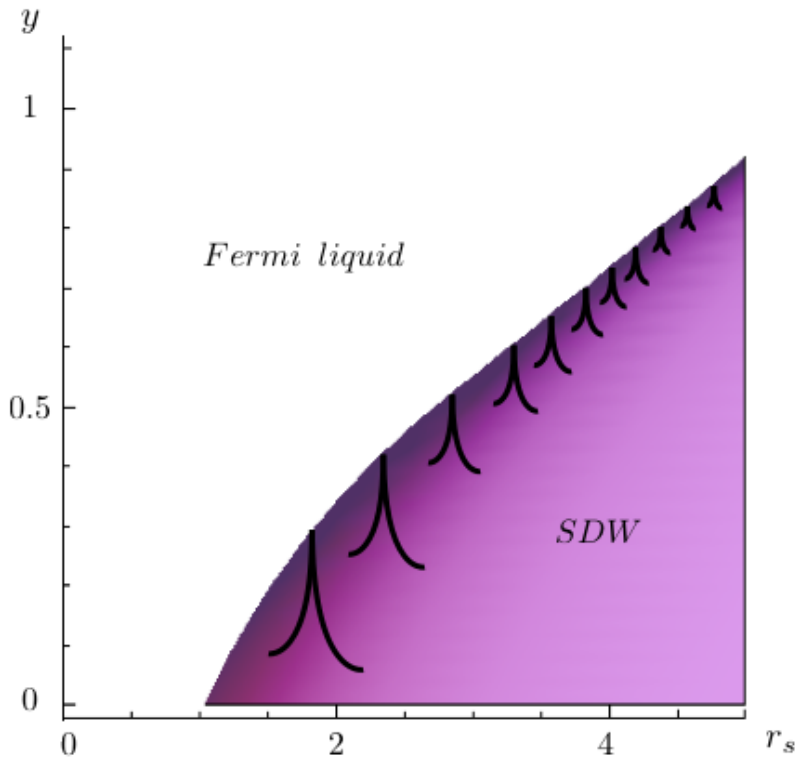

Figure 3.10: Phase diagram of the bilayer cold polar molecules under interlayer interaction. The instability is shown as a function of the interlayer separation $y = lk_F$ and the strength of the interaction $r_s = md_{eff}^2 k_F/\hbar^2$. The first order phase transition from SDW to SDW phase, at the commensurate points are shown schematically by the narrow angles.

It is worthwhile to compare the phase diagram that have been derived for SDW instability with another one which is derived by a group in university of Maryland [29], over the same bilayer system. They have studied the instability of the system versus the interlayer

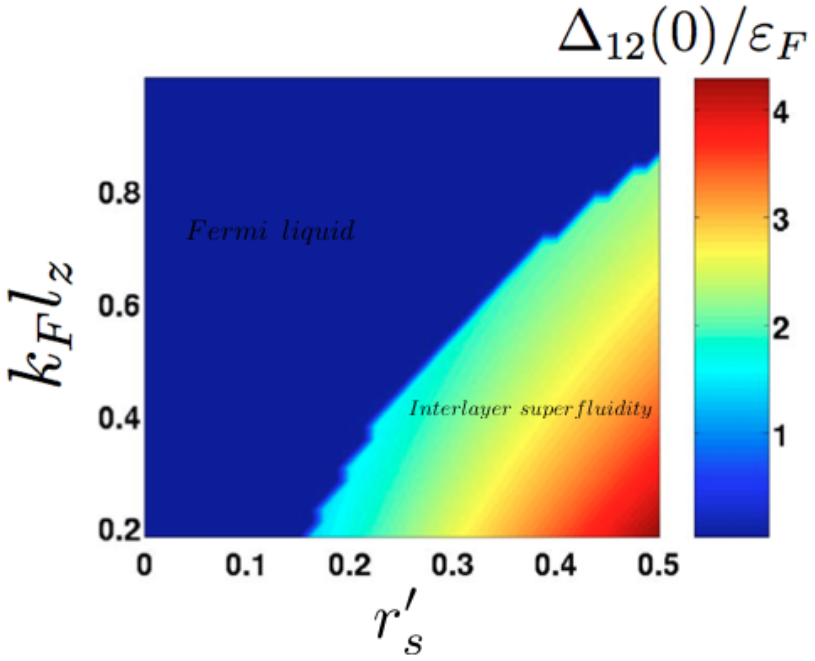

Figure 3.11: The phase diagram of the bilayer system of cold polar molecules which is reported in Ref. [29]. It is predicted that the system show a phase transition to interlayer superfluidity as a function of the interlayer separation $y = k_F l_z$ ($l_z \equiv l$ in our convention) and the strength of the interlayer interaction r'_s(The image is adopted from Ref. [30])

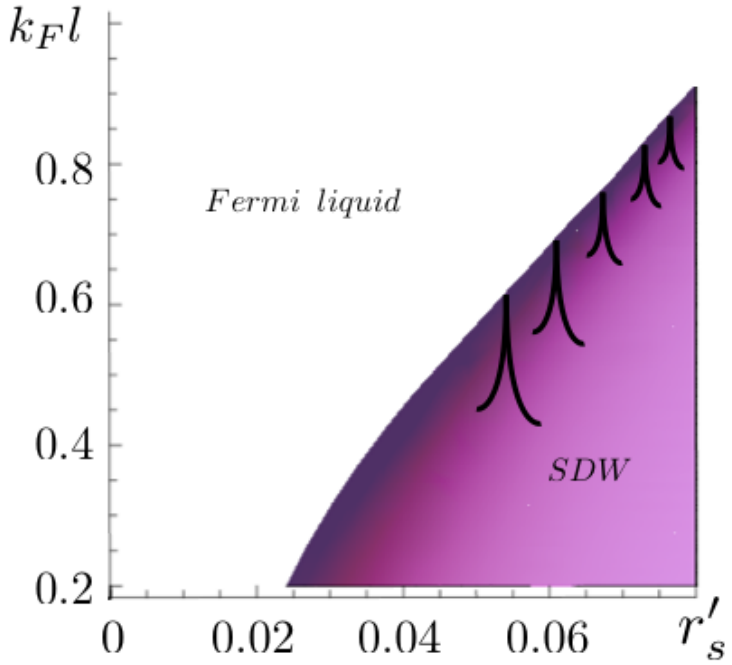

Figure 3.12: The phase diagram of the bilayer system for the SDW instability. The strength of the interaction is rescaled as $r'_s = d_{eff}^2 m k_F / 4\pi^{3/2}\hbar^2$, following the convention of Ref. [29].

superfluidity. The ground state of the superfluid is obtained as

$$|\psi_{FM}\rangle = \prod_{|\boldsymbol{k}|\leq\sqrt{2}k_F} \left(\frac{c^\dagger_{\boldsymbol{k}1} + e^{i\varphi} c^\dagger_{\boldsymbol{k}2}}{\sqrt{2}} \right) |0\rangle, \tag{3.156}$$

where subscript FM stands for the ferromagnetic state upon the pseudospin idea. The field operator $c^\dagger_{i\boldsymbol{k}}$ creates a molecule with the momentum $\boldsymbol{k}$ in the layer i. The phase difference between different layers is φ. Thus, in spin analogy, the ground state has the nonzero magnetization $\mathbf{M} = \langle\psi_{FM}|\sum_i \mathbf{m}_i|\psi_{FM}\rangle \neq 0$, quite on the contrary with the ground state of the normal phase. The ground state in Eq. (3.156) can be compared with one which we have derived in Eq. (3.56) for the SDW phase. The Fermi wavevector in Eq. (3.156) is entirely scaled by a factor of $\sqrt{2}$ versus the Fermi liquid one. But in the calculation over the SDW phase, the modification of the Fermi surface is characterized by its relative configuration with respect to the boundary zone of the lattice.

The order parameter for the interlayer superfluidity, as is suggested in Ref. [29] reads as

$$\Delta_{12}(k) = \frac{1}{2}\sum_q V_{12}(q) e^{-i\varphi} \langle c^\dagger_1(k+q) c_2(k+q)\rangle, \tag{3.157}$$

which takes into account interlayer correlations. The dependence of the order parameter, at zero-momentum $\Delta_{12}(0)$, is shown in Fig. 3.11 versus $r'_s = d^2_{eff} m k_F / 4\pi^{3/2}\hbar^2$ and $y = l k_F$. In order to compare the instabilities, we reprint our phase diagram in Fig. 3.12, versus the same dimensionless parameter r'_s as in Fig. 3.11. It shows that the instability for the SDW phase starts much more sooner than the interlayer superfluidity as a function of the strength of interaction.

Chapter 4

Interlayer superfluidity

In the preceding chapter, the instability of the bilayer system versus the spin density wave phase has been studied. In this chapter, we examine the circumstances in which the bilayer system undergoes a phase transition toward superfluidity as a function of interlayer distance $y = lk_F$ or the strength of interaction $r_s = md_{eff}^2 k_F/\hbar^2$. Due to the attractive long-tail of the interlayer interaction, which decays as $\propto 1/r^3$, molecules from different layers can form bound state [40]. In the weekly interacting regime, the Bardeen-Cooper-Schrieffer (BCS) theory would suffice to explain the superfluidity within the bilayer system of polar molecules [43].

Examination of the two dimensional Fermi liquid against superconductivity, dates back to decades ago [37, 38]. Superfluidity in two dimensional cold polar molecules have been recently studied in diverse topological configuration, accompanied by different interaction design (see for example [9, 10, 36, 44, 7, 13, 28, 29]). In the references [7, 28] the designed interaction is analytically similar to the interaction of the system which is considered up to now in this thesis. Therefore we use their results, after examining their consistency with the characteristic features of our system.

In the Ref. [7], the s-wave superfluid has been studied over a bilayer system of cold polar molecules. On the other side, in Ref. [28] the instability of the 2D system of cold polar molecules versus p-wave pairing is examined. In the both reports, the many-body effects have been contributed to the calculations, upon the Gor'kov-Melik-Barkhudarov corrections [21]. Hence, they go beyond the standard BCS approach.

In the following, first we review two references and the common general tools. Afterwards, we present the examination of the instability of our system versus the superfluidity, in the s-wave and p-wave channels.

4.1 Review of the models

In reference [7] a bilayer system of cold polar molecules has been considered, with the electric dipole moments polarized perpendicular to the layers by means of an external dc field, which is shown schematically in Fig. 4.1. The critical temperature of the interlayer superfluidity under s-wave pairing is calculated by means of the analysis of the interlayer scattering.

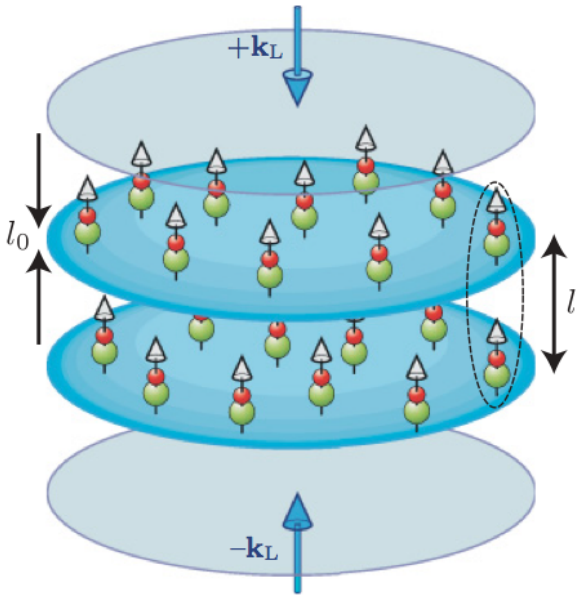

Figure 4.1: The setup of bilayer dipolar molecules, considered in Ref. [7]. Molecule are confined in the layers, with the thickness l_0, by means of two counterpropagating laser waves $\boldsymbol{k}_L$ and $-\boldsymbol{k}_L$. The dipoles are oriented perpendicular to the layers. The interlayer Cooper pairs are shown schematically by the dashed oval. (The image is taken from Ref. [7])

The system is characterized with two dimensionless parameters as

$$g = \frac{m\, d_{eff}^2}{l\hbar^2}, \qquad y = k_F l,$$

where d_{eff} is the effective electric dipole moment of the molecules and l is the interlayer separation. Actually, g is the measure of the interlayer interaction strength and y measures the interlayer separation in units of the mean interparticle distance in each layer, which is proportional to k_F^{-1}. One can draw the relation between those parameters and our dimensionless parameter as

$$\begin{aligned} g &= r_s/y, \\ k_F l &= y \end{aligned} \tag{4.1}$$

where $r_s = m\, d_{eff}^2\, k_F/\hbar^2$. We will use these relations to transform the results of this report to our system.

The relations between two parameters g and $k_F l$ determine three different regimes of scattering and thus the BCS pairing: regime (**A**) for $g < k_F l \lesssim 1$, regime (**B**) when $\exp(-1/g^2) \ll k_F l < g < 1$, and regime (**C**) as the $\exp(-1/g^2) \lesssim k_F l \ll g < 1$. We will examine the consistency of the critical temperature and order parameter in these regimes with the characteristic features of our system.

The interlayer interaction of the system in Ref.[7] is

$$V_{+-}(\boldsymbol{r}) = V_{-+}(\boldsymbol{r}) \equiv V^S(\boldsymbol{r}) \approx d_{eff}^2 \, \frac{r^2 - 2l^2}{(r^2 + l^2)^{5/2}}. \tag{4.2}$$

We have introduced the superscript S to prevent the confusion of the interaction potentials with our system one. The intralayer interaction of their system reads as

$$V_{++}^S(\boldsymbol{r}) \approx \begin{cases} d_{eff}^2/r^3 & r \gg l_0, \\ \sqrt{2/\pi}(d_{eff}^2/l_0^2)\ln(l_0/r) & r \ll l_0, \end{cases} \tag{4.3}$$

by l_0 as the confinement length. Our interlayer interaction can be obtain from Eq. (4.2) by multiplying a prefactor as

$$V(\mathbf{r}) = d_{eff}^2 \, \frac{l^2 - r^2/2}{(r^2 + l^2)^{5/2}} = -\frac{1}{2} V^S(\mathbf{r}). \tag{4.4}$$

The Fourier transform of interlayer interaction has the form as

$$\tilde{V}^S(\mathbf{q}) = \int d\boldsymbol{r} \, V^S(\boldsymbol{r}) \, e^{-i\mathbf{q}\boldsymbol{r}} = -\frac{2\pi\hbar^2}{m} \, gql \, e^{-ql}, \tag{4.5}$$

and the Fourier transform of the intralayer interaction reads

$$\tilde{V}_{++}^S(\mathbf{k}) = \sqrt{2\pi} \, \frac{4}{3} \, \frac{d_{eff}^2}{l_0} + \tilde{V}_{++}'^S(\mathbf{k}), \tag{4.6}$$

where in the regime $kl_0 \ll 1$, the second part is approximated as

$$\tilde{V}_{++}'^S(\mathbf{k}) \approx -\frac{2\pi\hbar^2}{m} gkl. \tag{4.7}$$

The interlayer interaction and its Fourier transform is shown in Fig. 4.2, which can be compare with our ones in Fig. 2.2 and Fig. 2.4. The interlayer interaction in Eq. (4.2) is attractive at the short distances $r < \sqrt{2}l$ and repulsive for $r > \sqrt{2}l$. On the contrary to the our interaction which is repulsive at the short distances and attractive at large distances and indeed causes different physical phenomena at short ranges. The intralayer interaction in Eq. (4.3) is repulsive at large long range limit, opposite to the our one. As will be shown later, the momentum-independent part of the intralayer interaction in Eq. (4.6) will have no contribution in the calculations. The Fourier transform of the interlayer interaction in Eq. (4.5) is negative for all values of $\mathbf{q}$. We use the following relation

$$-(1/2)g \to g, \tag{4.8}$$

to translate their results correspond to our system.

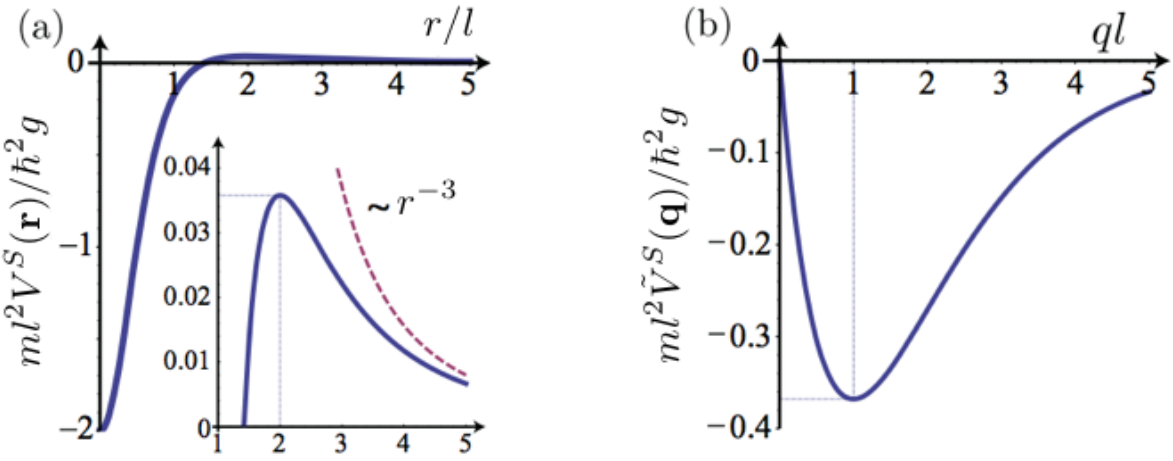

Figure 4.2: The interlayer interaction potential $V^S(\mathbf{r})$ of the setup in Ref. [7], and its Fourier transform $\tilde{V}^S(\mathbf{q})$. (The image is adopted from Ref. [7])

In reference [28] a two dimensional system of single-component fermionic has been studied. The polar molecules dressed by a circularly polarized microwave field and oriented perpendicular to the confinement plane by a dc field (see Fig. 4.3). The interaction potential has an attractive $1/r^3$ tail, similar to the our potential which causes the emergence of the p-wave superfluid. For two molecules far from each other $r \to \infty$ is given as

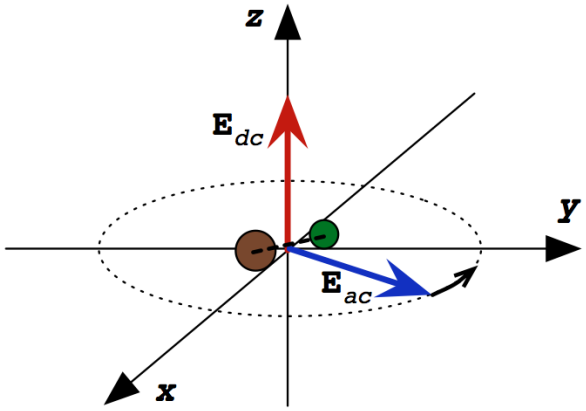

Figure 4.3: Dressed polar molecules in Ref. [28]. The molecules have been dressed by means of and a *dc* field, and a *ac* MW field, rotates with the frequency ω perpendicular to the confinement plane. (The image is taken from Ref. [28]

$$V^P(r \to \infty) = -\frac{\hbar^2}{m}\frac{r_*}{r^3}. \tag{4.9}$$

Once again, we have labeled the interaction potential by superscript P to prevent confusion. The length scale r_* has been introduced as

$$r_* = \frac{md_{eff}^2}{3\hbar^2}\frac{(\Omega_R/\delta)^2}{1+4(\Omega_R/\delta)^2}\left\{1-3\beta^2\left[\frac{49}{2160}+\left(\frac{7+13\sqrt{1+4(\Omega_R/\delta)^2}}{600\Omega_R/\delta}\right)^2\right]\right\},$$

where Ω_R is the Rabi frequency, δ is the frequency detuning of the MW field and the frequency of the transition between ground state and first excited state of internal states of a molecules, and $\beta = d_{eff}E_{dc}/B$ is a perturbation parameter, in which E_{dc} is the strength of dc field and B is the rotational constant of molecules. The length scale r_* in Eq .(4.9) is directly related to the parameters of our system at the same limit as

$$k_F\, r_* = \frac{m\, d_{eff}^2\, k_F}{2\hbar^2} = \frac{r_s}{2}, \tag{4.10}$$

where r_s is the measure of interaction in our system.

4.2 Superfluid gap equation

We now discuss superfluid pairing of the bilayer system following Ref. [28] and Ref. [28] within our system. The Hamiltonian of the bilayer system has been represented in the previous chapter in Eq. (3.1). In order to derive the gap equation it is convenient to work with Hamiltonian in the coordinate representation. By engaging the pseudospin proposal the Hamiltonian reads as

$$H = \sum_{\lambda=\uparrow\downarrow} \int d^2r\, \hat{\psi}^\dagger_\lambda(\mathbf{r}) \left(-\frac{\hbar^2}{2m}\nabla^2 - \mu\right) \hat{\psi}_\lambda(\mathbf{r}) + \int d^2r\, d^2r'\, \hat{\psi}^\dagger_\uparrow(\mathbf{r})\, \hat{\psi}^\dagger_\downarrow(\mathbf{r}')\, V(\mathbf{r}-\mathbf{r}')\, \hat{\psi}_\downarrow(\mathbf{r}')\, \hat{\psi}_\uparrow(\mathbf{r}),$$

where μ is the chemical potential, m mass of molecules and $\hat{\psi}_\lambda$ is the field operator of molecules in layer λ which interact by means of the interlayer potential $V(\mathbf{r}) = d_{eff}^2\,(l^2 - r^2/2)/(r^2 + l^2)^{5/2}$, introduced in the preceding chapter. The pairing stems from the attractive interaction between the fermions at long distance $r \gg l$. Following the BCS approach (see Sec. 2.3 or Ref. [43], the mean-field Hamiltonian looks like

$$H_{BCS} = \sum_{\lambda=\uparrow\downarrow} \int d^2r\, \hat{\psi}^\dagger_\lambda(\mathbf{r}) \left(-\frac{\hbar^2}{2m}\nabla^2 - \mu\right) \hat{\psi}_\lambda(\mathbf{r}) + \int d^2r\, d^2r' \left[\Delta^*(\mathbf{r},\mathbf{r}')\, \hat{\psi}_\downarrow(\mathbf{r}')\, \hat{\psi}_\uparrow(\mathbf{r}) + h.c.\right].$$

The order parameter obeys the gap equation as

$$\Delta(\mathbf{r},\mathbf{r}') = V(\mathbf{r}-\mathbf{r}')\langle\hat{\psi}_\downarrow(\mathbf{r}')\, \hat{\psi}_\uparrow(\mathbf{r})\rangle.$$

Similar to the approach of preceding chapter for SDW phase, we diagonalized the mean-field Hamiltonian by using Bogolyubov canonical transformation, which reduced Hamiltonian to the bilinear one as

$$H_{BCS} = \sum_{\substack{k \\ \lambda=\uparrow\downarrow}} \epsilon_k \hat{b}^\dagger_{\mathbf{k}\lambda} \hat{b}_{\mathbf{k}\lambda} + const.$$

The transformation is done by means of

$$\hat{\psi}(\mathbf{r}) = \frac{1}{L}\sum_{k}\left[u_{\mathbf{k}}\exp(i\mathbf{kr})\,\hat{b}_{\mathbf{k}} + v^{*}_{\mathbf{k}}\exp(-i\mathbf{kr})\,\hat{b}^{\dagger}_{\mathbf{k}}\right],$$

where L^2 is the volume of the system, $\hat{b}^{\dagger}_{\mathbf{k}}$ and $\hat{b}_{\mathbf{k}}$ are creation and annihilation operator for single-particles with dispersion relation of $\epsilon_{\mathbf{k}} = \sqrt{\xi^2_{\mathbf{k}} + \Delta^2_{\mathbf{k}}}$ while $\xi_{\mathbf{k}} = E_{\mathbf{k}} - \mu$, and $E_{\mathbf{k}} = \hbar^2k^2/2m$. The coefficients $u_{\mathbf{k}}$ and $v_{\mathbf{k}}$ obey the relations required for canonical transformation of the fermionic operators, given by

$$u_{\mathbf{k}} = \frac{\xi_{\mathbf{k}} + \epsilon_{\mathbf{k}}}{\sqrt{2\epsilon_{\mathbf{k}}(\xi_{\mathbf{k}} + \epsilon_{\mathbf{k}})}}, \qquad v_{\mathbf{k}} = \frac{\Delta_{\mathbf{k}}}{\sqrt{2\epsilon_{\mathbf{k}}(\xi_{\mathbf{k}} + \epsilon_{\mathbf{k}})}},$$

where $\Delta_{\mathbf{k}}$ is the Fourier transform of the order parameter. In the momentum space, the gap equation takes the form

$$\Delta_{\mathbf{k}} = -\int \frac{d\mathbf{q}}{(2\pi)^2}\,\tilde{V}(\mathbf{q}-\mathbf{k})\,\Delta_{\mathbf{q}}\,\frac{\tanh(\epsilon_{\mathbf{q}}/2T)}{2\epsilon_{\mathbf{q}}}, \tag{4.11}$$

where $\tilde{V}(\mathbf{q}) = \pi\, d^2_{eff}\, q\, \exp(-lq)$ is the Fourier transform of the interaction potential and T is the temperature. Actually the calculations would be for non-zero temperature and at the end we derived the band gap at zero temperature by means of a relation which will be presented later.

In the dense regime ($k_F l > 1$), Eq. (4.11) can be solved directly. But for a dilute gas ($k_F l < 1$) this equation mixed many-body physics (BCS) pairing with two-body scattering [7]. It is convenient to renormalize the gap equation by means of off-shell scattering amplitude. Actually, the renormalization procedure in Ref.[7] is done by means of the vertex function (see for example Ref. [19]) as

$$\Gamma(E,\mathbf{k},\mathbf{k}') = \tilde{V}(\mathbf{k}-\mathbf{k}') + \int \frac{d\mathbf{q}}{(2\pi)^2}\tilde{V}(\mathbf{k}-\mathbf{q})\frac{1}{E - \hbar^2q^2/m + i0}\Gamma(E,\mathbf{q},\mathbf{k}'), \tag{4.12}$$

by E being arbitrary chosen relative energy. The off-shell scattering amplitude (see for example Ref. [19]) reads as

$$f(\mathbf{k}',\mathbf{k}) = \tilde{V}(\mathbf{k}'-\mathbf{k}) + \int \frac{d\mathbf{q}}{(2\pi)^2}\,\frac{\tilde{V}(\mathbf{k}'-\mathbf{q})}{2(E_k - E_q - i0)}\,f(\mathbf{q},\mathbf{k}), \tag{4.13}$$

which can be obtained from the vertex function by putting $E = \hbar^2k^2/m$ in Eq. (4.12). We continue formally with the off-shell scattering amplitude and return to the vertex function in the sections associated with the s-wave scattering.

Multiplying Eq. (4.13) by $\Delta_{\mathbf{k}'}\tanh(\epsilon_{\mathbf{k}'}/2T)/2\epsilon_{\mathbf{k}'}$ and integrating over $d\mathbf{k}'$, by employing Eq. (4.11), there would be

$$\Delta_{\mathbf{k}} = -\int \frac{d\mathbf{k}'}{(2\pi)^2} f(\mathbf{k}',\mathbf{k})\,\Delta_{\mathbf{k}'}\left[\frac{\tanh(\epsilon_{\mathbf{k}'}/2T)}{2\epsilon_{\mathbf{k}'}} - \frac{1}{2(E_{k'}-E_k-i0)}\right]. \tag{4.14}$$

Taking into account the conservation of angular momentum it is possible to decompose the scattering amplitude in Eq. (4.14) into the different channels. In this chapter, we just analyze s-wave ($l=0$) and p-wave ($l=1$) scattering. Now we review the contribution of the many-body effects in Eq. (4.14), as the correction to the interparticle interaction $\delta\tilde{V}(\mathbf{q},\mathbf{k})$, and the mass renormalization m_*.

4.2.1 Many-body contributions to the interparticle interaction

The leading terms of the correction $\delta\tilde{V}(\mathbf{q},\mathbf{k})$, are in second order in $\tilde{V}(\mathbf{q})$ (see Ref .[21]), which is shown diagrammatically in Fig. 4.4. In panel (***d***) of Fig. 4.4 just the interlayer interaction is taken into account, while panels (***a***), (***b***) , and (***c***) both inter- and intralayer interactions contribute. The corresponding analytical expressions of Fig. 4.4 are

$$\begin{aligned}
\delta\tilde{V}_a(\mathbf{k},\mathbf{k}') &= 2\int \frac{d\mathbf{q}}{(2\pi)^2}\frac{N(\mathbf{q}+\mathbf{k}_-/2)-N(\mathbf{q}-\mathbf{k}_-/2)}{\xi_{\mathbf{q}+\mathbf{k}_-/2}-\xi_{\mathbf{q}-\mathbf{k}_-/2}}\,\tilde{V}(\mathbf{k}_-)\tilde{V}_{++}(\mathbf{k}_-),\\
\delta\tilde{V}_b(\mathbf{k},\mathbf{k}') &= -\int \frac{d\mathbf{q}}{(2\pi)^2}\frac{N(\mathbf{q}+\mathbf{k}_-/2)-N(\mathbf{q}-\mathbf{k}_-/2)}{\xi_{\mathbf{q}+\mathbf{k}_-/2}-\xi_{\mathbf{q}-\mathbf{k}_-/2}}\,\tilde{V}(\mathbf{k}_-)\tilde{V}_{++}(\mathbf{q}-\mathbf{k}_+/2),\\
\delta\tilde{V}_c(\mathbf{k},\mathbf{k}') &= -\int \frac{d\mathbf{q}}{(2\pi)^2}\frac{N(\mathbf{q}+\mathbf{k}_-/2)-N(\mathbf{q}-\mathbf{k}_-/2)}{\xi_{\mathbf{q}+\mathbf{k}_-/2}-\xi_{\mathbf{q}-\mathbf{k}_-/2}}\,\tilde{V}(\mathbf{k}_-)\tilde{V}_{++}(\mathbf{q}+\mathbf{k}_+/2),\\
\delta\tilde{V}_d(\mathbf{k},\mathbf{k}') &= -\int \frac{d\mathbf{q}}{(2\pi)^2}\frac{N(\mathbf{q}+\mathbf{k}_+/2)-N(\mathbf{q}-\mathbf{k}_+/2)}{\xi_{\mathbf{q}+\mathbf{k}_+/2}-\xi_{\mathbf{q}-\mathbf{k}_+/2}}\,\tilde{V}(\mathbf{q}-\mathbf{k}_-/2)\tilde{V}(\mathbf{q}+\mathbf{k}_-/2),
\end{aligned} \tag{4.15}$$

where $\mathbf{k}_\pm = \mathbf{k}\pm\mathbf{k}'$ and $\tilde{V}(\mathbf{q}) = \pi\, q\exp(-lq)$ being the interlayer interaction, while $\tilde{V}_{++}(\mathbf{q}) = \pi\, q$ is the intralayer interaction potential. In $\delta\tilde{V}_a$ the spin degeneracy of the loop has been counted by a 2 prefactor. The Eq. (4.14), by including the many-body corrections as $\delta\tilde{V}(\mathbf{k},\mathbf{k}') = \sum_j \delta\tilde{V}_j(\mathbf{k},\mathbf{k}')$, takes the form

$$\begin{aligned}
\Delta(\mathbf{k}) = &- \int \frac{d\mathbf{k}'}{(2\pi)^2} f(\mathbf{k}',\mathbf{k})\,\Delta(\mathbf{k}')\left[\frac{\tanh(\epsilon_{\mathbf{k}'}/2T)}{2\epsilon_{\mathbf{k}'}} - \frac{1}{2(E_{k'}-E_k-i0)}\right]\\
&- \int \frac{d\mathbf{k}'}{(2\pi)^2}\,\delta\tilde{V}(\mathbf{k}',\mathbf{k})\,\frac{\tanh(\epsilon_{\mathbf{k}'}/2T)}{2\epsilon_{\mathbf{k}'}}\,\Delta(\mathbf{k}').
\end{aligned} \tag{4.16}$$

To get rid of the azimuthal integral part in the gap equation, we average over the directions of $\mathbf{k}$ and $\mathbf{k}'$ *i.e.* integrating over φ and φ' corresponds to the s-wave scattering; and multiplying Eq. (4.16) by $\exp(-i\varphi_{\mathbf{k}})$ and integrate over $\varphi_{\mathbf{k}}$ and $\varphi_{\mathbf{k}'}$ for the p-wave symmetry is $\Delta_{\mathbf{k}} =$

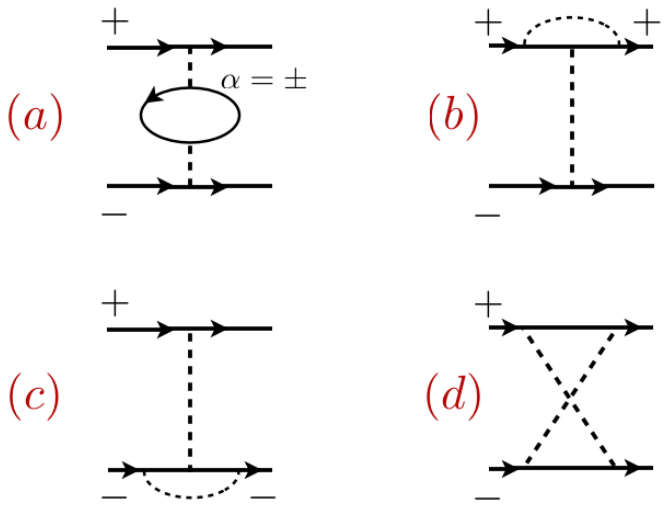

Figure 4.4: The second-order contribution to the interlayer interaction. The solid lines presents propagators of the particles from different layers, which labeled by + and −. The dashed lines show the dipole-dipole interaction. Panel (**d**) contains only the interlayer interaction. Since, panels (**a**), (**b**), and (**c**) include both inter- and intralayer interactions. (The image is reproduced from Ref. [7] and Ref. [28])

$\Delta(\boldsymbol{k})\exp(i\varphi_{\mathbf{k}})$. Thus we present the gap equation generally for both of the partial waves, by replacing $\Delta(\mathbf{k})$ with $\Delta(k)$, scattering amplitude $f(\mathbf{k}',\mathbf{k})$ with $f(k',k)$, and $\delta\tilde{V}(\mathbf{k}',\mathbf{k})$ with $\delta\tilde{V}(k',k)$. Hence it reads

$$\begin{aligned}\Delta(k) = &- \int \frac{d^2k'}{(2\pi)^2}\, f(k',k)\,\Delta(k')\left[\frac{\tanh(\epsilon_{k'}/2T)}{2\epsilon_{k'}} - \frac{1}{2(E_{k'}-E_k-i0)}\right] \\ &- \int \frac{d^2k'}{(2\pi)^2}\,\delta\tilde{V}(k',k)\,\frac{\tanh(\epsilon_{k'}/2T)}{2\epsilon_{k'}}\,\Delta(k'). \end{aligned} \tag{4.17}$$

Later we decompose the gap equation into the partial-waves, associated with the desired s-wave or p-wave scattering amplitude.

4.2.2 Effective mass

It is straightforward to renormaize particles' mass by means of the self-energy as $m/m_* = (1+2m\partial\Sigma(\omega,p)/\partial p^2)(1-\partial\Sigma(\omega,p)/\partial p)|_{p=p_F,\omega=0}$ (see for example [19, 31]). It is important to note that the most contribution in gap equation (4.17) comes from the momenta close to the Fermi surface and it suffices to restrict the many-body effect at the Fermi surface in mass renormalization. The self-energy up to first order is shown in Fig. 4.5 where the first two diagrams contain just intralayer interaction, while the third one engages the interlayer potential.

The corresponding terms in Fig. 4.5 are the so-called Hartree-Fock diagrams which are frequency-independent, $\Sigma_\alpha^{(1)}(\omega,p) = \Sigma_\alpha^{(1)}(p)$. The analytical for $\Sigma_\alpha^{(1)}(p)$ takes the form

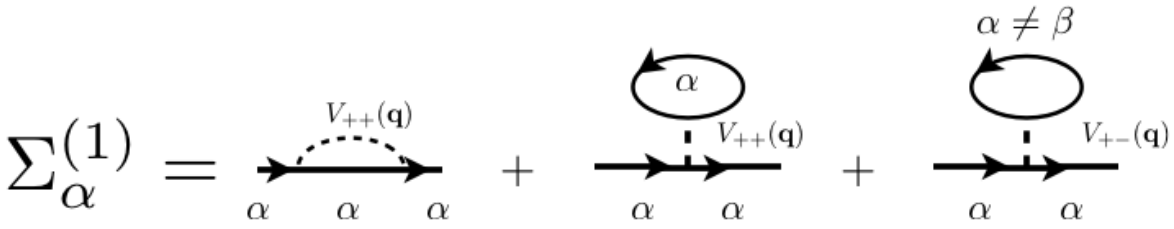

Figure 4.5: The fermionic self-energy up to the first order in the interaction. Dashed lines correspond to dipole-dipole interaction. The label α specifies the layer. The first two diagrams contain the intralayer interaction, and the third diagram corresponds interlayer interaction. (The image is reproduced from Ref. [7])

$$\begin{aligned}\Sigma_\alpha^{(1)}(k) &= -\int \frac{d\mathbf{q}}{(2\pi)^2}\left[\tilde{V}_{++}(\mathbf{k}-\mathbf{q})-\tilde{V}_{++}(0)\right] N(\mathbf{q}) + V(0) \\ &= -\int \frac{d\mathbf{q}}{(2\pi)^2}\left[\tilde{V}_{++}(\mathbf{k}-\mathbf{q})-\tilde{V}_{++}(0)\right] N(\mathbf{q}),\end{aligned} \tag{4.18}$$

where $N(\mathbf{q}) = \theta(\mathbf{k}_F - \mathbf{q})$ is Fermi-Dirac distribution function at zero-temperature. Due to exponential smallness of the critical temperature T_c, it makes no contribution by engaging the zero-temperature one. Remembering that $\tilde{V}(\mathbf{q}) = \pi\, q \exp(-lq)$ being the interlayer interaction and $\tilde{V}_{++}(\mathbf{q}) = \pi\, q$, the intralayer interaction potential Eq. (4.18) can be readily calculated which gives

$$\begin{aligned}\frac{m_*}{m} &= 1 + \frac{2}{3\pi}\frac{m\, d_{eff}^2\, k_F}{\hbar^2} \\ &= 1 + \frac{2}{3\pi}\frac{g k_F l}{2} \\ &= 1 + \frac{2}{3\pi} k_F r_* \\ &= 1 + \frac{2}{3\pi}\frac{r_s}{2}.\end{aligned} \tag{4.19}$$

It has to be noted that in Eq. (4.18) for self-energy, the momentum-independent part of intralayer interaction of Ref. [7], presented in Eq. (4.6), would be canceled and does not contribute to the results. Hence, by following the replacement of the parameter of our system as noted in Eq. (4.8) we can use the results in Ref. [7] without any further manipulation (as we have represented their approach to renormalize the mass).

The effective mass has to be replaced instead of the bare mass in the gap equation in Eq. (4.17). Following Ref.[7], we rewrite the gap equation as

$$\begin{aligned}\Delta(k) = &- \frac{m_*}{m}\int \frac{d^2k'}{(2\pi)^2} f(k',k)\,\Delta(k')\left[\frac{\tanh(\epsilon_{k'}/2T)}{2\epsilon_{k'}} - \frac{1}{2(E_{k'}-E_k-i0)}\right] \\ &- \int \frac{d^2k'}{(2\pi)^2}\,\delta\tilde{V}(k',k)\,\frac{\tanh(\epsilon_{k'}/2T)}{2\epsilon_{k'}}\,\Delta(k'),\end{aligned} \tag{4.20}$$

in order to cancel the bare mass in the off-shell scattering amplitude and replaced it by effective mass. In Ref. [28], the effective mass calculated according to the Landau Fermi-liquid theory which obviously gives the same results for our system by changing the parameters as given in Eq. (4.10). In Ref. [28], they have contributed the effective mass at the end of calculations, as will be discussed in the p-wave pairing section.

4.3 Relation of $\Delta(k_F)$ and T_c at zero-temperature

Upon the reasoning of the Ref. [28], the most contribution in the integral of the gap equation in Eq. (4.14) comes from a narrow vicinity of Fermi surface. Singling out this main contribution it is possible to make a relation between the order parameter $\Delta(k)$ and the order parameter on the Fermi surface $\Delta(k_F)$ as

$$\Delta(k) = \Delta(k_F)\frac{f(k_F,k)}{f(k_F)}, \tag{4.21}$$

where $f(k,k')$ is the off-shell scattering amplitude and $f(k) = f(k,k)$ is the on-shell one. Once again, considering the rotational invariance, this relation is valid for the partial waves components too. The same relation as in Eq. (4.21) is derived in Ref.[7] in a more details which we present it later.

Employing Eq. (4.21) makes it possible to construct a relation between the zero-temperature order parameter on the Fermi surface $\Delta_0(k_F)$ and critical temperature T_c. The weak coupling regime implies that $\Delta(k), T_c \ll E_F$. Therefore, we divide the region of the integrals in Eq. (4.20) into two regions: the first region would be states which are in a narrow annulus around the Fermi energy as $\mathbf{\Omega} \equiv \{\mathbf{k}'|\,\mathbf{k}' \in |E_{k'} - E_F| < \omega\}$ and the second, states out of this region by the constraint that $\Delta(k), T_c \ll \omega \ll E_F$. Putting $k = k_F$ in Eq. (4.20), in the integral over the first region, we put $f(k', k_F) \approx f(k_F, k_F) = f(k_F)$, $\Delta(k') \approx \Delta(k_F)$, and $\delta\tilde{V}(k', k) = \delta\tilde{V}(k_F, k_F) = \delta\tilde{V}(k_F)$, which is legitimate through the similar reasoning as is mentioned before in Eq. (4.21). In the integral over the second region, we may put $\epsilon_{k'} = |\xi_{k'}|$, $\tanh(\epsilon_{k'}/2T) = 1$ and also replacing $\Delta(k')$ by Eq. (4.21) we have

$$\begin{aligned}
\Delta(k_F) = &- \int_{k'\in\mathbf{\Omega}} \frac{d^2k_F}{(2\pi)^2}\, f(k_F)\,\Delta(k_F) \left[\tanh\left(\frac{\sqrt{\xi_{k'}^2+\Delta_{k_F}^2}}{2T}\right)\frac{1}{2\sqrt{\xi_{k'}^2+\Delta_{k_F}^2}} - \frac{1}{2(E_{k'}-E_{k_F}-i0)}\right] \\
&- \int_{k'\in\mathbf{\Omega}} \frac{d^2k'}{(2\pi)^2}\, \delta\tilde{V}(k_F)\,\tanh\left(\frac{\sqrt{\xi_{k'}^2+\Delta_{k_F}^2}}{2T}\right)\frac{1}{2\sqrt{\xi_{k'}^2+\Delta_{k_F}^2}}\,\Delta(k_F) \\
&- \int_{k'\notin\mathbf{\Omega}} \frac{d^2k'}{(2\pi)^2}\, f(k',k_F)\,\Delta(k_F)\frac{f(k_F,k')}{f(k_F)}\left[\frac{1}{2|\xi_{k'}|} - \frac{1}{2(E_{k'}-E_F-i0)}\right] \\
&- \int_{k'\notin\mathbf{\Omega}} \frac{d^2k'}{(2\pi)^2}\, \delta\tilde{V}(k',k_F)\,\frac{1}{2|\xi_{k'}|}\,\Delta(k_F)\frac{f(k_F,k')}{f(k_F)}.
\end{aligned}$$

By canceling $\Delta(k_F)$ from both side and rearranging the terms to the temperature-dependent and -independent parts, and by switching to the integral over energy it takes the form

$$1 = -\frac{m}{2\pi\hbar^2}\int_0^{\omega}\left[f(k_F)+\delta\tilde{V}(k_F)\right]\tanh\left(\frac{\sqrt{\xi_{k'}^2+\Delta_{k_F}^2}}{2T}\right)\frac{d\xi_{k'}}{2\sqrt{\xi_{k'}^2+\Delta_{k_F}^2}}+\Lambda, \tag{4.22}$$

where Λ contains all the temperature-independent terms. On one hand, at the critical point as $T \to T_c$ the order parameter vanishes and we put $\Delta(k_F) = 0$ in Eq. (4.22). On the other hand, at zero-temperature the hyperbolic tangent tend to one. By subtracting these two extreme cases, we have

$$\int_0^{\omega}\left\{\frac{\tanh\left(\xi_{k'}/2T_c\right)}{\xi_{k'}}-\frac{1}{\sqrt{\xi_{k'}^2+\Delta_0(k_F)^2}}\right\}d\xi_{k'}=0. \tag{4.23}$$

The integral is convergent by extending the upper cutoff to infinity. By running the integral and solving for critical temperature there would be

$$T_c = \frac{e^{\gamma}}{\pi}\Delta_0(k_F), \tag{4.24}$$

where γ is the Euler's constant $\gamma = 0.5772$. We use Eq. (4.24) as a relation to transfer the critical temperatures, which have been derived in the references [7, 28], to the order parameter at zero-temperature that fits the framework of this thesis. Actually, by help of Eq. (4.21) and Eq. (4.22) it is possible to find the relation between the critical temperature T_c and the order parameter on Fermi surface $\Delta(k_F)$ at any temperature.

4.4 S-wave superfluidity

It is shown in Ref.[37] that "*a two-body* [s-wave] *bound state in vacuum is a necessary and sufficient condition for the many-body instability.*" Although it is not the case for the p-wave bound state in vacuum. Following the approach of Ref.[7], first we show the existence of such s-wave bound state in vacuum. Afterwards, we present the scattering amplitude in the different regimes and discuss the circumstances for the s-wave superfluidity.

4.4.1 Interlayer s-wave bound state

We start by solving the two dimensional Schrödinger equation for a two-body bound state by the wavefunction of relative motion as $\psi(\mathbf{r}) = \chi_{m_z}(r)\exp\left(im_z\phi\right)$ with shallow binding energy of E_b which reads like

$$\left[\frac{d^2}{d^2r}+\frac{1}{r}\frac{d}{dr}-\frac{m_z}{r^2}-\frac{E_b+V(r)}{\hbar^2/m}\right]\chi_{m_z}(r)=0. \tag{4.25}$$

where $V(r) = d_{eff}^2\,(l^2 - r^2/2)/(l^2 + r^2)^{5/2}$. By concentrating over the states by axial symmetry as $m_z = 0$ we attempt to drive the binding energy as a perturbative series of $g^{-1} = \hbar^2 l/m\, d_{eff}^2 = y/r_s$. We solve the axial symmetric Schrödinger in two extreme limit of large and small distances in compare with $r^\star = (d_{eff}^2/E_b)^{1/3}$ and by matching the logarithmic derivative of the two asymptotic results we find the binding energy E_b.

On the one hand, at large distances, $r \gg r^\star$ we can neglect the potential and so take the particles as they are free. In this limit the wavefunction reads

$$\chi_0(r) \approx C K_0(\sqrt{mE_b}r/\hbar),$$

where C being the normalization constant. For $r \ll r_\kappa = \sqrt{mE_b}/\hbar$, we expand the wavefunction to have

$$\chi_0(r) \approx C \ln \frac{2\hbar e^{-\gamma}}{\sqrt{mE_b}r},$$

with $\gamma = 0.5772$ the Euler constant. The logarithmic derivation take the form

$$r\frac{d}{dr}\ln\chi_0(r) \approx -\left[\ln\left(\frac{2\hbar}{\sqrt{mE_b}r}\right) - \gamma\right]^{-1}. \tag{4.26}$$

On the other hand, for sufficiently small distances as $r \ll r^\star$ upon the constraint that $E_b \ll U_0 = d_{eff}^2/l^3$, we neglect the binding energy versus interlayer potential which can be written as $V(x = r/l) = U_0(1 - x^2/2)/(1 + r^2)$. Expanding the wavefunction in powers of g as

$$\chi_0(r) \approx N\left[\chi_0^{(0)}(r) + \sum_{n=1}^{\infty} g^n \chi_0^{(n)}(r)\right],$$

where N would be the overall normalization factor. Inserting this wavefunction in Schrödinger equation, there would be a set of differential equations concerning the powers of the perturbative term g as

$$\frac{1}{r}\frac{d}{dr}r\frac{d}{dr}\chi_0^{(n)}(r) = \frac{mV(r)}{\hbar^2 g}\chi_0^{(n-1)}(r), \tag{4.27}$$

with the constraint $\chi_0^{(-1)}(r) \equiv 0$ and the boundary condition $\chi_0^{(n)}(0) = \delta_{n,0}$. Therefore from differential equation in Eq. (4.27), we obtain an integral form for each power series term iteratively as

$$\chi_0^{(n)}(r) = \int_0^r dr_1 \int_0^{r_1} dr_2 \frac{l^2 - r_2^2/2}{(l^2 + r_2^2)^{5/2}}\,\frac{r_2}{r_1}\,\chi_0^{(n-1)}(r_2). \tag{4.28}$$

Concerning the boundary condition, the terms up to fourth order, which suffices in the current approximation, take the forms

$$\begin{aligned}
\chi_0^{(0)}(r) &= 1, \\
\chi_0^{(1)}(r) &= -\frac{1}{2}\left(\frac{1}{z}-1\right), \\
\chi_0^{(2)}(r) &= \frac{1}{4}\left(\frac{3}{8z^2}-\frac{1}{z}+\frac{5}{8}-\frac{1}{4}\ln z\right), \\
\chi_0^{(3)}(r) &= -\frac{1}{8}\left(\frac{3}{40z^3}-\frac{3}{8z^2}+\frac{47}{120z}-\frac{11}{120}-\frac{z-1}{4}\ln z-\frac{4}{15}\ln\frac{1+z}{2}\right), \\
\chi_0^{(4)}(r) &= \frac{1}{16}\left[\frac{3}{320z^4}-\frac{3}{40z^3}+\frac{11}{128z^2}-\frac{17}{120z}-\frac{311}{1920}+\frac{\ln^2 z}{32}+\left(-\frac{3}{32z^2}+\frac{1}{4z}+\frac{257}{960}\right)\ln z\right. \\
&+ \left.\frac{4}{15}\left(\frac{1}{z}+1\right)\ln\frac{2}{z+1}+\frac{\mathbf{Li}_2(1-z^2)}{64}\right],
\end{aligned}$$

where $z=\sqrt{r^2+l^2}$, and $\mathbf{Li}_n(x)=\sum_i^\infty x^i/i^n$ is the polylogarithm function. Moreover, upon the boundary condition and the constraint of $\chi_0^{(-1)}(r)=0$, the zero-order term is chosen equal unity as it has to be constant. The logarithmic derivative is

$$r\frac{d}{dr}\ln\chi_0(r) \approx r\frac{d}{dr}\ln\left(\sum_{n=0}^{j} g^n\chi_0^{(n)}(r)\right)\equiv\Lambda_0^j,$$

and as we kept up to the forth order, for $r\gg l$ it would be

$$\begin{aligned}
\Lambda_0^4 &\approx \left\{\ln\frac{r}{l}-(1-\frac{g}{30}-\frac{g^2}{960})^{-1}\right. \\
&\times \left.\left[\frac{16}{g^2}+\frac{8}{g}+\frac{5}{2}-\frac{1}{60}g\left(-11+32\ln 2\right)+g^2\left(-\frac{311+5\pi^2}{1920}+\frac{4}{15}\ln 2\right)\right]\right\}^{-1},
\end{aligned} \tag{4.29}$$

Matching the latter with the solution of the long distances limit in Eq. (4.26), we have

$$\begin{aligned}
\ln\left(\frac{\sqrt{mE_b}le^\gamma}{2\hbar}\right) &= (1-\frac{g}{30}-\frac{g^2}{960})^{-1} \\
&\times \left[\frac{16}{g^2}+\frac{8}{g}+\frac{5}{2}-\frac{1}{60}g\left(-11+32\ln 2\right)+g^2\left(-\frac{311+5\pi^2}{1920}+\frac{4}{15}\ln 2\right)\right] \\
&\approx -\frac{16}{g^2}-\frac{128}{15g}-\frac{2521}{900},
\end{aligned}$$

thus readily we solve it to obtain the binding energy

$$E_b = \frac{4\hbar^2}{ml^2}\exp\left[-\frac{32}{g^2}-\frac{256}{15g}-\frac{2521}{450}-2\gamma+O(g)\right]. \tag{4.30}$$

Upon the particular behavior of the interaction potential, with the vanishing zero-momentum Born approximation as $\int V(r)rdr = 0$, the same type of the shallow binding energy is derived in Ref.[26] which would be accurate up to the leading order of the binding energy in Eq. (4.30), as the higher orders are determined by contributions of higher order terms in the scattering amplitude in Ref.[26].

4.4.2 Low-energy s-wave scattering

In the following part, we derive the scattering amplitude for the low energy in 2D. The quantum mechanical character of the scattering in 2D is considered in details in Ref.[2]. In preceding part, we have shown the shallow binding energy and its relation with the wavefunction of the two-body system. In the framework of the scattering theory, it is convenient to write down the asymptotic form of the wavefunction in the large distances $r \gg r^\star$, as a combination of incoming plane wave and an scattered wave with the scattering amplitude f_k as the weight

$$\Psi_k^s(\mathbf{r}) \approx \exp(i\mathbf{k}r) - \frac{if_k}{4}H_0^{(1)}(kr),$$

where $H_0^{(1)}$ being the Hankel function. In low energy regime $kr^\star \ll 1$, we can further expand the wavefunction for $r \ll 1/k$ to have

$$\Psi_k^s(\mathbf{r}) \approx 1 + \frac{f_k}{2\pi}\left[\ln\left(\frac{kr}{2}+\gamma-\frac{i\pi}{2}\right)\right],$$

and its logarithmic derivative reads

$$r\frac{d}{dr}\ln\Psi_k^s(\mathbf{r}) \approx \left[\ln\left(\frac{kr}{2}\right)+\gamma+\frac{2\pi}{f_k}-\frac{i\pi}{2}\right]^{-1}.$$

We have derived the wavefunction for the small distances regime $r \ll r^\star$, and its logarithmic derivative too, which reads as

$$r\frac{d}{dr}\ln\Psi_k^s(\mathbf{r}) \approx \left[\ln\left(\frac{kr}{2}\right)+\frac{\Lambda(g)}{2}\right]^{-1},$$

where $\Lambda(g)$ is obtained in Eq. (4.29) as

$$\begin{aligned}
\Lambda(g) &= -\frac{1}{(1-\frac{g}{30}-\frac{g^2}{960})}\left[\frac{16}{g^2}+\frac{8}{g}+\frac{5}{2}-\frac{1}{60}g(-11+32\ln 2)+g^2\left(-\frac{311+5\pi^2}{1920}+\frac{4}{15}\ln 2\right)\right] \\
&\approx -\frac{32}{g^2}-\frac{256}{15g}-\frac{2521}{450} \\
&\approx \ln\left(\frac{ml^2E_b}{4\hbar^2e^{-2\gamma}}\right),
\end{aligned}$$

with E_b being the binding energy as is shown in Eq. (4.30). Matching the wavefunctions in the two regimes, we obtain the scattering amplitude as

$$f_k \approx \frac{2\pi}{\ln(2/kl) - \gamma + \Lambda(g)/2 + i\pi/2} = \frac{4\pi}{\ln(E_b/E) + i\pi}, \tag{4.31}$$

with $E = \hbar^2 k^2/m$ being the relative energy. Eq. (4.31) recovers the universal low-energy behavior of 2D scattering amplitude. For later convenience, we expand Eq. (4.31) up to the fourth order in g to have

$$\frac{f_k}{2\pi} \approx -\frac{g^2}{16} + \frac{g^3}{30} - \frac{g^4}{256}\left[\ln(\frac{2i}{kl}) - \gamma + \frac{7}{4}\right]. \tag{4.32}$$

4.4.3 Born series for the s-wave scattering

As we had mentioned before, we return to the the vertex function, which is introduced in Eq. (4.12), as it is considered in Ref .[7] to analysis the scattering in the s-wave channel. By iteration of Eq. (4.12), we obtain Born series and keeping up to the forth-order term in the interlayer interaction potential $\tilde{V}(\mathbf{q}) = \pi d_{eff}^2 q \exp(-lq) = (\pi\hbar^2 g/m) lq \exp(-lq)$ it reads

$$\begin{aligned}
\Gamma(E,\mathbf{k},\mathbf{k}') &= \tilde{V}(\mathbf{k}-\mathbf{k}') + \int \frac{d\mathbf{q}}{(2\pi)^2} \frac{\tilde{V}(\mathbf{k}-\mathbf{q})\tilde{V}(\mathbf{q}-\mathbf{k}')}{E - \hbar^2 q^2/m + i0} \\
&+ \int \frac{d\mathbf{q}_1 d\mathbf{q}_2}{(2\pi)^4} \frac{\tilde{V}(\mathbf{k}-\mathbf{q}_1)\tilde{V}(\mathbf{q}_1-\mathbf{q}_2)\tilde{V}(\mathbf{q}_2-\mathbf{k}')}{(E - \hbar^2 q_1^2/m + i0)(E - \hbar^2 q_2^2/m + i0)} \\
&+ \int \frac{d\mathbf{q}_1 d\mathbf{q}_2 d\mathbf{q}_3}{(2\pi)^6} \frac{\tilde{V}(\mathbf{k}-\mathbf{q}_1)\tilde{V}(\mathbf{q}_1-\mathbf{q}_2)\tilde{V}(\mathbf{q}_2-\mathbf{q}_3)\tilde{V}(\mathbf{q}_3-\mathbf{k}')}{(E - \hbar^2 q_1^2/m + i0)(E - \hbar^2 q_2^2/m + i0)(E - \hbar^2 q_3^2/m + i0)} + \cdots \\
&\equiv \Gamma^{(1)}(E,\mathbf{k},\mathbf{k}') + \Gamma^{(2)}(E,\mathbf{k},\mathbf{k}') + \Gamma^{(3)}(E,\mathbf{k},\mathbf{k}') + \Gamma^{(4)}(E,\mathbf{k},\mathbf{k}') + \cdots .
\end{aligned} \tag{4.33}$$

In the small energy limit $k \sim k' \sim \sqrt{mE/\hbar^2} \ll 1/l$, the leading contribution of these terms as the perturbation in $g = m d_{eff}^2/\hbar^2 < 1$ can be estimated as

$$\begin{aligned}
\Gamma^{(1)}(E,\mathbf{k},\mathbf{k}') &= \tilde{V}(\mathbf{k}-\mathbf{k}') \approx \frac{\pi\hbar^2}{m} g l |\mathbf{k}-\mathbf{k}'|, \\
\Gamma^{(2)}(E,\mathbf{k},\mathbf{k}') &\approx -\frac{\pi\hbar^2}{m}\frac{g^2}{8}, \\
\Gamma^{(3)}(E,\mathbf{k},\mathbf{k}') &\approx \frac{\pi\hbar^2}{m}\frac{g^3}{60}, \\
\Gamma^{(4)}(E,\mathbf{k},\mathbf{k}') &\approx -\frac{\pi\hbar^2}{m}\frac{g^4}{256}\left[\ln\left(\frac{\hbar^2}{mEl^2}\right) + i\pi\right].
\end{aligned}$$

The leading order for $\Gamma^{(1)}(E,\mathbf{k},\mathbf{k}')$ is repulsive which has significant consequence in the examination of our system in s-wave superfluidity, that in contrast with the model in Ref.[7] there would not be any instability in this regime respect to the superfluidity in our system. The

estimate for the leading order in $\Gamma^{(2)}(E,\mathbf{k},\mathbf{k}')$ and $\Gamma^{(3)}(E,\mathbf{k},\mathbf{k}')$ comes from large q ($q \gg k$) and large q_1, q_2 (q_1, $q_2 \gg k$) regions; and the leading contributions to $\Gamma^{(4)}(E,\mathbf{k},\mathbf{k}')$ stem from large q_1 ($q_1 \gg k$) and q_3 ($q_3 \gg k$) and small q_2 ($q_2 \sim \sqrt{mE/\hbar^2}$), respectively, correspond to the integrals in Eq. (4.33).

As it was mentioned in Sec. 4.1, through Ref.[7], concerning the above considerations, three different regimes of scattering for dilute weekly interacting regime *i.e.* $g < 1$, $kl < 1$ and $k \sim k_F$ have been introduced: regime (**A**) for $g < k_F l \lesssim 1$, regime (**B**) when $\exp(-1/g^2) \ll k_F l < g < 1$, and regime (**C**) as the $\exp(-1/g^2) \lesssim k_F l \ll g < 1$.

In regime (A) for $g < k_F l \lesssim 1$. The leading contribution to the scattering comes from the first-order Born series

$$\Gamma_{\mathbf{A}}(E,\mathbf{k},\mathbf{k}') \approx \Gamma^{(1)}(E,\mathbf{k},\mathbf{k}') = \tilde{V}(\mathbf{k}-\mathbf{k}') \approx \frac{\pi\hbar^2}{m} g l |\mathbf{k}-\mathbf{k}'|. \tag{4.34}$$

In regime (B) for $\exp(-1/g^2) \ll k_F l < g < 1$. In this case the dominant scattering term is given by the second-order Born series as

$$\Gamma_{\mathbf{B}}(E,\mathbf{k},\mathbf{k}') \approx \Gamma^{(2)}(E,\mathbf{k},\mathbf{k}') \approx -\frac{\pi\hbar^2}{m}\frac{g^2}{8}, \tag{4.35}$$

which is momentum-independent.

In regime (C) for $\exp(-1/g^2) \lesssim k_F l \ll g < 1$. In this regime the second- and the forth-order contribute in the same order and the entire leading order of Born series have to be summed, which results

$$\Gamma_{\mathbf{C}}(E,\mathbf{k},\mathbf{k}') \approx \frac{2\pi\hbar^2}{m}\frac{2}{\ln(E_b/E) + i\pi}, \tag{4.36}$$

where E_b is the binding energy and is derived in Sec. 4.4.1. Indeed, the scattering amplitude in regime (**C**) has the same form as the standard low-energy scattering amplitude in 2D which is derived in Sec.4.4.2. Note that within the lowest-order terms, the three terms in different regions can be expressed in the form

$$\Gamma(E,\mathbf{k},\mathbf{k}') \approx -\frac{2\pi\hbar^2}{m}\left[g l|\mathbf{k}-\mathbf{k}'| - \frac{2}{\ln(E_b)/E + i\pi}\right].$$

It has to be noted that the scattering amplitude is a complex parameter. The relation of imaginary and real part can be establish by means of Eq. (4.12) as

$$\text{Im}\ \Gamma(E,\mathbf{k},\mathbf{k}') = -\frac{m}{4\hbar^2}\int \frac{d\varphi_{\mathbf{q}}}{2\pi}\Gamma^*(E,\mathbf{k},\mathbf{q}_E)\Gamma(E,\mathbf{q}_E,\mathbf{k}'), \tag{4.37}$$

where $|\mathbf{q}_E| = \hbar^{-1}\sqrt{mE}$ and the integration would be performed over direction of this vector. The same relation as Eq. (4.37) is valid for the partial wave decomposition $\Gamma_m(E, \mathbf{k}, \mathbf{k}')$ with azimuthal quantum number m. The s-wave scattering channel can be obtained by

$$\Gamma_s(E, k, k') = \langle \Gamma(E, \mathbf{k}, \mathbf{k}') \rangle_{\varphi, \varphi'}.$$

The relation in Eq. (4.37) for s-wave channel $m = 0$ takes the form

$$\text{Im } \Gamma_s(E, k, k') = -\frac{m}{4\hbar^2} \Gamma_s^*(E, k, q_E) \Gamma_s(E, q_E, k').$$

The on-shell scattering amplitude, $k = k' = q_E = \hbar^{-1}\sqrt{mE}$ has the form

$$\text{Im } \Gamma_s(k) = -\frac{m}{4\hbar^2} |\Gamma_s(k)|^2. \tag{4.38}$$

This implies that up to the second-order we have

$$\text{Im } \Gamma_s(k) = -\frac{m}{4\hbar^2} \left[\text{Re } \Gamma_s(k)\right]. \tag{4.39}$$

In the following part, we review the s-wave scattering amplitude within a Born series. The on-shell s-wave vertex function can be written as a sum of power series in $g < 1$ as

$$\langle \Gamma_s(E, \mathbf{k}, \mathbf{k}') \rangle_{\varphi, \varphi'}|_{k=k'=\sqrt{mE/\hbar^2}} = \sum_{n=1}^{\infty} \Gamma_s^n(k),$$

where the average is performed over azimuthal angles φ and φ' and The Born series are presented in Eq. (4.33). For later calculations we mention the s-wave potential as

$$\begin{aligned} \tilde{V}_s(q_1, q_2) &= \langle \tilde{V}_s(\mathbf{q}_1 - \mathbf{q}_2) \rangle_{\varphi_1, \varphi_2} = \langle \tilde{V}_s(\mathbf{q}_1 - \mathbf{q}_2) \rangle_{\varphi} \\ &= \int \frac{d\varphi}{2\pi} \tilde{V}(\sqrt{q_1^2 + q_2^2 - 2q_1 q_2 \cos\varphi}) \\ &= -gl \frac{\pi\hbar^2}{m} \frac{\partial}{\partial l} \int \frac{d\varphi}{2\pi} e^{-l\sqrt{q_1^2 + q_2^2 - 2q_1 q_2 \cos\varphi}}, \end{aligned}$$

where has the form for $q_1 = 0$ (or $q_2 = 0$) as

$$\tilde{V}_s(q, 0) = \tilde{V}_s(0, q) = \tilde{V}(q) = gl \frac{\pi\hbar^2}{m} q e^{-lq},$$

and for $q_1 = q_2 = q$ it reads

$$\tilde{V}(q, q) = gl \frac{\pi\hbar^2}{m} q \left[\mathbf{L}_{-1}(2ql) - \mathbf{I}_1(2ql)\right],$$

where $\mathbf{L}_n(z)$ being the modified Struve function and $\mathbf{I}_n(z)$ is the modified Bessel function of the first kind. We represent the Born series up to fourth-order.

The first-order contribution of the Born series in s-wave channel happens as

$$\begin{aligned}\Gamma_s^{(1)}(k) &= \langle \tilde{V}(\mathbf{k}-\mathbf{k}')\rangle_{\varphi_1,\varphi_2} = \tilde{V}_s(k,k) \\ &= gl\frac{\pi\hbar^2}{m}k\left[\mathbf{L}_{-1}(2kl)-\mathbf{I}_1(2kl)\right],\end{aligned}$$

that for low momenta $kl \ll 1$ takes the form

$$\Gamma_s^{(1)}(k) = g\frac{\pi\hbar^2}{m}\left[\frac{4kl}{\pi}-2(kl)^2+O(k^3)\right]. \tag{4.40}$$

The second-order contribution to the s-wave scattering reads

$$\begin{aligned}\Gamma_s^{(2)}(k) &= \int \frac{d\mathbf{q}}{(2\pi)^2}\frac{\langle \tilde{V}(\mathbf{k}-\mathbf{q})\tilde{V}(\mathbf{q}-\mathbf{k}')\rangle_{\varphi,\varphi'}}{E-\hbar^2q^2/m+i0^+} \\ &= \fint \frac{qdq}{2\pi}\frac{\tilde{V}_s(k,q)\tilde{V}_s(q,k)}{E-\hbar^2q^2/m}-i\frac{m}{4\hbar^2}\tilde{V}_s(k,k)^2,\end{aligned}$$

where $\fint$ being the principle value integral. The integral of the real part has to be evaluated numerically; but the leading contribution for small momenta $kl \ll 1$ is

$$\begin{aligned}\mathrm{Re}[\Gamma_s^{(2)}(k)] &\approx -\frac{\pi\hbar^2}{2m}g^2l^2\int_0^\infty qdqe^{-2ql}+O(k) \\ &= -\frac{\pi\hbar^2}{2m}\frac{g^2}{4}+O(k).\end{aligned} \tag{4.41}$$

The imaginary part is

$$\begin{aligned}\mathrm{Im}[\Gamma_s^{(2)}(k)] &= -\frac{m}{4\hbar^2}\tilde{V}_s(k,k)^2 \\ &= -\frac{\pi\hbar^2}{2m}g^2(kl)^2 2\pi\left[\mathbf{L}_{-1}(2kl)-\mathbf{I}_1(2kl)\right] \\ &\approx -\frac{4\hbar^2}{m}g^2(kl)^2+O(k^3),\end{aligned} \tag{4.42}$$

where once again it is approximated for small momenta $kl \ll 1$.

The third-order contribution to the s-wave scattering takes the integral form as

$$\begin{aligned}
\Gamma_s^{(3)}(k) &= \int \frac{d\mathbf{q}_1 d\mathbf{q}_2}{(2\pi)^4} \frac{\langle \tilde{V}(\mathbf{k}-\mathbf{q}_1)\tilde{V}(\mathbf{q}_1-\mathbf{q}_2)\tilde{V}(\mathbf{q}_2-\mathbf{k})\rangle_{\varphi,\varphi'}}{(E-\hbar^2 q_1^2/m+i0^+)(E-\hbar^2 q_2^2/m+i0^+)} \\
&= \int \frac{q_1 dq_1}{2\pi} \int \frac{q_2 dq_2}{2\pi} \frac{\tilde{V}_s(k,q_1)\tilde{V}_s(q_1,q_2)\tilde{V}_s(q_2,k)}{(E-\hbar^2 q_1^2/m+i0^+)(E-\hbar^2 q_2^2/m+i0^+)} \\
&= \fint \frac{q_1 dq_1}{2\pi} \fint \frac{q_2 dq_2}{2\pi} \frac{\tilde{V}_s(k,q_1)\tilde{V}_s(q_1,q_2)\tilde{V}_s(q_2,k)}{(E-\hbar^2 q_1^2/m)(E-\hbar^2 q_2^2/m)} \\
&- i\frac{\tilde{V}_s(k,k)}{2\hbar^2/m} \fint \frac{qdq}{2\pi} \frac{\tilde{V}_s(k,q)\tilde{V}_s(q,k)}{E-\hbar^2 q^2/m} - \frac{m^2}{16\hbar^4}\tilde{V}_s(k,k)^3.
\end{aligned}$$

The real part has its minimum at $k=0$, where it reads

$$\begin{aligned}
\mathrm{Re}[\Gamma_s^{(3)}(k)] &= \int_0^\infty dq_1 \int_0^\infty dq_2 \frac{\tilde{V}_s(0,q_1)\tilde{V}_s(q_1,q_2)\tilde{V}_s(q_2,0)}{4\pi^2\hbar^4 q_1 q_2/m^2} \\
&= \frac{g^2 l^2}{4} \int_0^\infty dq_1 \int_0^\infty dq_2 e^{-q_1 l - q_2 l} \tilde{V}_s(q_1,q_2) \\
&= \frac{\pi}{2} g^2 l^2 \int_0^\infty r dr \frac{V(r)}{r^2+l^2} = \frac{\pi\hbar^2 g^3}{15m},
\end{aligned} \tag{4.43}$$

where for the s-wave potential the following representation is used

$$\tilde{V}_s(q_1,q_2) = 2\pi \int_0^\infty r dr V(r) J_0(q_1 r) J_0(q_2 r),$$

and for the convolution of the Bessel function

$$\int_0^\infty dq e^{-ql} J_0(qr) = \frac{1}{\sqrt{r^2+l^2}}.$$

The imaginary part of $\Gamma_s^{(3)}(k)$ has the form

$$\begin{aligned}
\mathrm{Im}[\Gamma_s^{(3)}(k)] &= -\frac{m}{2\hbar^2} V_s(k,k) \mathrm{Re}[\Gamma_s^{(2)}(k)] \\
&\approx \frac{\pi\hbar^2}{4m} g^3 kl + O(k^2).
\end{aligned} \tag{4.44}$$

The fourth-order contribution to the s-wave scattering by splitting it into its real and imaginary part reads as

$$
\begin{aligned}
\Gamma_s^{(4)}(k) &= \int \frac{d\mathbf{q}_1 d\mathbf{q}_2 d\mathbf{q}_3}{(2\pi)^6} \frac{\langle \tilde{V}(\mathbf{k}-\mathbf{q}_1)\tilde{V}(\mathbf{q}_1-\mathbf{q}_2)\tilde{V}(\mathbf{q}_2-\mathbf{q}_3)\tilde{V}(\mathbf{q}_3-\mathbf{k})\rangle_{\varphi,\varphi'}}{(E-\hbar^2 q_1^2/m+i0^+)(E-\hbar^2 q_2^2/m+i0^+)(E-\hbar^2 q_3^2/m+i0^+)} \\
&= \int \frac{q_1 dq_1}{2\pi} \int \frac{q_2 dq_2}{2\pi} \int \frac{q_3 dq_3}{2\pi} \frac{\tilde{V}_s(k,q_1)\tilde{V}_s(q_1,q_2)\tilde{V}_s(q_2,q_3)\tilde{V}_s(q_3,k)}{(E-\hbar^2 q_1^2/m+i0^+)(E-\hbar^2 q_2^2/m+i0^+)(E-\hbar^2 q_3^2/m+i0^+)} \\
&= \fint \frac{q_1 dq_1}{2\pi} \fint \frac{q_2 dq_2}{2\pi} \fint \frac{q_3 dq_3}{2\pi} \frac{\tilde{V}_s(k,q_1)\tilde{V}_s(q_1,q_2)\tilde{V}_s(q_2,q_3)\tilde{V}_s(q_3,k)}{(E-\hbar^2 q_1^2/m)(E-\hbar^2 q_2^2/m)(E-\hbar^2 q_3^2/m)} \\
&- 3\left[\frac{\tilde{V}_s(k,k)}{4\hbar^2/m}\right]^2 \fint \frac{qdq}{2\pi} \frac{\tilde{V}_s(k,q)\tilde{V}_s(q,k)}{E-\hbar^2 q^2/m} \\
&- 2i\frac{\tilde{V}_s(k,k)}{4\hbar^2/m} \fint \frac{q_1 dq_1}{2\pi} \fint \frac{q_2 dq_2}{2\pi} \frac{\tilde{V}_s(k,q_1)\tilde{V}_s(q_1,q_2)\tilde{V}_s(q_2,k)}{(E-\hbar^2 q_1^2/m)(E-\hbar^2 q_2^2/m)} \\
&- i\frac{m}{4\hbar^2}\left[\fint \frac{qdq}{2\pi} \frac{\tilde{V}_s(k,q)\tilde{V}_s(q,k)}{E-\hbar^2 q^2/m}\right]^2 \\
&+ i\left(\frac{m}{4\hbar^4}\right)^3 \tilde{V}_s(k,k)^4.
\end{aligned}
$$

The imaginary part of $\Gamma_s^{(4)}(k)$ in the limit $k \to 0$ approaches

$$
\begin{aligned}
\mathrm{Im}[\Gamma_s^{(4)}(k)] &= -\frac{m}{4\hbar^2}\left[\fint \frac{qdq}{2\pi} \frac{\tilde{V}_s(k,q)\tilde{V}_s(q,k)}{E-\hbar^2 q^2/m}\right]^2 \\
&= -\frac{\pi\hbar^2}{m}\frac{g^4\pi}{256}. \qquad (4.45)
\end{aligned}
$$

The real part of $\Gamma_s^{(4)}(k)$ diverges for $k \to 0$ as (for $kl \ll 1$)

$$
\begin{aligned}
\mathrm{Re}[\Gamma_s^{(4)}(k)] &\approx \left(\frac{m}{2\pi\hbar^2}\right)^3 \fint \frac{q_1 dq_1}{k^2-q_1^2} \fint \frac{q_2 dq_2}{k^2-q_2^2} \fint \frac{q_3 dq_3}{k^2-q_3^2} \tilde{V}_s(k,q_1)\tilde{V}_s(q_1,q_2)\tilde{V}_s(q_2,q_3)\tilde{V}_s(q_3,k) + O(k^2) \\
&\approx \left(\frac{m}{2\pi\hbar^2}\right)^3 \fint \frac{q_2 dq_2}{k^2-q_2^2}\left[\fint \frac{qdq}{q}\tilde{V}_s(0,q)\tilde{V}_s(q,q_2)\right]^2 + O(k) \\
&= \frac{\pi\hbar^2 g^4}{8m} \fint \frac{qdq}{k^2-q^2}\left[\fint lrldr \frac{(r^2-2l^2)}{(r^2+l^2)^3} J_0(rq)\right]^2 + O(k) \\
&= \frac{\pi\hbar^2 g^4}{8m} \fint \frac{qdq}{k^2-q^2}\left[\frac{ql}{2}\mathbf{K}_1(ql) - \frac{3(ql)^2}{8}\mathbf{K}_2(ql)\right]^2 + O(k) \\
&\approx -\frac{\pi\hbar^2 g^4}{8m}\frac{1}{16}\left[\ln(\frac{2}{kl}) + \frac{7}{4} - \gamma\right] + O(k), \qquad (4.46)
\end{aligned}
$$

where it is expanded for small momenta $kl \ll 1$ in the last line. By summing up the terms up to fourth order in low-energy regime as $kl \ll 1$ we have

$$\Gamma_s(k) \approx \sum_1^4 \Gamma_s^{(n)}(k) \approx -\frac{2\pi\hbar^2}{m}\Big\{ -\frac{g^2}{16} + \frac{g^3}{30} - \frac{g^4}{256}\left[\ln(\frac{2i}{kl}) - \gamma + \frac{7}{4}\right]\Big\}, \tag{4.47}$$

which coincides with the low energy scattering amplitude that is represented in Eq. (4.32).

4.4.4 Many-body corrections to the s-wave scattering amplitude

In Sec. 4.2.1, we have shown the general contribution of the many-body correction into the gap equation, upon the Gor'kov-Melik-Barkhudarov method [21]. In the following part, we discuss this many-body modification through s-wave channel. The analytical expression for such many-body contribution is given in Eq. (4.15), and correspond to the each triple regions, their participation would be presented. It is sufficient to consider the lowest many-body contributions to the effective interaction.

In the regime (A) $g < k_F l < 1$ the contribution of $\delta\tilde{V}_a(\mathbf{k},\mathbf{k}')$ for $k = k' = k_F$ reads

$$\begin{aligned}
\delta\tilde{V}_a(\mathbf{k},\mathbf{k}') &= -2\nu_F \tilde{V}(\mathbf{k}_-)\tilde{V}_{++}(\mathbf{k}_-) \\
&\approx -\frac{m}{\pi\hbar^2}\left(\frac{\pi\hbar^2}{m} g|\mathbf{k}-\mathbf{k}'|\right)^2 \\
&= -\frac{\pi\hbar^2}{m}(gl)^2(\mathbf{k}-\mathbf{k}')^2,
\end{aligned}$$

where $\mathbf{k}_\pm = \mathbf{k} \pm \mathbf{k}'$, and $\nu_F = m/2\pi\hbar^2$ density of state in 2D, $\tilde{V}_{++}(\mathbf{q}) = (\pi\hbar^2/m)gql$ being intralayer interaction, and $\tilde{V}(\mathbf{q}) = (\pi\hbar^2/m)gqlexp(-ql)$ is the interlayer interaction. The other three terms of many-body contribution have to be calculated numerically by averaging over the directions of $\mathbf{k}$ and $\mathbf{k}'$ corresponding to the s-wave channel as

$$\delta\bar{V}_i \equiv \langle\delta\tilde{V}_i(\mathbf{k},\mathbf{k}')\rangle_{\varphi,\varphi'} \equiv \int_0^{2\pi} \frac{d\varphi d\varphi'}{(2\pi)^2}\tilde{V}_i(\mathbf{k},\mathbf{k}'), \qquad i = a,\, b,\, c,\, d$$

where can be written as

$$\delta\bar{V}_i = \frac{\pi\hbar^2}{2m}(gk_F l)^2\eta_i,$$

and the coefficients being $\eta_a = -4$, $\eta_b = \eta_c = 1.148$, $\eta_d = 0.963$. Summing the effect of the terms gives

$$\delta\bar{V} = \frac{\pi\hbar^2}{2m}(gk_F l)^2\sum_i \eta_i = -0.741\frac{\pi\hbar^2}{2m}(gk_F l)^2. \tag{4.48}$$

In the regime (B) $exp(-1/g^2) \ll k_F l < g < 1$ the leading contribution to the interlayer two-body scattering is in the second-order Born term as g^2, while the leading order of the

intralayer scattering is in the first-order Born term proportional to gk_Fl and the dominant contribution is the p-wave one. Therefore, the many-body correction is given by the same diagram as in Fig. 4.4, in which all interlayer interactions are replaced with the second-order Born scattering amplitude $\Gamma^{(2)}$ and the whole many-body correction is written as

$$\delta\tilde{V}(\mathbf{k},\mathbf{k}') \approx \frac{2\pi\hbar^2}{m}\left(\frac{g^2}{16}\right)^2. \tag{4.49}$$

In the regime (C) $exp(-1/g^2) \lesssim k_Fl \ll g < 1$ the leading contribution of interlayer scattering is $\Gamma(E,\mathbf{k},\mathbf{k}') \approx (4\pi\hbar^2/m)[\ln(E_b/E) + i\pi]^{-1}$, which similar to the region (**B**) the leading order-term is proportional g^2 (see Eq. (4.47)). Thus, similar to the reasoning in regime (**B**), the many-body contribution comes from the same diagram as in Fig. 4.4, by replacing the interaction lines with the scattering amplitude. The many-body contribution reads as

$$\delta\tilde{V}(\mathbf{k},\mathbf{k}') \approx \frac{2\pi\hbar^2}{m}\left(\frac{2}{\ln(E_b/E)}\right)^2. \tag{4.50}$$

The leading many-body contribution to the effective interlayer interaction in the regimes (**B**) and (**C**), by taking into account the expansion of the scattering amplitude in Eq. (4.47), can be written as

$$\delta\tilde{V}(\mathbf{k},\mathbf{k}') = \frac{2\pi\hbar^2}{m}\left(\frac{g^2}{16}\right)^2, \tag{4.51}$$

that is independent of $\mathbf{k}$ and $\mathbf{k}'$.

4.4.5 Critical temperature and order parameter in the dilute regime

In the dilute regime $kl < 1$, we work out the critical temperature and the order parameter by means of Eq. (4.20) projected into the s-wave channel. As it was noted before, the many-body corrections contribute to the second-order in the small parameter $g < 1$, and they would be taken at Fermi surface. Hence, all second-order terms would be treated perturbatively. In the first-order, we solve the gap equation in the BCS approach similar to the calculation method which is presented in Sec. 4.3 and then add the many-body contribution.

BCS approach

We use the gap equation of the Eq. (4.14), linearized in term of the vertex function in Eq. (4.12) and are projected to the s-wave channel $\Gamma(2\mu,k,k')$. The energy of the pair is chosen at the Fermi energy $E = 2\mu$. The gap equation reads

$$\Delta(\xi) = -\int_{-\mu}^{\infty} d\xi'\, R(\xi,\xi')\,\Delta(\xi')\left[\frac{\tanh(\xi_{k'}/2T_c)}{2\xi_{k'}} - \frac{1}{2\xi_{k'} - i0}\right], \tag{4.52}$$

where $R(\xi,\xi') = \nu_F \Gamma(2\mu, k_\xi, k'_{\xi'})$ with $\xi = \hbar^2 k^2/2m - \mu$, and $\nu_F = m/2\pi\hbar^2$ being the density of state in 2D. introducing energy ω with characteristic relation as $\Delta(k), T_c \ll \omega \lesssim E_F$, we divide the integral in Eq.(4.52) into three parts: (a) the integration of $R(\xi,0)\Delta(0)$ in the interval of $(-\omega,\omega)$; (b) integral of $R(\xi,\xi')\Delta(\xi') - R(\xi,0)\Delta(0)$ throughout the same interval of $(-\omega,\omega)$; and the last one, integral of $R(\xi,\xi')\Delta(\xi')$ from $(-\mu,-\omega)$ and from $(-\omega,\infty)$. By engaging the asymptotic formula in the integral of part (a), there is

$$\int_{-\omega}^{\omega} d\xi' \frac{\tanh(\xi_{k'}/2T_c)}{2\xi_{k'}} \approx \ln\frac{2e^\gamma\omega}{\pi T_c}.$$

In part (b) and (c) we replace $\tanh(\xi_{k'}/2T_c)$ by the step function and integrate by parts, Eq. (4.52) reads as

$$\begin{aligned}
\Delta(\xi) &= -\left[\ln\frac{2e^\gamma\omega}{\pi T_c} - i\frac{\pi}{2}\right] R(\xi,0)\Delta(0) \\
&- R(\xi,-\mu)\Delta(-\mu)\ln\frac{\mu}{\omega} \\
&- \int_{-\mu}^{0} d\xi' \ln\left|\frac{\xi'}{\omega}\right| \frac{d}{d\xi'}\left[R(\xi,\xi')\Delta(\xi')\right].
\end{aligned} \tag{4.53}$$

In order to solve Eq. (4.53), we choose ω to satisfies the following equation at the Fermi surface

$$R(0,-\mu)\Delta(-\mu)\ln\frac{\mu}{\omega} + \int_{-\mu}^{0} d\xi' \ln\left|\frac{\xi'}{\omega}\right| \frac{d}{d\xi'}\left[R(0,\xi')\Delta(\xi')\right] = 0. \tag{4.54}$$

We solve the latter for ω to have

$$\begin{aligned}
\ln\omega &= \ln\mu\frac{R(0,-\mu)\Delta(-\mu)}{R(0,0)\Delta(0)} + \frac{1}{R(0,0)\Delta(0)}\int_{-\mu}^{0} d\xi' \ln|\xi'| \frac{d}{d\xi'}\left[R(0,\xi')\Delta(\xi')\right] \\
&= \ln\mu + \frac{1}{R(0,0)\Delta(0)}\int_{-\mu}^{0} d\xi' \ln\frac{|\xi'|}{\mu}\frac{d}{d\xi'}\left[R(0,\xi')\Delta(\xi')\right].
\end{aligned} \tag{4.55}$$

Now putting $\xi = 0$ in Eq. (4.53) and using Eq. (4.54), we obtain

$$\Delta(0) = -\left[\ln\frac{2e^\gamma\omega}{\pi T_c} - i\frac{\pi}{2}\right] R(0,0)\Delta(0). \tag{4.56}$$

Readily solve it for the critical temperature, we have

$$T_c^{BCS} = \frac{2e^\gamma}{\pi}\omega\exp\left[\frac{1}{R'(0,0)}\right], \tag{4.57}$$

where R' is the real part of R such that $R = R' + iR''$ according to the Eq. (4.39). Replacing Eq. (4.55) multiplied by $R(\xi,0)\Delta(0)$ and also Eq. (4.56) in the Eq. (4.53) to omit the ω-dependent terms in it, we obtain

$$\Delta(\xi) = \frac{R(\xi,0)}{R(0,0)}\Delta(0) + \int_{-\mu}^{0} d\xi' \ln\left|\frac{\xi'}{\mu}\right| \frac{d}{d\xi'}\left\{ \left[\frac{R(\xi,0)}{R(0,0)}R(0,\xi') - R(\xi,\xi')\right]\Delta(\xi')\right\}, \qquad (4.58)$$

where the second term is smaller in compare with the first term, in the regime of the week interaction. Hence, it can be treated perturbatively and to the first order we have

$$\Delta(\xi) \approx \frac{R(\xi,0)}{R(0,0)}\Delta(0), \qquad (4.59)$$

which is the same as Eq. (4.21) that had been derived by just reasoning intuitively. Using this relation in Eq. (4.55) to obtain

$$\ln\omega \;=\; \ln\mu + \frac{1}{R(0,0)^2}\int_{-\mu}^{0} d\xi' \ln\frac{|\xi'|}{\mu}\frac{d}{d\xi'}\left[R(0,\xi')R(\xi',0)\right]. \qquad (4.60)$$

This expression and one in Eq. (4.57) determine the critical temperature in BCS regime.

Many-body correction

Now, after by use of BCS critical temperature, we account the many-body effects, which contribute at the Fermi surface to the Eq. (4.56) as

$$\Delta(0) = -\frac{m_*}{m}\left[\ln\frac{2e^\gamma\omega}{\pi T_c} - i\frac{\pi}{2}\right]R(0,0)\Delta(0) - \ln\frac{2e^\gamma\omega}{\pi T_c}\nu_F\delta\bar{V}\Delta(0).$$

By use of Eq. (4.57), we solve it for critical temperature to obtain

$$\begin{aligned} T_c &= \frac{2e^\gamma\omega e^{1/R'(0,0)}}{\pi} exp\left[-\frac{m_*/m-1}{R'(0,0)} - \frac{\nu_F\delta\bar{V}}{R'(0,0)^2}\right] \\ &= T_c^{BCS}\exp\left[-\frac{m_*/m-1}{R'(0,0)} - \frac{\nu_F\delta\bar{V}}{R'(0,0)^2}\right], \end{aligned} \qquad (4.61)$$

and by use of Eq. (4.24) we can translate it to the order parameter at the Fermi energy, at zero-temperature

$$\Delta_0(k_F) = 2\omega e^{1/R'(0,0)} exp\left[-\frac{m_*/m-1}{R'(0,0)} - \frac{\nu_F\delta\bar{V}}{R'(0,0)^2}\right], \qquad (4.62)$$

where ω and m_* are given by Eq. (4.60) and Eq. (4.19), respectively. The scattering amplitude and many-body contribution depend on the regime of scattering.

In the regime (A), $g < k_F l < 1$, the leading contribution to the scattering amplitude is given by the first-order Born series where in s-wave channel. It is derived in Eq. (4.40) and the many-body correction is obtained in Eq. (4.48); therefore we have

$$
\begin{aligned}
R'(0,0) &\approx \nu_F\Gamma_s^{(1)} - \frac{g^2}{16}\left\{1 - 2(k_Fl)^2\left[5.4 + 3\ln(k_Fl)\right]\right\} + \frac{g^3}{30} \\
&\approx gk_Fl\frac{2}{\pi}\left(1 - \frac{\pi}{2}k_Fl\right) - \frac{g^2}{16}\left\{1 - 2(k_Fl)^2\left[5.4 + 3\ln(k_Fl)\right]\right\} + \frac{g^3}{30}, \\
\frac{m_*}{m} - 1 &= \frac{2}{3\pi}gk_Fl, \\
\nu_F\delta\bar{V} &= -0.741(\frac{gk_Fl}{2})^2. \qquad (4.63)
\end{aligned}
$$

Without consideration of the prefactor of the critical temperature, it is apparent that T_c^a is proportional with a exponentially diverging function of the interaction strength

$$T_c^a \propto \exp\left(\frac{1}{gk_Fl}\right),$$

which means that the highest critical temperature results by vanishing the interaction $g \to 0$. So there is not any superfluidity in regime (**A**) in our system. The reason obviously is the repulsive potential at small distances. The potential in this regime has a linear dependence to the momentum *i.e.* so-called anomalous term. The leading contribution to the scattering is given by the first Born term which is repulsive in our case as $\Gamma_a(E,\mathbf{k},\mathbf{k}') \approx (\pi\hbar^2/m)gl|\mathbf{k}-\mathbf{k}'|$, on the contrary to the term in Ref. [7] which is attractive $\Gamma_a^S(E,\mathbf{k},\mathbf{k}') \approx -(2\pi\hbar^2/m)gl|\mathbf{k}-\mathbf{k}'|$ and contributes to the pairing.

In the regime (B), $k_Fl < g < 1$, the second-order Born term is dominated as is derived in Eq. (4.41). The many-body correction is also has been shown in Eq. (4.48); thus we write

$$
\begin{aligned}
R'(0.0) &\approx -\frac{g^2}{16} + gk_Fl\frac{2}{\pi}\left(1 - \frac{\pi}{2}k_Fl\right) + \frac{g^3}{30} - \frac{g^4}{512}\left[\ln\left(4\hbar^2/m\mu l^2\right) + \frac{7}{2} - 2\gamma\right] \\
&\approx \frac{2}{\ln\left(E_b/\mu\right)} + gk_Fl\frac{2}{\pi}\left(1 - \frac{\pi}{2}k_Fl\right),
\end{aligned}
$$

with many-body correction as

$$\nu_F\delta\bar{V} \approx \left[\frac{g^2}{16}\right]^2,$$

and the renormalized mass

$$\frac{m_*}{m} - 1 \approx \frac{2}{3\pi}k_Fl.$$

The leading-order contribution of the scattering amplitude in $R'(0,0)$ is momentum-independent. Thus $\omega = \mu$ is chosen and we have

$$\frac{1}{R'(0,0)} \approx -\left[\frac{g^2}{16} - gk_F l\frac{2}{\pi}\left(1-\frac{\pi}{2}k_F l\right)\right]^{-1} + \frac{1}{2}\left[\ln\left(\frac{4\hbar^2}{m\mu l^2}\right) + \frac{7}{2} - 2\gamma\right],$$

and

$$\begin{aligned}\frac{m_*/m-1}{R'(0,0)} &\approx \frac{28}{3\pi}\frac{k_F l}{g} \ll 1,\\ \frac{\nu_F \delta\bar{V}}{[R'(0,0)]^2} &\approx 1.\end{aligned}$$

Thereby, we write the critical temperature as

$$T_c^b = \frac{2e^\gamma}{\pi}\mu \exp\left\{-\left[\frac{g^2}{16} - gk_F l\frac{2}{\pi}\left(1-\frac{\pi}{2}k_F l\right)\right]^{-1} + \frac{1}{2}\left[\ln\left(\frac{4\hbar^2}{m\mu l^2}\right) + \frac{7}{2} - 2\gamma\right] - 1\right\}, \quad (4.64)$$

and by use of Eq. (4.24) we write down the order parameter at zero temperature on the Fermi energy

$$\frac{\Delta_0^b(k_F)}{2\mu} = \exp\left\{-\left[\frac{g^2}{16} - gk_F l\frac{2}{\pi}\left(1-\frac{\pi}{2}k_F l\right)\right]^{-1} + \frac{1}{2}\left[\ln\left(\frac{4\hbar^2}{m\mu l^2}\right) + \frac{7}{2} - 2\gamma\right] - 1\right\}. \quad (4.65)$$

Finally, by means of the relation in Eq. (4.1), we translate the constraint of the regime (**A**) to the our dimensionless parameter as

$$y < r_s/y < 1 \equiv \begin{cases} r_s < y, \\ \\ y < \sqrt{r_s}, \end{cases} \quad (4.66)$$

which specifies an area in the phase diagram that is depicted in Fig. 4.6.

In the regime (C), $\exp(-1/g^2) \lesssim k_F l \ll g < 1$, the leading contributions to the scattering amplitude come from the entire Born series, as derived in Eq. (4.47) and the many-body corrections also presented in Eq. (4.51). Therefore, we write

$$R'(0,0) \approx \frac{2}{\ln(E_b/\mu)},$$

and the renormalized mass as

$$\left|\frac{m_*}{m} - 1\right| \approx \frac{2}{3\pi} g k_F l \ll 1,$$

and the many-body correction in this regime being

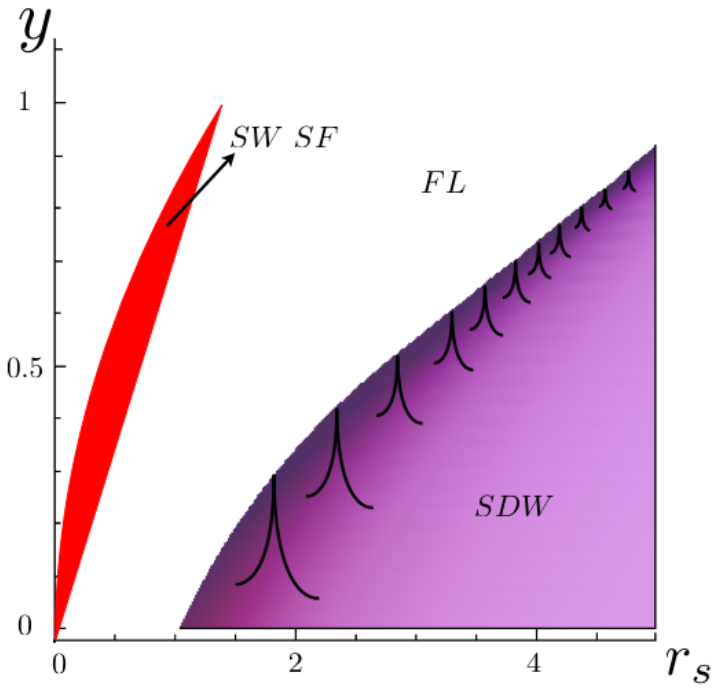

Figure 4.6: The area of the the validity of the order parameter (red area) for the s-wave superfluidity (**SW SF**), in the regime (**B**), is shown schematically. The spin density wave (**SDW**) phase is also presented for the comparison.

$$\nu_F \delta\bar{V} \approx \left[\frac{2}{\ln\left(E_b/\mu\right)}\right],$$

where E_b is the shallow binding energy and has been derived in Eq. (4.30). Similar to the regime (**B**) by $\omega = \mu$, we have for critical temperature

$$\begin{aligned} T_c^c &= \frac{2e^{\gamma}}{\pi}\mu \exp\left[\frac{1}{2}\ln\left(E_b/\mu\right) - 1\right] \\ &= \frac{2e^{(\gamma-1)}}{\pi}\sqrt{\mu E_b}, \end{aligned} \tag{4.67}$$

and thus the order parameter as

$$\Delta_0^c(k_F) = \frac{2}{e}\sqrt{\mu E_b}, \tag{4.68}$$

where coincides with the order parameter of the superfluidity in the short range potentials in 2D (see Ref. [38]).

By engaging the relation in Eq. (4.1), we translate the constraint of the regime (**C**) into our dimensionless parameters as

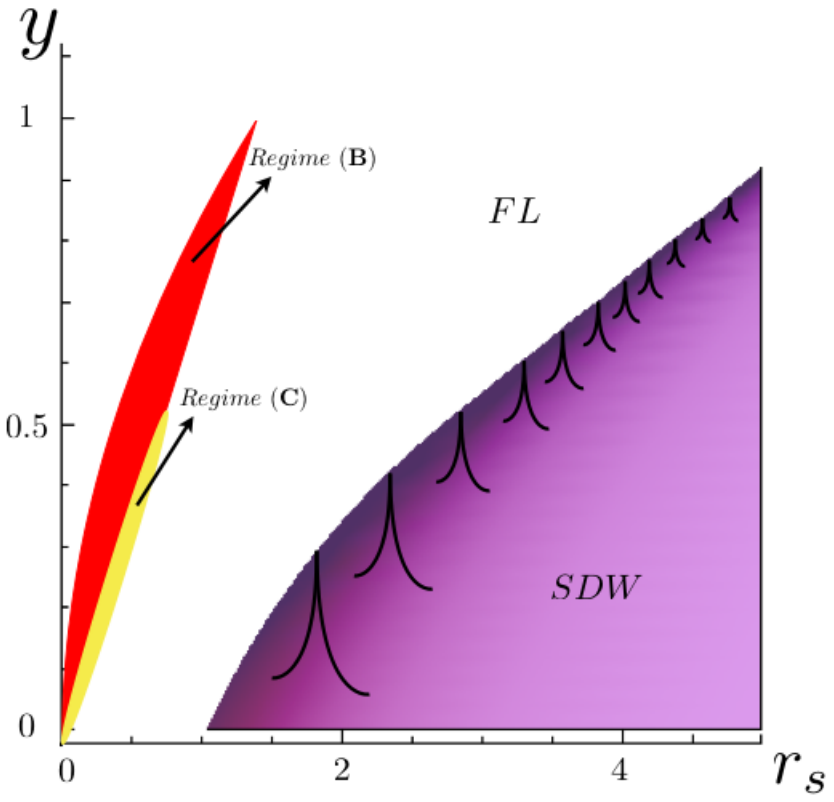

Figure 4.7: The area of the validity for the s-wave superfluidity in the regime (**C**) is shown in yellow color, schematically.

$$y \ll r_s/y < 1 \equiv \begin{cases} r_s < y, \\ \\ y \ll \sqrt{r_s}, \end{cases} \tag{4.69}$$

which defines a tiny area in the phase diagram that is shown in Fig. 4.7, in addition to the superfluidity corresponds to the regime (**B**), Fermi liquid, and spin density wave phases.

In the leading-order of the terms, we can rewrite the expressions for regime (**B**) and (**C**) as

$$\frac{\Delta_0^{b,c}(k_F)}{2\mu} = \exp\left\{\left[\frac{2}{\ln\left(E_b/\mu\right)} + gk_Fl\frac{2}{\pi}\left(1-\frac{\pi}{2}k_Fl\right)\right]^{-1}\right\}. \tag{4.70}$$

In the regimes (**B**) and (**C**) the order parameter in the leading-order is momentum-independent.

In the Ref. [7] the instability respect superfluidity in the dense regime corresponds to $k_Fl > 1$ is also considered. Obviously, in the dense regime the behavior of the potential in smaller distances would be much more important and due to the repulsive character of our potential in these distances, it fails to contribute to the superfluidity; hence we would not discuss the dense regime further.

4.5 P-wave superfluidity

Instability with respect to p-wave pairing superfluidity can occur, in our system, due to the attractive long-tail interaction, which decays by $1/r^3$. The present case is entirely similar to the situation in Ref. [28]. We follow their approach to map the gap equation in Eq. (4.17) into p-wave channel.

4.5.1 P-wave scattering amplitude

The off-shell scattering amplitude is defined as

$$f(\mathbf{k}', \mathbf{k}) = \int \exp\left(-i\mathbf{k}'\mathbf{r}\right) V_0(r) \tilde{\psi}_{\mathbf{k}}(\mathbf{r}) d^2r, \tag{4.71}$$

where $\tilde{\psi}_{\mathbf{k}}(\mathbf{r})$ is the the two-body wavefunction with relative momentum of $\mathbf{k}$. The potential is the large distances limit as

$$\begin{aligned} V_0(r) \equiv \lim_{r\to\infty} V(r) &= \lim_{r\to\infty} d_{eff}^2 \frac{l^2 - r^2/2}{(l^2 + r^2)^{5/2}} \\ &= -\frac{d_{eff}^2}{2}\frac{1}{r^3} \\ &= -\frac{\hbar^2}{m}\frac{r_*}{r}. \end{aligned} \tag{4.72}$$

Ww decompose the scattering amplitude into its p-wave partial wave amplitude, that would be $f(k', k) \exp i\phi$, where ϕ is the angle between $\mathbf{k}$ and $\mathbf{k}'$. The p-wave scattering amplitude is given by

$$f(k', k) = \int_0^\infty J_1(k'r) V_0(r) \tilde{\psi}(k, r) 2\pi r dr, \tag{4.73}$$

with J_1 being the Bessel function. The wavefunction is obtained by solving the Schrödinger equation for $m_z = 1$

$$-\frac{\hbar^2}{m}\left[\frac{d^2}{d^2r} + \frac{1}{r}\frac{d}{dr} - \frac{1}{r^2} - V_0(r)\right]\tilde{\psi} = \frac{\hbar^2 k^2}{m}\tilde{\psi}. \tag{4.74}$$

The on-shell scattering in term of the p-wave scattering phase shift $\delta(k)$ (see Re. [2]), reads

$$f(k, k) = f(k) = -\frac{2\hbar^2}{im}\left[\exp\left(2i\delta(k)\right) - 1\right] = -\frac{4\hbar^2}{m}\frac{\tan\delta(k)}{1 - i\tan\delta(k)}. \tag{4.75}$$

In the regime $r \to \infty$, we write the wavefunction as

$$\tilde{\psi}(k, r) = J_1(kr) - \frac{if(k)}{4} H_1(kr),$$

where $H_1 = J_1 + iN_1$ is the Hankel function, and N_1 being the Neumann function. The wavefunction is supposed to be normalized in such way that for $r \to \infty$, it would be real as

$$\psi(k,r) = [J_1(kr) - \tan\delta(k)\, N_1(kr)] \propto \cos(kr - 3\pi/4 + \delta), \tag{4.76}$$

where we have $\tilde{\psi}(k,r) = \psi(k,r)/(1 - i\tan\delta(k))$. By inserting this relation into Eq. (4.73), we rewrite the off-shell scattering amplitude as

$$f(k',k) = \frac{\bar{f}(k',k)}{1 - i\tan\delta(k)}, \tag{4.77}$$

where $\bar{f}(k',k)$ is achieved by replacing $\tilde{\psi}$ with ψ in Eq. (4.73) as

$$\bar{f}(k',k) = \int_0^\infty J_1(k'r)V_0(r)\psi(k,r)2\pi r dr. \tag{4.78}$$

For $k = k'$, by comparing with Eq. (4.75), we have

$$\bar{f}(k,k) \equiv \bar{f}(k) = -(4\hbar^2/m)\tan\delta(k). \tag{4.79}$$

We obtain the scattering amplitude by solving the Schrödinger equation in the large and short distances limit, and matching the asymptotic wavefunctions. To do so, a length scale r_0 is introduced and the wavefunctions will be solved in two regions correspond to $r < r_0$ and $r > r_0$, where r_0 lies in the interval $r_* \ll r_0 \ll k^{-1}$ and r_* is introduced in Eq. (4.72) (two regions are shown in Fig. 4.8).

In region I for $r < r_0$, we can neglect the kinetic energy versus the interaction potential, and solve the Schrödinger equation in the p-wave channel

$$-\frac{\hbar^2}{m}\left(\frac{d^2}{d^2r} + \frac{1}{r}\frac{d}{dr} - \frac{1}{r^2} - V_0(r)\right)\psi_I = 0. \tag{4.80}$$

The solution can be written as

$$\psi_I(r) \propto \left[AJ_2\left(2\sqrt{\frac{r_*}{r}}\right) + N_2\left(2\sqrt{\frac{r_*}{r}}\right)\right], \tag{4.81}$$

where A depends to the behavior of the potential $V(r)$ at short distances, and some estimation would be shown later. In the region II, for $r > r_*$ the relative motion could be given free and the potential $V_0(r)$ would be contributed perturbatively. In the zeroth order the wavefunction reads

$$\psi_{II}^{(0)}(r) = J_1(kr) - \tan\delta_I(k)N_1(kr), \tag{4.82}$$

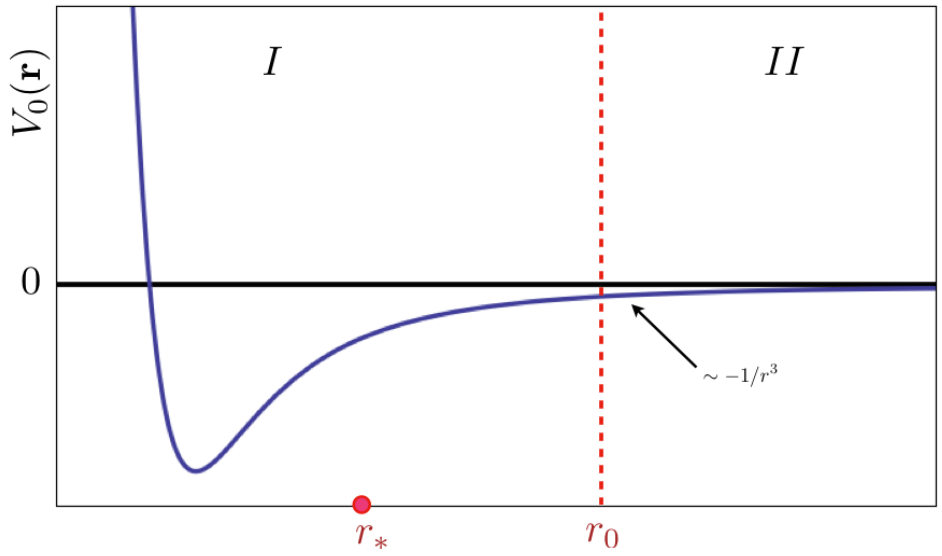

Figure 4.8: The ranges of the interaction is split into two regions: region $I$for $r < r_0$ and region II for $r > r_0$. The length scale r_* is shown schematically and the length scale r_0 with the constrain $r_* \ll r_0$. (The image is reproduced from Ref. [28])

that the phase shift $\delta_I(k)$ stems from scattering in region I. Matching the logarithmic derivative of the wavefunctions of two regions at $r = r_0$, we find the phase shift

$$\tan\delta_I(k) = \frac{\pi k^2 r_0 r_*}{8}\left[1 - \frac{r_*}{r_0}\left(2\gamma - \frac{1}{2} + \pi A - \ln\frac{r_0}{r_*}\right)\right], \tag{4.83}$$

where $\gamma = 0.5772$ is the Euler's constant. It is taken into account, in Eq. (4.83), that $r \gg r_*$ and $kr_0 \ll 1$. In the first order, we contribute the interaction $V_0(r)$ and by means of the Green function method (see Ref. [18]) we have

$$\psi^{(1)}_{II}(r) = \psi^{(0)}_{II}(r) - \int_{r_0}^{\infty} G(r,r')V_0(r')\psi^{(0)}_{II}(r')2\pi r' dr', \tag{4.84}$$

where the Green function for p-wave channel follows the radial equation as

$$-\frac{\hbar^2}{m}\left(\frac{d^2}{d^2r} + \frac{1}{r}\frac{d}{dr} - \frac{1}{r^2} + k^2\right)G(r,r') = \frac{\delta(r-r')}{2\pi r}.$$

Using the asymptotic wavefunction introduced in Eq. (4.76) for Green function we have

$$G(r,r') = -\frac{m}{4\hbar^2}\begin{cases} \psi^{(0)}_{II}(r')\,N_1(kr) & r > r', \\ \psi^{(0)}_{II}(r)\,N_1(kr') & r < r'. \end{cases}$$

Substituting the Green function in Eq. (4.84) in $r \to \infty$ limit, and once again, matching the wavefunctions at $r = r_0$, we have for the phase shift

$$\begin{aligned}\tan\delta^1(k) &= \tan\delta_I(k) - \frac{m}{4\hbar^2}\int_{r_0}^{\infty}\left[\psi_{II}^{(0)}(r)\right]^2 V_0(r)2\pi r dr \\ &\approx \frac{2}{3}kr_* - \frac{\pi(kr_*)^2}{8}\left[\ln\frac{r_*}{r_0} + 2\gamma - \frac{3}{2} + \pi A\right] + O(k^3).\end{aligned}$$

For the second order contribution, by iteration we have

$$\psi_{II}^{(2)}(r) = \psi_{II}^{(1)}(r) + \int_{r_0}^{\infty} G(r,r')V_0(r')2\pi r' dr' \int_{r_0}^{\infty} G(r',r'')V_0(r'')\psi_{II}^{(0)}(r'')2\pi r'' dr'',$$

and matching the logarithmic derivative, we obtain

$$\begin{aligned}\tan\delta(k) &= \tan\delta^{(1)}(k) - \frac{(\pi kr_*)^2}{2}\int_{kr_0}^{\infty}\frac{J_1^2(x)}{x^2}\left[\frac{2}{3}x\left(N_0(x)J_2(x) - N_1(x)J_1(x)\right)\right. \\ &- \left.\frac{1}{2}N_0(x)J_1(x) + \frac{1}{6}N_1(x)J_2(x) - \frac{1}{\pi x}\right]dx \\ &\approx \tan\delta^{(1)}(k) - \frac{(\pi kr_*)^2}{8}\left\{\frac{7}{12} + \gamma + -\ln 2 + \ln kr_0\right\} + O(k^3) \\ &\approx \frac{2}{3}kr_* - \frac{(\pi kr_*)^2}{8}\ln\rho kr_*, \qquad (4.85)\end{aligned}$$

where

$$\rho = \exp\left\{3\gamma - \ln 2 - 11/12 + \pi A\right\} \approx 1.13\exp(\pi A). \qquad (4.86)$$

By engaging Eq. (4.79) and Eq. (4.75), we find the on-shell scattering amplitude, represented by two terms $\bar{f}(k) = \bar{f}_1(k) + \bar{f}_2(k)$ as

$$\begin{aligned}\bar{f}_1(k) &= -\frac{8}{3}\frac{\hbar^2}{m}kr_*, \\ \bar{f}_2(k) &= \frac{\pi}{2}\frac{\hbar^2}{m}(kr_*)^2\ln\rho kr_*, \qquad (4.87)\end{aligned}$$

in which the term $\bar{f}_1(k)$ is dominant in the low-momentum limit. The leading low-momentum contribution of the off-shell scattering amplitude $\bar{f}(k',k)$ can be obtained by replacement $J_1(kr) \to \psi(k,r)$ in Eq. (4.78), which gives

$$\begin{aligned}\bar{f}(k',k) &= \int_{r_0}^{\infty} J_1(k'r)J_1(kr)V_0(r)2\pi r dr \\ &= -\frac{\pi\hbar^2}{m}kr_* F(-\frac{1}{2},\frac{1}{2},2,\frac{k^2}{k'^2}), \qquad (4.88)\end{aligned}$$

where it is taken into account that for $r > r_0$ the interaction potential has the form $V_0 = -\hbar^2 r_*/mr^3$. The parameter F in Eq. (4.88) is the hypergeometric function, where it is written for $k < k'$. For $k > k'$, the k and k' have to be interchanged.

4.5.2 Many-body corrections to the p-wave scattering amplitude

In this part, we project the many-body contributions, which are given in Eq. (4.15), into the p-wave channel. The correponding partial-wave of the diagrams in Fig. 4.4 would be achieved by integrating out the azimuthal symmetry corresponds to the p-wave symmetry as

$$\delta V(k',k) = \sum_{j\in\{a,b,c,d\}} \delta V_j(k',k) = \int_0^{2\pi} \frac{d\phi}{2\pi} e^{-i\phi} \sum_{j\in\{a,b,c,d\}} \delta V_j(\mathbf{k}',\mathbf{k}), \tag{4.89}$$

where ϕ is the angle between k and k'. The interaction potential, which contributes into many-body corrections as in Eq. (4.15), is taken like

$$V_0(r) \approx \begin{cases} 0 & r < r_0, \\ \\ -(\hbar^2/m) r_*/r^3 & r > r_0, \end{cases}$$

Its Fourier transform takes the form

$$V_0(\mathbf{q}) \approx -\frac{2\pi\hbar^2}{m}\frac{r_*}{r_0} + \frac{2\pi\hbar^2}{m}\mathbf{q}r_*.$$

The momentum-independent term of the interaction potential would not contribute to the diagrams as it will be cancelled. For analytical calculation of critical temperature T_c, it is only needed to calculate the contribution of many-body correction on the Fermi surface for $k = k' = k_F$, where each term in Eq. (4.15) takes the form $\delta V_j(k_F, k_F) = \alpha_j(\hbar^2/m)(k_F r_*)^2$. The coefficients reads

$$\alpha_a = 4\pi, \quad \alpha_b = \alpha_c = -1.5, \quad \alpha_d = -1.0.$$

Therefore the total correction reads as

$$\delta V(k_F, k_F) \equiv \alpha \frac{\hbar^2}{m}(k_F r_*)^2, \tag{4.90}$$

with $\alpha = \sum_j \alpha_j = 8.6$.

It should be noted that in Ref. [28], as the system is constructed upon a single layer of particles, the layer (spin) degeneracy correspond to the $\delta\tilde{V}_a(k',k)$ in Fig. 4.4 has not been included. Hence, α_a associated with our system is doubled in comparison with the coefficient in Ref. [28].

4.5.3 Critical temperature and order parameter

We return to the gap equation in (4.20). we attempt to obtain the critical temperature T_c, and afterwards, we will obtain the order parameter at zero-temperature on Fermi energy $\Delta_0(E_F)$ by engaging Eq. (4.24). Once again, we perform the integrals in Eq. (4.20) by dividing their region into two parts: $|E_{k'} - E_F| < \omega$ and $|E_{k'} - E_F| > \omega$. We start by calculating $\Delta(k_F)$ and calculate the contribution of each region separately.

In the first region, the parameters would be replaced as $\Delta(k_F) \to \Delta(k')$ and $\bar{f}(k', k_F) = \bar{f}(k_F) \to f(k', k_F)$, where $\bar{f}(k_F) = \bar{f}_1(k_F) + \bar{f}_2(k_F)$ which is derived in Eq. (4.87). Therefore the second term in the square brackets would contribute negligibly. We put in the first term $\epsilon_{k'} = |\xi_{k'}|$.Thus the result of the integral in this region is

$$\Delta_1(k_F) = \Delta(k_F)\frac{4k_F r_*}{3\pi}\left(1 - \frac{3\pi}{16}k_F r_* \ln\left(\rho k_F r_*\right)\right)\ln\left(\frac{2e^{\gamma}\omega}{\pi T_c}\right), \tag{4.91}$$

where ρ is introduced in Eq. (4.86).

In the second region, we put $\tanh\left(\epsilon_{k'}/2T_c\right)/2\epsilon_{k'} = 1/2\xi_{k'}$. The contribution of this region, in compare with the with latter result, is so small$\sim k_F r_*$ and it suffices to keep just the leading low-momentum term of the off-shell scattering amplitude in Eq. (4.88). By use of Eq. (4.24), we write the gap equation in this region

$$\Delta_2(k_F) = \Delta(k_F)\frac{3\pi r_*}{8k_F}\int_0^{k_\omega}\frac{k'^3 dk'}{(k_F^2 - k'^2)}F^2\left(-\frac{1}{2}, \frac{1}{2}, 2, \frac{k'^2}{k_F^2}\right),$$

where $k_\omega = \sqrt{2m(E_F - \omega)/\hbar^2}$. By remembering the limit $\omega \ll E_F$, we obtain

$$\Delta_2(k_F) = \Delta(k_F)\frac{4k_F r_*}{3\pi}\left[\ln\left(\frac{E_F}{\omega}\right) - \eta\right], \tag{4.92}$$

where

$$\eta = 1 - \frac{9\pi^2}{64}\int_0^1\left[F^2\left(-\frac{1}{2}, \frac{1}{2}, 2, x\right) - F^2\left(-\frac{1}{2}, \frac{1}{2}, 2, 1\right)\right]\frac{xdx}{1-x} \approx 0.78. \tag{4.93}$$

The main contribution of the many-body correction comes from the vicinity of the Fermi surface in second integral of Eq. (4.20). Therefore, we used the $\delta V(k_F, k_F)$ which is presented in Eq. (4.90) and the integral reads

$$\Delta_3(k_F) = -\Delta(k_F)\frac{\delta V(k_F, k_F)}{2\pi}\ln\left(\frac{2e^{\gamma}\omega}{\pi T_c}\right). \tag{4.94}$$

Sum the whole separate terms, by canceling Δ_F we obtain a equation for the critical temperature as

$$1 = \frac{4k_F r_*}{3\pi}\left[\ln\left(\frac{2e^\gamma E_F}{\pi T_c}\right) - \eta\right] - (k_F r_*)^2 \ln\left(\frac{E_F}{T_c}\right)\left\{\frac{1}{4}\ln(\rho k_F r_*) + \frac{\alpha}{2\pi}\right\}, \tag{4.95}$$

where it is chosen that $\omega = E_F$, as the terms which contain ω are small as $k_F r_* \ll 1$ in comparison with the leading term.

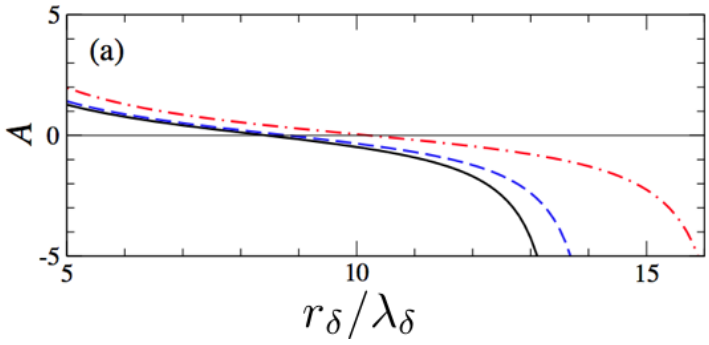

Figure 4.9: The coefficient A is depicted versus r_δ/λ_δ for $\Omega_R/\delta = 0.25$ and $\beta = 0$ (black, solid line), $\beta = 0.1$ (blue, dashed line), and $\beta = 0.2$ (red, dash-dotted line), where Ω_R being the Rabbi frequency, δ the frequency detuning, and $\beta = dE_{dc}/B$ (see the Sec. 2.1). In our system, there is no dc field, hence, the solid line corresponds to $\beta = 0$ would be favorable. (The image is taken from Ref. [28])

For contributing the renormalized mass (see Eq. (4.19)) into the calculation, we see that the relative difference between m_* and m is proportional to $k_F r_* \ll 1$. By replacing m_* instead of the bare mass m in Eq. (4.95), a new term $(16/9\pi^2)\ln(E_F/T_c)$ would be introduced. Thus by replacing $\tilde{\alpha} = \alpha - 32/9\pi$ and considering the limit of $k_F r_* \ll 1$ we have for critical temperature

$$\frac{T_c}{2E_F} = \frac{e^\gamma}{\pi}\frac{\kappa}{(k_F r_*)^{9\pi^2/64}}\exp\left(-\frac{3\pi}{4k_F r_*}\right), \tag{4.96}$$

where

$$\begin{aligned}\kappa &= \exp\left\{-\frac{9\pi^2}{64}\ln\rho - \frac{9\pi}{32}\tilde{\alpha} - \eta\right\} \\ &\approx 0.00053\exp\left(-\frac{9\pi^3 A}{64}\right),\end{aligned} \tag{4.97}$$

in which ρ and η are introduced in Eq. (4.86) and Eq. (4.93), respectively. By use of Eq. (4.24) we translate the critical temperature into the order parameter at zero-temperature on the Fermi energy as

$$\frac{\Delta_0(k_F)}{2E_F} = \frac{\kappa}{(k_F r_*)^{9\pi^2/64}}\exp\left(-\frac{3\pi}{4k_F r_*}\right). \tag{4.98}$$

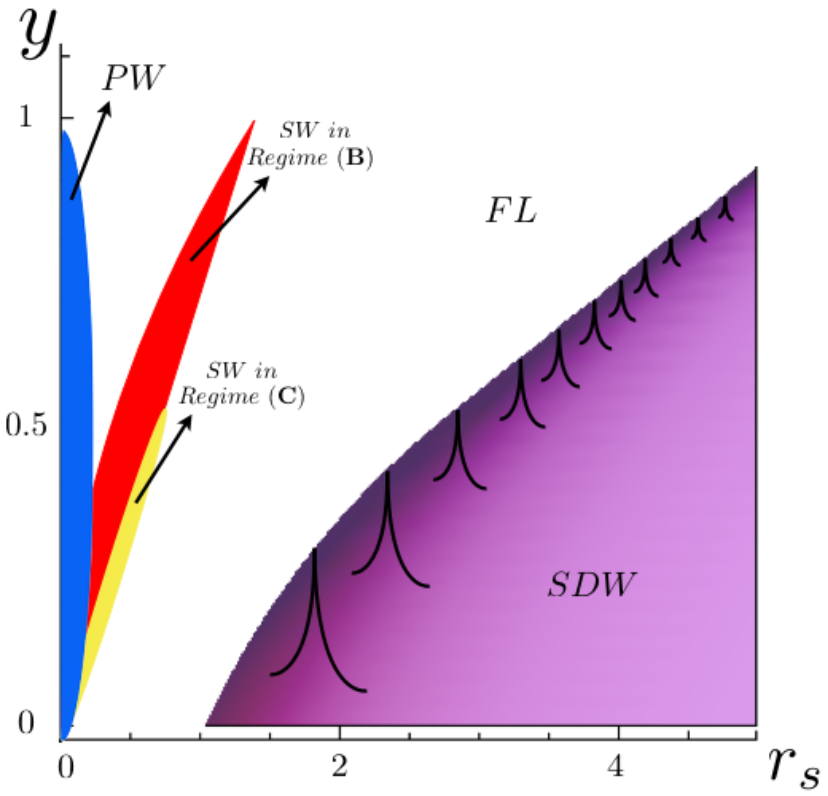

Figure 4.10: The area of the validity for the order parameter of the p-wave superfluidity is presented roughly in blue color. Other phases are also added, including s-wave superfluidity associated with two overlapping regions, and the SDW phase.

The dependence of the order parameter on the short distances is included in κ through the coefficient A. In Fig. 4.9 parameter A is depicted versus parameter of the system $(r_\delta/\lambda_\delta)$, where $r_\delta = (d_c^2/\hbar\delta)$ and $\lambda_\delta = \sqrt{\hbar/m\delta}$, where $\delta = \omega - \omega_0$ is the frequency detuning, the difference between microwave external field ω and the transition frequency between internal states of molecules $|\phi_{00}\rangle$ and $|\phi_{11}\rangle$; and $d_c = (d/\sqrt{3})(1-49\beta^2/1440)$ is the transition dipole moment between the mentioned states by static external field $\beta \propto E_{dc}$ (see the Sec. 2.1). Actually, in our system there is not any dc field, so $\beta = 0$, which corresponds to the black solid line in Fig. 4.9.

At the end, the area in the phase diagram corresponds to the p-wave super fluidity (weak interaction $k_F r_* \sim r_s \ll 1$ and dilute system $lk_F < 1$), has been presented in Fig. 4.10 schematically, besides other phases of the system..

4.6 Summary

Throughout this chapter, the instability of the system respect to the interlayer superfluidity through s-wave and p-wave pairing has been analyzed. We have adopted the approach of two references [7, 28] to analyze the superfluidity of the system. The interaction potentials in the corresponding references have close similarity with the interaction our system. It should be

noted that the both references go beyond the standard BCS approach by involving many-body corrections, based upon the Gor'kov-Melik-Barkhudarov method [21].

We have used Ref. [7] to examine the s-wave superfluidity in Sec. 4.4. Upon the criterions presented in this reference, three regimes have been introduced correspond to the relation of the natural length scale of the system. Our system shows instability in two of those regions: (**B**) $exp(-1/g^2) \ll k_F l < g < 1$ and (**C**) $exp(-1/g^2) \lesssim k_F l \ll g < 1$. Within accepted accuracy, it is possible to unified the expressions of the order parameters for these two regime as is presented in Eq. (4.70). The area in phase diagram associated with the s-wave superfluidity is depicted roughly in Fig. 4.10.

To study the p-wave bilayer superfluidity we have followed Ref. [28]. Their interaction potential, indeed, coincides with our one at large distances. Although the system in Ref. [28] is composed of a single layer, their analysis would be applicable for our system by some modifications. The order parameter of the p-wave superfluidity is presented in Eq. (4.98), which is valid for the dilute system $k_F l \ll 1$ with weak interaction $k_F r_* \sim r_s \ll 1$. Thus, it enhances the phase diagram of the system, as is shown in Fig. 4.10, schematically.

It can be seen in Fig. 4.10 that there is a competition between the interlayer superfluidity in s-wave and p-wave pairing channels around the origin of the diagram. The winner ground state would be determined by the constraint of the lowest ground state energy. We have not calculated the ground state energies of those state. By the way, we adopt the claim mentioned in Ref. [28], that the p-wave superfluidity phase is the most stable phase, since it fully gaps the Fermi surface, in contrast to the competing phases. Hence, the p-wave superfluidity would be the dominant ground state, wherever there is a competition between p-wave and s-wave superfluidity in the diagram. It must be noted that the examination of the p-wave pairing at short distances would be a prospective to extend the calculation of the considered system.

Chapter 5

Summary and outlook

In the preceding chapters, we have analyzed the instability of the system versus a number of phases at zero-temperature. Generally speaking, The phase transition is associated with the broken symmetries of the system. In the classical phase transition, thermal fluctuation is responsible for such broken symmetry phenomenas. But at zero-temperature, it is merely the quantum fluctuation who is responsible for the broken symmetry and labeled by the quantum phase transition (see Ref. [39]).

In this thesis, we have analyzed a bilayer system of cold polar molecules, which have been introduced in Sec. 2.1. The striking feature of the cold polar molecules is the tunable interparticle interaction. In the considered system, the interaction of the polar molecules are dressed by means of a circularly polarized MW field. The designed bilayer interaction of the system shows a repulsive behavior and an attractive long-tail at large distances (see Fig. 2.2). These characters of the interaction potential put the system on the verge of the instability toward various quantum phases.

In chapter 3, the instability of the bilayer system versus spin density wave phase has been examined. Due to the repulsive interlayer interaction, and particularly, the repulsive interaction potential in the momentum space, the system undergoes a phase transition toward SDW as a function of the external parameter of the system, say interlayer separation $y = lk_F$ and the strength of the interaction $r_s = md_{eff}^2 k_F/\hbar^2$. It has been discussed that whenever the system is in the SDW phase, by variation of the external parameter $y = lk_F$, there would be further phase transitions from SDW to SDW, whenever the commensurability happens as $q = (m/n)k_F$ (m and n are integer and q is the coupling vector of the particle-hole pair). In the mean-field framework, it is shown that within the SDW phase the symmetry of the system would be broken from invariant translational symmetry to the discrete translational symmetry associated with the triangular lattice, as is depicted in Fig.3.5. The ground state energy and the order parameter are calculated, correspond to the different area of the phase diagram, as far as was analytically possible. The phase diagram is shown in Fig. 3.10.

In chapter 4, bilayer superfluidity of the system has been examined following the reports of the references [7, 28]. Both references contribute the many-body effects, upon the Gor'kov-Melik-Barkhudarov idea [21], and go beyond the standard BCS theory. We analyzed the bilayer superfluidity through s-wave and p-wave channels separately, and it has been shown

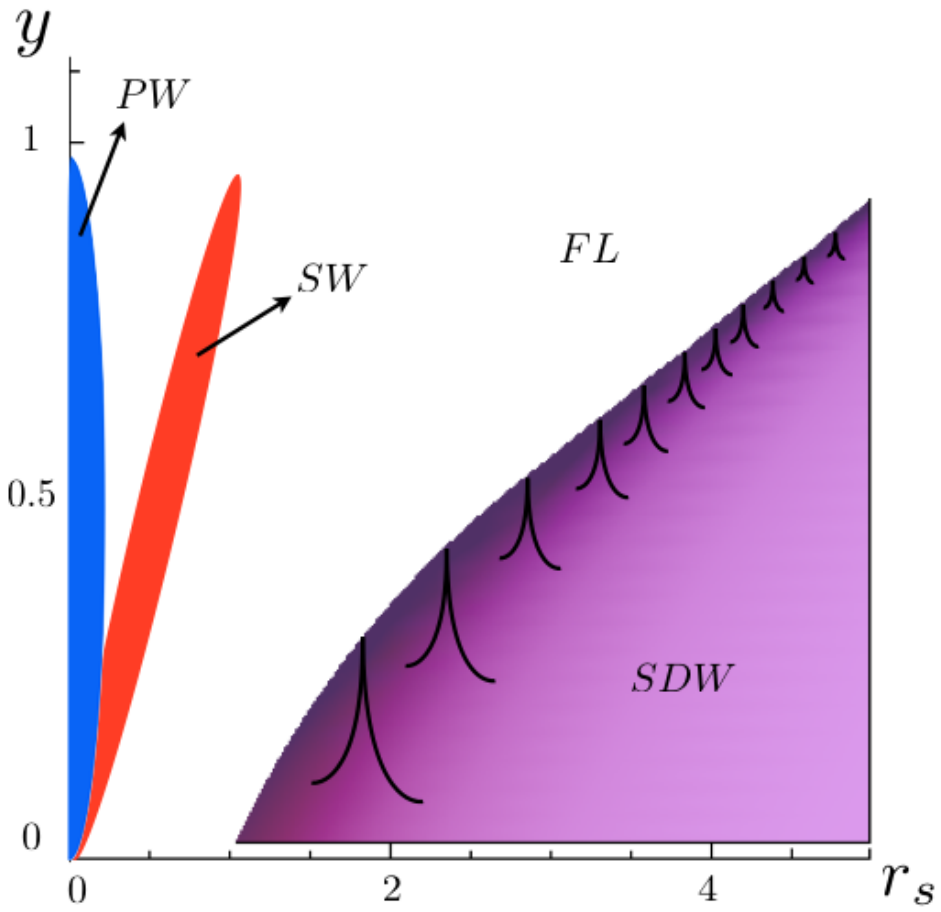

Figure 5.1: The phase diagram of the bilayer cold polar molecules versus $y = lk_F$ and $r_s = md_{eff}^2 k_F/\hbar^2$. The areas associated with the s-wave (**SW**) superfluidity, p-wave (**PW**) superfluity, and spin density (**SDW**) phases, which are competing with the Fermi liquid (**FL**) phase, are shown in red, blue, purple, and white area, respectively. The two regions of the s-wave superfluidity, presented in Fig. 4.10, are coincided into one area of the phase diagram (red color area).

that due to the attractive long-tail of the interlayer interaction, molecules from different layers could form s-wave or p-wave bound state. The order parameter and critical temperature have been extracted correspond to the particular regime of the external parameter of the system. The phase diagram, included all of the phases which the system shows instability, is presented in Fig. 5.1.

It can be seen in the phase diagram that there is a competition between s-wave and p-wave superfluidity at extremely week interaction. It is discussed that the p-wave superfluidity would be the dominant phase as it fully gaps the Fermi surface, in contrast to the other competing phases. As it has been mentioned, the p-wave pairing is examined in the large distances regime and its behavior in the small distances, in which the repulsive interaction potential comes into stage, is left as a prospective.

Appendix A

Linear response theory

In this appendix, we review the effect of an weak external potential $H^{ext}(t)$ on the Hamiltonian of the system H. In the other words, we examine the response of the system with respect to a weak external field. The external potential is given to be weak, so can be treated perturbatively (see for example Ref. [42, 20]).

We start by writing full Hamiltonian as $H^T(t) = H + H^{ext}(t)$, where H is the unperturbed Hamiltonian. The Schrödinger equation for total Hamiltonian reads

$$i\hbar\frac{\partial}{\partial t}|\Psi_S(t)\rangle = H^T(t)|\Psi_S(t)\rangle, \tag{A.1}$$

where subscript S indicates we are working in the Schrödinger picture (see [19, 20]). We define the evolution operator $U^T(t, t_0)$ as

$$|\Psi_S(t)\rangle = U^T(t, t_0)|\Psi_S(t_0)\rangle. \tag{A.2}$$

Inserting this in the Schrödinger we have

$$i\hbar\frac{\partial}{\partial t}U^T(t, t_0) = H^T(t)U^T(t, t_0). \tag{A.3}$$

By use of the boundary condition for the unitary evolution operator as $U^T(t_0, t_0) = 1$, we readily solve Eq. (A.3) to have

$$U^T(t, t_0) = 1 - \frac{i}{\hbar}\int_{t_0}^{t} dt' H^T(t')U^T(t', t_0). \tag{A.4}$$

It is possible to construct the same equation for the evolution operator of the unperturbed Hamiltonian as

$$i\hbar\frac{\partial}{\partial t}U(t, t_0) = H(t)U(t, t_0). \tag{A.5}$$

We suggest a relation between evolution operator of full Hamiltonian $U^T(t,t_0)$ and the one for unperturbed Hamiltonian $U(t,t_0)$ as

$$U^T(t,t_0) = U(t,t_0)\tilde{U}(t,t_0), \tag{A.6}$$

where $\tilde{U}(t,t_0)$ would be determined by means of the external perturbation. Inserting Eq. (A.6) in Eq. (A.3), there would be

$$i\hbar\frac{\partial}{\partial t}\left[U(t,t_0)\tilde{U}(t,t_0)\right] = \left(H(t)+H^{ext}(t)\right)U(t,t_0)\tilde{U}(t,t_0). \tag{A.7}$$

By use of Eq. (A.5), we obtain a familiar form like

$$\begin{aligned} i\hbar\frac{\partial}{\partial t}\tilde{U}(t,t_0) &= U^\dagger(t,t_0)H^{ext}(t)U(t,t_0)\tilde{U}(t,t_0) \\ &\equiv \tilde{H}^{ext}(t)\tilde{U}(t,t_0), \end{aligned} \tag{A.8}$$

where $\tilde{H}^{ext}(t) = U^\dagger(t,t_0)H^{ext}(t)U(t,t_0)\tilde{U}(t,t_0)$ being the external potential in Heisenberg picture. In the same approach as the Eq. (A.4) obtained we solve Eq. (A.8) and keep the terms up to first order in $\tilde{H}^{ext}(t)$ by iteration to obtain

$$\tilde{U}(t,t_0) = 1 - \frac{i}{\hbar}\int_{t_0}^{t} dt'\,\tilde{H}^{ext}(t'). \tag{A.9}$$

Inserting this result in Eq. (A.6), we obtain

$$\begin{aligned} U^T(t,t_0) &= U(t,t_0) - \frac{i}{\hbar}\int_{t_0}^{t} dt' \underbrace{U(t,t_0)}_{U(t,t')U(t',t_0)} U^\dagger(t',t_0)H^{ext}(t')U(t',t_0) \\ &= U(t,t_0) - \frac{i}{\hbar}\int_{t_0}^{t} dt' U(t',t_0)H^{ext}(t')U(t',t_0), \end{aligned} \tag{A.10}$$

where the unitarity relation $U^\dagger U = 1$ is used in the first line. Now by use of this evolution operator, we derive the eigenstate of the system at any arbitrary time

$$\begin{aligned} |\Psi_S(t)\rangle &= \exp\left[-\frac{i}{\hbar}H(t-t_0)\right]|\Psi_S(t_0)\rangle \\ &- \frac{i}{\hbar}\int_{t_0}^{t} dt' \exp\left[-\frac{i}{\hbar}H(t-t')\right]H^{ext}(t')\exp\left[-\frac{i}{\hbar}H(t-t_0)\right]|\Psi_S(t_0)\rangle. \end{aligned} \tag{A.11}$$

It is possible now to construct the expectation value of any observable and thus obtain the effect of the external potential. Write down the expectation value generally for a operator $\hat{O}$, by choosing $t_0 = 0$ we have

$$\begin{aligned}\langle\hat{O}(t)\rangle_{H^T} &= \langle\Psi_S|\hat{O}|\Psi_S\rangle \\ &= \langle\Psi_H|\hat{O}|\Psi_H\rangle + \frac{i}{\hbar}\int_{\tilde{t}_0}^{t} dt'\langle\Psi_H|\left[H_H^{ext}(t'),\,\hat{O}_H\right]|\Psi_H\rangle, \end{aligned} \tag{A.12}$$

where subscript H indicates the representation in Heisenberg picture in which $|\Psi_H\rangle = |\Psi_S(t = 0)\rangle$. The lower limit of the integral is taken at $0 < \tilde{t}_0 < t$ when the external field is switched on. We then arrive at the general form for the response of the system corresponds to the external field, which leads to the modification of the systems' observable as

$$\begin{aligned}\delta\langle\hat{O}(t)\rangle &= \delta\langle\hat{O}(t)\rangle_{H^T} - \delta\langle\hat{O}(t)\rangle_H \\ &= \frac{i}{\hbar}\int_{\tilde{t}_0}^{t} dt'\langle\Psi_0|\left[H_H^{ext}(t'),\,\hat{O}_H\right]|\Psi_0\rangle, \end{aligned} \tag{A.13}$$

where the expectation value is taken at the ground state of the system.

A.0.1 Density-density response function

A particular important case is the response of the system to an external potential coupled to the charge-density of the system. As far as the system is not polarized $\epsilon_\uparrow(\mathbf{k}) = \epsilon_\downarrow(\mathbf{k})$, the result would be applicable for the response of the system respect to an external field that is coupled with the spin-density of the system. By the way, suppose the external potential is given as

$$H^{ext}(t) = \int d\mathbf{r}\,\hat{n}_H(\mathbf{r},t)\varphi^{ext}(\mathbf{r},t),$$

which change in the charge density of the system is

$$\begin{aligned}\delta\langle\hat{n}(\mathbf{r},t)\rangle &= \frac{i}{\hbar}\int_{\tilde{t}_0}^{t} dt'\int d\mathbf{r}'\langle\Psi_0|\left[\hat{n}_H(\mathbf{r}',t'),\,\hat{n}_H(\mathbf{r},t)\right]|\Psi_0\rangle\varphi^{ext}(\mathbf{r}',t') \\ &= \int_{-\infty}^{\infty} dt'\int d\mathbf{r}'\chi(\mathbf{r},\mathbf{r}')\varphi^{ext}(\mathbf{r}',t'), \end{aligned} \tag{A.14}$$

where we have introduced the generalized susceptibility as

$$\chi(\mathbf{r},\mathbf{r}') = -\frac{i}{\hbar}\theta(t-t')\frac{\langle\Psi_0|\left[\hat{n}_H(\mathbf{r}',t'),\,\hat{n}_H(\mathbf{r},t)\right]|\Psi_0\rangle}{\langle\Psi_0|\Psi_0\rangle}. \tag{A.15}$$

The relation in Eq. (A.14) takes a simple form in the momentum-frequency space as

$$\delta\langle\hat{n}(\mathbf{q},\omega)\rangle = \chi(\mathbf{q},\omega)\varphi^{ext}(\mathbf{q},\omega). \tag{A.16}$$

A.0.2 Lehmann's representation

In the following section we attempt to obtain the density-density response function for a Fermi gas *i.e.* a non-interacting system, by engaging generalized susceptibility in Eq. (A.15). We work over the normalized ground state $\langle\Psi_0|\Psi_0\rangle = 1$. Therefore, the generalized susceptibility take the form

$$\chi(\mathbf{r},\mathbf{r}') = -\frac{i}{\hbar}\theta(t-t')\langle\Psi_0|\left[\hat{n}_H(\mathbf{r},t),\,\hat{n}_H(\mathbf{r}',t')\right]|\Psi_0\rangle.$$

As it contains a commutator, we calculate one of the products and then apply the result for the other one by $\mathbf{r}\leftrightarrow\mathbf{r}'$. By inserting a complete set of eigenstates $\sum_n |\Psi_n\rangle\langle\Psi_n| = 1$, it takes the form

$$\begin{aligned}
&\langle\Psi_0|\hat{n}_H(\mathbf{r},t),\hat{n}_H(\mathbf{r}',t')|\Psi_0\rangle \\
=\;& \sum_n \langle\Psi_0|e^{iHt/\hbar}\sum_\alpha \hat{\psi}^\dagger_\alpha(\mathbf{r})\hat{\psi}_\alpha(\mathbf{r})e^{-iHt/\hbar}|\Psi_n\rangle\langle\Psi_n|e^{iHt'/\hbar}\sum_\beta \hat{\psi}^\dagger_\beta(\mathbf{r}')\hat{\psi}_\beta(\mathbf{r}')e^{-iHt'/\hbar}|\Psi_0\rangle \\
=\;& \sum_n e^{-i(E_n-E_0-i\eta)(t-t')/\hbar}\sum_{\alpha,\,\beta}\langle\Psi_0|\hat{\psi}^\dagger_\alpha(\mathbf{r})\hat{\psi}_\alpha(\mathbf{r})|\Psi_n\rangle\langle\Psi_n|\hat{\psi}^\dagger_\beta(\mathbf{r}')\hat{\psi}_\beta(\mathbf{r}')|\Psi_0\rangle,
\end{aligned}$$

where we have introduced the small factor $i\eta$ to prevent the oscillation of the exponential term at infinity. By performing the Fourier transform to frequency space and adding the other term we have

$$\begin{aligned}
\chi(\mathbf{r},\mathbf{r}';\omega) \;=\; \sum_{\substack{n\\ \alpha,\,\beta}}\Bigg[&\frac{\langle\Psi_0|\hat{\psi}^\dagger_\alpha(\mathbf{r})\hat{\psi}_\alpha(\mathbf{r})|\Psi_n\rangle\langle\Psi_n|\hat{\psi}^\dagger_\beta(\mathbf{r}')\hat{\psi}_\beta(\mathbf{r}')|\Psi_0\rangle}{\hbar\omega-(E_n-E_0)+i\eta} \\
&-\frac{\langle\Psi_0|\hat{\psi}^\dagger_\alpha(\mathbf{r}')\hat{\psi}_\alpha(\mathbf{r}')|\Psi_n\rangle\langle\Psi_n|\hat{\psi}^\dagger_\beta(\mathbf{r})\hat{\psi}_\beta(\mathbf{r})|\Psi_0\rangle}{\hbar\omega+(E_n-E_0)-i\eta}\Bigg].
\end{aligned}$$

The field operators in the momentum space have the form

$$\begin{aligned}
\hat{\psi}_\alpha(\mathbf{r}) &= \frac{1}{\sqrt{V}}\sum_{\mathbf{k}}\hat{f}_{\mathbf{k}\alpha}\exp(i\mathbf{k}.\mathbf{r}), \\
\hat{\psi}^\dagger_\beta(\mathbf{r}) &= \frac{1}{\sqrt{V}}\sum_{\mathbf{k}}\hat{f}^\dagger_{\mathbf{k}\beta}\exp(-i\mathbf{k}.\mathbf{r}).
\end{aligned}$$

Therefore, we write for the expectation value of the field operators as

$$\begin{aligned}
&\langle\Psi_0|\hat{\psi}^\dagger_\alpha(\mathbf{r})\hat{\psi}_\alpha(\mathbf{r})|\Psi_n\rangle\langle\Psi_n|\hat{\psi}^\dagger_\beta(\mathbf{r}')\hat{\psi}_\beta(\mathbf{r}')|\Psi_0\rangle = \\
&\frac{1}{V^2}\sum_{\mathbf{k}_1,\cdots\mathbf{k}_4}\exp\left[-(\mathbf{k}_1-\mathbf{k}_2).\mathbf{r}\right]\exp\left[-(\mathbf{k}_3-\mathbf{k}_4).\mathbf{r}'\right]\langle\Psi_0|\hat{f}^\dagger_{\mathbf{k}_1\alpha}\hat{f}_{\mathbf{k}_2\alpha}|\Psi_n\rangle\langle\Psi_n|\hat{f}^\dagger_{\mathbf{k}_3\beta}\hat{f}_{\mathbf{k}_4\beta}|\Psi_0\rangle.
\end{aligned}$$

As $|\Psi_0\rangle$ is the ground state, we have these relations among the wavevectors

$$\begin{aligned} \mathbf{k}_4 &\equiv \mathbf{k}, \qquad |\mathbf{k}| < k_F, \\ \mathbf{k}_3 &\equiv \mathbf{k}', \qquad |\mathbf{k}'| > k_F, \\ \mathbf{k}_2 &\equiv \mathbf{k}', \\ \mathbf{k}_1 &\equiv \mathbf{k}. \end{aligned} \tag{A.17}$$

By writing the excitation energy like as $E_n = E_0 + \epsilon_{\mathbf{k}+\mathbf{q}} - \epsilon_{\mathbf{k}}$, we have for the susceptibility in momentum space

$$\begin{aligned} \chi^0(\mathbf{q},\omega) &= \frac{1}{V^2}\sum_{\substack{\mathbf{k}\\ \alpha,\,\beta}} \left[\frac{\langle\Psi_0|\hat{f}^\dagger_{\mathbf{k}\alpha}\hat{f}_{\mathbf{k}'\alpha}|\Psi_n\rangle\langle\Psi_n|\hat{f}^\dagger_{\mathbf{k}'\beta}\hat{f}_{\mathbf{k}\beta}|\Psi_0\rangle}{\hbar\omega - (\epsilon_{\mathbf{k}+\mathbf{q}} - \epsilon_{\mathbf{k}}) + i\eta} \right. \\ &\quad \left. - \frac{\langle\Psi_0|\hat{f}^\dagger_{\mathbf{k}'\alpha}\hat{f}_{\mathbf{k}\alpha}|\Psi_n\rangle\langle\Psi_n|\hat{f}^\dagger_{\mathbf{k}\beta}\hat{f}_{\mathbf{k}'\beta}|\Psi_0\rangle}{\hbar\omega + (\epsilon_{\mathbf{k}-\mathbf{q}} - \epsilon_{\mathbf{k}}) - i\eta} \right] \\ &= \frac{2}{V^2}\sum_{\mathbf{k}} \left[\frac{\theta(|\mathbf{k}+\mathbf{q}| - k_F)\theta(k - k_F)}{\hbar\omega - (\epsilon_{\mathbf{k}+\mathbf{q}} - \epsilon_{\mathbf{k}}) + i\eta} \right. \\ &\quad \left. - \frac{\theta(|\mathbf{k}-\mathbf{q}| - k_F)\theta(k - k_F)}{\hbar\omega + (\epsilon_{\mathbf{k}-\mathbf{q}} - \epsilon_{\mathbf{k}}) - i\eta} \right] \\ &= \frac{2}{V^2}\sum_{\mathbf{k}} \frac{\theta(k_F - k) - \theta(k_F - |\mathbf{k}+\mathbf{q}|)}{\hbar\omega - (\epsilon_{\mathbf{k}+\mathbf{q}} - \epsilon_{\mathbf{k}}) + i\eta}, \end{aligned} \tag{A.18}$$

where after renaming the variable in the second term, we have used the relation $\theta(x) = 1 - \theta(-x)$. The spin-degeneracy is compensated by the prefactor 2 in the third line. The integral form for the static response function $\omega = 0$ can be written as

$$\chi(\boldsymbol{q}) = \int \frac{d\boldsymbol{k}}{(2\pi)^d} \frac{f_{\boldsymbol{k}} - f_{\boldsymbol{k}+\boldsymbol{q}}}{\epsilon_{\boldsymbol{k}} - \epsilon_{\boldsymbol{k}+\boldsymbol{q}}}. \tag{A.19}$$

where $f_{\boldsymbol{k}}$ is the Fermi distribution function. We report the explicit forms of the response function at zero-temperature $T = 0$ correspond to 1D, 2D, and 3D space as

$$\begin{aligned} \chi^0_{1D}(\mathbf{q}) &= -2\omega^{1D}(E)\frac{1}{2x}\ln\left|\frac{1+x}{1-x}\right|, \\ \chi^0_{2D}(\mathbf{q}) &= -2\omega^{2D}(E)\begin{cases} 1 & x < 1, \\ 1 - \sqrt{1-x^{-2}} & x \geqslant 1, \end{cases} \\ \chi^0_{3D}(\mathbf{q}) &= -2\omega^{3D}(E)\left[\frac{1}{2} - \frac{1}{4x}(1-x^2)\ln\left|\frac{1-x}{1+x}\right|\right], \end{aligned} \tag{A.20}$$

where $x = q/2k_F$ and $\omega^{iD}(E)$ is the density of state per spin, corresponds to the i-th dimension(s). The response functions are depicted in Fig. A.1. The particular behavior of the response functions at $q = 2k_F$ would have significant physical effect. It can be seen that response function in 1D is divergent at $q = 2k_f$, which implies the instability of the free system with respect to the even extremely small perturbation. In 2D, at the same value $q = 2k_F$ the response function shows a non-analytical behavior, and in 3D the derivative has a logarithmic singularity.

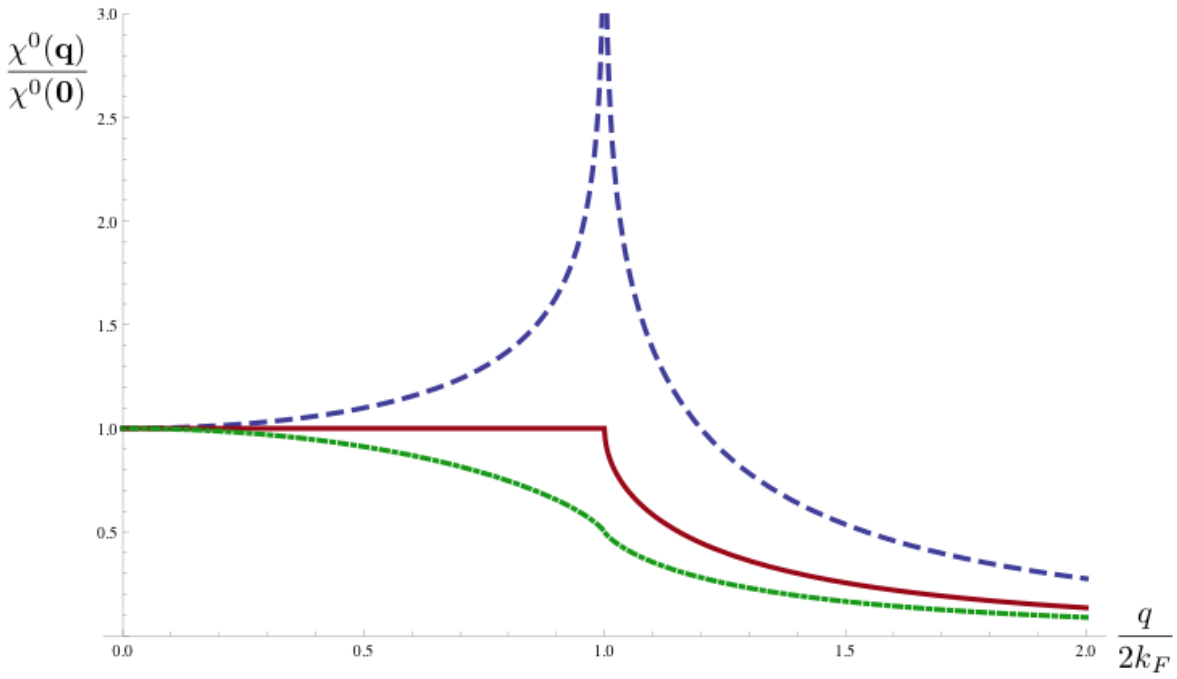

Figure A.1: Wavevectore dependent Lindhard response function for one- (dark blue dashed line), two- (solid red line), and three-dimensional (dash-dotted green line) system of free fermionic gas at zero-temperature.

Bibliography

[1] A. A. Abrikosov, L. P. Gorkov, and I. E. Dzyaloshinski. *Methods of quantum field theory in statistical physics.* Prentice-Hall Inc., 1963.

[2] Sadhan K. Adhikari. Quantum scattering in two dimensions. *American Journal of Physics*, 54(4):362–367, 1986.

[3] A. Altland and B. Simons. *Condensed Matter Field Theory.* Cambridge University Press, second edition, 2010.

[4] M. H. Anderson, J. R. Ensher, M. R. Matthews, C. E. Wieman, and E. A. Cornell. Observation of bose-einstein condensation in a dilute atomic vapor. *Science*, 269(5221):198–201, 1995.

[5] M. R. Andrews, J. Stenger, H.-J. Miesner, D. M. Stamper-Kurn, and W. Ketterle. Observation of feshbach resonances in a bose-einstein condensate. *Nature*, 392(6672):151–154, 1998/03/12/print.

[6] Neil W. Ashcroft and David N. Mermin. *Solid State Physics.* Harcourt College, 1976.

[7] M. A. Baranov, A. Micheli, S. Ronen, and P. Zoller. Bilayer superfluidity of fermionic polar molecules: Many-body effects. *Phys. Rev. A*, 83:043602, Apr 2011.

[8] Jason Socrates Bardi. Landmarks: Laser cooling of atoms. *Phys. Rev. Focus*, 21:11, Apr 2008.

[9] G. M. Bruun and E. Taylor. Quantum phases of a two-dimensional dipolar fermi gas. *Phys. Rev. Lett.*, 101:245301, Dec 2008.

[10] H. P. Büchler, E. Demler, M. Lukin, A. Micheli, N. Prokof'ev, G. Pupillo, and P. Zoller. Strongly correlated 2d quantum phases with cold polar molecules: Controlling the shape of the interaction potential. *Phys. Rev. Lett.*, 98:060404, Feb 2007.

[11] Lincoln D Carr, David DeMille, Roman V Krems, and Jun Ye. Cold and ultracold molecules: science, technology and applications. *New Journal of Physics*, 11(5):055049, 2009.

[12] Claude N. Cohen-Tannoudji and William D. Phillips. New mechanisms for laser cooling. *Physics Today*, 43(10):33–40, 1990.

[13] N. R. Cooper and G. V. Shlyapnikov. Stable topological superfluid phase of ultracold polar fermionic molecules. *Phys. Rev. Lett.*, 103:155302, Oct 2009.

[14] Johann G. Danzl, Manfred J. Mark, Elmar Haller, Mattias Gustavsson, Russell Hart, Jesus Aldegunde, Jeremy M. Hutson, and Hanns-Christoph Nagerl. An ultracold high-density sample of rovibronic ground-state molecules in an optical lattice. *Nat. Phys.*, 6(10.1038/nphys1533):265 – 270, February 2010.

[15] K. B. Davis, M. O. Mewes, M. R. Andrews, N. J. van Druten, D. S. Durfee, D. M. Kurn, and W. Ketterle. Bose-einstein condensation in a gas of sodium atoms. *Phys. Rev. Lett.*, 75:3969–3973, Nov 1995.

[16] M. H. G. de Miranda, A. Chotia, B. Neyenhuis, D. Wang, G. Quemener, S. Ospelkaus, J. L. Bohn, J. Ye, and D. S. Jin. Controlling the quantum stereodynamics of ultracold bimolecular reactions. *Nat. Phys.*, 7(10.1038/nphys1939):502–507, 2011/06.

[17] J. Deiglmayr, A. Grochola, M. Repp, K. Mörtlbauer, C. Glück, J. Lange, O. Dulieu, R. Wester, and M. Weidemüller. Formation of ultracold polar molecules in the rovibrational ground state. *Phys. Rev. Lett.*, 101:133004, Sep 2008.

[18] E. N. Economou. *Green's Functions in Quantum Physics*. Springer, third edition, 2006.

[19] Alexander L. Fetter and John Dirk Walecka. *Quantum theory of many-particle systems*. McGraw-Hill Inc., 1971.

[20] G. F. Giuliani and Vignale. *Quantum theory of the electron liquid*. Cambridge University Press, 2005.

[21] L. P. Gor'kov and T. K. Melik-Barkhudarov. Contribution to the theory of superfluidity in an imperfect fermi gas. *Sov. Phys. JETP*, 13:1018–1022, 1962.

[22] A. V. Gorshkov, P. Rabl, G. Pupillo, A. Micheli, P. Zoller, M. D. Lukin, and H. P. Büchler. Suppression of inelastic collisions between polar molecules with a repulsive shield. *Phys. Rev. Lett.*, 101:073201, Aug 2008.

[23] George Grüner. *Density Waves In Solids*. Frontiers In Physics, first edition, 1994.

[24] Hermann Haken and Hans Christolph Wolf. *The Physics of Atoms and Quanta*. Springer-Verlag, 5th edition, 1996.

[25] Deborah S. Jin and Jun Ye. Polar molecules in the quantum regime. *Physics Today*, 64:27, 2011 2011.

[26] Michael Klawunn, Alexander Pikovski, and Luis Santos. Two-dimensional scattering and bound states of polar molecules in bilayers. *Phys. Rev. A*, 82:044701, Oct 2010.

[27] Roman V. Krems, William C. Stwalley, and Bretislav. Friedrich. *Cold molecules : theory, experiment, applications*. CRC Press, Boca Raton, 2009.

[28] J. Levinsen, N. R. Cooper, and G. V. Shlyapnikov. Topological $p_x + ip_y$ superfluid phase of fermionic polar molecules. *Phys. Rev. A*, 84:013603, Jul 2011.

[29] Roman M. Lutchyn, Enrico Rossi, and S. Das Sarma. Spontaneous interlayer superfluidity in bilayer systems of cold polar molecules. *Phys. Rev. A*, 82:061604, Dec 2010.

[30] Roman M. Lutchyn, Enrico Rossi, and S. Das Sarma. Spontaneous interlayer superfluidity in bilayer systems of cold polar molecules. *arXic*, (arXiv:0911.1378v1 [cond-mat.quant-gas]), 8 Nov 2009.

[31] Richard D. Mattuck. *A guide to Feynman diagrams in the many-body problem.* MacGraw-Hill Inc., second edition, 1976.

[32] A. Micheli, G. Pupillo, H. P. Büchler, and P. Zoller. Cold polar molecules in two-dimensional traps: Tailoring interactions with external fields for novel quantum phases. *Phys. Rev. A*, 76:043604, Oct 2007.

[33] K.-K. Ni, S. Ospelkaus, M. H. G. de Miranda, A. Pe'er, B. Neyenhuis, J. J. Zirbel, S. Kotochigova, P. S. Julienne, D. S. Jin, and J. Ye. A high phase-space-density gas of polar molecules. *Science*, 322(5899):231–235, 2008.

[34] K.-K. Ni, S. Ospelkaus, D. Wang, G. Quemener, B. Neyenhuis, M. H. G. de Miranda, J. L. Bohn, J. Ye, and D. S. Jin. Dipolar collisions of polar molecules in the quantum regime. *Nature*, 464(10.1038/nature08953):1324–1328, 2010/04/29.

[35] S. Ospelkaus, K.-K. Ni, D. Wang, M. H. G. de Miranda, B. Neyenhuis, G. Qu?)m?)ner, P. S. Julienne, J. L. Bohn, D. S. Jin, and J. Ye. Quantum-state controlled chemical reactions of ultracold potassium-rubidium molecules. *Science*, 327(5967):853–857, 2010.

[36] A. Pikovski, M. Klawunn, G. V. Shlyapnikov, and L. Santos. Interlayer superfluidity in bilayer systems of fermionic polar molecules. *Phys. Rev. Lett.*, 105:215302, Nov 2010.

[37] Mohit Randeria, Ji-Min Duan, and Lih-Yir Shieh. Bound states, cooper pairing, and bose condensation in two dimensions. *Phys. Rev. Lett.*, 62:981–984, Feb 1989.

[38] Mohit Randeria, Ji-Min Duan, and Lih-Yir Shieh. Superconductivity in a two-dimensional fermi gas: Evolution from cooper pairing to bose condensation. *Phys. Rev. B*, 41:327–343, Jan 1990.

[39] Subir Sachdev. *Quantum Phase Transitions.* Cambridge University Press, second edition, 2011.

[40] Barry Simon. The bound state of weakly coupled schrödinger operators in one and two dimensions. *Annals of Physics*, 97(2):279 – 288, 1976.

[41] J. Sólyom. The fermi gas model of one-dimensional conductors. *Advances in Physics*, 28(2):201–303, 1979.

[42] Jenő Sólyom. *Fundamentals of the Physics of Solids*, volume 3. Springer, 2010.

[43] Michael Tinkham. *Introduction To Superconductivity.* Dover Publication, INC., second edition, 1996.

[44] N. T. Zinner, B. Wunsch, D. Pekker, and D. W. Wang. Bcs-bec crossover in bilayers of cold fermionic polar molecules, 2010.

[45] Daniel Zwillinger. *Standard Mathematical Tables And Formulae.* CHAPMAN and HALL/CRC Press, 31 edition, 2003.

Statutory Declaration

I declare that I have written this thesis independently and have not used any other sources or aids than those have been referenced in this work.

January 18, 2012 *Amin Naseri Jorshari*

Acknowledgements

From the moment that I have arrived in Germany, to start my master program at Stuttgart University, up to now that I am getting to be graduated, there have been several people I met who I feel deeply indebted. Although, first of all I need to express my eternal gratitude toward my parents for their dedication and many years of support throughout my life. Afterwards, I have to acknowledge my debt to dear Madam Eva Rose, my course director in the International Master Program at the Stuttgart University, who far beyond the formal frame of her position, assists international students included me, and who without her unexpectedly kind consultation, I would have never reached to the end of my master program. Also, I would like to say my deep thanks to Prof. Kurt Lassmann who cares his students paternally.

During the past year, I have encountered with my first experience in research period and I was very indeed fortunate to have the opportunity of working under the supervision of Prof. Hans Peter Büchler. I would like to acknowledge my gratitude to him and say my thanks for his support and tolerance during. I would like also to appreciate my colleagues in the Institut für Theoretische Physik III, Alexander Janisch, Adam Bühler, Thorsten Beck, and Mohammad Rezai, for all of their friendly companionship and helps.

I would like also to say my gratefulness toward my dear friends Nasim Rafie Fard, Carolina Trichet Paredes, and Nima Farahmand Bafi, for all memorable moments we shared together. And for sure, I need to thank Dr. Johannes Roth in ITAP who accepted me for a HIWI job which helped me to run my life throughout my inhabitant in Germany.

And the last but not the least, I appreciate the care of Prof. Günter Wunner as the second supervisor of my thesis.